The design and development of new anti-trypanosomal agents

A Thesis submitted to the University of Strathclyde for the degree of Doctor of Philosophy by

Bilal Ali AlJaidi

2010

Strathclyde Institute of Pharmacy and Biomedical Sciences

University of Strathclyde

Glasgow

"This thesis is the result of the author's original research. It has been composed by the author and has not been previously submitted for examination which has led to the award of a degree"

Author's signature:

Date

For my sweetheart Shoruq

For my lovely children, Omar and Salma

For my great mother

Acknowledgment

I would like to thank my supervisors Professor Simon P. Mackay and Dr. Geoffrey D. Coxon for their endless help, support and guidance throughout my PhD work. I realy appreciate it and will never forget their endless efforts in making my PhD programme a success.

Special thanks to Carol Clements (Strathclyde Institute for Drug Research) for her time in teaching and guiding me in the techniques of screening my compounds for activity against *T. brucei*. This allowed me to gain invaluable experience of assay procedures. Thanks also to Louise Young for running the cytotoxicity assay. I am also thankful to Dr. Judith Huggan for her enormous effort and guidance throughout my chemistry work as well as her valuable advice regarding my thesis writing.

I thank my friend Nizar Al-shar'i for his help in teaching me the techniques used for the pharmacophore modelling. Thanks to Dr. Nahoum Anthony, Dr. Murray Robertson and Dr. Rachel Clark for their continuous advice and support regarding the molecular modelling and docking experiments. I also would like to thank Mr. Steve Steer for his assistance with the use of IR instrument, as well as Denise Gelmour for running the elemental analysis of my compounds, and Dr. Tong Zhang for his assistance in performing the MS. Many thanks to Gavin Bain (Chemistry Department, University of Strathclyde) for all his help in teaching me how to use the hydrogenator.

I would like also to thank all my colleagues in SIPBS 312 and 309; Murad, Hasan, Giacomo, Sabin, Jessica, James, and Dr. Fang for making life in the laboratory a pleasant one, as if we are one family.

Very special thanks to Philadelphia University/Jordan for sponsoring my study; I realy appreciate this sponsorship which has made my dreams come true.

Endless thanks to all my family members there in Jordan who have been with me all the time in their hearts and prayers, especially my great Mother, my dear brothers and sisters.

To my soul mate and sweetheart, my wife Shoruq, who was always beside me, caring about my PhD progress and trying her best to make life easier and supporting me toward a successful conclusion of my PhD studies, I say: you are the best and the sweetest thing to happen to me in my life, thank you so much. To my son Omar and daughter Salma, my treasures in this life, who give meaning to our life, may Allah bless you all and help me take care of you through all my life.

Table of Contents

Abbreviations

μM	Micromolar concentration
^{13}C NMR	Carbon NMR
^{1}H NMR	Proton NMR
3D	Three dimensional
ADP	Adenosine diphosphate
ATC	2-aminothiazole-4-carboxylate
ATP	Adenosine triphosphate
BBB	Blood brain barrier
BrCN	Cyanogen bromide
bs	Broad singlet
BSF	Blood stream form
CADD	Computer aided drug design
CDK	Cyclin-dependent kinase
CNS	Central nervous system
CoA	Coenzyme A
CSF	Cerebrospinal fluid
d	Doublet
D. H_2O	Distilled water
DCM	Dichloromethane
dd	Doublet of doublet
DHFR	Dihydrofolate reductase
DMF	Dimethylformamide
DFMO	α-difluoromethylornithine
DMSO-d_6	Deuterated dimethylsulfoxide
DNA	Deoxyribonucleic acid
DYRK	Dual specificity tyrosine-phosphorylation-regulated kinases
E. coli	*Escherichia coli*
ED_{50}	Half maximal effective dose
ELO's	Elongase enzymes
eq	Equivalent
FAS-I	Fatty acid synthase type I
FAS-II	Fatty acid synthase type II

FTIR	Fourier-transformmed infra-red spectroscopy
FTMS-ESI	Fourier-transformed mass spectroscopy-electron spray ionization
G.	*Glossina*
GPI	Glycosyl phosphatidylinositol
GSK3	Glycogen synthase kinase
HAT	Human African Trypanosomiasis
H_2O	Water
HCl	Hydrochloric acid
HS27	Human fibroblast cell lines
HTS	High throughput screening
Hz	Hertz
IC_{50}	Half maximal inhibitory concentration
IPC	Inositol phosphorylceramide
IR	Infra-red Spectroscopy
J	Coupling constant
KBr	Potassium bromide
K_i	Dissociation constant for inhibitor binding
LBDD	Ligand-based drug design
m	Multiplet
m.p	Melting point
MAPK	Mitogen activated protein kinase
MaxOmitFeat	Maximum omitted features
$MgSO_4$	Magnesium sulfate
MIC	Minimum inhibitory concentration
Mwt	Molecular weight
Na_2CO_3	Sodium carbonate
NAD^+	Nicotinamide adenine dinucleoptide
NADPH	Nicotinamide adenine dinucleoptide phosphate
NaOH	Sodium hydroxide
nM	Nanomolar
NMR	Nuclear magnetic resonance spectroscopy
NTR	Nitroreductase
O_2	Oxygen
ODC	Ornithine Decarboxylase
p	Pentet

P2	Purine transporter type 2
PCF	procyclic form
PNT2A	normal prostatic cell line
ppm	Part per million
PtO_2	Platinum oxide IV
PTR1	Pteridine reductase 1
q	Quartet
r.t	Room temperature
RNA	Ribonucleic acid
s	Singlet
SBDD	Structure-based drug design
t	Triplet
T.b.	*Trypanosoma brucei*
T3P	Propane phosphonic acid anhydride
*Tb*AT1	*Trypanosoma brucei* adenosine transporter 1
*Tb*ECT	*Trypanosoma brucei* ethanolamine-phosphate cytidyltransferase
*Tb*MRPA	*Trypanosoma brucei* multi-drug resistant associated protein A
TEA	Triethylamine
THF	Tetrahydrofuran
TLM	Thiolactomycin
TryS	Trypanothione synthetase
VS	Virtual screening
WHO	World Health Organisation

Abstract

Human African Trypanosomiasis (HAT) is considered one of the most dangerous parasitic infections, killing over 60,000 people each year and is endemic to tropical and sub-Saharan Africa, threatening more than 70 million lives. Currently, only five drugs are used for the treatment of HAT, most of which have serious adverse effects, some of which are fatal. No new drugs have been introduced for the treatment of HAT over the last 40 years, and those available agents have undesirable side effects as well as problems with increasing resistance. There is therefore an urgent need to develop new agents with novel modes of action to combat this life threatening infection.

This work utilised computational techniques to generate a pharmacophore based on results obtained from screening a library of compounds for anti-trypanosomal activity. The active compounds from the *in vitro* assay were mapped onto the pharmacophore and used as hits in a medicinal chemistry lead optimisation programme. Several series were designed and synthesised utilising efficient synthetic methodologies.

Biological evaluation of the compounds resulted in a range of activities against *Trypanosoma* species with some compounds having activity in the sub-micromolar range and with no observed toxicity on human cells. These results were used to further optimise the most active compounds, which resulted in very active compounds being obtained (MICs of 195-490 nM) with no apparent toxic effect on human cell lines.

Chapter One: Introduction

1.1 Introduction to Human African Trypanosomiasis

Human African Trypanosomiasis (HAT) is considered to be one of the most dangerous parasitic infections and kills more than 60,000 people each year. This disease, which is caused by the *Trypanosoma* parasite and transmitted by the tsetse fly, is endemic to most of tropical and sub-Saharan African regions covering 36 countries. It affects more than 70 million people and 700,000 new cases are reported each year according to World Health Organisation (WHO) reports.[1]

The trypanosoma parasite is amongst the most extensively studied organism of all the flagellated protozoa. Most of the *Trypanosoma* genus is non-pathogenic to wild mammals, and the disease is restricted to human or domestic animals. *Trypanosoma brucei* (*T.b*) is the pathogenic species among the *Trypanosoma* genus, with *rhodesiense* and *gambiense* the subspecies pathogenic to humans. *T.b. rhodesiense* is the causative agent of East African sleeping sickness, whereas *T.b. gambiense* causes the West and Central African sleeping sickness. Although these two subspecies are morphologically indistinguishable from each other, *rhodesiense* is more virulent and the infection develops rapidly compared to the *gambiense* subspecies.[2] The other subspecies, *T.b. brucei*, is non pathogenic to humans under normal conditions because it is rapidly lysed by human serum, but infects domestic animals and causes Nagana disease.[3] In addition to the *brucei* species, there are many others such as *T. congolense*, *T. vivax*, *T. evansi* and *T. equiperdum*, which primarily infect domestic animals. *T. cruzi* is the other pathogenic species in humans; it is prevalent in Central and South America and causes Chagas' disease.

1.2 Epidemiology of HAT

HAT is restricted to sub-Saharan Africa which has a suitable habitat for its vector, the tsetse fly. It mainly affects poor and rural regions in 36 countries. There is no overlap between the two subspecies; *gambiense* and *rhodesiense*. The former is normally prevalent in west and central Africa causing West African or Gambian Sleeping Sickness, whereas the latter is found in East Africa and results in East African or Rhodesian Sleeping Sickness (**Figure 1**).

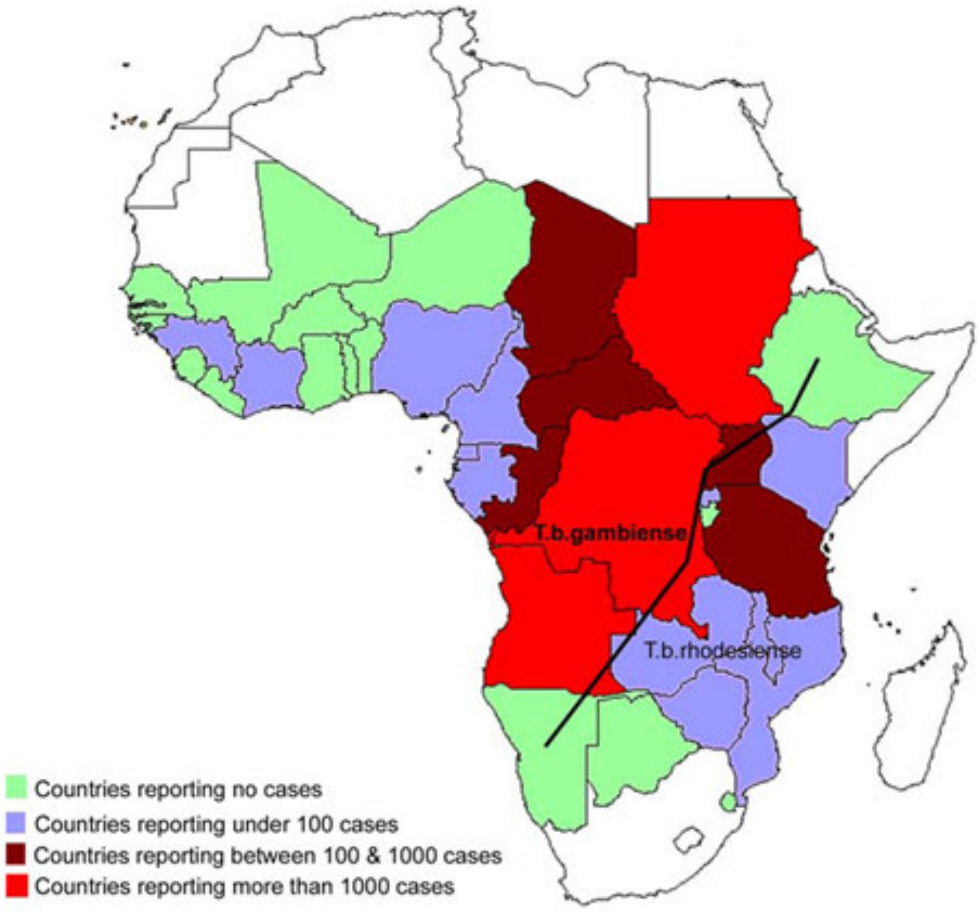

Figure 1: Countries infected with HAT in Africa.[4]

Generally the Rhodesian form of the disease is acute and is fatal within weeks to months, with 80% of deaths happening within six months of infection.[2] The Gambian form takes several years to develop and has a long asymptomatic stage, which is followed by a sub-acute illness before entering into the fatal late-stage menigoencephalitis.[2] Three major epidemics have been reported for HAT in the past century. The first, which largely affected equatorial Africa and killed more than 800,000 people, took place between 1896 and 1906.[5] The second epidemic was between the 1920s and 1940s and covered a wider region of sub Saharan Africa. Since then, a huge effort has been invested in controlling the vector and undertaking active surveillance of the population, both of which led to the near eradication of the disease. However, in the late 1990s there was a collapse in these control strategies primarily caused by war that resulted in a progressive re-emergence of the third HAT

epidemic primarily in the Democratic Republic of the Congo, Angola, Central African Republic southern Sudan and Uganda.

T. b. gambiense is considered as the predominant cause of HAT and is responsible for nearly 97% of the reported cases.[6]

1.3 Transmission of HAT

HAT is considered a vector-born parasitic disease and is transmitted through bites from the tsetse flies of the genus *Glossina* from the Diptera (*Glossinidae*) family. Tsetse flies are robust, 6-15 mm long flies that can be distinguished from other biting flies by their forward pointing mouthparts and characteristic wing venation (**Figure 2**).

Figure 2: The tsetse fly.

Thirty known species have been identified from the genus *Glossina*, but only nine belonging to either *G. palpatis* or *G. moristans* are known to transmit HAT. Wild and domestic animals like cattle are the common primary hosts of the parasite. The flies are known to be viviparous; the female fly deposits a fully developed larva into the soil where it develops into the adult flies within a month. These newly-hatched flies are not infected with the *Trypanosoma* parasites. Both the male and the female flies are haemtophagous and normally ingest the parasite during a blood meal from an infected host. Once ingested, the parasite goes through different development stages into the infective form that is stored in the fly's saliva, ready to be injected into the human blood stream during the next blood meal.[7]

Chagas' disease, which is caused by *T. cruzi*, is transmitted to humans mainly by the insect *Triatoma infestans* (also known as kissing bugs), in addition to other vectors such as *Rhodnius prolixus* and *Panstrongylus megistus* from *Reduviidae* family (**Figure 3**).[8]

Figure 3: *Triatoma* insect

1.4 The *Trypanosoma* parasite

Trypanosoma is a unicellular protozoan organism that belongs to the family *Trypanosomatidae*. The mature cell is 15-30 µm long and has a flagellum to help movement in the host blood stream (**Figure 4**).

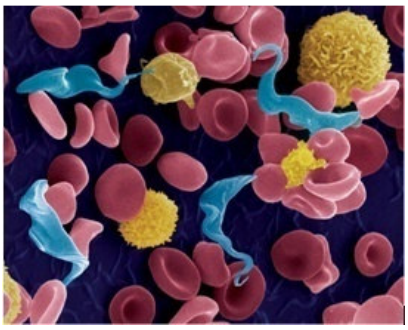

Figure 4: *Trypanosoma brucei* (in blue) in human blood.[5]

The *Trypanosoma* parasite is eukaryotic. It has tubular mitochondrion that contains the kinetoplast which stores circular mitochondrial DNA. The parasite cell has a unique surface of glycosyl phosphatidylinositol (GPI) molecules attached to a variant surface glycoprotein, which protects the parasite from the lytic factors in human plasma.[9]

1.5 The life cycle of *Trypanosoma brucei*

The life cycle starts when the tsetse fly bites its victim and injects the metacyclic forms of the *Trypanosoma* (the trypomastigotes) deep into the skin tissue. The parasite reaches the lymphatic system, then the blood stream where it normally multiplies by binary fission and develops into the blood stream forms (BSF). In the late stage of the disease, the BSF parasite penetrates the blood brain barrier (BBB) to

invade the cerebrospinal fluid (CSF). During its presence in the blood stream, the BSF parasite differentiates into a short form that is ingested into the tsetse fly during a blood meal. Inside the insect's midgut and within 3-5 weeks, the parasite undergoes several differentiation steps to form the procyclic form (PCF), which in turn differentiates into an epimastigote that travels to the salivary glands where it replicates by binary fission to the metacyclic trypomastigotes. This is the form that is transferred to another mammalian host to complete the life cycle during the next blood meal (**Figure 5**).[10]

Domestic and wild animals can also become infected with human *T.b. gambiense* and *T.b. rhodesiense* but without becoming ill. These animals play a major role as carriers and hosts for the disease from which the tsetse flies can acquire an infection and then transfer to humans. In *T.b. rhodesiense*, cattle are the most important host for the parasite. *T.b. gambiense* mostly depends on human-to-human transmission and man is considered the main host, although animals such as pigs and some other domestic species have been reported as possible hosts for the diasease.[11]

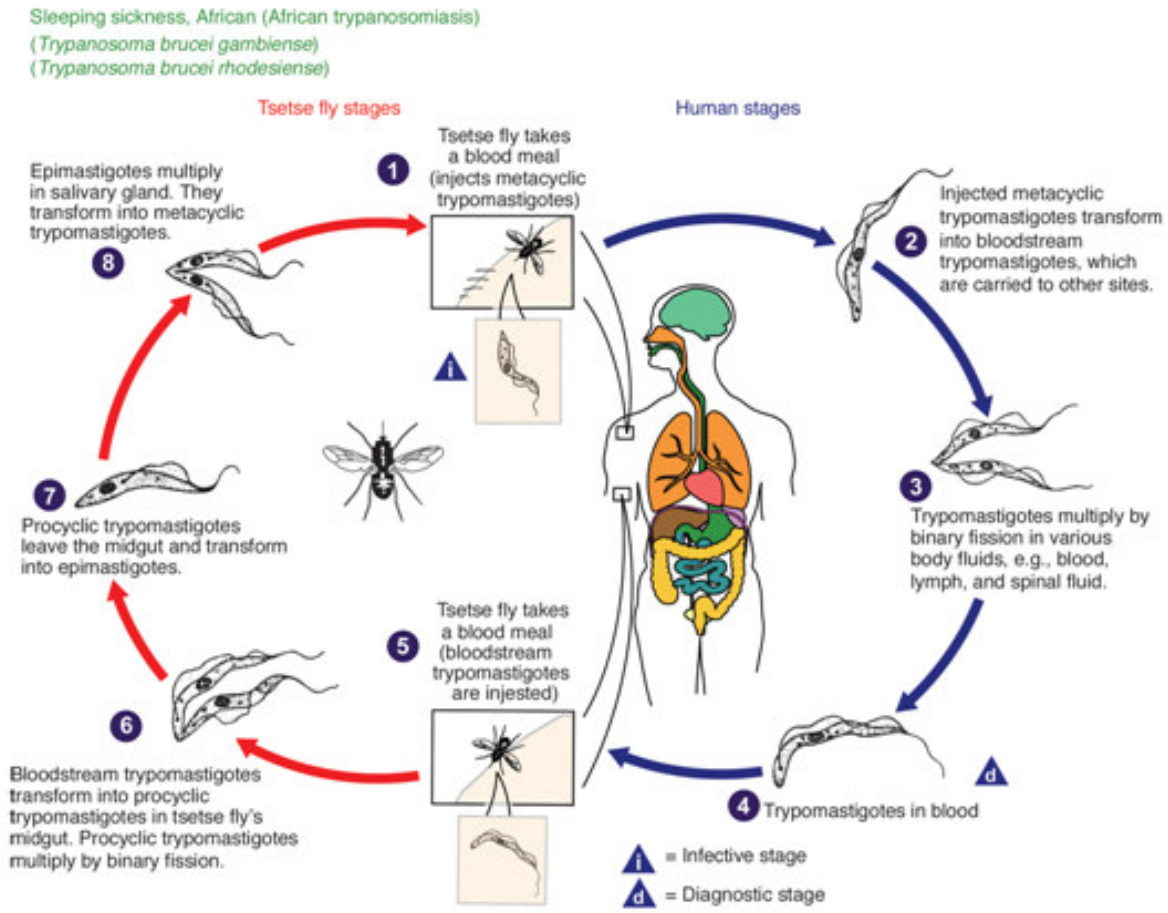

Figure 5: The life cycle of *Trypanosoma brucei*.[10]

1.5 Clinical features and diagnosis of HAT

The disease normally manifests in two stages, the early hemolymphatic stage and the late meningo-encephalitic stage after CNS invasion. In the hemolymphatic stage, a trypanosomal skin chancre can be seen accompanied with fever, headache and pruritus. As the parasite travels to the lymph nodes, signs of lymphadenopathy and to a lesser extent hepatosplenomegaly have been observed, especially with *T.b. rhodesiense* infections.[8]

In the late meningo-encephalitic stage, sleep disturbances and neuropsychiatric disorders dominate. Sleep disorder is the major symptom of this disease, which is how the disease gets its name of sleeping sickness. This stage is normally characterized by daytime somnolence followed by insomnia at night. Other neurological symptoms reported are tremor, general motor weakness, limb paralysis, hemiparesis and abnormal movements such as dyskinesia. In some cases Parkinson-like movements can be observed along with speech disorders and psychiatric symptoms such as psychotic reactions and aggressive behaviours.

Diagnosis of infection must be made as early as possible in order to prevent progression into the latter stage which may lead to impaired mental function, coma and even death. Early diagnosis is therefore very important in preventing the progression of the disease into the lethal stage as well as preventing its transmission.[8] However, diagnosis of HAT is difficult, especially in the *T.b. gambiense* infection because of the long asymptomatic early stage, and relies on laboratory examinations because the clinical features of the disease are not sufficiently specific. The card agglutination test for HAT, especially infections with *T.b. gambiense*, is a fast and practical serological test that allows hundreds of individuals to be screened daily and is reported to be 87–98% sensitive. [12, 13] In addition, microscopic examination of lymph nodes and blood, or both, is needed for parasitological confirmation.

The diagnostic approach for *T.b. rhodesiense* differs in several ways; firstly, there is no serological screening test available. Instead, the identification of suspected cases relies on the non-specific clinical presentation and history of exposure. Secondly, parasitological confirmation is easier since the density of blood circulating parasites

is higher than that for *T.b. gambiense*, and blood smear is usually sufficient to confirm diagnosis.[5]

1.6 Control and prevention of HAT

To date, there is no vaccine available for the prevention of HAT, primarily because eukaryotic pathogens such as protozoa and parasites are genetically and biologically complex organisms with elaborate life cycles and specialized immune evasion mechanisms.[14] Recent research has focussed on developing DNA vaccines as both therapy and protection against many protozoan infections such as leishmaniasis, trypanosomiasis and malaria.[15]

Since the vaccination approach has so far proved to be unsuccessful, efforts have focussed on preventing further transmission of HAT to reduce the spread of the disease. WHO have put a comprehensive programme in place to tackle and control HAT in which two thirds of African countries have taken part in.[16] It is based first on applying mobile medical surveillance which guarantees continuous and regular visits to the area of high risk by specialized staff equipped with accurate and effective diagnostic tools to identify the infected people as fast as possible. These people are then sent to specific referral centres, where the disease stage is determined and the proper treatment given, with follow-up for possible side effects. The next step in the programme is post-medical surveillance, involving both local health centres and hospitals in blood sample analysis to identify cases. These are sent for further diagnosis and confirmation, after which the infected patients are sent to special centres for treatment and post therapeutic follow-up. These steps have been very successful at preventing the incidence of disease transmission between human and animal hosts.

Another important part of the control programme is related to the vector. Since tsetse flies play a fundamental role in the transmission of HAT between humans and animals, the reduction of tsetse fly bites is the best preventive measure. The flies are attracted to dark colours, in particular blue and black, and also to the motion of vehicles and they have the ability to bite through clothes. The primary preventive

measure is to avoid areas where tsetse flies are known to be present and to encourage people to travel in covered cars with closed windows, especially in endemic areas. Other measures include the use of insect repellents and the wearing of clothes of wrist and ankle length.[17] Since the fly remains infected for life by the parasite, human-fly contact is considered the crucial component of the HAT transmission,[10] and most efforts have focussed on eradicating and controlling the spread of tsetse flies.

Finally, eliminating HAT requires robust, reliable methods for effective early diagnosis of the disease, and safe, efficacious drugs to treat the haemolymphatic and the CNS stages of the disease.

1.7 Current chemotherapy for HAT

It is important to correctly diagnose the stage of the disease in order to choose a suitable treatment regime because most of the drugs currently used for HAT treatment do not penetrate blood brain barrier (BBB). In order to determine whether the parasite has crossed the BBB, a lumber puncture is used to draw cerebrospinal fluid for examination. Five compounds are clinically available and licensed for the treatment of the different stages of HAT; suramin and pentamidine are only active in the early hemolymphatic stage; melarsoprol and eflornithine are used for the treatment of the late CNS stage; and nifurtimox is used in the treatment of latter stages of melarsoprol resistant HAT.

1.7.1 Suramin

Suramin is a polysulfonated symmetrical naphthalene derivative that was first used against sleeping sickness in 1922.[6, 18] It is usually used against early stage *T.b. rhodesience* infections. Suramin should be administered intravenously in complex dose regimens that can last for 30 days.[5] In most cases, suramin should be given as a course of five injections, every 3-7 days over a period of one month. Since it is ionized at physiological pH, suramin is highly bound to serum protein, and does not freely cross the BBB and cannot be used in the late stage of the disease. Its high

molecular weight means it is only slowly excreted in the urine and leads to drug accumulation. The mechanism by which suramin exerts its anti-trypanosomal action has not been established. Glycolysis has been proposed as a possible target and evidence of 6-phosphogluconate dehydrogenase inhibition from the pentose phosphate shunt has been reported.[19] Many adverse effects have been reported including neuropathy, rash, fatigue, anaemia, hyperglycaemia, neuropaenia and bone marrow toxicity with agranulocytosis and thrombocytopenia.

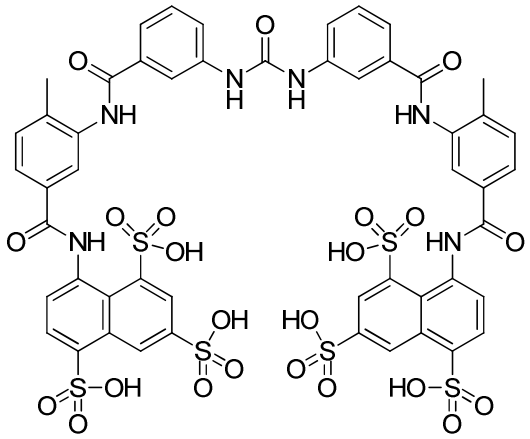

Suramin

1.7.2 Pentamidine

Pentamidine is an aromatic diamidine anti-protozoan agent first used for the treatment of *T.b. gambiense* in 1937. It is used in the early stages of the disease against *T.b. rhodesience* only when suramin is contraindicated.

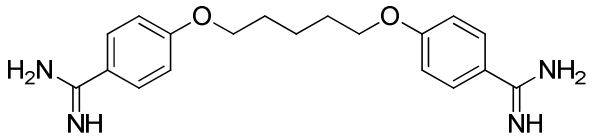

Pentamidine

Pentamidine is normally given by intramuscular injection for a week in a unit dose of 4mg/ kg body weight on a daily or alternate day basis. Since it is positively charged

at physiological pH it binds to blood serum proteins, and passes into the CSF only very slowly,[20] where it has been detected at concentrations of 0.5-0.8% of plasma levels, probably due to BBB damage that results from the inflammatory responses associated with CNS infections.[21] The mode of action is not well defined. It is a positively charged di-cationic compound that binds to DNA, RNA, proteins and phospholipids, and recent studies have shown that it binds to the minor groove of DNA in the parasite mitochondria, induces changes in DNA topology, inhibits topoisomerases and leads to DNA damage.[22] Pentamidine is believed to enter the trypanosomal cell by active transport using at least three membrane transporters; P2 aminopurine permease (also called *Tb*AT1, *Trypanosoma brucei* adenosine transporter 1), a high affinity pentamidine transporter 1 and a low affinity pentamidine transporter 1. Resistant cases have been reported and are believed to be due to an absence of P2 transporter activity.[23]

Pentamidine has serious adverse effects which include leucopoenia, thrombocytopenia, hyperkalaemia, as well as hepatotoxicity, tachycardia and pain and tenderness at the site of injection.[24]

1.7.3 Melarsoprol

Melarsoprol is an organoarsenic compound and is most widely used for the treatment of the late stage of *T.b. gambiense*. It is the main choice for the treatment of the late stage of *T.b. rhodesiense* despite its extremely toxic effects.[5, 6] The recommended dose in *T.b. gambiense* infections is ten intravenous injections of a 3.6% solution in propylene glycol in doses of 2.2-3.6mg/kg body weight once a day.[21] These injections are highly irritant because of the propylene glycol vehicle.

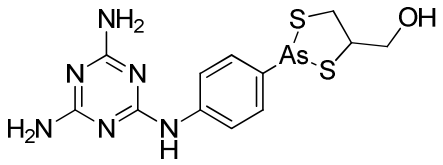

Melarsoprol

It is still not clear how melarsoprol exerts its trypanocidal action, but it is believed to inhibit the trypanosomal glycolysis pathway. Arsenic can form stable interactions with thiol containing enzymes such as glycerol-3-phosphate dehydrogenase (G3PDH),[25] and with substances such as trypanothione and lipoic acid to from a reversible but stable compound that acts as a competitive inhibitor of trypanothione reductase, an important enzyme for the parasite.[26] Melarsoprol is a prodrug and is metabolized inside the human body to the active species, melarsan oxide and phenylarsan, which can be taken up by the P2 transporter to bind trypanothione and then inhibit trypanothione reductase enzyme.

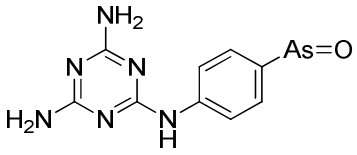

Melarsan oxide

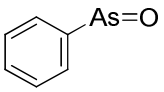

Phenylarsan

Although melarsoprol crosses the BBB at levels of around 1-2% of its maximum plasma levels, this amount is sufficient to kill *Trypanosoma* parasites. However, the side effects of melarsoprol are severe. In 5-10% of the cases, severe convulsions and encephalopathy might lead to coma and death. Other common adverse events include pyrexia, headache, thrombocytopenia and heart failure.[25]

1.7.4 Eflornithine

Eflornithine (or α-difluoromethylornithine-DFMO) is an analogue of the amino acid ornithine. It was first introduced for the treatment of HAT in 1990 under the trade name Ornidyl® by Aventis. It is considered the drug of choice for the treatment of late stage *T.b. gambiense* infections and several studies have revealed that DFMO has reduced mortality compared to melarsoprol.[27] DFMO has much lower activity against *T.b. rhodesiense*; which may be due to the innate tolerance of this subspecies to the drug.

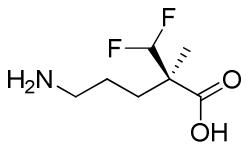

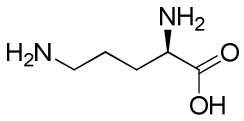

DFMO **L-Ornithine**

DFMO should be given *via* intravenous infusion at a dose of 400mg/ kg body weight four times daily for 7 to 14 days.[28] A high dose is required since only small amounts cross the BBB. Despite this problem, DFMO is still the first line therapy for late stage *T.b. gambiense* infections. It enters the parasite through either passive diffusion or *via* amino acid carrier mediated transport. Once inside the parasite, it irreversibly inhibits ornithine decarboxylase (ODC), the rate-controlling enzyme in polyamine biosynthesis.[29] Although DFMO has similar affinity for both mammalian and trypanosomal ODC's, it specifically affects the trypanosomal enzymes because the degradation half life of the DFMO–mammalian ODC complex is very short and is replaced by newly synthesised ODC; the DFMO-parasitic ODC complex has a longer half life and is only slowly replaced by new ODC's, which leads to impaired growth.[30]

Side effects with DFMO are much milder than melarsoprol, and include fever, headache, hypertension, peripheral neuropathy and gastrointestinal problems such as diarrhoea.

1.7.5 Nifurtimox

Nifurtimox is a 5-nitrofuran containing compound first introduced for the treatment of Chagas' disease in the early 1970s. It is commonly used in combination with other trypanocidal agents to avoid treatment failure, particularly in the case of melarsoprol. Recent trials of Nifurtimox in combination with DFMO have shown promising results.[31]

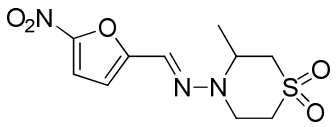

Nifurtimox

Nifurtimox mainly acts on the circulating trypomastigotes, but the precise mode of action is unknown. Single reduction of the nitro group by trypanosomal nitroreductase (NTR), especially prokaryote-related type I nitroreductase forms reactive oxygen species (**Scheme 1**) which are believed to cause damage to DNA, membrane lipids and proteins, leading to cell death.[8, 32]

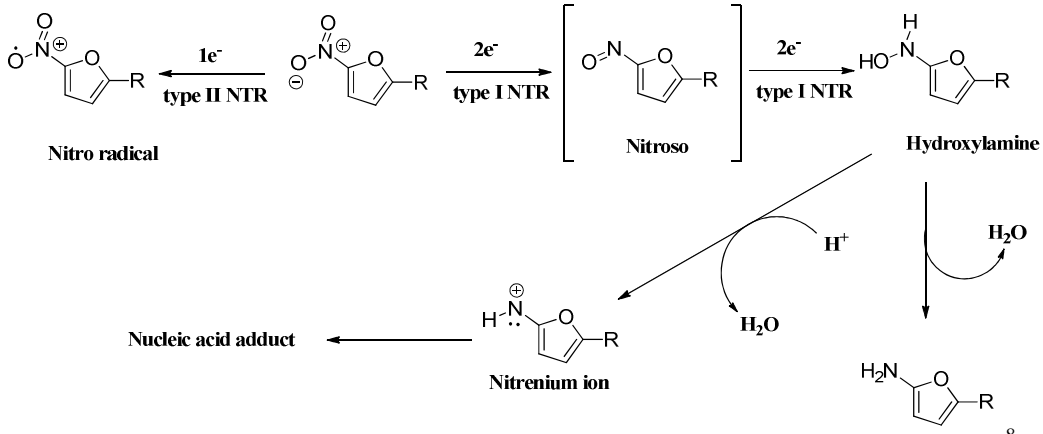

Scheme 1: Reduction of nitrofuran from nifurtimox with nitroreductase enzymes.[8]

Nifurtimox can cross the BBB to levels around half of its concentration in plasma. Its clearance is fast with a half life of around 3 hours. It is commonly used in combination since it is much less active than melarsoprol with an IC_{50} of 5 μM compared to 10 nM for melarsan oxide against cell proliferation. Although nifurtimox has good activity against the *Trypanosoma* parasite, it is generally toxic to humans and may be carcinogenic. It can also affect the central and peripheral nervous systems resulting in mood or mental changes, muscle weakness, numbness tingling, sleeping disorders, and in some cases convulsions and seizures.

1.8 Development of resistance in *Trypanosoma* parasites

Due to the extensive use of the clinically available anti-trypanosomal agents over a very long time and no development of new agents for HAT, multiple drug resistance has developed in both *T.b. gambiense* and *T.b. rhodesiense*, along with cross resistance between animals and humans. The emergence of drug-resistant

Trypanosoma strains is considered the most serious problem in HAT control, particularly for the populations at risk in tropical and sub-Saharan Africa.

The occurrence of resistance in *Trypanosoma* parasites was first observed over 100 years ago when Paul Ehrlich showed that drug-resistant *Trypanosoma* did not stain with acridine dyes. Based on these results, Ehrlich developed the "chemoreceptor" hypothesis, which stated that drugs act *via* specific receptors, and that drug resistance is caused by a reduced affinity for the respective receptor.[33]

Understanding the mechanisms of drug resistance is important as it can lead to the identification of potential and novel drug targets as well as provide direction for new chemotherapeutic strategies targeted against the development of resistance.

1.8.1 Resistance mechanisms in *T. brucei*

There are three main mechanisms by which *T. brucei* has developed resistance. The first is by reducing drug uptake into cells, which is mediated *via* the loss or mutation in the genes which encode the protein transporters. For example, resistance in *T.b. gambiense* and *T.b. rhodesiense* to melarsoprol is mainly mediated *via* mutations in the P2 transporter, which lead to decreased uptake of melarsan oxide, and cross-resistance to diamidine drugs such as pentamidine.

The second mechanism for resistance is the over expression of the efflux pump, which is responsible for pumping the drug molecules out of cells against a concentration gradient.[22] *T. brucei* has a multi-drug resistant associated protein A (*Tb*MRPA) efflux pump integrated in its plasma membrane, which is one of three ATP-binding transporters that are responsible for transporting molecules out of the cell. Resistance to melarsoprol is believed to be also mediated by a 10-fold over expression of the *TbMRPA* gene.[34]

The third mechanism by which *T. brucei* develops resistance is by interference with drug receptor interactions which is a consequence of:

- mutations that lead to structural modifications in the macromolecular target that prevent the drug from binding to its receptor as effectively;
- over expression and faster enzyme turnover. For example, *Trypanosoma* parasites, especially *T.b. rhodesiense* became resistant to DFMO by increasing ODC activity and production to compensate for inhibition;[35]

- increasing the uptake of the natural substrate to compete with the drug for the active site. For example, the resistance of *T.b. brucei* to DFMO is due to the increased uptake of ornithine, the natural substrate for ODC, leading to sufficient biosynthesis of polyamines and trypanothione.[36]

Unfortunately, many cases of the early and late stage HAT have became resistant to melarsoprol, pentamidine and eflornithine, which complicates the eradication strategies of HAT and slows down the preventive measures against the spread and progression of both *T.b. gambiense* and *T.b. rhodesiense* infections. As a result, new strategies are required to treat the existing resistant cases and to minimize the development of new resistance in the future.

1.8.2 Strategies for combating drug resistance in *Trypanosoma* parasites

Due to the fact that no new drugs have been recently introduced in clinic for the treatment of Trypanosomiasis, the control of the disease has to rely on the use of existing drugs which, apart from having been developed more than 100 years ago, suffer from many limitations such as toxicity and drug resistance. As a result, efforts are being focused on finding suitable and effective strategies to overcome drug resistance.

The first strategy to be used was called sanative pairs, which was proposed by Whiteside in 1958 and is based on the use of two drugs that are not susceptible to cross-resistance.[37] This method has shown promising results in resistant HAT cases in cattle. In human HAT, combined use of pentamidine and melarsoprol in early stage cases and nifurtimox with melarsoprol for the treatment of late CNS infections have proved to be successful.

Another method of overcoming drug resistance has been to use high dose regimens. Although this offers an efficient way to eliminate resistant trypanosomal infections, it increases the risk of drug toxicity because of the very high drug concentrations needed. However, in a recent study, the use of repeated treatments with lower doses proved to be as effective as using high doses in infected cattle.[38]

Another strategy to combat drug resistance is the use of combination therapy, which has the added advantage of lowering doses through the synergistic effects between

the combined drugs. This can reduce the incidence of adverse effects and improve cost-effectiveness.

Many drug combinations for HAT are under investigation; the combination therapy of eflornithine with nifurtimox against the late CNS stage of *T.b. gambiense* is in phase III clinical trials. The preliminary results from a multi-country nifurtimox-eflornithine combination therapy where eflornithine was administered as an intravenous infusion of 200 mg/kg every 12 hours for 7 days along with 5 mg/kg oral dose of nifurtimox every 8 hours for 10 days, indicate a reduction in the number of infusions from 56 to 14 with a reduced regimen duration from 14 days to 10 days.[5, 39] Other combinations that are in phase II trials are also showing promising results (**Table 1**).[30, 40]

Suramin, Eflornithine	In phase II clinical trials
Suramin, Pentamidine	
Melarsoprol, Nifurtimox	
Suramin, Metronidazole	
Melarsoprol, Eflornithine	
Eflornithine, nifurtimox	In phase III clinical trials

Table 1: Drug combinations against HAT under investigations.

Although these strategies to combat drug resistance in HAT look promising with respect to the effectiveness of currently available drugs, there is an urgent need to develop new agents with novel modes of actions.

1.9 The need for new anti-trypanosomal agents

The fact that almost all current drugs were first introduced several decades ago, and that no new drugs except eflornithine and nifurtimox have been developed over the last 40 years, means that new agents to tackle this life threatening disease are desperately required, particularly since most of the drugs in use have serious adverse effects that can be fatal in more than 5% of cases.

While formulation and chemical strategies to modify existing drugs to improve pharmacokinetic properties and reduce toxicity are being used, the modes of action

for these therapies remain the same, and does not address the possibility of resistance development and treatment failure. Therefore, new strategies require the development of new chemical scaffolds with novel modes of action against new targets.

Recently, deciphering the trypanosomal genome has helped in identifying novel drug targets which might play an important role in improving efficacy and preventing further development of resistance. The identification of these new targets should enable the process of finding new agents with novel mode of actions against both early stage and late stage HAT over next decade. In the following section, the most important metabolic pathways in *Trypanosoma brucei* are described and their credentials as suitable targets for the development of anti-trypanosomal agents discussed.

1.10 Metabolic pathways in *Trypanosoma brucei* as possible targets for chemotherapy

Much is known about the biochemical pathways and genomic sequences of Trypanosoma parasites.[6, 41] Since their cell organization and metabolic pathways differ considerably from mammalian cells, trypanosomal biochemical pathways, especially those which are absent in their hosts, should provide excellent targets for rational drug design.[42]

Target validation is a key step in any rational drug design program and the gene knockout approach is considered the best way to investigate whether a specific protein is or is not essential for the parasite's survival. In the following sections, some of the biochemical pathways that are considered promising targets for trypanocidal drugs will be discussed briefly along with some compounds that have been developed as possible inhibitors.

1.10.1 Trypanosomal lipid biosynthesis

Research has revealed that the *T. brucei* bloodstream form (BSF) has the ability to synthesise fully saturated fatty acids using butyryl-CoA as a primer and NADPH as a

reducing agent, and the major product in this process is myristate.[43] The synthesised myristate is incorporated into the surface glycosyl phosphatidylinositol (GPI) which is essential for parasitic pathogenesis. Most organisms such as mammalian and fungal cells synthesise fatty acids using fatty acid synthase type I (FAS-I), bacteria and plants use FAS-II, whereas *T. brucei* uses groups of enzymes called elongases.[44] These elongases (ELO's), in contrast to FAS-I and FAS-II enzymes, are integral membrane proteins in the endoplasmic reticulum. Whether the inhibition of ELO's or targeting fatty acid biosynthesis could potentially kill the parasites was not revealed until thiolactomycin (TLM), a natural product isolated from *Nocardia* bacteria, was examined. TLM effectively inhibits trypanosomal fatty acid synthesis *in vitro* with an IC_{50} of 150 μM and kills the parasite at the same concentration.[45]

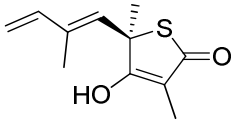

Thiolactomycin (TLM)

The ELO system in *T.brucei* is structurally and functionally different from the mammalian FAS-I system, and is also essential for parasitic survival. Lipid biosynthesis can therefore be considered a good target for the development of selective and potent anti-trypanosomal agents, and TLM analogues such as those shown in **Figure 6** have shown promising activity against *T.brucei*.[45, 46]

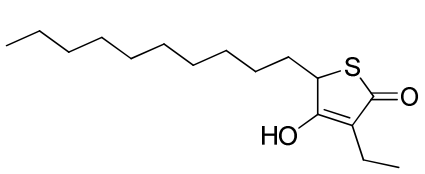

MIC = 6 μM

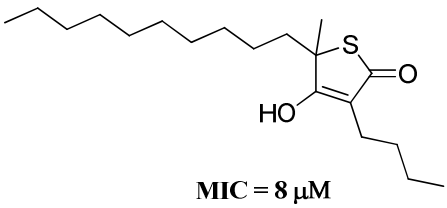

MIC = 8 μM

Figure 6: TLM analogues as anti-trypanosomal agents.

Other important lipids in *Trypanosoma* are the phosphatidylethanolamine and sphingolipid membrane constituents. Phosphatidylethanolamine is the major phospholipid component in Trypanosoma membranes, and *T.brucei* has the ability to

de novo synthesise this phospholipid through the Kennedy pathway. Cytosolic ethanolamine-phosphate cytidyltransferase (*Tb*ECT) is an important enzyme in this pathway that is essential for growth and survival, which makes it possible target for trypanocidal agents.[47]

Sphingolipids play a very important role in signal transductions through the plasma membrane. *T. brucei* synthesise inositol phosphorylceramide (IPC) as the primary phosphosphingolipid using sphingolipid synthase, which has been identified as an essential enzyme for parasite survival. Since this enzyme is structurally and functionally different from mammalian sphingomyelin synthase, it represents a promising target for developing selective trypanocidal agents. Recently, the fungal inhibitor of sphingolipid synthase, aureobasidin A has shown good activity against *T. brucei* at sub-micromolar concentrations.[48]

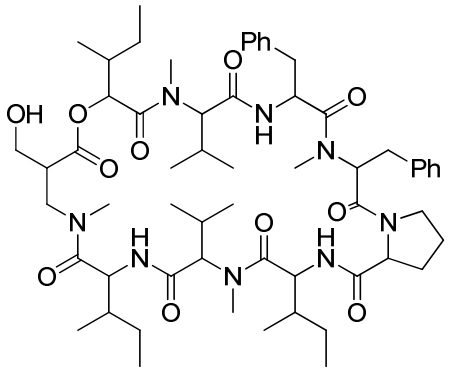

Aureobasidin A

1.10.2 Kinetoplast DNA replication

T. brucei has a unique network of interlocked DNA rings called kinetoplast DNA (**Section 1.4**) with a unique topology and its replication process is a target for new anti-trypanosomal drugs. Many enzymes are involved in kinetoplast DNA replication and some, such as the topoisomerases, are essential for the process. Recently, topoisomerase-II inhibitors such as aclarubicin, doxorubicin and mitoxantrone showed activity against *T. brucei* with ED_{50} values in the low nanomolar region (**Figure 7**).[49, 50] Although these agents have potent anti-

trypanosomal activity, almost all topoisomerase-II inhibitors have toxic effects on human cells, which renders their development as anti-trypanosomal agents problematic.

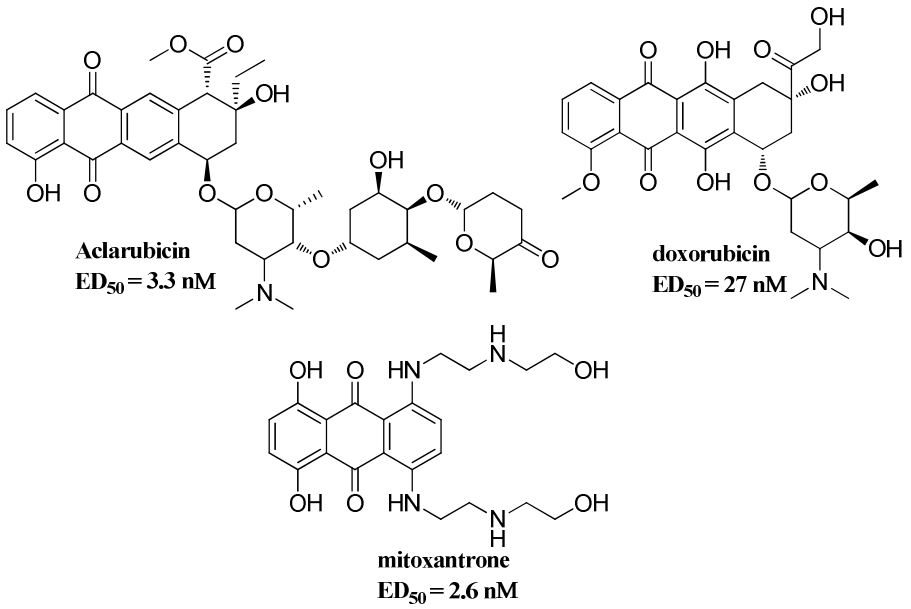

Figure 7: Some Topoisomerase II inhibitors with their ED_{50} against *T. brucei*.

Like pentamidine, some alkanediamide-linked bisbenzamidines have been designed as DNA binders and show good activity against *T. brucei* with IC_{50}'s in the 2 nM range (**Figure 8**). Although DNA binders are known to be toxic in human cells, these agents have shown no toxic effects on A549 human lung carcinoma cell line.[51]

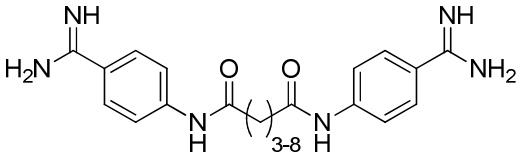

Figure 8: Alkanediamide-linked bisbenzamidines derivatives as trypanocidal agent.

1.10.3 Purine and pyrimidine metabolism and salvage

Unlike their mammalian hosts, *Trypanosoma* parasites lack the metabolic capability to make purine nucleotides *de novo* and must get them from the host *via* purine salvage, which offers a potential target for drug discovery. In the purine salvage pathway, the most extensively studied targets are nucleoside hydrolase, purine nucleoside phosphorylase, inositol monophosphate dehydrogenase, methylthioadenosine phosphorylase, and adenosine kinase. The hyperactivation of the last enzyme, which is a border enzyme between the purine salvage and polyamine biosynthesis pathways, has shown good trypanocidal activity,[52] and recently adenosine kinase activators have shown good anti-trypanosomal activity with MIC's of 1 μM against *T.b rhodesiense* (**Figure 9**).[53]

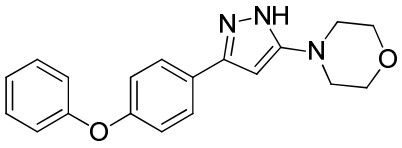

Figure 9: An adenosine kinase activator as an anti-trypanosomal agent.

1.10.4 Trypanosomal carbohydrate biosynthesis and glycolysis

Almost all trypanosomatids use carbohydrates as the main source for energy metabolism through glycolysis. Trypanosomal glycolysis is a good and selective target for the development of trypanocidal agents because the first reactions in this pathway occur inside unique organelles called glycosomes.[54] Glycosomes in *T. brucei* consist mainly of glycolytic enzymes that are essential for carbohydrate catabolism (**Figure 10**). Glycolysis in Trypanosomas as well as in other kinetoplastida members differs from the corresponding pathways in other organisms in many aspects. Firstly, the flux of glucose into the glycosome is controlled by glucose transporters which is believed to be the rate-limiting step in the glycolytic pathway; in humans, any undesired inhibition can be compensated by increasing the blood insulin levels.[54] Secondly, the first seven steps take place in the glycosomes which have impermeable membranes. Thirdly, the cycle under anaerobic conditions produces one molecule of ATP per glucose. Forthly, the glycosomal enzymes are not regulated by any of the intermediates in the cycle compared to other organisms;

for example, fructose-2,6-bisphosphate allosterically activates pyruvate kinase rather than the glycosomal phosphofructokinase in humans.[55]

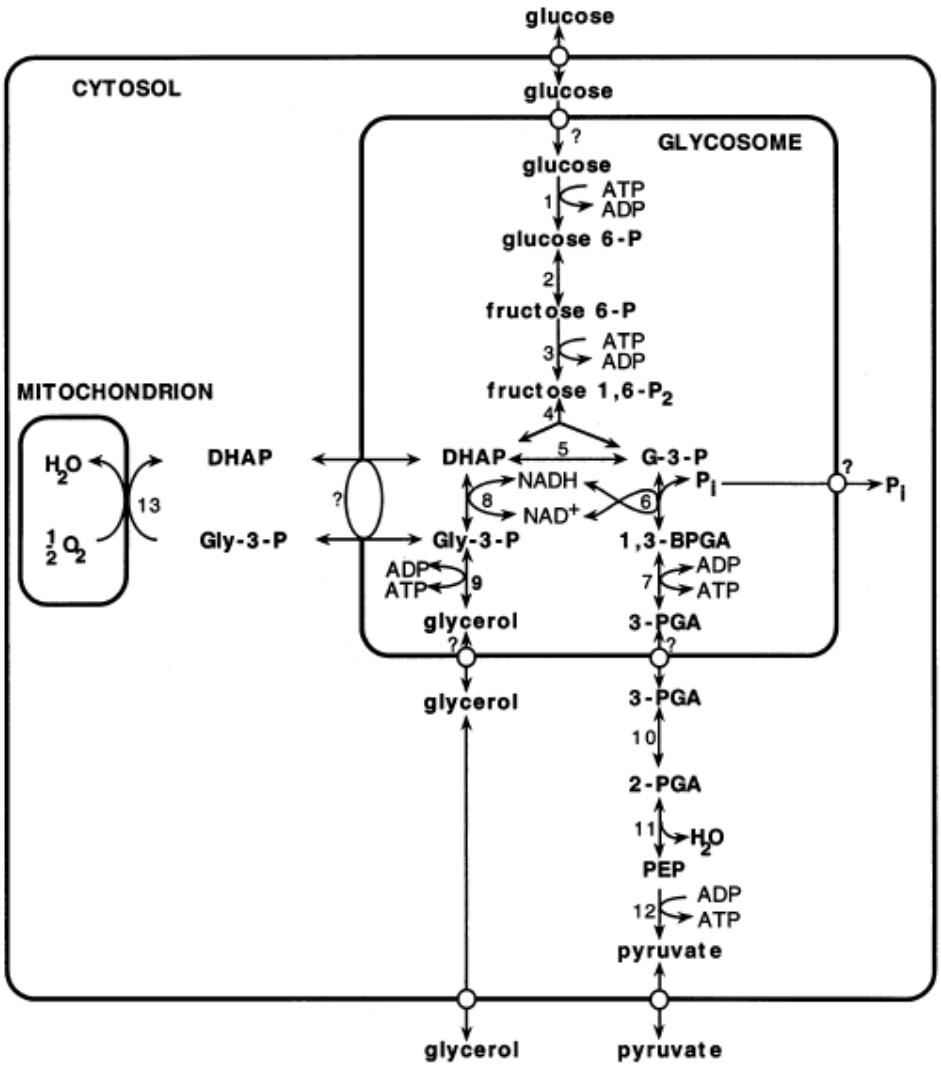

Figure 10:[56] glycolysis in bloodstream-form *T. brucei*. (1) Hexokinase: (2) glucose-6-phosphate isomerase; (3) phosphofructokinase; (4) aldolase; (5) triosephosphate isomerase: (6) glyceraldehyde-3-phosphate dehydrogenase; (7) phosphoglycerate kinase; (8) glycerol-3-phosphate dehydrogenase; (9) glycerol kinase; (10) phosphoglycerate mutase; (11) enolase; (12) pyruvate kinase; (13) glycerol-3-phosphate oxidase. Substrate and metabolite transporters in membranes are represented by circles; the carrier molecules postulated for translocation of metabolites across the glycosomal membrane remain to be identified. Abbreviations: 1,3-PGA, 1,3-bisphosphoglycerate; DHAP, dihydroxyacetone phosphate; G-3-P, glyceraldehyde 3-phosphate; Gly-3-P, glycerol 3-phosphate; PEP, phospho*enol*pyruvate; 2-PGA, 2-phosphoglycerate; 3-PGA, 3-phosphoglycerate.

Finally, most of the glycosomal enzymes are more than 70% structurally and topologically different from their human homologues. All these differences suggest that targeting the glycosomal enzymes could result in the selective killing of the parasite without exerting any undesired effect on the human glycolytic pathway.

Recent research has been focussed on understanding and characterizing the glycolytic enzymes from trypanosomes and the three dimensional (3D) structures of most of the key enzymes such as hexokinase,[57] fructose-1,6-bisphosophate aldolase,[58] triosephosphate isomerise,[59] glyceraldehydes-3-phosphate dehydrogenase,[58] phosphoglycerate kinase, pyruvate kinase, glycerol-3-phosphate dehydrogenase and phosphofructokinase have been solved.[60, 61] These structures help our understanding of the mechanisms of these proteins and their superimposition with host enzymes can reveal differences that can be exploited in the design of specific and selective inhibitors. Many of the glycolytic enzymes mentioned earlier have been targeted either by analogues of their substrates or by finding possible hits through the use of computational drug design and molecular modelling studies (**Table 2**).

Inhibitor	Target	Activity	Ref.
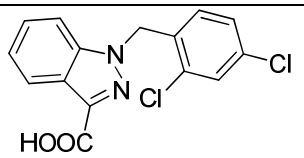 lonidamide	Hexokinase	IC_{50} = 50μM	62
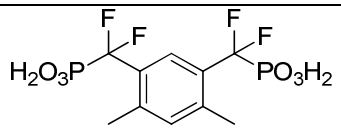 Bisphosphonate derivatives	phosphoglycerate kinase	IC_{50} = 0.84 μM	63
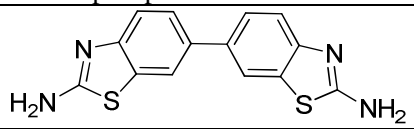	triosephosphate isomerise	IC_{50} = 50 μM	59
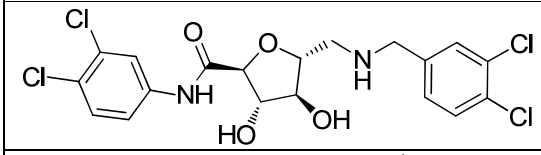	phosphofructokinase	IC_{50} = 23 μM	64
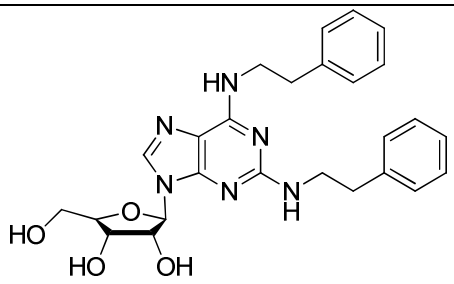 Adenosine analogues	phosphoglycerate kinase	IC_{50} = 30 μM	65

Table 2: Some glycolytic enzyme inhibitors.

1.10.5 Folate and pterin metabolism

Pterins and folates are essential biomolecules for growth in living organisms including trypanosomatids. Studies have revealed that the genes encoding enzymes for the *de novo* synthesis of folates and pterin in *Trypanosoma* are not present. Trypanosomatids require oxidized pteridines such as biopterin and folate from the host which they subsequently reduce to the active cofactors such as tetrahydrobiopterin and tetrahydrofolate by means of pteridine reductase 1 (PTR1).[66] Most of the PTR1 inhibitors have similar chemical scaffolds to dihydrofolate reductase (DHFR) inhibitors which contain either a 2,4- diaminopteridine, 2,4-

diaminoquinazoline, or 2,4-diaminopyrimidine core (**Figure 11**),[67] all of which have shown toxic effects on human cells.

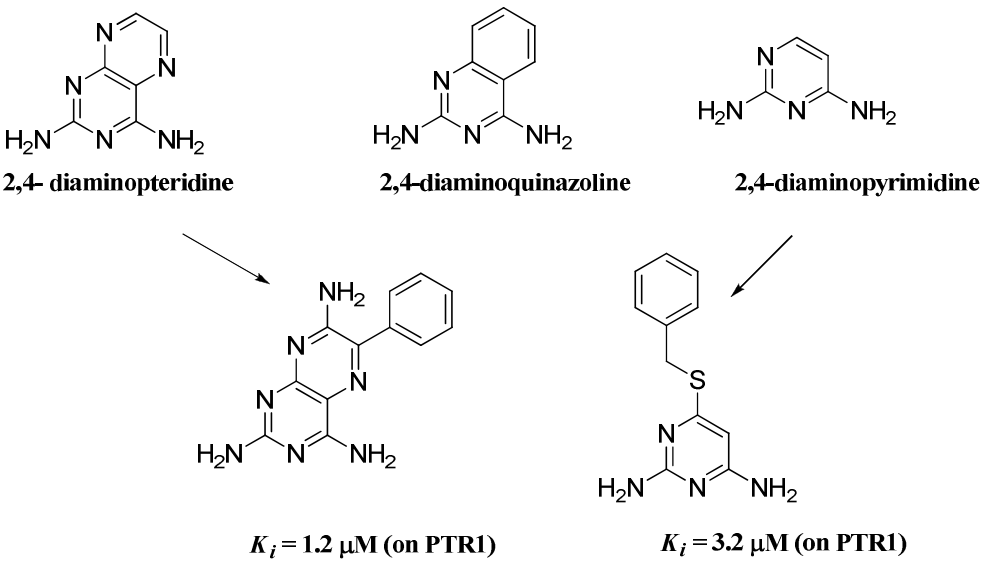

Figure 11: The main scaffolds for PTR1 and DHFR inhibitors.

Recently, 2-aminobenzothiazole and benzimidazole derivatives have been developed as PTR1 inhibitors with promising activity against *T.b. brucei*, having MICs as low as 10 μM and dissociation constants (K_i) against PTR1 in the low nanomolar region with negligible effects on human DHFR.[66] Since these compounds selectively inhibit the trypanosomal PTR1, they have potential as safe and effective anti-trypanosomal agents (**Figure 12**).

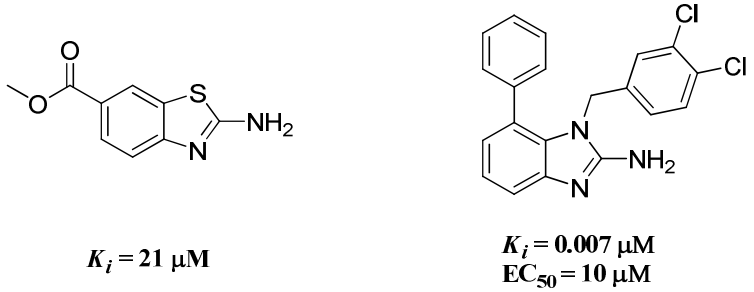

Figure 12: Some 2-aminobenzothiazole and benzimidazole PTR1 inhibitors.

1.10.6 Trypanosomal thiol metabolism

Trypanothione is a low molecular weight thiol containing compound that is unique to trypanosomes. Both bloodstream and procyclic forms *T. brucei* use trypanothione synthetase (TryS) to synthesise trypanothione from glutathione. TryS has been validated by gene knock-out studies as a possible drug target in both BSF and PCF.[30] Since TryS is absent from human cells, it is considered a promising target for the development of selective anti-trypanosomal agents.

A number of compounds have been developed and shown inhibition of TryS with potencies of at least 100 nM, and have comparable activity in whole cell assays with EC_{50}s in the low micromolar region (**Figure 13**).[68]

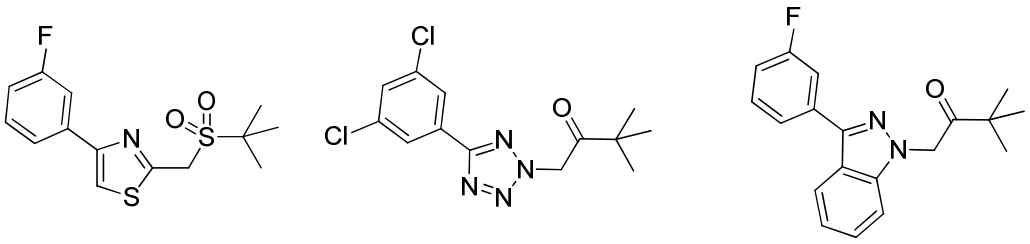

IC_{50} = 0.273 μM
EC_{50} = 27.10 μM

IC_{50} = 0.317 μM
EC_{50} = 21.2 μM

IC_{50} = 0.095 μM
EC_{50} = 8.8 μM

Figure 13: Some Trypanothione synthetase inhibitors.

1.10.7 Trypanosomal protein kinases

Protein kinases are important regulators of many cellular processes in humans such as transcriptional control, cell cycle progression and differentiation, and have received great attention as potential drug targets in many disorders such as cancer, cardiovascular diseases and Alzheimer's disease. The elucidation of the complete genomic sequence of trypanosomatids has resulted in the identification of many protein kinases that are likely to be involved in regulating cell cycle control and response to stress during their complex life cycle. Many kinase families are relatively abundant in trypanosomatids such as cyclin-dependent kinases (CDK), mitogen activated protein kinases (MAPK), glycogen synthase kinase (GSK3), and dual specificity tyrosine-phosphorylation-regulated (DYRK) kinases.[69-71] Several of

these enzymes have been found to be essential for the proliferation and viability of parasite life cycle stages. Moreover, the fact that some of the protein kinases, such as Polo-like kinases,[72] Aurora kinase [73] and Casein kinase [74] of trypanosomatids have significant sequence differences from the mammalian homologues, makes them suitable targets for new anti-trypanosomal agents.

Several compounds have been designed to target certain protein kinases such as the aurora and casein kinases in *T. brucei*, and they have shown promising activity with limited degrees of toxicity against human cells (**Figure 14**).[73, 74]

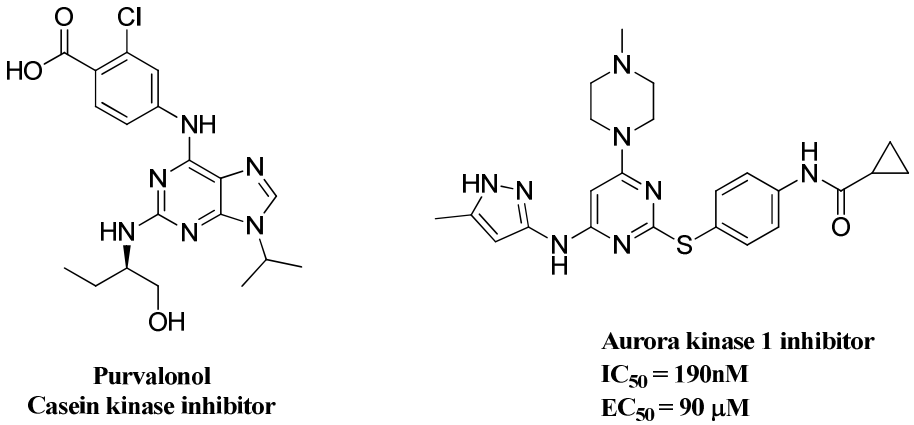

Purvalonol
Casein kinase inhibitor

Aurora kinase 1 inhibitor
IC_{50} = 190nM
EC_{50} = 90 μM

Figure 14: Some trypanosomal kinase inhibitors.

Many other metabolic pathways have been reported in the literature and are characterized as challenging targets for the development of selective anti-trypanosomal agents. Among these targets are polyamine metabolism,[75] amino acid/ protein metabolism, [76-79] and sterol biosynthesis (**Table 3**).[80]

Compound	Target	Ref.
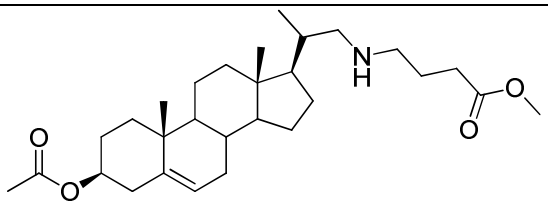	sterol biosynthesis	80
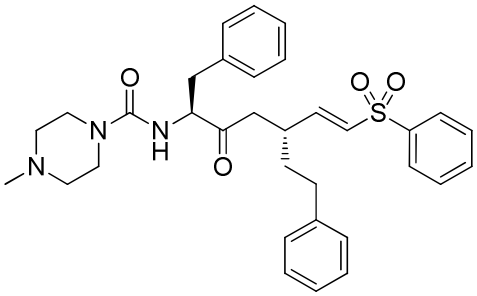	Protein biosynthesis	78
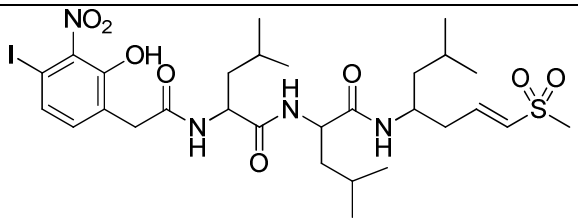	Protein biosynthesis	79

Table 3: Inhibitors of some trypanosomal metabolic processes.

1.11 Identifying new anti-trypanosomal agents by using virtual screening and computer aided drug design

It is estimated that on average it can take 14 years to bring a compound from hit identification through to an approved drug,[81] and the costs associated with this process are enormous. Since the threat of HAT and other infectious diseases are growing exponentially, immediate new solutions and novel agents are required. Medicinal chemistry has traditionally been a long process, first to discover the best hit compounds, then to perform lead optimisation.[82] Many efforts are directed to reduce the hit-to-drug timeline and increase the number of promising candidates that make the transition from discovery to clinical development. Computer aided drug design (CADD) and virtual screening (VS) have emerged as reliable, inexpensive

and fast methods for identifying hits. In contrast to experimental high throughput screening (HTS), which is based on *in vitro* screening, VS selects compounds by predicting their binding to a macromolecular target using computer programs. 3D structures of macromolecular targets achieved by crystal structure analyses or nuclear magnetic resonance spectroscopy (NMR) has provided the input for CADD in the development of new agents (**Figure 15**).

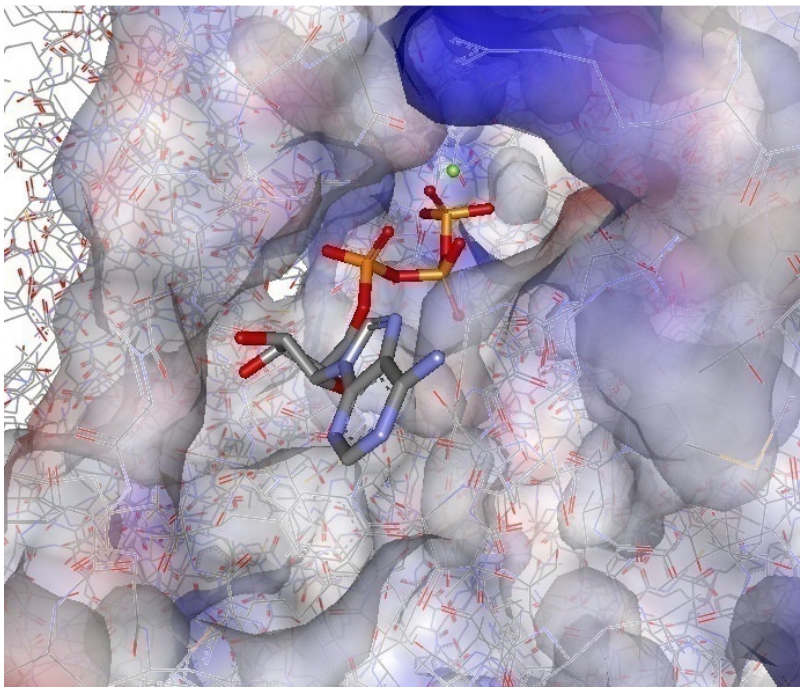

Figure 15: ATP bound to the active site of trypanosomal phosphofructokinase.

Two major types of CADD approaches are used; structure-based or ligand-based drug design. In structure-based drug design (SBDD), the information contained in the 3D crystal structure can be used in the virtual screening of large numbers of compounds. Database searching utilises docking software such as GOLD®, Autodock®, FlexX®, Glide®, Fred®, and Slide® to dock compound structures into assigned binding sites. The compounds are then rank-ordered with respect to their "goodness of fit" using scoring functions specific for each docking software.[83]

The best fit compounds can then be classified according to desired molecular properties such as Lipinski's rule of five and other physicochemical properties that

are appropriate for the target.[84] SBDD can also be used by building a pharmacophore of the binding site based upon information from the co-crystal structure of the target with its natural ligand or a known inhibitor. Chemical libraries can then be screened against the pharmacophore to find which hits are screened as described above. The hits from these two methods are then tested *in vitro* to study their actual effect on the target; VS is essentially an enrichment process for *in vitro* hit identification.

The ligand-based drug design (LBDD) approach is used when the 3D crystal structure of the enzyme is not available or is not of sufficient high resolution to be used for VS. A theoretical receptor can be built from overlaying known active compounds and the common features of the molecular interactions used to generate an interaction map or what is called a pharmacophore map (**Figure 16**).[85]

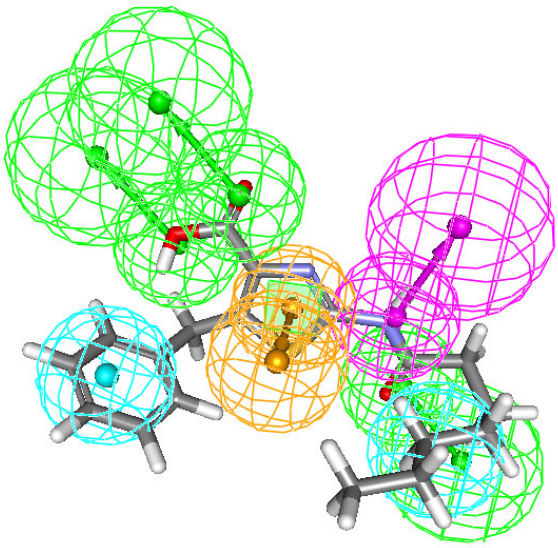

Figure 16: Screened compound mapped onto ligand pharmacophore: green spheres represent hydrogen bond acceptors, pink spheres hydrogen bond donors, orange spheres ring aromatics and cyan spheres hydrophobic groups

The pharmacophores are then used to screen large chemical databases and the hits from these VS runs can be ranked using suitable scoring functions to select for *in vitro* testing.

1.12 Aims and objectives

The aim of this work is to design and synthesise a series of novel anti-trypanosomal agents. LBDD will be used to build a common feature pharmacophore based on our in-house library of compounds that have promising activity against *T. brucei*. The pharmacophore will be used to virtually screen chemical libraries from commercial sources to find possible hits that can be used as hits for structural optimisation in attempts to improve the activity and develop potent and safe agents to combat HAT.

The objectives of this work are as follows:

- To build the best common feature pharmacophore based on an in-house chemical library with activity against *T. brucei*.
- To use this pharmacophore to screen chemical databases to find suitable hits.
- To select the best hits that have the potential to be used as possible trypanocidal candidates based on physicochemical properties as well as the ease of synthesis.
- To make structural modifications and synthesise derivatives of the hit compounds.
- To test the synthesised compounds *in vitro* against *T.b. brucei* and establish the toxicity levels on human normal cell lines.
- To use the results obtained to construct structure activity relationships (SAR) that can be used in the optimization program in order to improve activity and/or reduce toxicity.
- To identify potent compounds with low toxicity for *in vivo* testing.

Chapter Two: The rational design of the target compound

2.1 Introduction

Previous published work in our laboratory (**Appendix A**) focused on synthesising a library of compounds containing a 2-aminothiazole-4-carboxylate (**ATC**) scaffold as anti-mycobacterial agents based on the structure of TLM (**Figure 17**).[86]

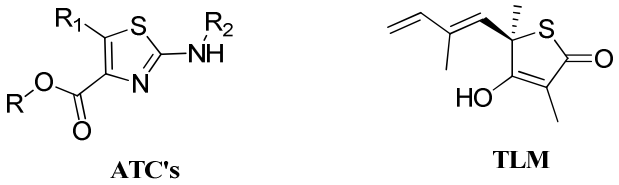

Figure 17: Chemical structure of ATC library and TLM.

TLM kills the mycobacterium by inhibiting the FAS-II system, which is an essential pathway for energy production and cell wall components in mycobacterial and many other organisms.[87] TLM has broad spectrum activity against a wide range of microorganisms such as *Escherichia coli* and *Plasmodium falciparum.*[46] Moreover, TLM had shown promising anti-trypanosomal activity with an IC_{50} of 150 µM against *T.b. brucei.*[43, 45] TLM has no effect on the human FAS-I system, which makes this compound a good hit for developing selective anti-microbial agents.

2.2 Anti-trypanosomal activity of ATC compounds

Based upon TLM having anti-trypanosomal activity, our **ATC** library was screened *in vitro* against *T.b. brucei* using the Alamar Blue® microplate assay protocol.[88] A selection of compounds was found to be active with MIC's as low as 0.78µM, and importantly, these compounds showed negligible cytotoxic effects on human fibroblast cell lines (HS27). These results indicate that the active compounds from this series may serve as hits for the development of safe and effective anti-trypanosomal agents (**Table 4**) (see **Appendix B** for the full library of **ATC** compounds assessed) .

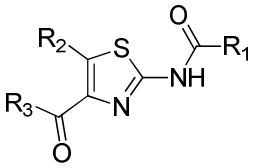

Compound	R_1	R_2	R_3	MIC (μM)	Cytotoxicity (% control)
1	CH_2CH_3	CH_3	OH	7.8	99
2	$(CH_2)_2CH_3$	CH_3	OH	31.3	99
3	phenyl	CH_3	OCH_3	12.2	96
4	phenyl	CH_3	OH	15.6	95
5	3-pyrrolyl	CH_3	OH	3.9	102
6	CH_2CH_3	benzyl	OH	15.6	114
7	cyclopropyl	benzyl	OH	15.6	108
8	cyclopropyl	phenyl	OCH_3	62.5	76
9	phenyl	3-chlorophenyl	OCH_3	15.6	87
10	phenyl	3-chlorophenyl	OH	15.6	92
11	cyclopropyl	3-chlorophenyl	OCH_3	31.3	69
12	$(CH_2)_4CH_3$	CH_3	OH	3.9	106
13	$(CH_2)_5CH_3$	CH_3	OCH_3	62.5	94
14	$(CH_2)_5CH_3$	CH_3	OH	15.6	99
15	$(CH_2)_6CH_3$	CH_3	OH	3.9	87
16	$(CH_2)_7CH_3$	CH_3	OCH_3	31.3	102
17	$(CH_2)_7CH_3$	CH_3	OH	3.9	64
18	$(CH_2)_8CH_3$	CH_3	OCH_3	31.3	117
19	$(CH_2)_8CH_3$	CH_3	OH	1.9	114
20	$(CH_2)_{10}CH_3$	CH_3	OCH_3	62.5	112
21	$(CH_2)_{10}CH_3$	CH_3	OH	1.9	120
22	4-nitrophenyl	CH_3	OH	15.6	96
23	4-methoxyphenyl	CH_3	OH	3.9	83
24	4-butoxyphenyl	CH_3	OH	3.9	78
25	$(CH_2)_5CH_3$	benzyl	OH	1.0	108
26	$(CH_2)_8CH_3$	benzyl	OCH_3	31.3	103
27	$(CH_2)_8CH_3$	benzyl	OH	0.78	106
28	benzyl	benzyl	OH	3.9	98
29	4-nitrophenyl	benzyl	OH	15.6	114
30	$(CH_2)_5CH_3$	phenyl	OCH_3	31.3	44
31	$(CH_2)_5CH_3$	phenyl	OH	3.9	105
32	$(CH_2)_8CH_3$	phenyl	OCH_3	31.3	94
33	$(CH_2)_8CH_3$	phenyl	OH	1.9	94
34	2-bromoacetyl	CH_3	OH	1.9	97
35	benzyl	3-chlorophenyl	OH	15.6	122
36	$(CH_2)_8CH_3$	3-chlorophenyl	OH	7.8	108
37	$(CH_2)_5CH_3$	3-chlorophenyl	OH	31.3	98
38	$(CH_2)_{14}CH_3$	CH_3	OH	3.9	95
39	$NH(CH)_5CH_3$	CH_3	OH	3.9	102

Table 4: MIC results for some **ATC** compounds against *T.b. brucei* with their cytotoxicity against human fibroblast cell lines (HS27).

As shown in **Table 4**, many of the compounds from this library showed good activity against *T.b. brucei*, especially compounds with a carboxylic acid moiety in position-4 and a hydrophobic amide side chain in position-2 of the thiazole ring. Although some of these compounds have MIC's ranging from 15.6 to as low as 0.78μM, the biological target for these compounds in the Trypanosoma is not known, which makes it difficult to fully characterize the mode of action and the suitable structural modifications that should be adopted to improve the activity.

2.3 Trypanosomal fatty acid synthesis as a possible target for ATC compounds

The **ATC** library was originally designed to target the elongation step (the β-ketoacyl ACP-synthase enzymes) in the FAS-II pathway of the mycobacterium,[89] which suggested that these compounds could target trypanosomal fatty acid synthesis. Furthermore, the library was based on TLM, which is active against the trypanosomal fatty acid elongase system. Two of the most active compounds (**6** and **27**) were tested for fatty acid synthesis inhibition in the trypanosome at the University of St. Andrews using the Bligh and Dyer method for lipid extraction from the trypanosomal cell after treating the cells with the test compounds,[90] followed by Electron Spray-Mass Spectroscopy and Gas Chromatography-Mass Spectroscopy (ES-MS and GC-MS) analysis. The results revealed that the tested compounds showed no inhibitory effect on lipid biosynthesis, and suggests that the target for the **ATC**s is not trypanosomal lipid biosynthesis.

In the absence of a defined molecular target for the **ATC**s, the LBDD approach was used as the basis for hit optimisation.

2.4 Ligand-based drug design of the target compounds

LBDD is based on building a pharmacophore hypothesis for a chemical library that has a wide range of activity against a specific disease target. In summary, this is normally achieved by selecting 10-15 compounds (training set) from that library that would have maximal structural diversity along with the best activities.[91] The resultant pharmacophores require validation against the rest the library to test their

selectivity and degree of activity prediction. The most selective pharmacophore is then used to screen chemical databases to find new hits which can be ranked and refined using different descriptors that take into consideration scoring functions as well as the ease of synthesis and derivatisation, pharmacokinetic properties and Lipinski's rule of five.[84] The top-ranked hits are then tested *in vitro* against the target, and the most active hits analysed and considered for possible structural modification to optimise activity.

2.4.1 Conformation generation of the test set

The Accelrys® Discovery Studio package was used in the generation of the pharmacophores for the **ATC** library; the full procedure is in **Chapter Five**. A brief overview of the theory is as follows; 10 compounds was selected as a training set from the most active compounds using an MIC of 15.6 μM as the cut-off value for activity. The conformation generation protocol was used to generate the most stable conformers from the training set compounds. Prior to pharmacophore generation, the key features selected for consideration during the hypothesis generation were: hydrogen bond donor, hydrogen bond acceptor, negative ionisable and hydrophobic and aromatic ring. Two important parameters were set prior to the protocol run; the first, the Principal Number parameter, was set 2 for **24**, **27** and **28** and assigns these three compounds as reference ligands. A Principal of 1 was assigned for the rest of the training set, indicating that these ligands were considered moderately active when generating the hypothesis. The other important parameter is the Maximum Omitted Features (MaxOmitFeat), which specifies how many features for each ligand can be missed during the generation of the hypothesis. For the training set, this parameter was set to 1, which means all the features except one must map the generated pharmacophore (**Table 5**).

Compound	MIC (μM)	Principal	MaxOmitFeat
1	7.8	1	1
35	15.6	1	1
22	15.6	1	1
23	3.9	1	1
24	3.9	2	1
27	0.78	2	1
28	3.9	2	1
12	3.9	1	1
36	7.8	1	1
34	1.9	1	1

Table 5: The ATC training set for the pharmacophore generation protocol.

2.4.2 Common features pharmacophore generation

For the common features pharmacophore generation, the HipHop® protocol was run for the training set conformers and the best ten hypotheses were obtained (**Figure 18**). The minimum number of features in each hypothesis was set to four and the maximum set to ten. The ten generated pharmacophores were then inspected to rank them according to their correlation with the trypanosomal MIC values and whether their coverage of features was representative of almost all the compounds in the training set. The ligand pharmacophore mapping protocol was used to screen the test set, which contains all **ATC** compounds apart from the training set against each hypothesis separately, and the selectivity of each pharmacophore was evaluated by calculating two ratios; the first was the % yield of actives (% of the active hits to the total number of hits), and the second was the % ratio of actives (% of the active hits to the total number of actives in the test set). To calculate these ratios, an MIC cut-off value of 7.8 μM was chosen.

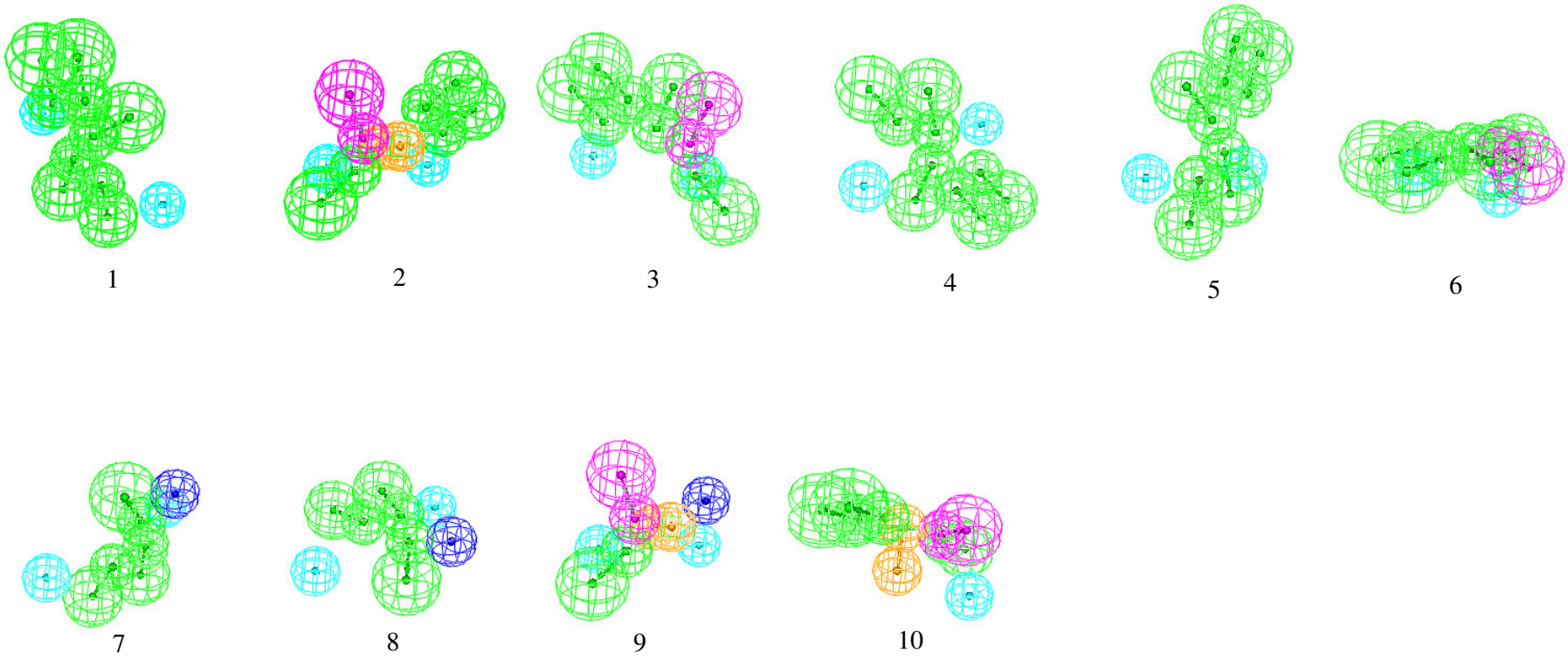

Figure 18: The ten pharmacophore hypotheses obtained for the ATC training set, the green spheres represent hydrogen bond acceptors, pink represents hydrogen bond donors, blue represents negative ionisable groups, orange represents ring aromatics and cyan represents hydrophobic groups.

The best hypothesis found was pharmacophore one, with six features that fall into two types; hydrogen bond acceptors and hydrophobics. However, this hypothesis was not selective enough to identify only the most active compounds, because it mapped 9 inactive compounds out of the 36 hits. To improve the selectivity of this hypothesis and minimise the possibility of false positives, the HipHopRefine® protocol was used. This algorithm identifies areas of space that are occupied by inactive ligands and then places excluded volumes in these regions to reduce the number of false positives that can map onto the pharmacophore.

In this protocol, a selection of inactive **ATC**s that have most of the common features of the pharmacophore in addition to extra features such as longer aliphatic amides or bulkier groups at position-5 of the thiazole ring were selected in order to add the exclusion volumes and prevent compounds with steric clashes from mapping to this new hypothesis. Unfortunately, no excluded volumes for the pharmacophore were generated, possibly because the structures of inactive compounds were very similar to the active ones, and the HipHopRefine® protocol was unable to discern these subtle differences.

Consequently, manual manipulation was required to add two additional features to the pharmacophore. The first was a hydrogen bond donor that fits to the amino group of the amide, and was selected because all active compounds have a 2-amido group which might play a role in activity. The second was an additional hydrophobic group proximal to the one mapped onto the 2-substituent, because all active compounds have a large and extended hydrophobic group in this position. The new pharmacophore contains five hydrogen bond donors, one hydrogen bond acceptor and three hydrophobic groups, giving a total of 9 pharmacophore features (**Figure 19**).

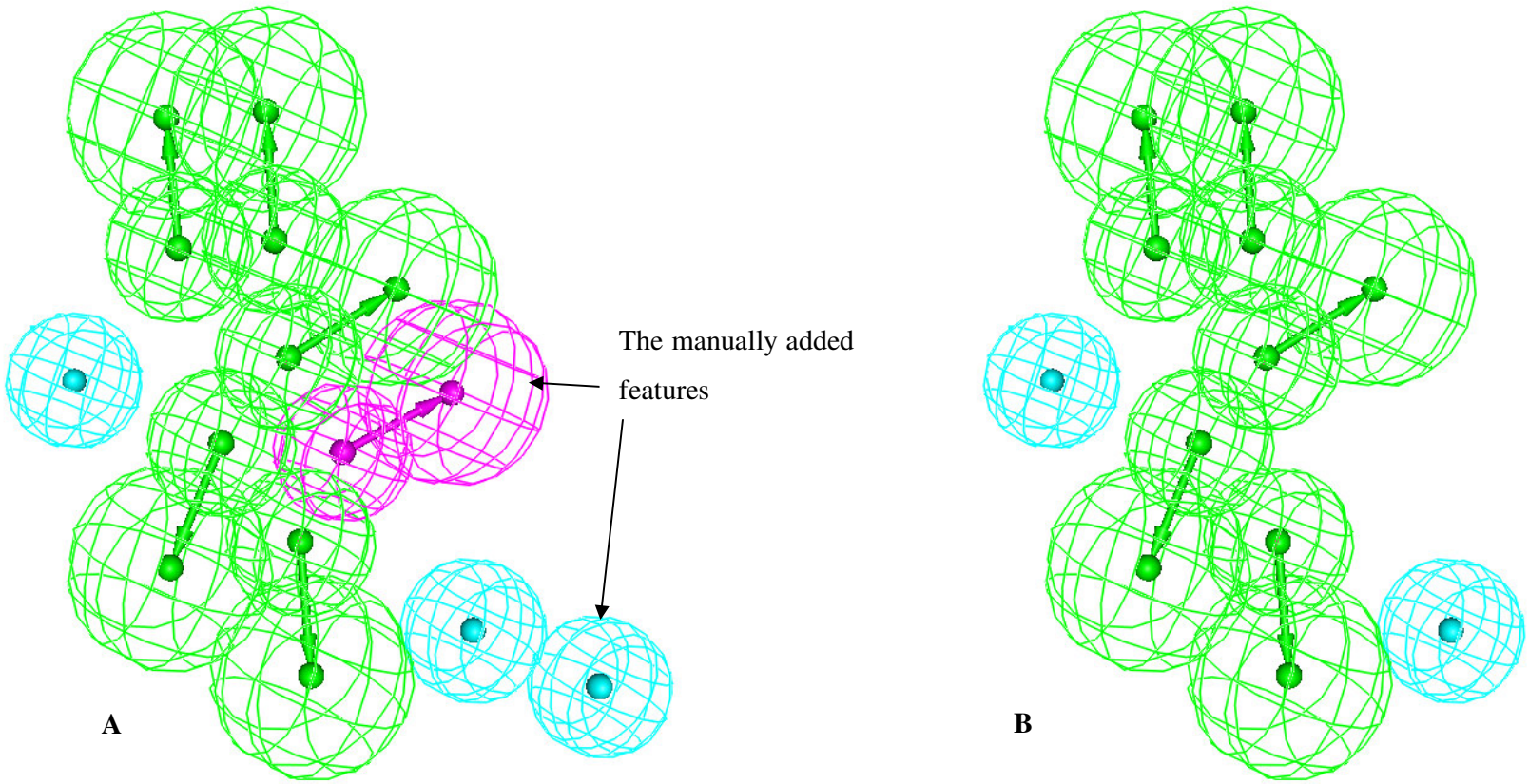

Figure 19: The new pharmacophore (A) compared to the original pharmacophore 1 (B): green spheres for hydrogen bond acceptors, pink spheres for hydrogen bond donors and cyan spheres for hydrophobic groups.

2.4.3 Validation of the modified pharmacophore hypothesis

To establish how the compounds from training set fitted to the new pharmacophore, compound **27** was superimposed onto the new hypothesis and the match is very clear; the additional hydrogen bond donor sphere is occupied by the amino group of the amide moiety and the new hydrophobic group was occupied by the extended aliphatic amide side chain (**Figure 20**).

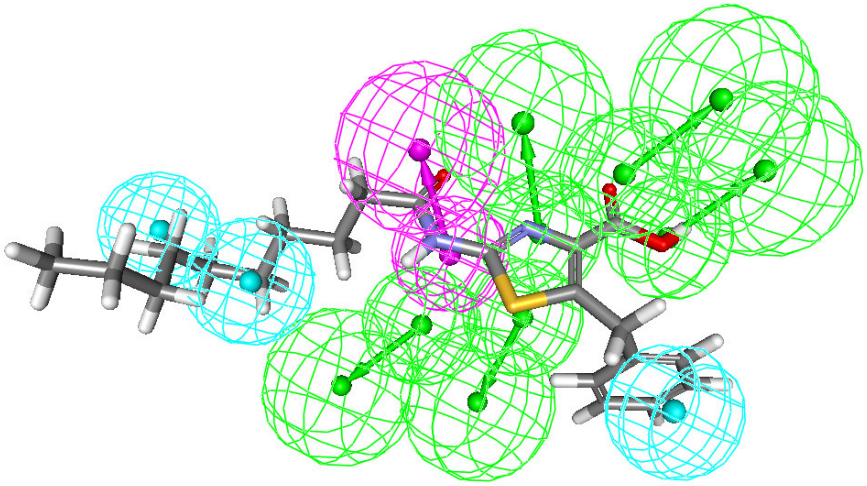

Figure 20: Compound **27** (sticks) superimposed on the new pharmacophore.

To test the selectivity of the modified pharmacophore, the ligand pharmacophore mapping protocol previously mentioned was applied to the test set; 10 hits out of 132 compounds mapped with fit values ranging from 5 to 8.2 (the fit value represents how many features from the pharmacophore were mapped for each compound) (**Table 6**).

Compound	MIC (μM)	Fit-value
25	1	8.18978
31	3.9	6.64699
37	31.3	6.53148
33	1.9	6.34854
21	1.9	5.9433
19	1.9	5.78792
38	1.56	5.77632
15	3.9	5.6642
17	3.9	5.62249
39	3.9	4.995

Table 6: The fit values of the mapped active **ATC** compounds.

Although the number of retrieved hits appears low, 9 out of 10 have activity below the assigned cut-off value of 7.8μM, with excellent mapping to the pharmacophore (**Figure 21**) and only one false positive hit (compound **37** with an MIC of 31.3μM) was identified, suggesting that this pharmacophore has sufficient selectivity to be used for compound identification during a virtual screening process.

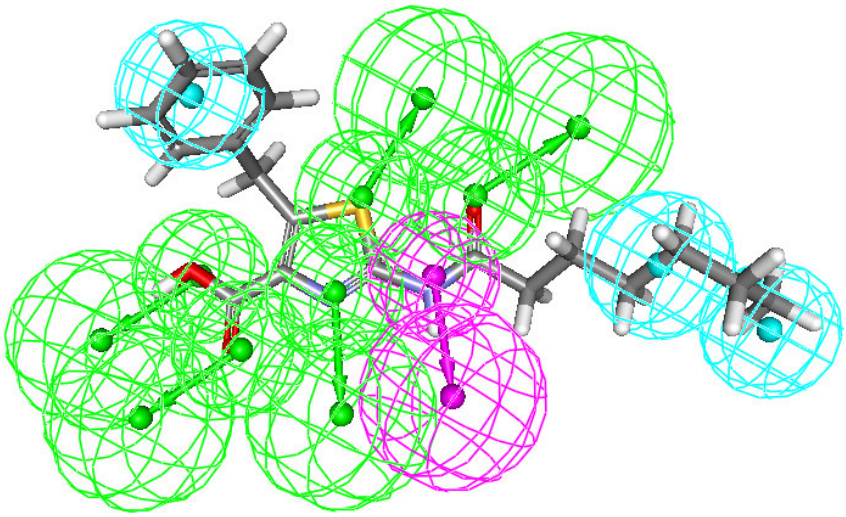

Figure 21: Compound **25** mapped to the **ATC** pharmacophore hypothesis.

2.4.4 Search for new hits from commercial chemical databases

In order to find new hits with new chemical scaffolds that fit the **ATC** pharmacophore, commercially available chemical libraries (Maybridge) containing 52,000 compounds were screened using the ligand pharmacophore mapping protocol. 923 hits were obtained from the Maybridge library and after filtering the structures according to fit value (more than or equal to 4.5), molecular weight (less than 500 Dalton), synthetic accessibility and Lipinski's rule of five; 150 compounds with good structural diversity were identified, and some are shown in **Table 7**.

Compound structure	Code	Fit value
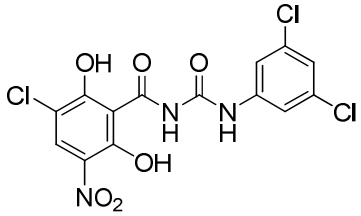	BTB07716 (**40**)	7.43475
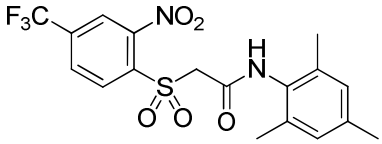	BTB05827 (**41**)	6.63916
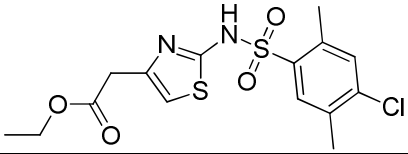	BTB06224 (**42**)	6.88148
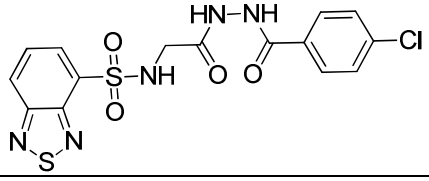	KM06430 (**43**)	6.44415
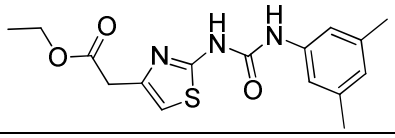	HTS08074 (**44**)	6.38415
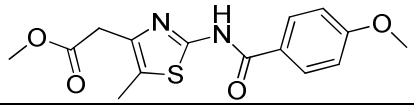	HTS00862 (**45**)	6.32124
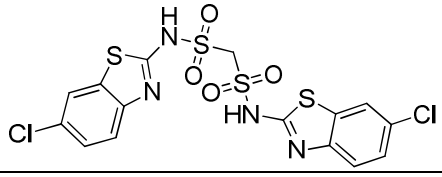	BTB06061 (**46**)	5.87525
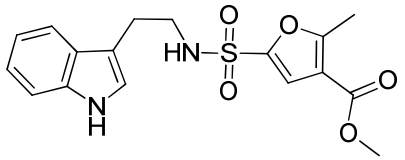	SCR00880 (**47**)	4.70901
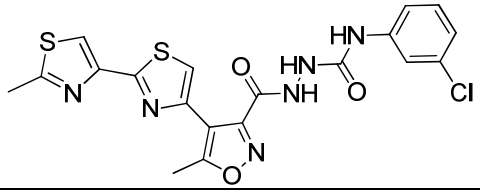	SPB03717 (**48**)	5.7415

Table 7: Some hits from ligand pharmacophore mapping of the Maybridge library.

Compound structure	Code	Fit value
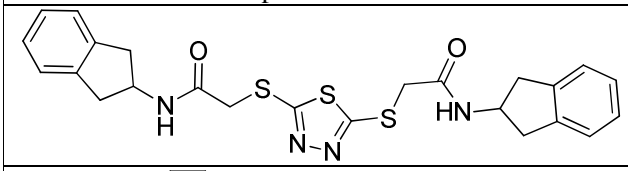	KM10557 (**49**)	4.75667
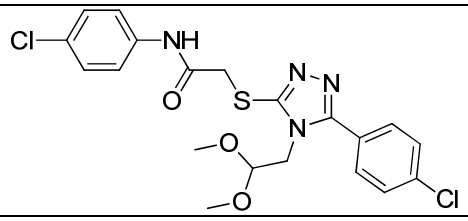	SPB04886 (**50**)	5.91562

Table 7: continued...

To study the activity of these compounds against the parasite, several compounds were selected according to their chemical accessibility, ease of synthesis, and druggability. Some moderate activities were obtained for several compounds with MIC's in the high micromolar range (**Table 8**).

Compound	MIC (µM)	Cytotoxicity on PNT2A % control
46	250	88.18
45	125	95.09
44	31.25	115.18
47	62.50	77.33
49	>250	85.32
40	>250	83.12
43	>250	91.30

Table 8: MICs of the hits obtained from the pharmacophore model against *T.b. brucei* and their toxicity on human prostatic cell lines (PNT2A).

2.5 Rational design of the target compounds

Based on the results obtained from screening the commercial chemical libraries on the assigned pharmacophore of the **ATC** compounds, and the promising anti-trypanosomal activity of some of the hits, their structures were assessed for their potential for library design and synthesis. Moreover, the fact that most of the active compounds from this screening did not show toxic effects on human normal cell lines, suggests that these compounds could be developed as active anti-trypanosomal agents.

2.5.1 Selection of the hit compounds

Three compounds were selected from the most active hits to be used in the design of new anti-trypanosomal agents (**Table 9**). The selection was based on group of criteria; the first one was meeting the Lipinski's rule of five,[84] because an orally available drug is required to treat HAT. The second was their fit value with the pharmacophore hypothesis, and the third was the ease of synthesis and derivatisation so that a comprehensive SAR profile could be established to direct hit to lead optimisation.

Compound	No. of H-bond donors	No. of H-bond acceptors	Mwt	cLogP	Fit value
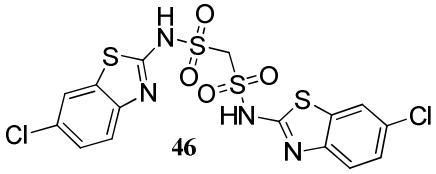 **46**	2	8	509.438	3.43	5.87525
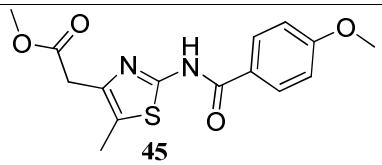 **45**	1	6	320.367	1.71	6.32124
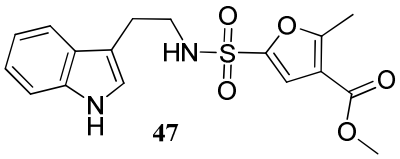 **47**	2	7	362.404	2.45	4.70901

Table 9: The selected lead compounds and their predicted properties and fit value to the **ATC** pharmacophore.

2.5.2 Design of the target compounds

The three compounds shown in **Table 9** were used as templates to design the target compounds. These compounds contain most of the structural features necessary for activity, including the main ring scaffold, the ester linkage and either the sulfonamide or the amide moieties (**Figure 22**).

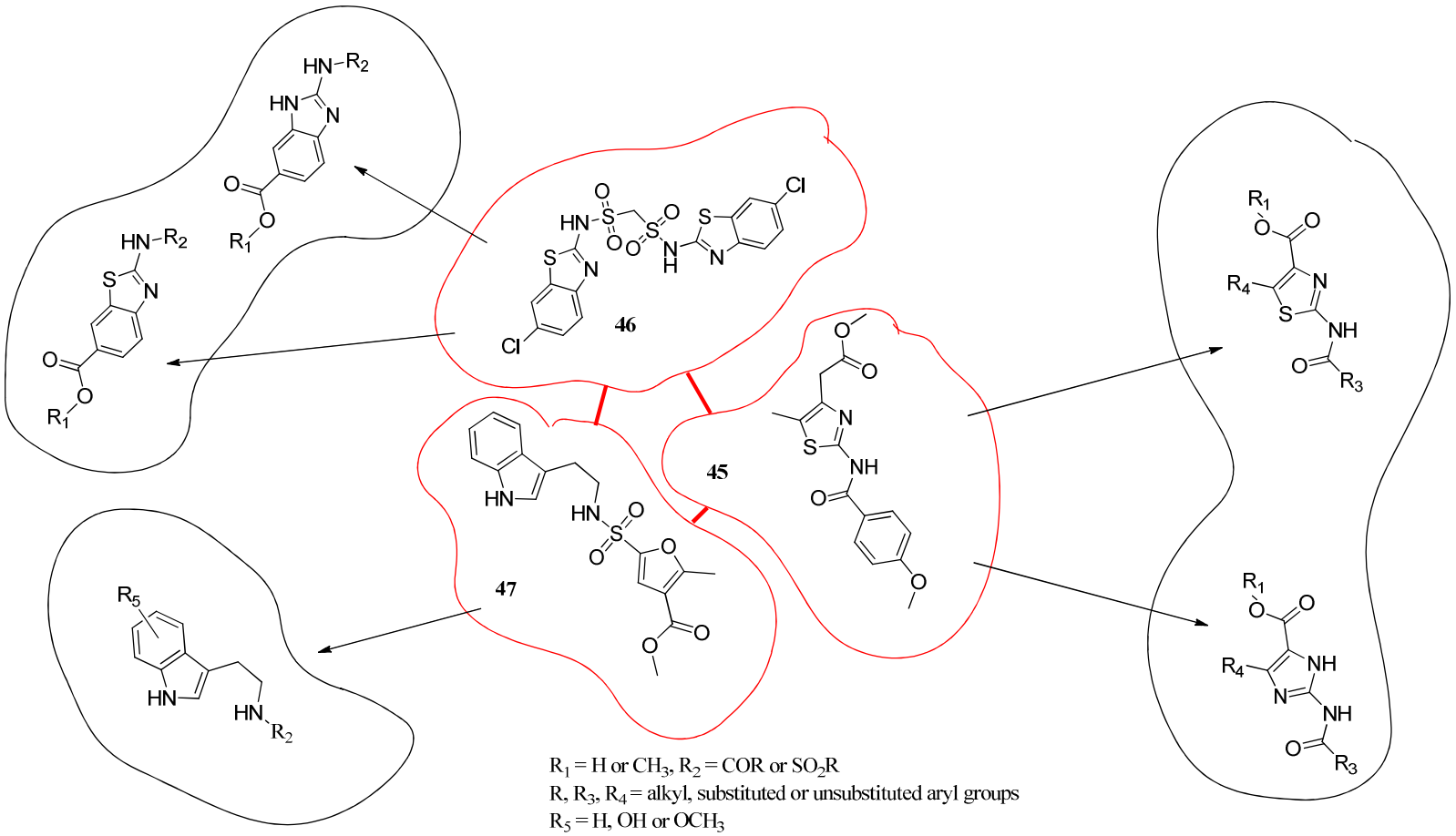

Figure 22: The design of the five libraries based on the structure of the three hits from the pharmacophore study.

To reduce the hydrophobic nature and the bulkiness of compound **46**, the two benzothiazole systems were replaced with either one benzothiazole or one benzimidazole ring. The benzimidazole is used to increase the number of hydrogen bond donors in the molecule, which might improve the interaction with the target. Another modification was the addition of a carbonyl moiety in place of the chlorine atom because the pharmacophore has a hydrogen bond acceptor pocket which a carboxylic acid or ester moiety could occupy. For compounds **45** and **47**, minor modifications have been made since they both have the amide and the ester groups attached to the core scaffold. In the analogues of **45**, two modifications were applied; the first was to directly attach the ester group to the thiazole ring rather than having a one carbon atom linker to simplify and enable rapid library generation. The second was to use an imidazole ring as a ring isostere for the thiazole to study whether other heterocyclic rings with different hydrogen bonding characteristics could retain or improve activity.

For the design of analogues of **47**, the effect of varying the sulfonamide substituents of the indole was investigated. Aromatic groups such as thiophene, thiazole, imidazole and phenyl linked *via* a sulfonamide and carboxamide group were assessed for their effect on activity. Indole ring substituents were also assessed. Cyclisation to the more rigid 1,2,3,4-tetrahydro-β-carboline derivatives (**Figure 23**) were performed to assess whether rotatable bonds were essential for activity.

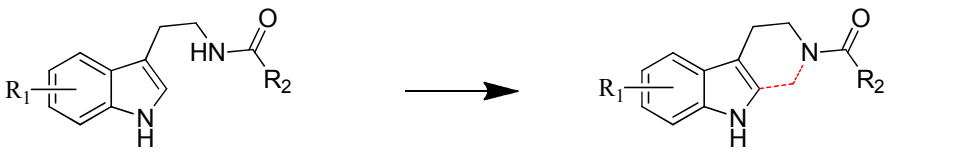

Indole derivatives 1,2,3,4-tetrahydro-β-carboline derivatives

Figure 23: The general structure of the proposed 1,2,3,4-tetrahydro-β-carboline derivatives.

Chapter Three: Biological evaluation of the target compounds

3.1 Biological screening tests

3.1.1 *T.b. brucei* testing

The blood stream form (BSF) of *T.b. brucei* was used as the test species in the assay. Although this species is not pathogenic to humans, it is structurally and morphologically similar to both the *gambiense* and *rhodesience* subspecies.[92] The only difference between *brucei* and both gambiense and *rhodesience* is the absence of the human serum protein resistance which means the parasite will be rapidly cleared out by the human immune system. [93] The *in vitro* assay described by Raz *et al*. was used for screening compounds for anti-trypanosomal activity.[88] In this method, the indicator Alamar Blue® was used to provide reproducible and quantitative data. Alamar Blue® (resazurin) is a non-fluorescent colorimetric dye which, upon reduction by living cells, turns to a fluorescent pink colour (**Figure 24**).

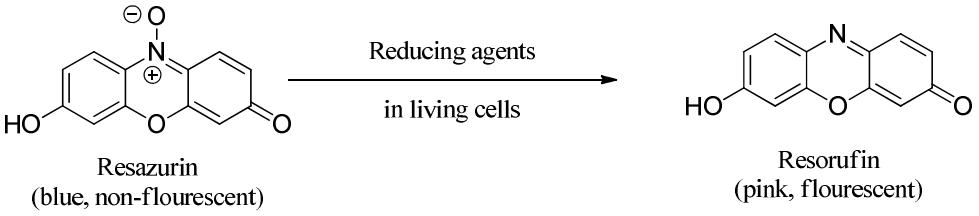

Figure 24: Reduction of Alamar Blue (Resazurin) by living cells to the fluorescent pink Resorufin.[94]

The reduction of Alamar Blue® in mammalian cells depends on the activity of unspecific dehydrogenases which are involved in the respiratory chain in the mitochondrion. In contrast to mammalian cells, BSF *Trypanosoma* lack a functional mitochondrion and rely on the glycolytic pathway for their energy production.[95] The reduction of Alamar Blue® is directly proportional to the number of viable cells in the sample and the intensity can be either measured by ultra-violet (UV) spectroscopy or a fluorescent reader.

3.1.2 Human cell line toxicity screening

Cytotoxicity against human normal prostatic cells (PNT2A) was determined using the well established Alamar blue microplate method. This was conducted to determine the toxicity levels of the synthesised compounds. The procedure is described in **Section 5.4.2**.

3.2 Anti-trypanosomal activities of the target compounds

3.2.1 Anti-trypanosomal activity of 2-aminobenzo[*d*]thiazole-6-carboxylate and 2-amino-1*H*-benzo[*d*]imidazole-5-carboxylate derivatives

The first hit to be derivatized was compound **46**. Since this compound has two benzothiazole rings bearing two chlorine atoms, it is relatively lipophilic with a high logP and molecular weight of more than 500 which makes this compound unsuitable as a drug candidate. Moreover, this compound does not fit the **ATC** pharmacophore very well; the algorithms mapped the two benzothiazole moieties to the hydrophobic regions of the pharmacophore, but the two sulfonamido groups did not adapt to the hydrogen bond acceptor pocket (**Figure 25**).

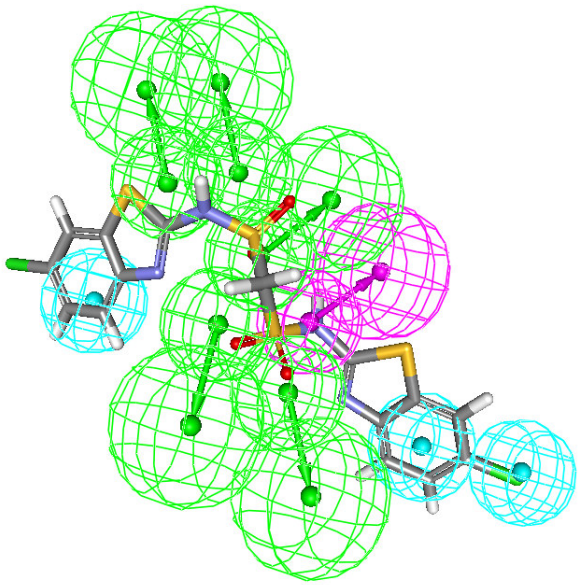

Figure 25: Compound **46** in the **ATC** pharmacophore: green spheres represent hydrogen bond acceptors, pink represents hydrogen bond donor and cyan represents hydrophobic groups.

To meet the essential features in the pharmacophore, a group of compounds was synthesised in which two functionalities were attached to the benzothiazole ring; an amide group at position-2 to map onto the hydrogen bond donor, and a carbonyl moiety at position-6 to interact with the hydrogen bond acceptor region (**Figure 26**).

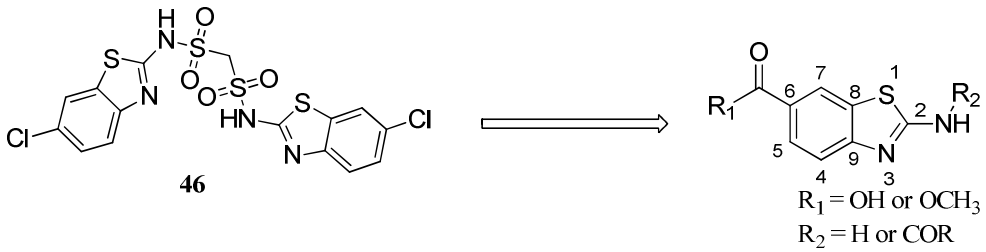

Figure 26: The 2-aminobenzo[*d*]thiazole-6-carboxylate scaffold based on compound **46**.

Aliphatic amide groups were first used in these compounds because the most active compounds from **ATC** library were those with long aliphatic chains in position-2. A group of compounds was synthesised with short, intermediate and long aliphatic amide side chains, with either an ester or carboxylic acid moieties at position-6 to occupy the hydrogen bond acceptor pocket of the pharmacophore. The compounds were screened for anti-trypanosomal activity and the cytotoxicity against human prostatic cell lines (PNT2A) was determined. The results are shown in **Table 10.**

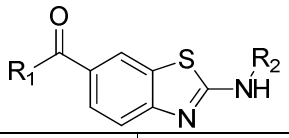

Compound	R_1	R_2	MIC (μM)*	Cytotoxicity % control	clogP
51	OCH_3	H	> 250	N.T	1.87
52	OH	H	> 250	N.T	1.84
53	OCH_3	$-CO(CH_2)_8CH_3$	> 250	N.T	6.27
54	OH	$-CO(CH_2)_8CH_3$	15.6	114.5	6.24
55	OCH_3	$-CO(CH_2)_4CH_3$	31.25	94.7	4.15
56	OH	$-CO(CH_2)_4CH_3$	15.63	103.7	4.12
57	OCH_3	$-COCH_3$	> 250	N.T	2.06

Table 10: Anti-trypanosomal activity and cytotoxicity results of aliphatic amide derivatives of 2-aminobenzo[*d*]thiazole-6-carboxylate: N.T = not tested.

* These values are the average of the dublicate results, applied for all MIC values in this work.

As expected, compounds with no amide side chain did not show any activity. The addition of an amido aliphatic side chain had mixed effects, and depended on whether the 6-substituent was the free acid or the methyl ester. The hexanoyl (**56**) and decanoyl (**54**) amides had MIC values of 15.6 μM as the free acids, but where the methyl ester of **55** with the shorter six carbon amide side chain had lower activity, the ten carbon amide ester was inactive. This trend in activity is similar to that observed for the **ATC** library where the longer the aliphatic chain, the better the activity, particularly as the free acids. To study the effect of replacing the amide group with a sulfonamide, two compounds with an aliphatic sulfonamide group were synthesised (**Table 11**). The use of sulfonamide functionality was to increase the capacity for hydrogen bonding with the target through the presence of two oxygen atoms as hydrogen bond acceptors.

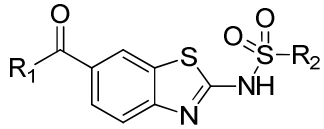

Compound	R_1	R_2	MIC (μM)	Cytotoxicity % control	clogP
58	OCH_3	CH_3	>250	N.T	1.59
59	OCH_3	$(CH_2)_3CH_3$	3.9	83.3	3.18

Table 11: Anti-trypanosomal activity and cytotoxicity results of aliphatic sulfonamide derivatives of 2-aminobenzo[*d*]thiazole-6-carboxylate.

Compound **59** with the longer aliphatic chain showed good activity with an MIC value of 3.9 μM which is better than the corresponding compounds with an aliphatic amide present. Unfortunately, the carboxylic acid equivalents of these compounds were not tractable for reasons that will be discussed in **Chapter Four**, so it is not possible to compare their activities with the ester derivatives.

It appeared that our strategy of replacing the two benzothiazoles in **46** with the smaller, less hydrophobic 2-aminobenzo[*d*]thiazole-6-carboxylate scaffold improved the anti-trypanosomal activity by more than 32 fold. As expected, compounds with no hydrophobic groups at position-2 did not show any activity, and highlighted the importance of a substituent for activity.

Since compounds with long aliphatic chains tend to be highly lipophilic as indicated from the clogP values in **Table 10**, which is an undesirable property in any drug candidate when greater than 5, a series of compounds with lower clogP's were synthesised using both aromatic amide and sulfonamide groups. Different substituents were added to the aryl group to explore the effect of such groups on activity (**Table 12)**.

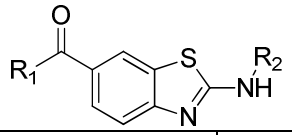

Compound	R_1	R_2	MIC (μM)	Cytotoxicity % control	clogP
60	OCH_3	-CO(phenyl)	>250	N.T	3.52
61	OCH_3	-CO(4-nitrophenyl)	>250	N.T	3.30
62	OCH_3	-CO(4-methoxyphenyl)	>250	N.T	3.60
63	OCH_3	-CO(4-chlorophenyl)	>250	N.T	4.20
64	OCH_3	$-SO_2$(phenyl)	125	110.5	3.22
65	OH	$-SO_2$(phenyl)	>250	N.T	3.21
66	OCH_3	$-SO_2$(4-methoxyphenyl)	125	116.3	3.32
67	OCH_3	$-SO_2$(4-nitrophenyl)	31.25	105.9	3.13
68	OCH_3	$-SO_2$(4-chlorophenyl)	125	108.4	3.97
69	OCH_3	$-SO_2$(4-methylphenyl)	125	103.7	3.72

Table 12: Anti-trypanosomal activity and cytotoxicity results of aromatic amide and sulfonamide derivatives of 2-aminobenzo[*d*]thiazole-6-carboxylate.

No improvement in activity was observed by replacing the aliphatic amide and sulfonamide with aromatic substituents although compound **67** showed moderate activity with an MIC of 31.25 μM.

To further explore the 2-aminobenzo[*d*]thiazole-6-carboxylate scaffold and study the importance of the benzothiazole heterocycle for activity, it was replaced with a benzimidazole ring. This should reduce the lipophilicity of the compounds as well as increase its ability to form hydrogen bonds. In the new scaffold, the amide, sulfonamide and the carboxylate moieties were conserved since they had proved to be important for activity. Additionally, compounds having a phenyl ketone at position-5 were prepared to determine whether a bulky aromatic group at this position was tolerated. The 2-amino-1*H*-benzo[*d*]imidazole-5-carboxylate derivatives in this series with their associated activities are shown in **Table 13**.

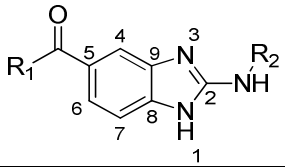

Compound	R_1	R_2	MIC (μM)	Cytotoxicity (% control)	clogP
70	OCH_3	H	>250	N.T	1.38
71	OC_2H_5	H	>250	N.T	1.91
72	phenyl	H	62.5	87.2	2.63
73	OH	H	>250	N.T	1.32
74	OC_2H_5	$-COCH_3$	>250	N.T	2.07
75	OCH_3	$-COCH_3$	125	44.5	1.54
76	phenyl	$-COCH_3$	125	68.6	2.80
77	phenyl	-CO(phenyl)	15.6	55.8	4.28
78	OCH_3	$-CO(CH_2)_8CH_3$	125	97.1	5.77
79	OH	$-CO(CH_2)_8CH_3$	>250	N.T	5.72
80	OCH_3	$-COCH_2CH_3$	>250	N.T	2.07
81	OH	$-COCH_2CH_3$	>250	N.T	2.02
82	OCH_3	-CO(benzyl)	200	N.T	3.08
83	OH	-CO(benzyl)	>250	N.T	3.03
84	OCH_3	$-CO(CH_2)_4CH_3$	25	79.1	3.66
85	OH	$-CO(CH_2)_4CH_3$	>250	N.T	3.61
86	phenyl	$-CO(CH_2)_8CH_3$	>250	N.T	7.03
87	OCH_3	-CO(phenyl)	31.3	69.6	3.04
88	OH	-CO(phenyl)	>250	N.T	2.98
89	phenyl	-CO(4-chlorophenyl)	62.5	13.5	5.02
90	phenyl	$-CO(CH_2)_5CH_3$	>250	N.T	5.44
91	phenyl	-CO(4-methylphenyl)	15.6	65.2	4.78
92	OCH_3	-CO(4-methylphenyl)	>250	N.T	3.53
93	phenyl	-CO(4-methoxyphenyl)	7.8	23.3	4.38
94	phenyl	-CO(4-nitrophenyl)	7.8	79.0	4.11
95	OCH_3	-CO(4-nitrophenyl)	15.6	73.2	2.84
96	OCH_3	-CO(4-methoxyphenyl)	62.5	90.8	3.13
97	OC_2H_5	$-SO_2$(phenyl)	25	70.0	3.24
98	OCH_3	$-SO_2$(4-chlorophenyl)	15.6	84.6	3.55
99	OCH_3	$-SO_2$(4-methoxyphenyl)	31.3	47.9	2.86
100	phenyl	$-SO_2$(phenyl)	31.3	40.4	3.99
101	phenyl	$-SO_2$(4-nitrophenyl)	7.8	2.7	3.96
102	OCH_3	$-SO_2$(3-dimethylaminonaphthyl)	31.25	80.8	4.24
103	OCH_3	$-SO_2$(4-methylphenyl)	31.25	86.7	3.24
104	phenyl	$-SO_2$(4-methylphenyl)	15.6	48.4	4.49
105	OCH_3	$-SO_2$(butyl)	62.5	95.8	2.71
106	phenyl	$-SO_2$(3-dimethylaminonaphthyl)	15.6	53.0	5.50
107	OCH_3	$-SO_2$(4-nitrophenyl)	15.6	2.9	2.71
108	OCH_3	$-SO_2$(3-nitrophenyl)	31.3	77.3	2.71

Table 13: Anti-trypanosomal activity and cytotoxicity results of the amide and sulfonamide derivatives of 2-amino-1*H*-benzo[*d*]imidazole-5-carboxylate.

It is clear from the assay data for the 2-amino-1*H*-benzo[*d*]imidazole-5-carboxylate series that both the aromatic amide and sulfonamide derivatives showed better activity than the compounds containing aliphatic amides, a trend which is different to 2-aminobenzo[*d*]thiazole-6-carboxylate series. One possible explanation for this difference could be that the benzimidazole ring, through its ability to donate a hydrogen bond, leads to a change in the orientation of the substituents relative to the biological target. Alternatively, the benzimidazole nucleus more closely resembles a purine, and could be a better substrate for transport into the parasite.

The compounds containing the phenyl ketone at position-5 showed improved activity over the ester and carboxylic derivatives which suggests a bulky group in this position promotes activity. Unfortunately, this series consistently showed greater toxicity in the human cell line, and negated further exploration.

Overall, replacement of the benzothiazole ring with a benzimidazole heterocycle improved activity against *T.b. brucei* furnishing MIC's as low as 7.8 μM, but with the disadvantage of introducing adverse effects in a human cell line.

3.2.2 Anti-trypanosomal activity of 2-aminothiazole-5-carboxylate derivatives

Another hit that was investigated further was compound **45**, which was active against *T.b. brucei* (MIC of 125μM). Upon studying the pharmacophore map of this compound in the **ATC** pharmacophore, it was evident that it matches some of the desired pharmacophoric features (**Figure 27**). For example, the 4-methoxybenzamido substituent occupied the two hydrophobic pockets of the pharmacophore, the methyl group at position-5 mapped onto the other hydrophobic pocket, and both the ester and the amino group of the amide mapped onto the hydrogen bond acceptor and donor regions, respectively.

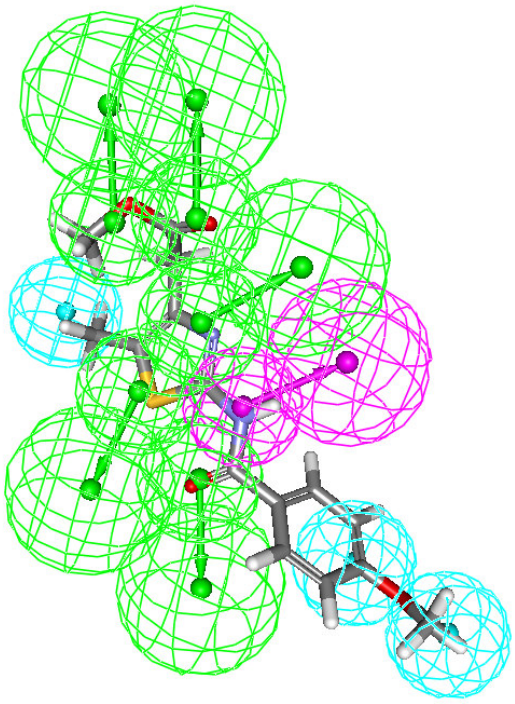

Figure 27: Compound **45** in **ATC** pharmacophore model.

This similarity between **45** and the **ATC** series suggested that a more thorough investigation of the thiazole scaffold was required.

The first batch of compounds contained the decanamido group found in the most active **ATC** compound, **27**, with diversity introduced at position-5 and ester and acid substituents at position-4 (**Figure 28**).

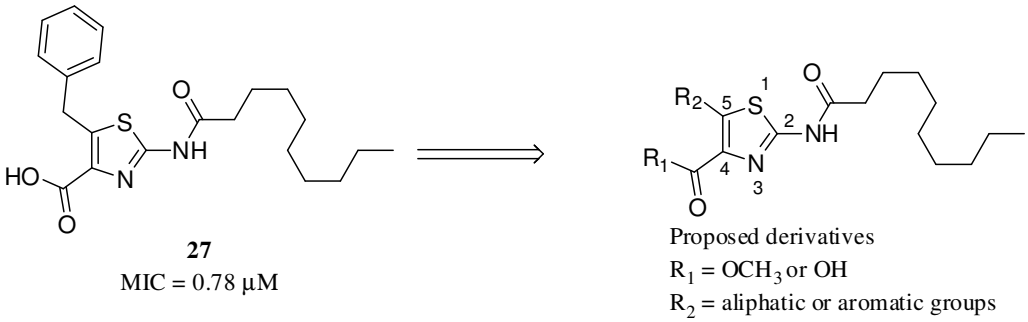

Figure 28: Proposed derivatives based on the structure of **27**.

Structurally diverse groups ranging from short and medium-sized alkyl groups and aryl rings with polar and non polar substituents were introduced at position-5 (**Table 14**).

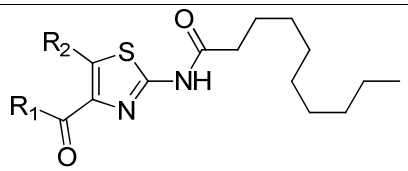

Compound	R_1	R_2	MIC (µM)	Cytotoxicity (% control)	clogP
109	OCH_3	-$(CH_2)_2$ phenyl	7.8	8.2	6.77
110	OH	-$(CH_2)_2$ phenyl	7.8	89.6	6.51
111	OCH_3	isopropyl	7.8	0.6	5.75
112	OH	isopropyl	0.97	49.0	5.29
113	OCH_3	Ethyl	15.6	0.7	5.35
114	OH	Ethyl	1.9	89.0	5.09
115	OCH_3	n-propyl	15.6	0.7	5.88
116	OH	n-propyl	1.9	50.9	5.62
117	OCH_3	n-butyl	15.6	0.4	6.41
118	OH	n-butyl	0.97	63.1	6.15
119	OCH_3	4-chlorophenyl	15.6	75.8	7.14
120	OH	4-chlorophenyl	1.9	96.8	6.95
121	OCH_3	4-methoxyphenyl	15.6	13.5	6.44
122	OH	4-methoxyphenyl	3.9	93.8	6.28

Table 14: Anti-trypanosomal activity and cytotoxicity of 5-substituted 2-decanamidothiazole-4-carboxylate derivatives.

Compounds **112** and **118** were the most active, with an isopropyl or butyl group at position-5, respectively, and a carboxylic acid at position-4. This was at least eight times more active than the ester derivatives, **111** and **117**, but only twice as active than compounds with ethyl, propyl and *p*-chlorophenyl groups, which suggests that while activity is improved by a carboxylic acid at position-4, position-5 is more tolerant, with a medium sized aliphatic or aromatic accepted. Compounds **110**, with a phenethyl group at position-5 was less active than **112**, **118**, **120** and **122**, and suggests that the bulkiness of this group is important, and that there is a limit to what can be accommodated. Furthermore, the phenethyl group is considerably more flexible than other substituents, which could mean that the position benefits from restricted conformation freedom. Interestingly, almost all the carboxylic acid

derivatives from this series were not toxic to the PNT2A cell lines, whereas some of the ester derivatives showed potential toxicity, and emphasises the importance a carboxylic acid moiety at position-4.

To further study the importance of the hydrophobic decanamido group for activity, two compounds that have polar carboxylate moieties in the aliphatic chains were synthesised to determine if the addition of polar group at this position is tolerated. A reduction in activity compared to compound **27** by at least 15 fold was observed with compound **123**, which was four times more active than the carboxylic acid derivative **124**, and suggests that a polar group in the hydrophobic side chain of the amide is not favoured (**Table 15**).

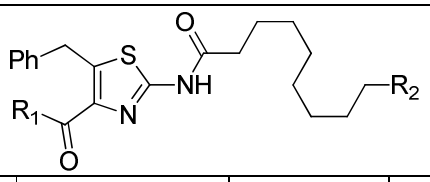

Compound	R_1	R_2	MIC (μM)	Cytotoxicity (% control)	clogP
27	OH	H	0.78	106 (in HS27)	6.39
123	OCH_3	-$COOCH_3$	12.5	97.0	4.84
124	OH	-COOH	50	108.0	4.18

Table 15: Anti-trypanosomal activity and cytotoxicity of 5-substituted 2-decanamidothiazole-4-carboxylate derivatives with polar groups at the terminal carbon.

Derivatives with a free carboxylic acid at position-4 consistently demonstrated higher activity than the corresponding ester derivatives, but whether this was due to the acidity of the carboxylic acid or its ability to donate a hydrogen bond had not been established. To explore this, four derivatives were synthesised related to compound **19** and **27**, but with the carboxylic acid at position-4 replaced with either a primary or secondary amide moiety (**Table 16**). Replacement of the carboxylic acid with the carboxamide group reduced the activity by 8 and 20 fold for the primary and the secondary amides, respectively. These data suggest that the carboxylic acid moiety functions as an acidic and ionisable group rather than as a hydrogen bond donor in turns of anti-trypanosomal activity. Additionally, a primary amide group

appeared to have the negative effect of introducing toxicity into the molecule, particularly for compound **127**.

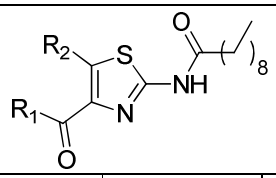

Compound	R_1	R_2	MIC (μM)	Cytotoxicity (% control)	clogP
19	OH	CH_3	1.9	98 (in HS27)	5.16
27	OH	benzyl	0.78	102 (in HS27)	6.39
125	NH_2	CH_3	15.6	44.0	4.28
126	$NHCH_3$	CH_3	31.2	106.0	4.60
127	NH_2	benzyl	15.6	0.5	5.85
128	$NHCH_3$	benzyl	>250	92.2	6.17

Table 16: Anti-trypanosomal activity and cytotoxicity of 2-decanamidothiazole-4-carboxamide derivatives.

All previous modifications of the **ATC** scaffold were applied to the substituents attached to the thiazole ring. Whether this heterocycle was essential for activity had not been explored. To investigate this, a group of compounds were synthesised in which either a phenyl or imidazole replaced the thiazole of the active series (**Table 17**).

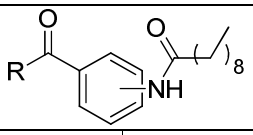

Compound	R	Amide position	MIC (μM)	Cytotoxicity (% control)	clogP
129	OCH_3	*p*	>125	N.T	5.83
130	OH	*p*	>125	N.T	5.43
131	OCH_3	*m*	62.5	98.2	5.83
132	OH	*m*	>125	N.T	5.43
133	OCH_3	*o*	>125	N.T	5.83
134	OH	*o*	125.0	87.3	5.43

Table 17: Anti-trypanosomal activity and cytotoxicity of *o*, *m* and *p*-decanamidobenzoate derivatives.

Replacement of the thiazole ring with a phenyl group markedly reduced activity; compound **131** was the most active with an MIC of 62.5 μM, which was still 33

times less active than the lead compound **19**. This suggests that not only are the decanamido and the carboxylate substituents essential for activity, but that the core ring is important also. To establish whether the thiazole ring was the best heterocyclic core ring for activity, the imidazole containing compounds **139** and **140** were synthesised (*via* the azo dye intermediates **135** and **136**, respectively). The decanamido and carboxylate moieties were retained along with a methyl group at position-4 in order to compare activities with compound **19** (**Figure 29**).

19

139 R = C_2H_5
140 R = H

Figure 29: Compounds **139** and **140** compared to **19.**

Although compounds **139** and **140** were active with MIC's of 31.25 µM, they were still much less active than compound **19**, as were the azo intermediates, **135** and **136**, which showed moderate activity with MIC's of 31.2 and 25 µM, respectively (**Table 18**).

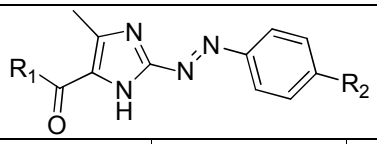

Compound	R_1	R_2	MIC (µM)	Cytotoxicity (% control)	clogP
135	OC_2H_5	Br	31.2	77.5	3.24
136	OC_2H_5	$COOCH_3$	25	73.9	2.35
137	OH	Br	>250	N.T	3.06
138	OH	COOH	>250	N.T	1.95

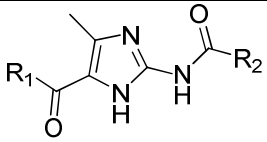

Compound	R_1	R_2	MIC (µM)	Cytotoxicity (% control)	clogP
19			1.9	98 (in HS27)	5.16
139	OC_2H_5	$(CH_2)_8CH_3$	31.25	87.7	4.62
140	OH	$(CH_2)_8CH_3$	31.25	83.9	4.45

Table 18: 2-amino-1*H*-imidazole-5-carboxylate derivatives.

Based on the data for the **ATC** library, the following conclusions could be drawn:

- The thiazole is the optimal core ring for activity, compared to the imidazole, benzimidazole, benzothiazole and phenyl isosteres.
- Position-5 should have a small to moderate-sized hydrophobic group such as a benzyl, isopropyl or butyl moiety.
- Position-2 should have hydrophobic amide functionality; compounds with a decanamido moiety were the most active.
- A carboxylic acid at position-4 is essential for activity; the ester equivalents were at least 8 fold less active.

All of these active compounds had the disadvantage of being highly lipophilic due to the 2-decanamido group, which reduces their druggabalility. Aromatic amides such as substituted benzamido and phenylacetamido groups were introduced in order to reduce lipophilicity. The substituents used were chloro, methoxy, butoxy and nitro groups with the carboxylate group at position-4 and the hydrophobic moiety (benzyl or isopropyl) at position-5 retained (**Table 19**). To establish whether a restrained aliphatic group at position-2 was tolerated, the 2-cyclohexylmethyleneamido derivatives were prepared (**157**-**159**).

All compounds in this series were active, including both acid and ester analogues for each derivative. The only derivatives that followed the previous trend in which the carboxylic acids were more active than the ester equivalents were those having a 4-butoxybenzamido group present at position-2. For example compound **162** was 16 times more active than its ester analogue **161**, whereas compound **164** showed 31 fold enhanced activity compared to **163**.

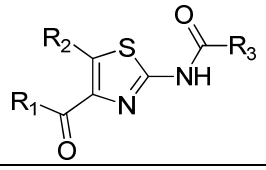

Compound	R_1	R_2	R_3	MIC (μM)	Cytotoxicity (% control)	clogP
141	OCH_3	isopropyl	-CH_2(4-methoxyphenyl)	7.80	81.9	2.98
142	OH	isopropyl	-CH_2(4-methoxyphenyl)	31.25	99.7	2.51
143	OCH_3	isopropyl	benzyl	31.25	81.0	3.06
144	OH	isopropyl	benzyl	31.25	89.0	2.59
145	OCH_3	isopropyl	-CH_2(3-methoxyphenyl)	7.8	71.50	2.98
146	OH	isopropyl	-CH_2(3-methoxyphenyl)	15.6	96.3	2.51
147	OCH_3	isopropyl	-CH_2(4-chlorophenyl)	7.8	90.2	3.77
148	OH	isopropyl	-CH_2(4-chlorophenyl)	7.8	84.9	3.31
149	OCH_3	benzyl	-CH_2(4-methoxyphenyl)	15.6	96.5	3.62
150	OH	benzyl	-CH_2(4-methoxyphenyl)	15.6	89.3	3.35
151	OCH_3	benzyl	-CH_2(3-methoxyphenyl)	7.8	101.4	3.62
152	OH	benzyl	-CH_2(3-methoxyphenyl)	3.9	89.4	3.35
153	OCH_3	benzyl	-CH_2(4-chlorophenyl)	7.8	84.9	4.41
154	OH	benzyl	-CH_2(4-chlorophenyl)	15.6	96.5	4.15
155	OCH_3	benzyl	-CH_2(4-nitrophenyl)	3.9	101.2	3.44
156	OH	benzyl	-CH_2(4-nitrophenyl)	15.6	107.4	3.18
157	OCH_3	benzyl	-CH_2(cyclohexyl)	3.9	7.2	4.81
158	OH	benzyl	-CH_2(cyclohexyl)	7.8	99.3	4.54
159	OCH_3	isopropyl	-CH_2(cyclohexyl)	7.8	69.3	4.17
160	OH	isopropyl	-CH_2(cyclohexyl)	3.9	90.1	3.71
161	OCH_3	ethyl	4-butoxyphenyl	15.6	97.2	4.28
162	OH	ethyl	4-butoxyphenyl	0.97	99.1	4.02
163	OCH_3	n-propyl	4-butoxyphenyl	15.6	97.6	4.81
164	OH	n-propyl	4-butoxyphenyl	0.49	87.7	4.54
165	OCH_3	n-butyl	4-butoxyphenyl	31.30	98.9	5.34
166	OH	n-butyl	4-butoxyphenyl	0.78	84.1	5.07
167	OCH_3	phenyl	4-butoxyphenyl	1.9	102.5	5.35
168	OH	phenyl	4-butoxyphenyl	1.9	100.2	5.19
169	OCH_3	benzyl	4-chlorophenyl	3.9	95.4	4.37
170	OH	benzyl	4-chlorophenyl	15.6	77.1	4.11
171	OCH_3	isopropyl	4-methoxyphenyl	3.9	48.3	3.09
172	OH	isopropyl	4-methoxyphenyl	7.8	78.5	2.63
173	OCH_3	isopropyl	4-chlorophenyl	15.6	91.2	3.73

Table 19: Anti-trypanosomal and cytotoxicity activity of substituted 2-bezamido and phenylacetamido thiazole-4-carboxylate derivatives.

Based on the results obtained so far, an improvement in anti-trypanosomal activity was obtained when the highly lipophilic decanamido group was replaced with lesser lipophilic, smaller aromatic moieties at position-2 such as 4-butoxybenzamido and substituted phenethyl groups. These results indicate that the long chain aliphatic

amides can be replaced by more druggable aromatic substituents. A 4-butoxyphenyl amido group conveys the greatest activity, particularly in association with the 4-carboxylate and a 5-alkyl substituent such as ethyl and n-propyl. Compound **164** was the most active to date, with a sub micromolar MIC of 0.49 μM, and was non-toxic in the human cell line.

3.2.3 Anti-trypanosomal activity of indole and 1,2,3,4-tetrahydro-*β*-carboline derivatives

The third hit compound selected for further investigation was the indole **47**. The fact that this compound is a small molecule with a predicted logP of 2.41 makes it a good candidate for development. This molecule also showed good mapping with the recommended features of the pharmacophore, with the indole moiety mapped onto the two hydrophobic features, the sulfonamido amino group occupying the hydrogen bond donor feature and the ester attached to the furan ring occupying the hydrogen bond acceptor pocket (**Figure 30**).

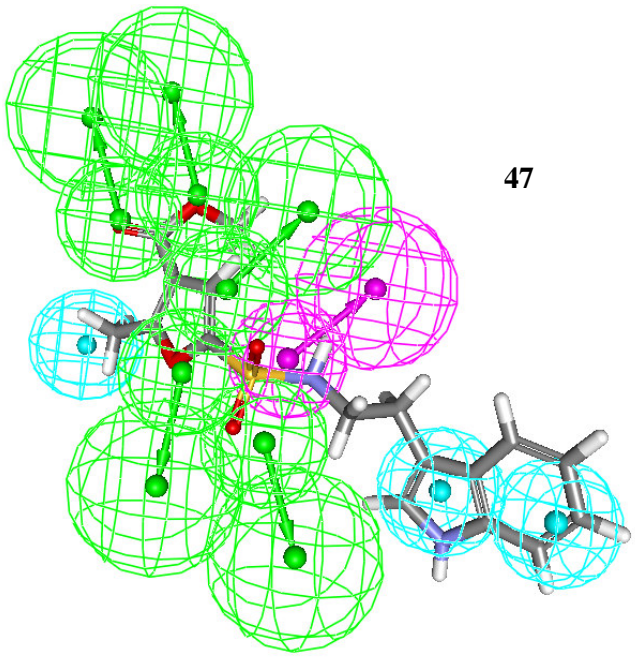

Figure 30: Compound **47** in the **ATC** pharmacophore model.

Before embarking on the synthesis of derivatives based on this compound, we assessed an in-house library of indoles that were closely related to structure **47** against *T.b. brucei.* The anti-trypanosomal activities of these compounds were promising and two of them, **174** and **175** were active, both with an MIC value of 0.40 µM, which is 150 times more active than **47** and twice as active as the lead **ATC** compound, **27** (**Table 20**).

Compound	structure	MIC (µM)
174	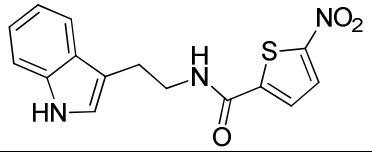	0.40
175	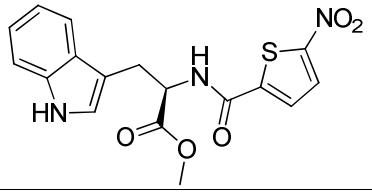	0.40
176	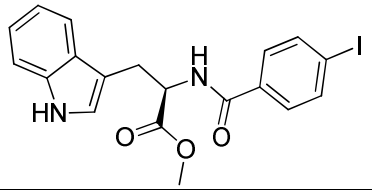	12.5
177	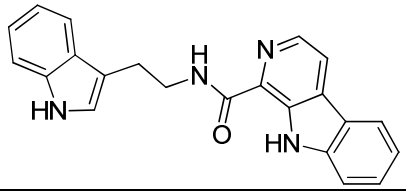	>250
178	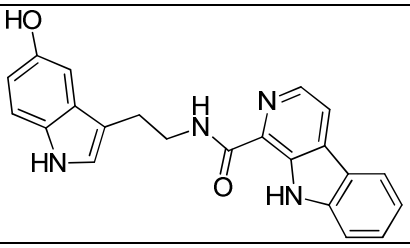	>250

Table 20: anti-trypanosomal activity of compounds from the in-house indole library.

Structural modifications were made to address the following features (**Figure 31**):

1. The importance of the nitro group for activity.

2. The role of stereochemistry in compound **175**.
3. Isosteric replacement of the thiazole ring.
4. Whether substituents in the indole ring could be tolerated.
5. Structural rigidification.

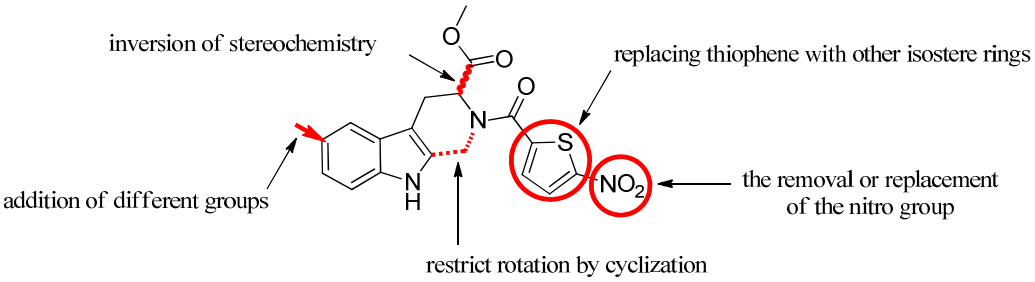

Figure 31: The proposed modifications to **174** and **175** to explore activity.

The nitro group was modified by either reduction to the corresponding amino group or by preparing compounds with a hydrogen atom in its place. Four compounds were synthesised and their anti-trypanosomal activities are shown in **Table 21**.

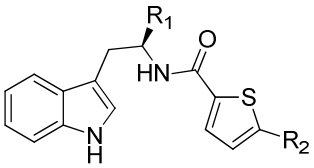

Compound	R_1	R_2	MIC (µM)	Cytotoxicity (% control)
179	-(*S*)$COOCH_3$	NH_2	125	104.5
180	H	NH_2	62.5	96.3
181	-(*S*)$COOCH_3$	H	31.25	102.1
182	H	H	62.5	83.7

Table 21: Anti-trypanosomal and cytotoxicity results of indole compounds without nitro group.

Results showed that the presence of the nitro group in both **174** and **175** plays an important role in activity since compounds **181** and **182** without it and compounds **179** and **180** with an amino group were much less active.

To further investigate whether the nitro group alone is essential, the three regioisomers of the nitrophenyl isostere were synthesised (**Table 22**).

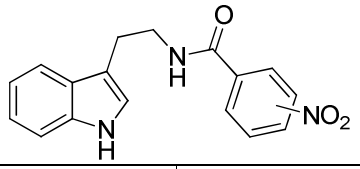

Compound	Nitro position	MIC (μM)	Cytotoxicity (% control)
183	*para*	62.5	92.5
184	*meta*	62.5	96.4
185	*ortho*	125	100.5

Table 22: Anti-trypanosomal and cytotoxicity results of indole compounds having nitrobenzamide substituent.

The three nitrobenzene isomers were more than 150 times less active than hit compounds **174** and **175**, which suggests that the nitrothiophene group plays a crucial role in the anti-trypanosomal activity of the indole derivatives. One possible explanation is that the thiophene ring has the required spatial arrangement for binding with the target. Moreover, the presence of a sulfur atom might play role in increasing the hydrogen bond acceptor capacity of the molecule.

To further study the indole structure, the nitrothiophene carboxamide moiety was retained and the stereochemistry in **175** was inverted (compound **186**) (**Figure 32**). *R* stereochemistry at α-position reduced activity four fold, which suggests that the *S* configuration is favoured for activity.

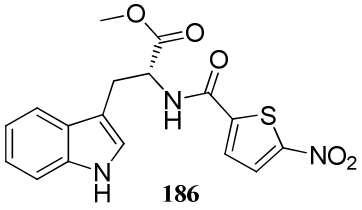

186

MIC = 1.9 μM

Cytotoxicty (% control) = 65.7 %

Figure 32: Compound **186** with its anti-trypanosomal and cytotoxicity results

However, the fact that **174**, which has no stereochemical centre at this position was as active as **175**, and does not contain the ester moiety means that absolute stereochemistry at this position is not a requirement for activity, rather that the conformation of the two heterocyclic rings with respect to each other is what governs activity (**Figure 33**).

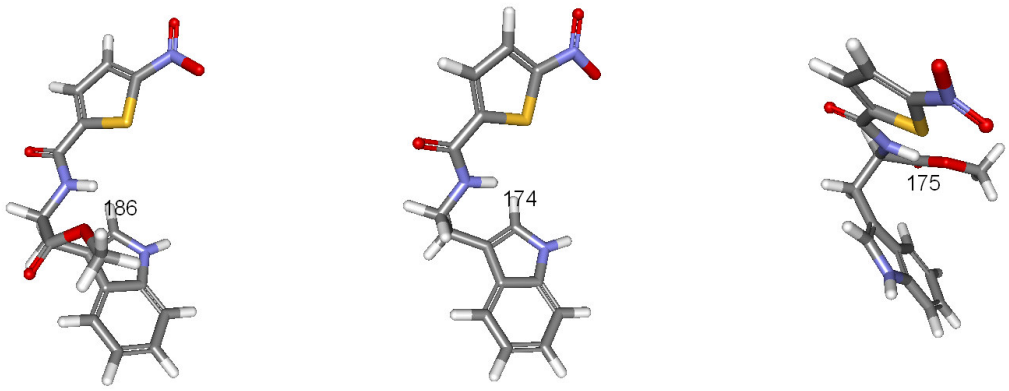

Figure 33: the most stable conformers of compound **174**, **175**, and **186**.

To study these three compounds in terms of the relationship between thiophene and indole rings, the three lowest energy conformers for compound **174**, **175**, and **186** were superimposed on top of each other (**Figure 34**). This experiment revealed that the thiophene ring as well as the amide moiety from compound **174** mapped to that of **175** whereas the indole rings were like mirror-images (**Figure 34A**), whereas, the indole rings from **174** and **186** can be superimposed, but not the thiophene ring. Moreover, enantiomeric compounds **175** and **186** do not superimpose and were perfect mirror-images to each other and no mapping between either thiophene or indole ring was observed. These findings suggest that the conformation of the thiophene ring relative to the indole ring plays an important role in activity since both **174** and **175** were more active than **186**.

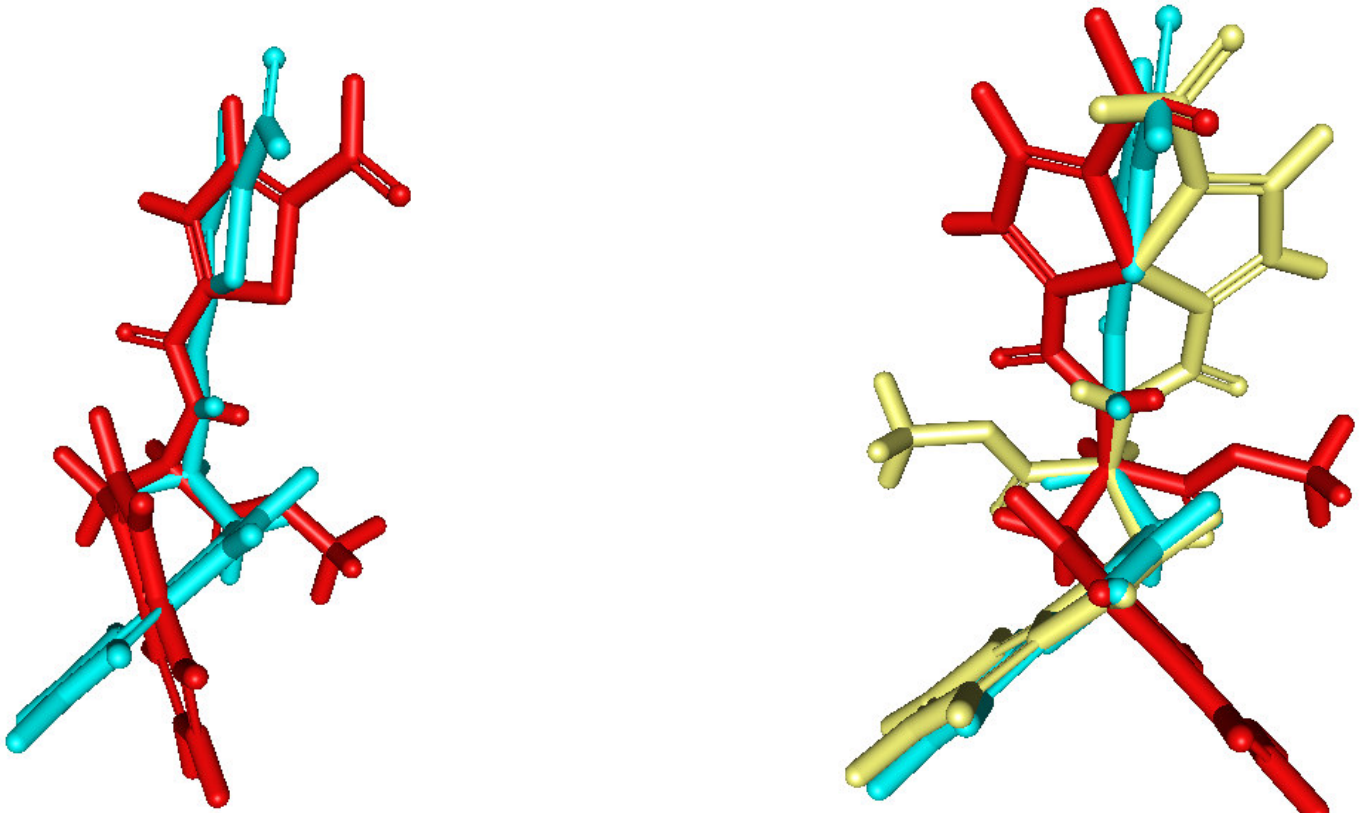

Figure 34: (**A)** The superimposition of compounds **174** (cyan) and **175** (red). (**B**) The superimposition of **174**, **175** and **186** (yellow).

A further modification applied to this scaffold was the addition of different groups at position-5 of the indole ring; a polar hydroxyl and methoxy group to examine whether a substituent in the indole ring could be tolerated (**Table 23**).

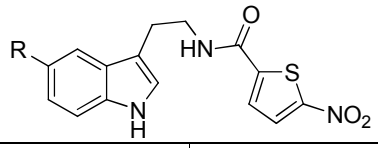

Compound	R	MIC (μM)	Cytotoxicity (% control)
187	OH	3.9	52.0
188	OCH_3	3.9	47.9

Table 23: Anti-trypanosomal and cytotoxicity results of 5-substituted indole derivatives.

The activity of both **187** and **188** was ten times less than **174**, which could suggest that the indole ring should be unsubstituted at position-5 for better anti-trypanosomal activity, although a wider range of substituents needs to be explored before this can be stated categorically. Both substituents had the negative effect of introducing cytotoxicity in the mammalian cell lines.

The last structural modification applied to this library was the synthesis of compound **190**, which is a 1,2,3,4-tetrahydro-*β*-carboline derivative and a rigid analogue of **186** in which the free rotation of the ethylene group is restricted by incorporation into a piperidine ring. This compound was tested against *T.b. brucei* and had an activity of 0.97 μM **(Figure 35**).

190
MIC = 0.97 μM
Cytotoxicity (% control) = 83.8 %

189
MIC > 250 μM

Figure 35: Compound **190** and its precursor **189** with their anti-trypanosomal and cytotoxicity results.

Since the activity of **190** was two fold higher than that of **186**, it appears that the restriction of the free rotation of the ethylene group has some effect. The inactivity of **189** again demonstrates the importance of the nitrothiophene for activity. The higher activity of compound **190** to **186** also illustrates the importance of conformation of the two heterocycles with respect to each other. Despite having R-stereochemistry, the carboline is more active because of the rigidified orientation of the two ring systems (**Figure 36**).

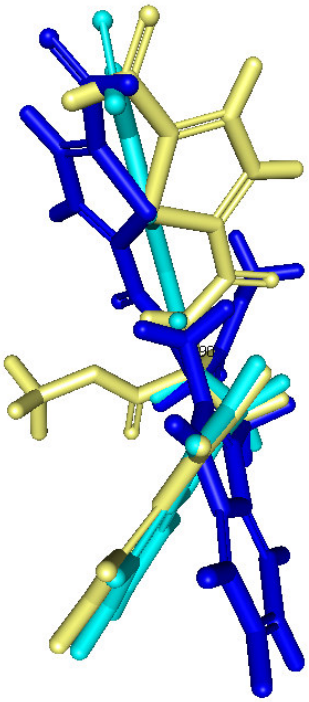

Figure 36: The superimposition of the most stable conformers of compound **174** (cyan), **186** (yellow) and **190** (blue).

It is obvious from the superimposition that there is poor mapping between **186** and the rigidified analogue, **190** in which neither the thiophene nor the indole fit to the same orientation, which demonstrates why these two compounds have different activities. The superimposition of **190** with **174** revealed better mapping between the thiophene rings (the blue and cyan structures in **Figure 36**, respectively), which could account for the superior activity of compound **190** compared to **186**.

Further work is needed to determine whether the 1,2,3,4-tetrahydro-*β*-carboline scaffold can deliver more active compounds compared to the indole series. For example, the rigid analogues of both **174** and **175**, the most active indole derivatives, have to be prepared to further assess the effect of conformational restraint on activity.

Based on the results shown for all indole and 1,2,3,4-tetrahydro-*β*-carboline derivatives tested, it can be concluded that:

- The nitrothiophene is essential for activity.
- The *S* configuration of the α-carbon to the amide group was superior in activity compared to the *R* isomer; this is applied to compounds with an ester group at α-position.
- The conformation of the two heterocycles; the indole and thiophene, with respect to each other plays important role in activity.
- Substitution at position-5 of the indole ring is tolerated, but lower activity was observed and toxicity appeared.

3.2.4 Anti-trypanosomal activity of thiazole derivatives with the nitrothiophenyl carboxamide moiety

The nitrothiophenyl carboxamide group significantly augmenting the anti-trypanosomal activity of the indole derivatives led to the synthesis of hybrid molecules of the indole and the thiazole scaffold; compounds **191** and **192**. Substituents from the most active **ATC** scaffold were retained (a carboxylate moiety at position-4 and a benzyl group at position-5), while the nitrothiophene was introduced as the 2-aminosubstituent of the thiazole ring (**Figure 37**).

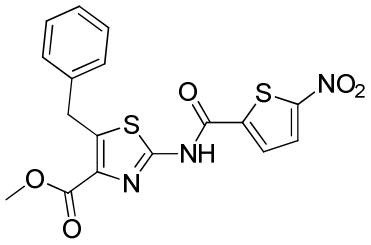

191
MIC = 0.78 μM
Cytotoxicity (% control) = 65%

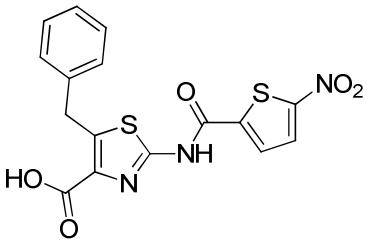

192
MIC = 0.195 μM
Cytotoxicity (% control) = 32% (LD_{50} = 300μM)

Figure 37: Nitrothiophenyl carboxamide derivatives of the **ATC**s with their anti-trypanosomal and cytotoxicity results.

A very promising result was obtained for compound **192** which had an MIC value of 195 nM, which was more active than the ester analogue, **191**, and the most active indole derivative **175**, and reinforces our previous findings that the nitrothiophenyl carboxamide plays an important role for activity. Other **ATC** compounds containing nitrophenyl groups (**Figure 38**) were less active (MIC range of 3.9-15.6 μM), which supports all our observations that the thiophene ring is required for optimum activity.

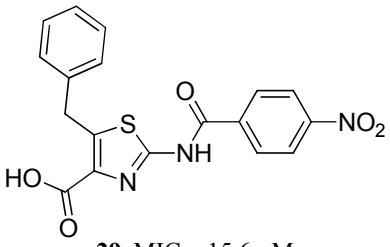

29, MIC = 15.6 μM

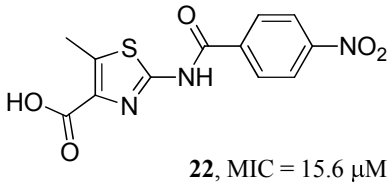

22, MIC = 15.6 μM

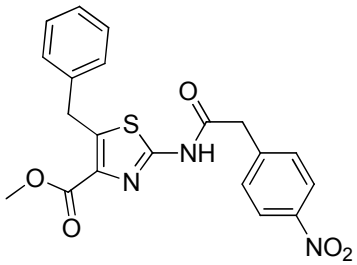

155, MIC = 3.9 μM

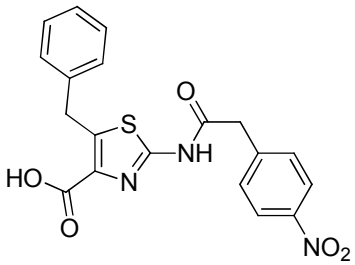

156, MIC = 15.6 μM

Figure 38: Some **ATC** compounds with nitro groups at position-2.

That the nitro containing group plays an important role in activity is supported by the fact that registered anti-trypanosomal agents such as nifurtimox and benznidazole (**Figure 39**), the frontline drugs used for the treatment of Chagas' disease, have nitroheterocycle moieties. The former has shown promising anti-trypanosomal activity especially in the late stage of HAT and its combination with eflornithine is currently in phase III clinical trials against the disease.[96]

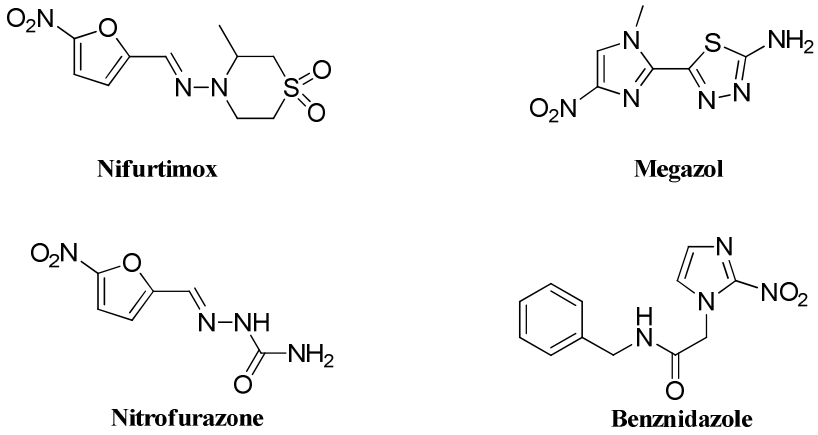

Figure 39: Chemical structure of some nitroheterocycle containing trypanocidal agents.

Both drugs are activated by a NADH-dependent I nitroreductase (NTR), and its down-regulation explains how resistance may emerge; loss of a single copy of this gene in *Trypanosoma cruzi* was found to cause significant cross-resistance to a wide range of nitroheterocyclic containing drugs. Furthermore, overexpression of NTRs increases sensitivity toward benznidazole and nifurtimox, and gene deletion of these enzymes causes cross resistance.

Many agents with nitroheterocyclic moieties have been developed and are in clinical trials for the treatment of HAT. For example, Megazol (**Figure 39**), which is in phase II clinical trials, showed promise when administered with suramin in late stage mice and rat models and is also able to cross the blood brain barrier in a considerable amount.[97] Nitrofurazone, a known antibacterial agent that showed good activity against Trypanosoma parasites entered human clinical trials in the mid-twentieth century. Its effect was attributed to inhibition of trypanothione-reductase, but because of toxicity issues, the trials were terminated.[98] All these agents are believed

to undergo activation by the trypanosomal nitroreductase enzyme to generate reactive radicals (**Section 1.7.5**) which may interact with cellular components, especially DNA such as the case with nifurtimox, Megazol and benznidazole, or generate reduced oxygen metabolites believed to cause parasite death.[6]

Research today is focusing in studying the role of trypanosomal NTR in parasite killing through the activation of nitroheterocyclic prodrugs to reactive radicals only inside the trypanosomal cells leading to cell death.[99] NTRs are of two types; type I NTRs are oxygen insensitive and contain flavin mononucleotide (FMN) as a cofactor; type II NTRs are oxygen sensitive and contain flavin adenine dinucleoptide and/or FMN as the cofactor. Type I NTRs are found in bacteria, and protozoan parasites, but not in any other eukaryotes. The absence of NTRs in humans raises the selectivity potential of these nitroheterocyclic prodrugs.

3.3 *In vivo* determination of acute toxicity and efficacy of the most active compounds

The most active compounds; **164**, **191** and **192**, were tested *in vivo* on both healthy and infected mice with *T.b. brucei* to study their toxicity and anti-trypanosomal efficacy, respectively. In summary, the three compounds were first injected intraperitoneally at different doses, starting with 1 mg/kg to study the maximum tolerable doses that show no signs of toxicity (continual staunching, laboured breathing, shivers, tremors and/or 25% body weight loss). The assay revealed that the three compounds did not show any toxicity in terms of weight loss at a maximum dose of 50 mg/kg (**Figure 40, 41 and 42**).

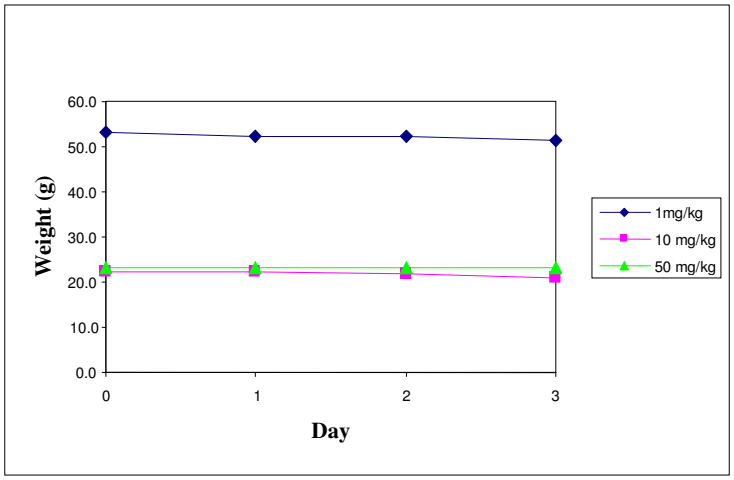

Figure 40: Body weight loss in the tested mice upon administration of **164**.

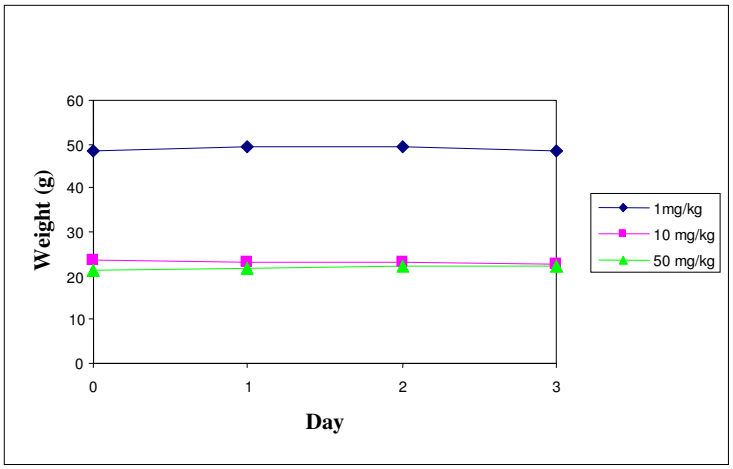

Figure 41: Body weight loss in the tested mice upon administration of **191**.

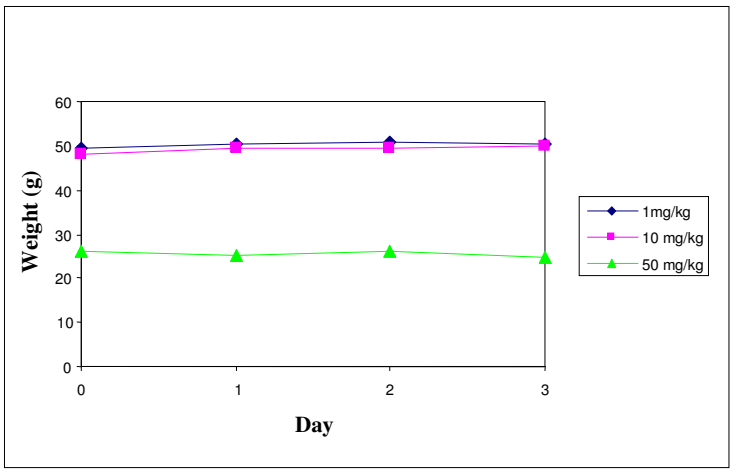

Figure 42: Body weight loss in the tested mice upon administration of **192**.

The highest tolerable dose of each test compound (50mg/kg) was then used *in vivo* (see **Section 5.4.3**). In summary, the infected mice were treated with the freshly prepared 200 µl solutions of compounds **164**, **191** and **192** in addition to pentamidine (4 mg kg^{-1}) as a positive control and one group was left untreated as the negative control. The treatments were repeated on a daily basis for another three days and the parasitaemia level was monitored by measuring parasite levels in the blood samples (**Figure 43**).

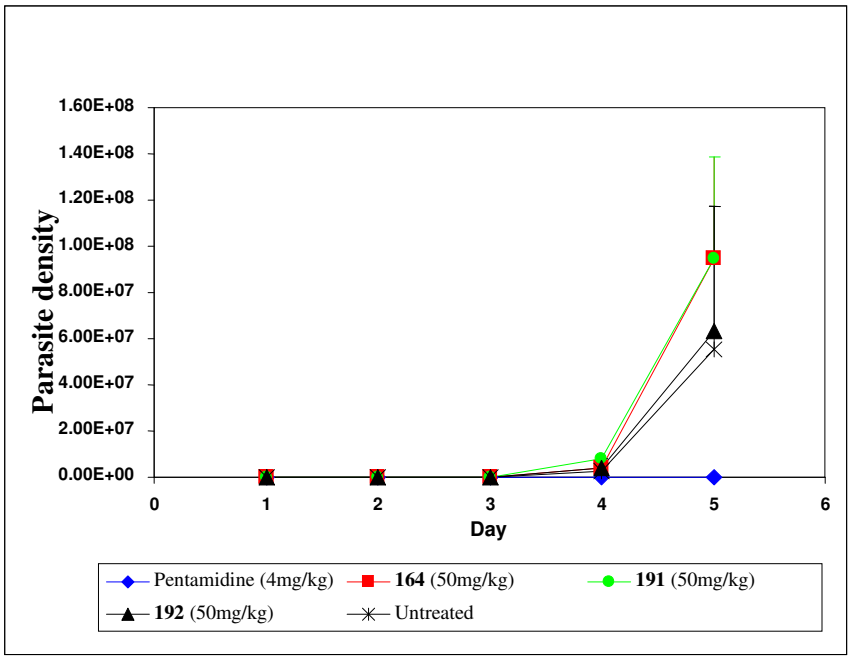

Figure 43: Treatment of *T.b. brucei* infected mice by compounds **164**, **191**, **192** and pentamidine.

As shown in **Figure 43**, the mice treated with **164**, **191** and **192** exhibited increasing levels of parasitaemia similar to the untreated group, whereas pentamidine as the positive control was effective in clearing out all parasites from blood. These results showed that the tested compounds did not have a trypanocidal effect *in vivo*, although they were among the most active *in vitro*. One possible explanation is that the three compounds precipitated out during the dilution process before administering to the animals. Despite the compounds being prepared directly prior to the injection, there was still precipitation directly after the injection, which will have a significant effect on activity. The main issue therefore appears to be solubility in

physiological aqueous solutions. To improve aqueous solubility, their salts should be prepared, either organic or inorganic, or by making water soluble esters as prodrugs.

Chapter Four: Synthesis of the target compounds

4.1 Synthesis of the 2-amino-1*H*-benzo[*d*]imidazole-5-carboxylate derivatives

A well known method for the synthesis of the 2-amino-1*H*-benzo[*d*]imidazole-5-carboxylate scaffold was used, in which the 3,4-diaminobenzene-5-carboxylate derivatives were treated with cyanogen bromide in water at room temperature followed by neutralization with ammonium hydroxide to give compounds **70**, **71** and **72** in good yields after either crystallization or column chromatography (**Scheme 2**).[100-103]

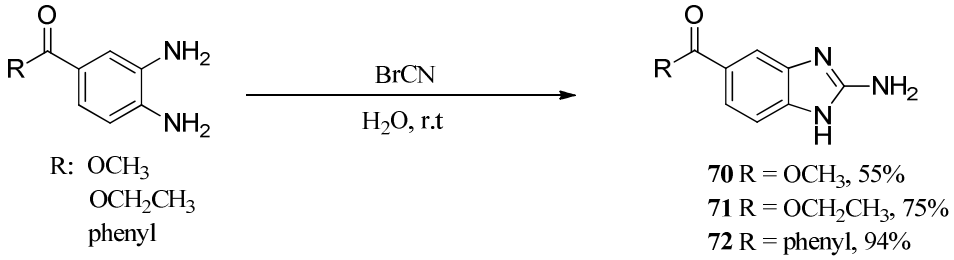

Scheme 2: Synthesis of **70**, **71** and **72** as precursors for 2-amino-1*H*-benzo[*d*]imidazole-5-carboxylate derivatives.

Cyanogen bromide is very reactive towards nucleophilic species because of the unusually electrophilic carbon atom. The reaction with the diamino reagent proceeds *via* the nucleophilic attack of the amino group on the cyanide carbon to form a highly reactive cyanamide intermediate, which is attacked by the second amino group to form the imidazole ring (**Scheme 3**).

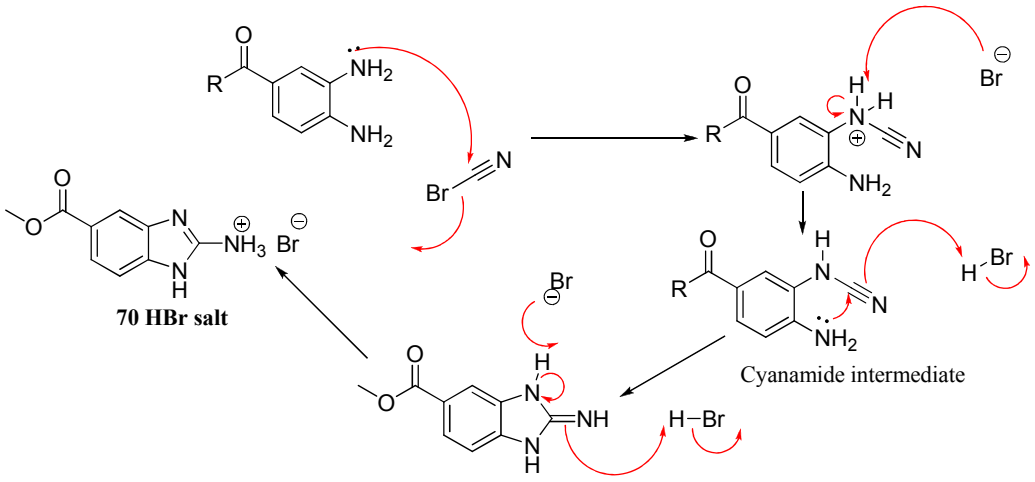

Scheme 3: Reaction mechanism of 2-amino-1*H*-benzo[*d*]imidazole formation.

Analysis of the proton (^{1}H) NMR spectrum of compound **70** (**Figure 44**) shows that there is a singlet around δ 3.79 ppm composed of three protons, which corresponds to the methyl ester (OCH_3), which is normally shifted downfield by the presence of the adjacent electronegative oxygen atom. The singlet at δ 6.53 represents the two protons of the amino group directly attached to the benzimidazole ring. Regarding the aromatic protons of the benzimidazole ring, the doublet at δ 7.12 with a coupling constant (*J*) of 8 Hertz (Hz) corresponds to H7. This proton is coupled to H6 which is represented by the doublet of doublets peak at δ 7.56 with coupling constants of 8 and 1.32 Hz. The large *J* coupling represents the *ortho* coupling with H7 while the smaller one corresponds to the *meta* coupling with H4. The doublet at δ 7.69 with *J* coupling of 1.32 Hz corresponds to H4 and finally the broad singlet at δ 10.96 corresponds to the imidazole NH proton.

The ^{13}C NMR spectrum of **70** (**Figure 45**) has nine peaks: one at δ 52.3 ppm represents the methoxy carbon; the signals at δ 112-123.5 ppm correspond to the aromatic carbons 4-7; the signals at δ 134.4 and 140.4 ppm correspond to the quaternary aromatic carbons 8 and 9, which are shifted downfield because they are attached to the electronegative imidazole nitrogen atoms; the highly deshielded carbon at δ 155.4 ppm corresponds to carbon 2 which is attached to three electron-withdrawing amino groups, which along with the carbon 8 and 9 signals confirms the formation of the 2-aminobenzimidazole ring. Finally, the signal at δ 167.15 ppm corresponds to the carbonyl carbon which is the most downfield signal due to sp^2 hybridization and the oxygen atom effect.

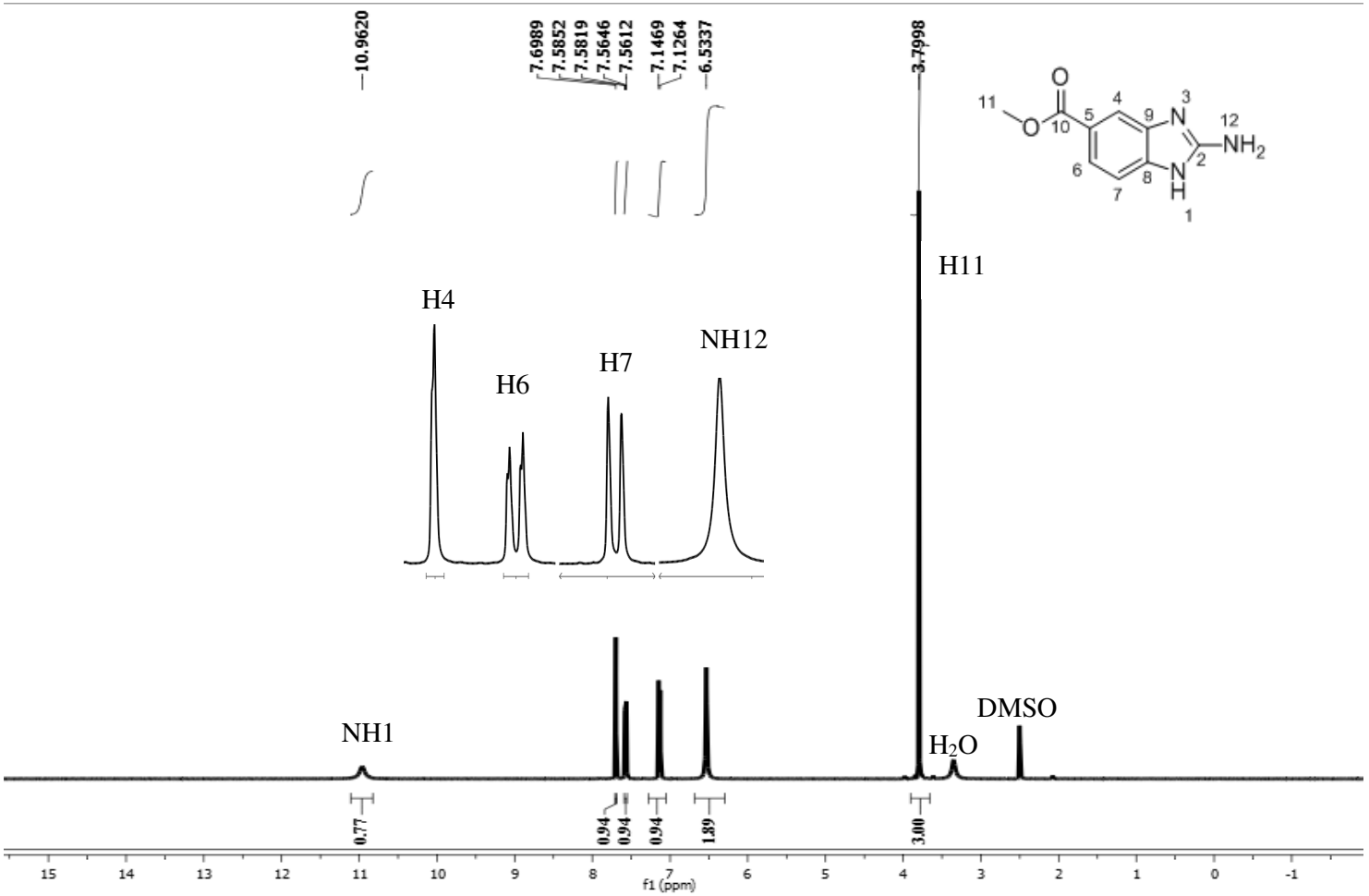

Figure 44: ^{1}H NMR spectrum for compound **70**.

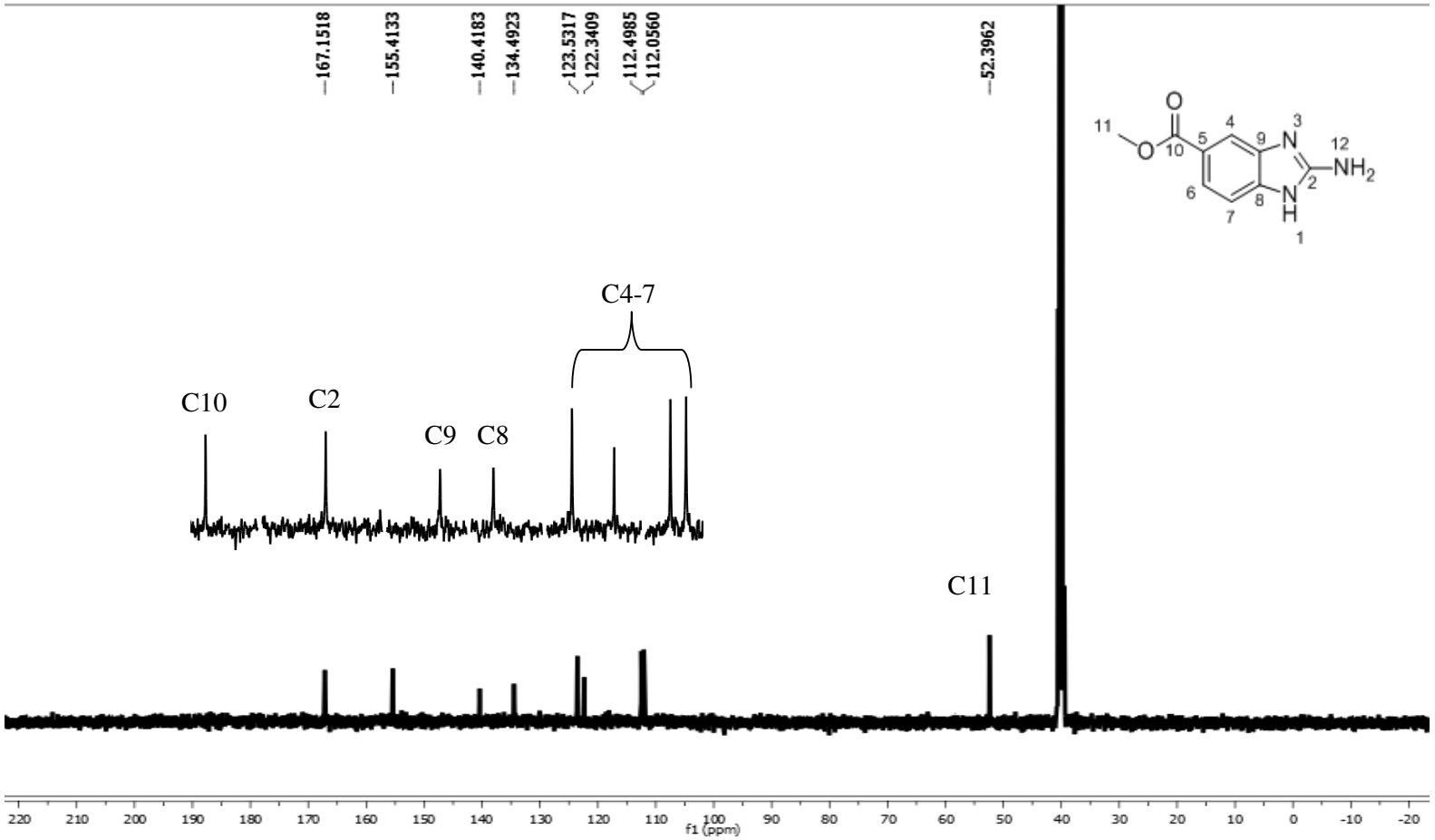

Figure 45: ^{13}C NMR spectra of compound **70**.

To synthesise different amide derivatives from this library, compounds **70**, **71** and **72** were treated with acid chlorides under anhydrous conditions in tetrahydrofuran or dichloromethane. Triethylamine was used to quench the formed hydrochloride and shift the reaction forward. The yields for these derivatives were relatively good and the final products were either crystallised or purified by column chromatography (**Scheme 4**).

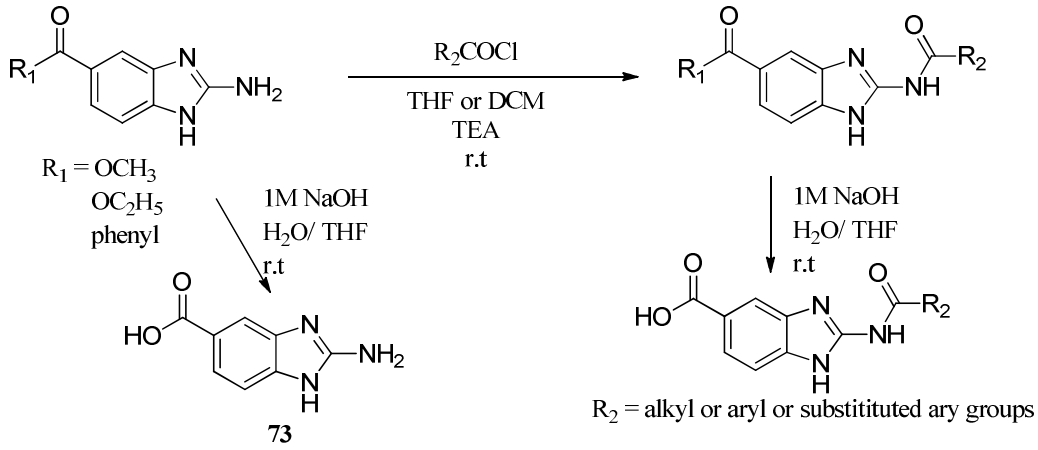

Scheme 4: Synthesis of 2-amido-1*H*-benzo[*d*]imidazole-5-carboxylate and its hydrolysis to the corresponding carboxylic acid.

The carboxylic acid derivatives from this library were obtained after basic hydrolysis of the ester analogues using aqueous sodium hydroxide (NaOH) at room temperature. This method was mild and did not affect the amide linkage and the yield was moderate to excellent. Most of the compounds were precipitated out in their pure form after neutralizing the reaction mixture with an aqueous HCl solution.[104-106]

As an alternative procedure for amide formation, compound **71** was treated with suitable acid anhydrides under anhydrous conditions to form the amide bond (**Scheme 5**).[107, 108] Although this method was milder and safer than using highly reactive and irritating acid chlorides, the availability of different acid anhydrides limited its use in the synthesis.

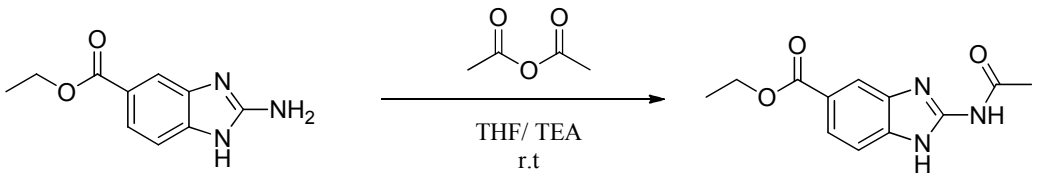

71 **74**, 43%

Scheme 5: Amide formation by using acid anhydride method.

Several compounds from this scaffold were synthesised to obtain amides bearing different moieties. These include short and long aliphatic amides in addition to substituted and unsubstituted aromatic groups differing in size. As expected, the yield of these compounds was good due to the strong nucleophilicity of the amino group as well as the highly reactive acid chlorides. A list of the synthesised amide derivatives and their yields is shown in **Table 24**.

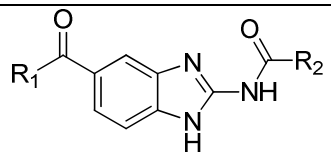

Compound	R_1	R_2	% Yield
75	OCH_3	CH_3	70
76	phenyl	CH_3	71
77	phenyl	phenyl	59
78	OCH_3	$(CH_2)_8CH_3$	71
79	OH	$(CH_2)_8CH_3$	83
80	OCH_3	CH_2CH_3	45
81	OH	CH_2CH_3	61
82	OCH_3	benzyl	60
83	OH	benzyl	57
84	OCH_3	$(CH_2)_4CH_3$	42
85	OH	$(CH_2)_4CH_3$	40
86	phenyl	$(CH_2)_8CH_3$	90
87	OCH_3	phenyl	62
88	OH	phenyl	64
89	phenyl	4-chlorophenyl	54
90	phenyl	$(CH_2)_5CH_3$	61
91	phenyl	4-methylphenyl	20
92	OCH_3	4-methylphenyl	35
93	phenyl	4-methoxyphenyl	67
94	phenyl	4-nitrophenyl	62
95	OCH_3	4-nitrophenyl	40
96	OCH_3	4-methoxyphenyl	42

Table 24: 2-amino-1*H*-benzo[*d*]imidazole-5-carboxylate amide derivatives.

As an example for the structural elucidation of the amide derivatives from this series, the ^{1}H NMR spectrum of compound **95** (**Figure 46**) shows the disappearance of the signal corresponds to primary amine at position-2. The signals for H4, 6 and 7 were almost the same as compound **70** in which the H7 signal appears as doublet at δ 7.52 ppm that is coupled with H6 at δ 7.81 ppm with *J* coupling of 8.36 Hz that characteristic of *ortho* coupling. The signal for H4 appears as singlet at δ 8.06 ppm although it should have a *meta* coupling with H6. It can be clearly seen that the signals for these protons are more deshielded than the corresponding ones in compound **70**, which is due to the introduction of the more electron withdrawing amide moiety at position-2. The sharp singlet at δ 8.35 ppm represents the four protons of the benzamido ring and is shifted downfield by the presence of both carbonyl and nitro electron withdrawing groups. Finally, the signals for both NH1 and NH12 appear together at δ 12.77.

In the ^{13} C NMR spectrum of this compound (**Figure 47**), the signal at δ 51.5 ppm corresponds to the deshielded methoxy carbon of the ester. The signals for C4-7 come at δ 113.4-122.8 ppm, and as expected, C8 and 9 were deshielded at δ 143.7-145 ppm. The most des-shielded carbon in the benzimidazole ring, as mentioned in compound **70** is C2, appears at δ 149.9 ppm. In addition to the carbonyl carbon (C10) signal at δ 169.7, this compound has a signal at δ 167.6 ppm, which represents the amide carbon (C13).

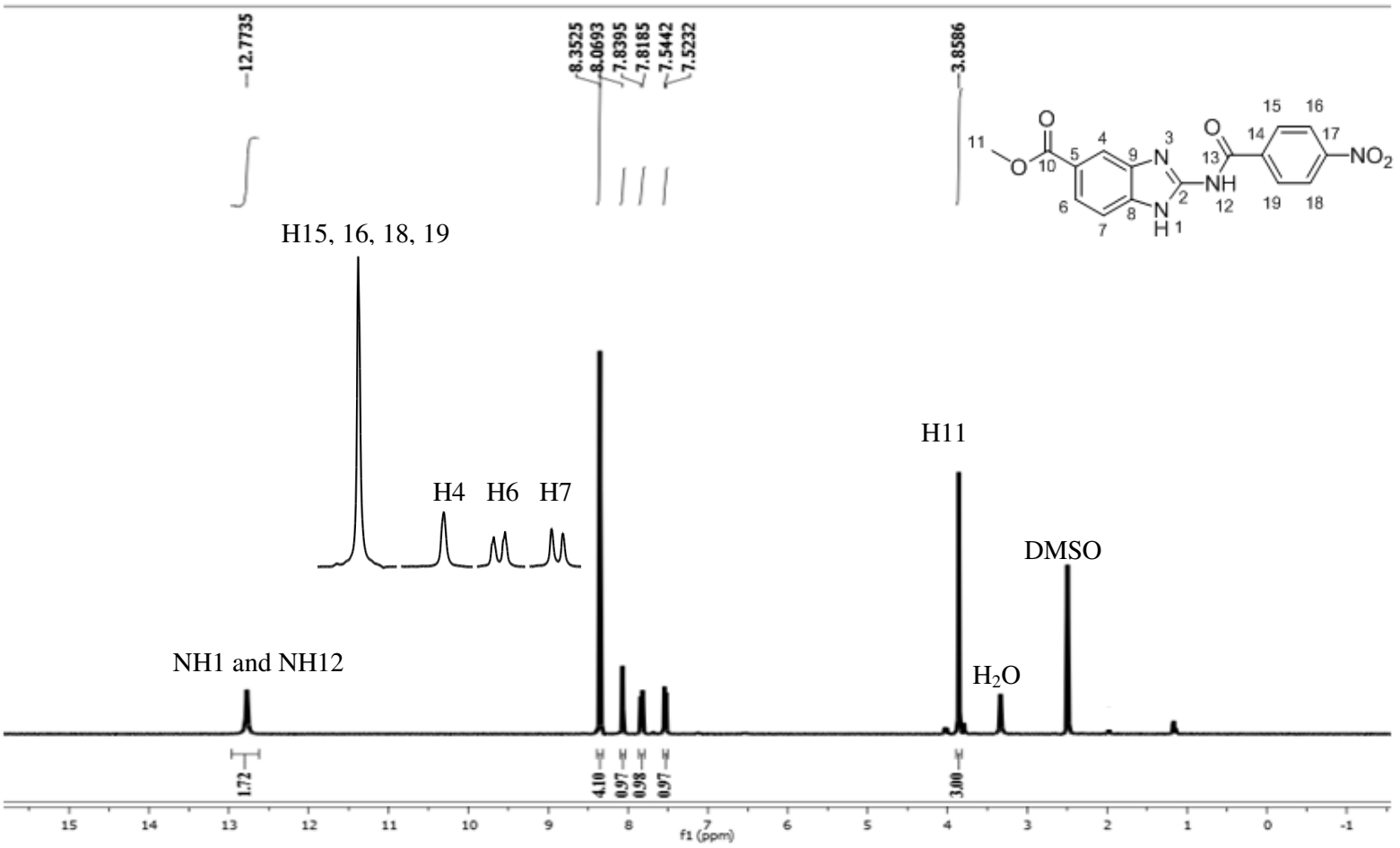

Figure 46: ^{1}H NMR spectrum of compound **95**.

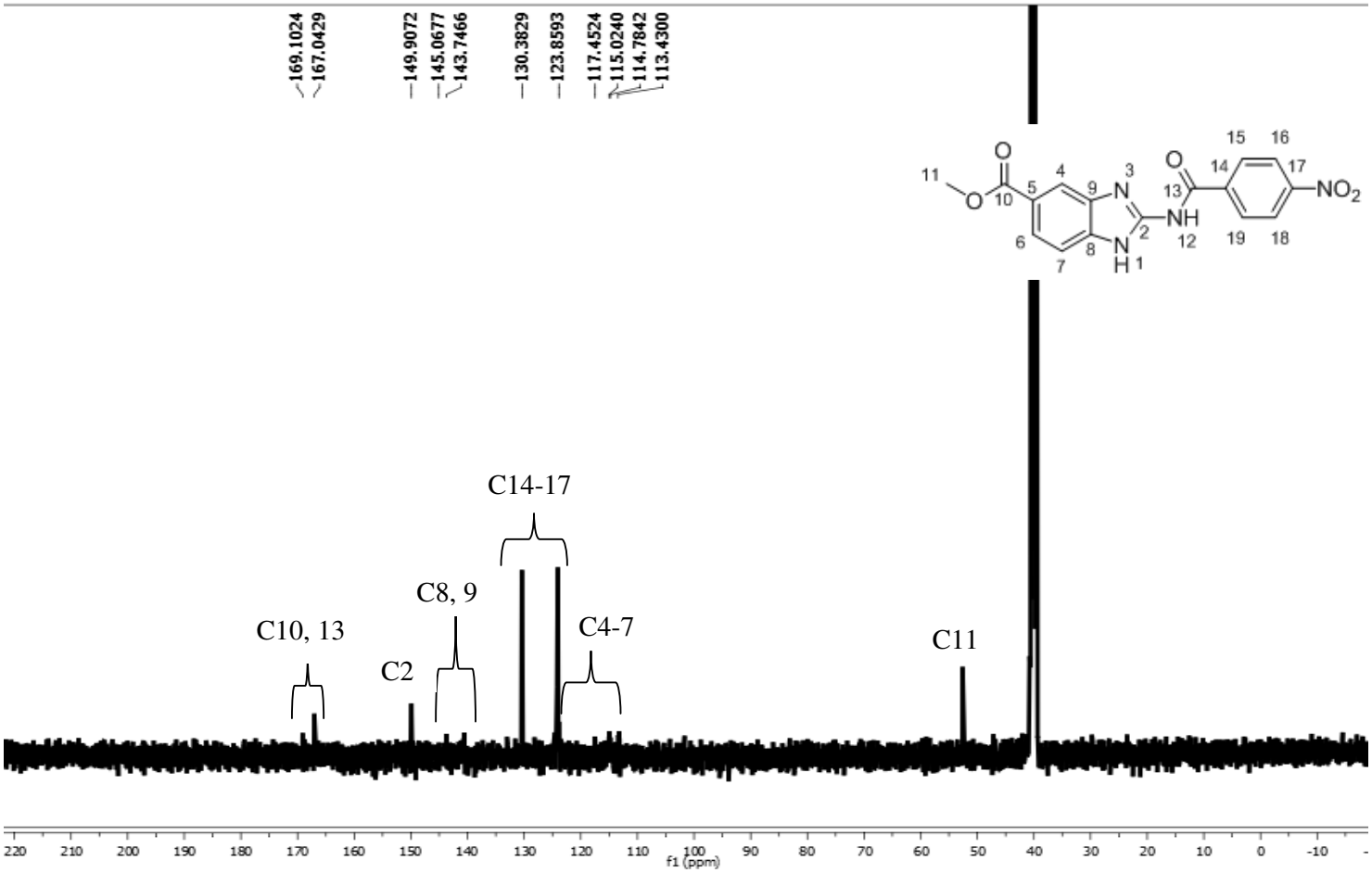

Figure 47: ^{13}C NMR spectrum of compound **95**.

The sulfonamide derivatives from this series were synthesised by two methods. Firstly, compound **70**, **71** or **72** were reacted with different sulfonyl chlorides under anhydrous conditions and using triethylamine (TEA) as a base (**Scheme 6**).[100]

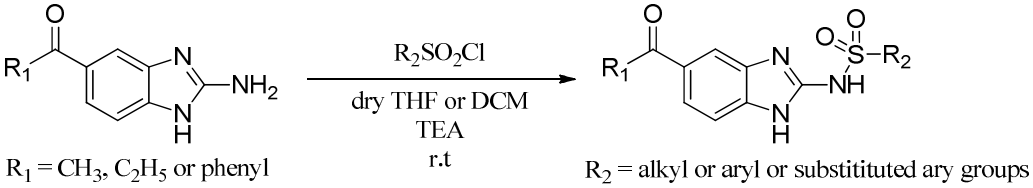

Scheme 6: Sulfonamide formation by using sulfonyl chloride.

The yield for this reaction was lower than that for amide formation (35-75%), which could be due to a steric factor that hinders nucleophilic attack of the amino group on the electrophilic sulphur compared with the carbon. Comparison of the two dihedral angles (Cl-CO-C *vs* Cl-SO_2-C) reveals that the angle in the sulfonyl chloride is 109°, which is narrower than the 120° angle of the acid chloride, and hinders access by the incoming nucleophile (**Figure 48**).

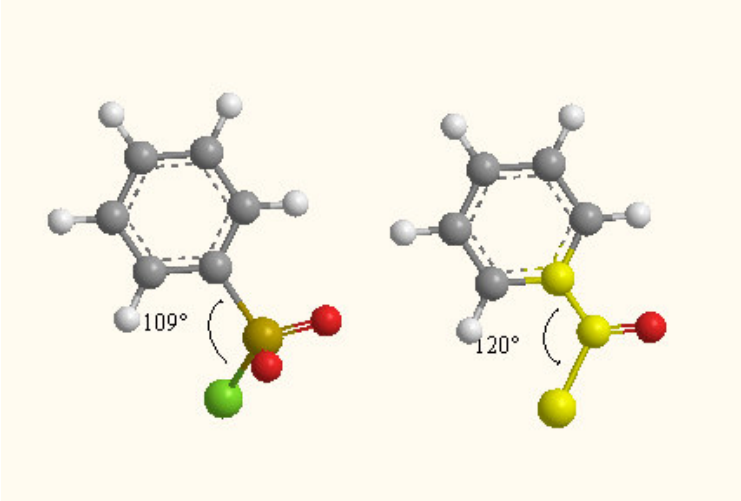

Figure 48: A comparison between the dihedral angle of Cl-SO_2-C (left) and Cl-CO-C (right) in benzenesulfonyl chloride and benzoyl chloride using the 3D ChemBioDraw® software prediction.

To improve the yield, an alternative method was used which involved mixing the amine and the sulfonyl chloride with pyridine as both base and solvent.[109-111] This improved the yield of the reaction as can be seen with compounds **99**, **100**, **101** and

108 compared to the others from this library (**Table 25**), probably through the formation of pyridinium salt intermediate that acts as a better leaving group than the chloride (**Scheme 7**). This seems to compensate for the steric hindrance of the amino group attack on sulfonyl chloride and was used in the synthesis of most of the sulfonamide derivatives from this library as well as other scaffolds.

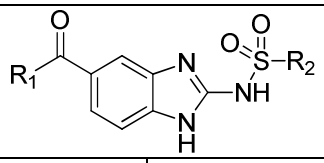

Compound	R_1	R_2	% yield
97	OC_2H_5	phenyl	47
98	OCH_3	4-chlorophenyl	44
99	OCH_3	4-methoxyphenyl	75
100	phenyl	phenyl	60
101	phenyl	4-nitrophenyl	62
102	OCH_3	3-dimethylaminonaphthyl	45
103	OCH_3	4-methylphenyl	58
104	phenyl	4-methylphenyl	45
105	OCH_3	butyl	35
106	phenyl	3-dimethylaminonaphthyl	55
107	OCH_3	4-nitrophenyl	42
108	OCH_3	3-nitrophenyl	60

Table 25: Sulfonamide derivatives of the 2-amino-1*H*-benzo[*d*]imidazole scaffold.

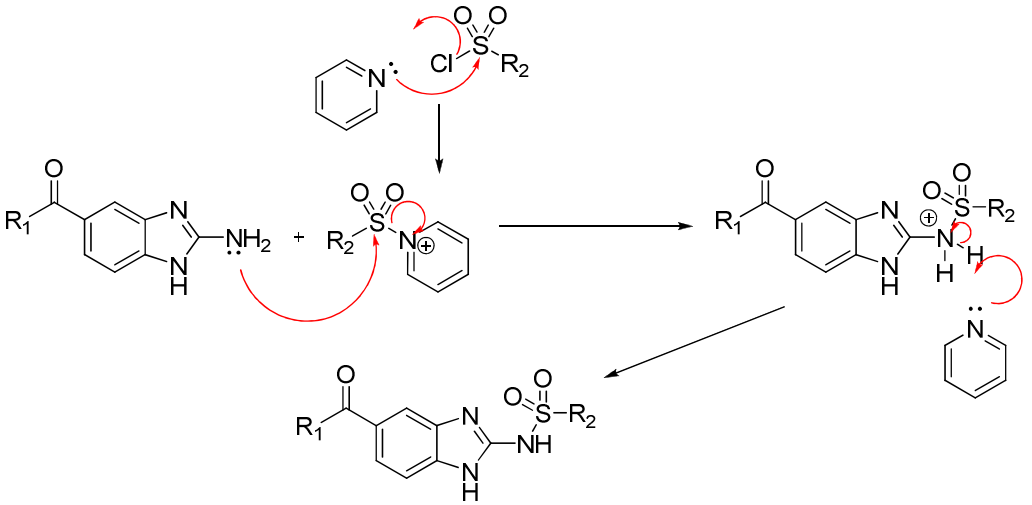

Scheme 7: Mechanism of sulfonamide formation using pyridine.

Hydrolysis of the ester using the basic hydrolysis conditions mentioned earlier in this section unfortunately cleaved both the ester and the sulfonamide despite literature precedence, [112] even when using a reduced amount of NaOH and shortening the reaction duration from 10-24 hours to 2 hours.

A milder method reported in literature in which the ester was added to a cooled solution of potassium tert-butoxide in an ether/water mixture [110] was also unsuccessful, and no hydrolysis was observed perhaps due to a solubility problem- almost all the compounds used here were sparingly soluble in the ether/water mixture.

The third attempt to hydrolyse the ester without affecting the sulfonamide moiety involved the use of 4-6 equivalents of lithium hydroxide in water/THF or methanol as a co-solvent at room temperature and over differing periods of time.[113] Again, these conditions either resulted in hydrolysing both the ester and sulfonamide linkage or did not hydrolyse either.

4.2 Synthesis of 2-aminobenzo[*d*]thiazole-6-carboxylate derivatives

The most practical and common method to synthesise the 2-aminobenzo[*d*]thiazole-6-carboxylate derivatives is through the reaction of commercially available methyl 4-aminobenzoate with potassium thiocayante and bromine in glacial acetic acid in a two step reaction (**Scheme 8**) at room temperature for 48 hours. Methyl 2-aminobenzo[*d*]thiazole-6-carboxylate, **51** was then purified by recrystallization from methanol.

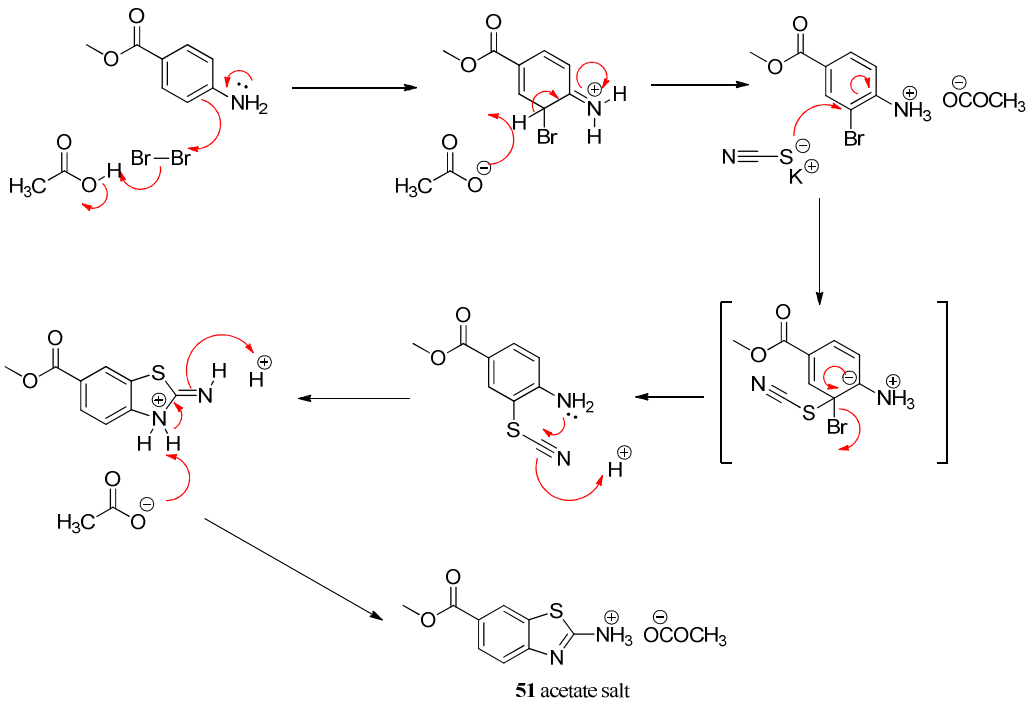

Scheme 8: Synthetic mechanism of **51** as the main precursor for 2 aminobenzo[*d*]thiazole-6-carboxylate derivatives.

Analysis of the ^{1}H NMR spectrum of compound **51** (**Figure 49**) shows that there is a doublet at δ 7.35 ppm that represents H4 which is *ortho* coupled to H5. The signal of the latter appears as doublet of doublets at δ 7.80 ppm with a *J* coupling constant of 8.36 Hz which represents *ortho* coupling to H5, and a smaller coupling of 1.76 Hz that corresponds to the *meta* coupling to H7. These coupling patterns confirm the formation of the benzothiazole ring substituted at both position 2 and 5. The broad singlet at δ 7.90 ppm corresponds to the primary amine attached to position-2, and the doublet at δ 8.28 ppm represents H7 *meta* coupled to H5.

The ^{13}C NMR spectrum (**Figure 50**) shows the same pattern found in benzimidazole **70**, in which signals for C4-7 appear at δ 117.6-123.2 ppm, but the more deshielded C8 and C9 signals appear at δ 157.4 and 166.7 ppm, respectively. As expected, C2 is the most deshielded in the ring since it is attached to two electronegative atoms and appears at δ 166.7 ppm. Finally the carbonyl carbon C10 is shifted downfield and found at δ 170.3 ppm.

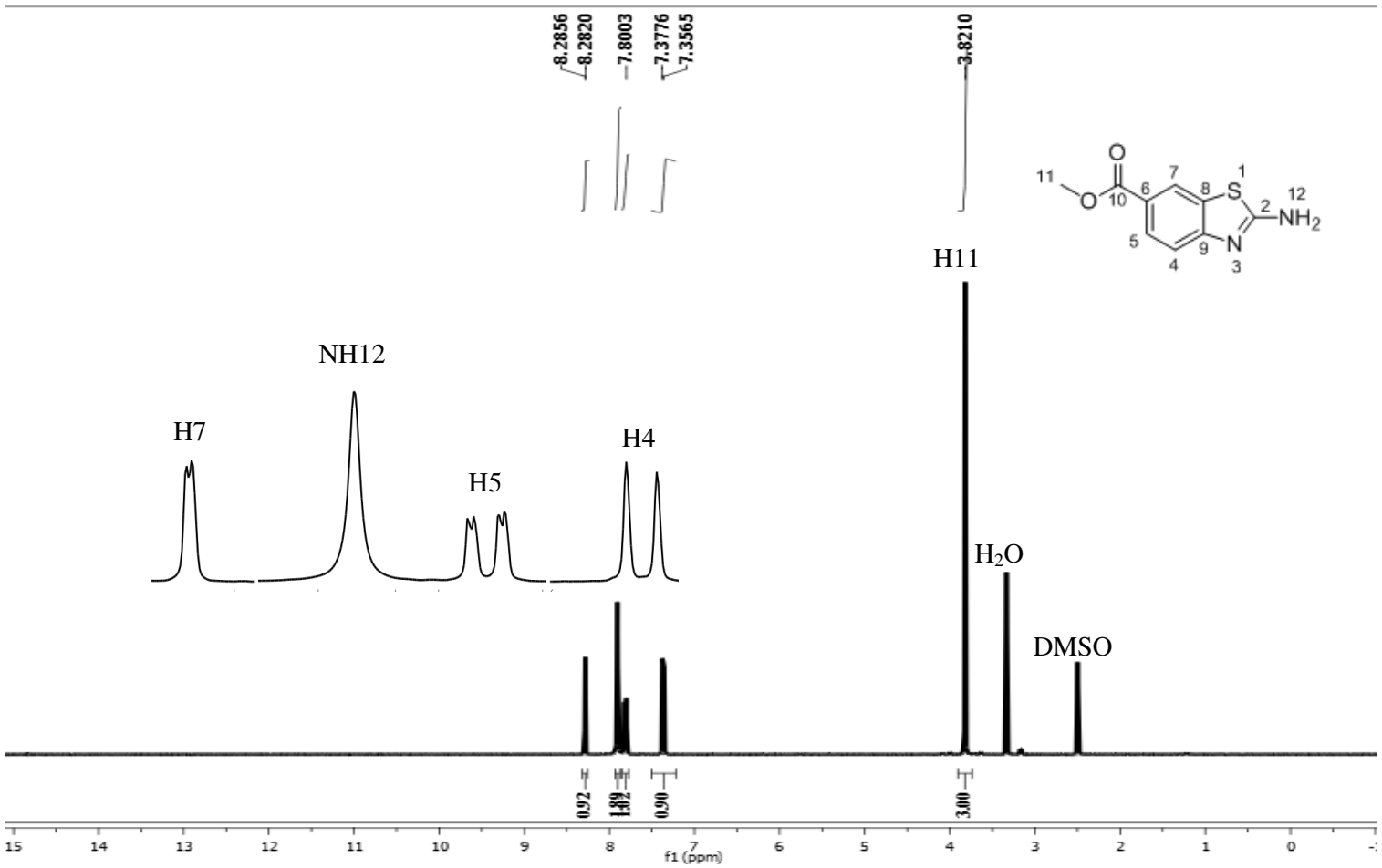

Figure 49: ^{1}H NMR spectrum of compound **51**.

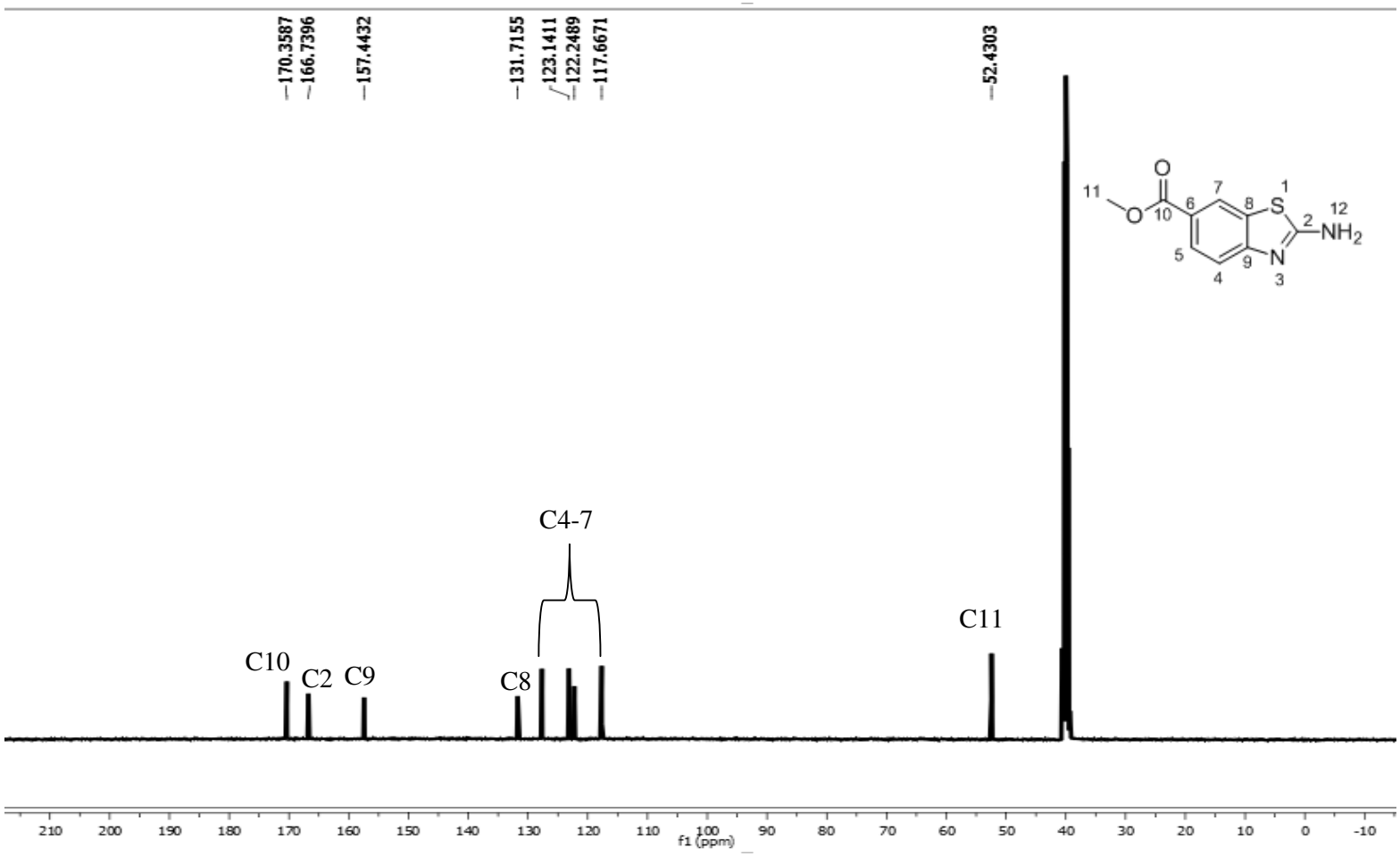

Figure 50: ^{13}C NMR spectrum of compound **51**.

The formation of the amide and sulfonamide derivatives from this library was achieved using the previously mentioned methods for the 2-amino-1*H*-benzo[*d*]imidazole-5-carboxylate library synthesis, although reaction times are longer and lower yielding.

The carboxylic acid derivatives from this library were obtained by basic hydrolysis of the ester derivatives to give the corresponding acids in good yields (**Scheme 9**). The derivatives synthesised are shown in **Table 26** and **27**.

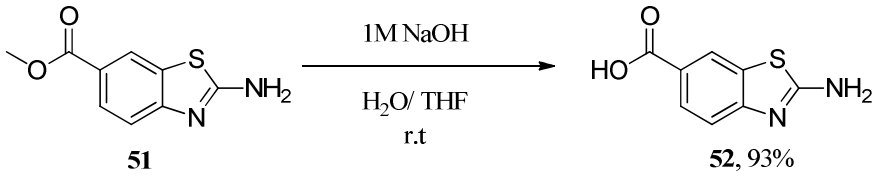

Scheme 9: Hydrolysis of ester derivatives from the 2-aminobenzo[*d*]thiazole-6-carboxylate library.

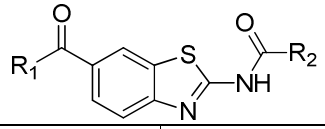

Compound	R_1	R_2	% yield
53	OCH_3	$(CH_2)_8CH_3$	54
54	OH	$(CH_2)_8CH_3$	52
55	OCH_3	$(CH_2)_4CH_3$	49
56	OH	$(CH_2)_4CH_3$	65
60	OCH_3	phenyl	60
57	OCH_3	CH_3	62
61	OCH_3	4-nitrophenyl	30
62	OCH_3	4-methoxyphenyl	25
63	OCH_3	4-chlorophenyl	45

Table 26: Amide derivatives from 2-aminobenzo[*d*]thiazole-6-carboxylate scaffold.

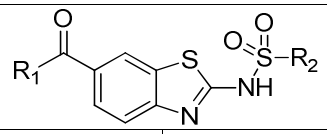

Compound	R_1	R_2	% yield
58	OCH_3	CH_3	25
59	OCH_3	$(CH_2)_2CH_3$	15
64	OCH_3	phenyl	55
65	OH	phenyl	45
66	OCH_3	4-methoxyphenyl	22
67	OCH_3	4-nitrophenyl	14
68	OCH_3	4-chlorophenyl	35
69	OCH_3	4-methylphenyl	43

Table 27: Sulfonamide derivatives from 2-aminobenzo[*d*]thiazole-6-carboxylate scaffold.

However, the same problem seen with the benzimidazole library was observed when attempting to hydrolyse the ester in the presence of the sulfonamide moiety. Compound **65** was the only free acid obtained using lithium hydroxide and this method was unsuccessful for the other derivatives.

Figure 51 represents the ^{1}H NMR for compound **64** as an example of structural elucidation applied to this series of compounds. The common signals found in compound **51** in which the doublet, doublet of doublets and doublet system corresponds to H4, 5 and 7, respectively, is conserved in all these compounds. H4 appears as a doublet at δ 7.36 ppm with *J* coupling of 8.36 Hz with H5, which is as doublet of doublets at δ 7.96 ppm. The latter has two coupling constants; *ortho* (8.36 Hz) with H4 and *meta* (1.36 Hz) with H7, which appears as a doublet with a coupling constant of 1.36 Hz. The five aromatic protons of the benzenesulfonamide appear as follows; the doublet at δ 7.57 ppm with *J* coupling of 7.38 Hz corresponds to H15 and 17; the triplet at δ 7.62 ppm with *J* coupling of 7.28 Hz is H16; and the doublet at δ 7.86 ppm with *J* coupling of 7.20 Hz corresponds to H14 and 18. The NH proton in this compound was not seen because of solvent exchange.

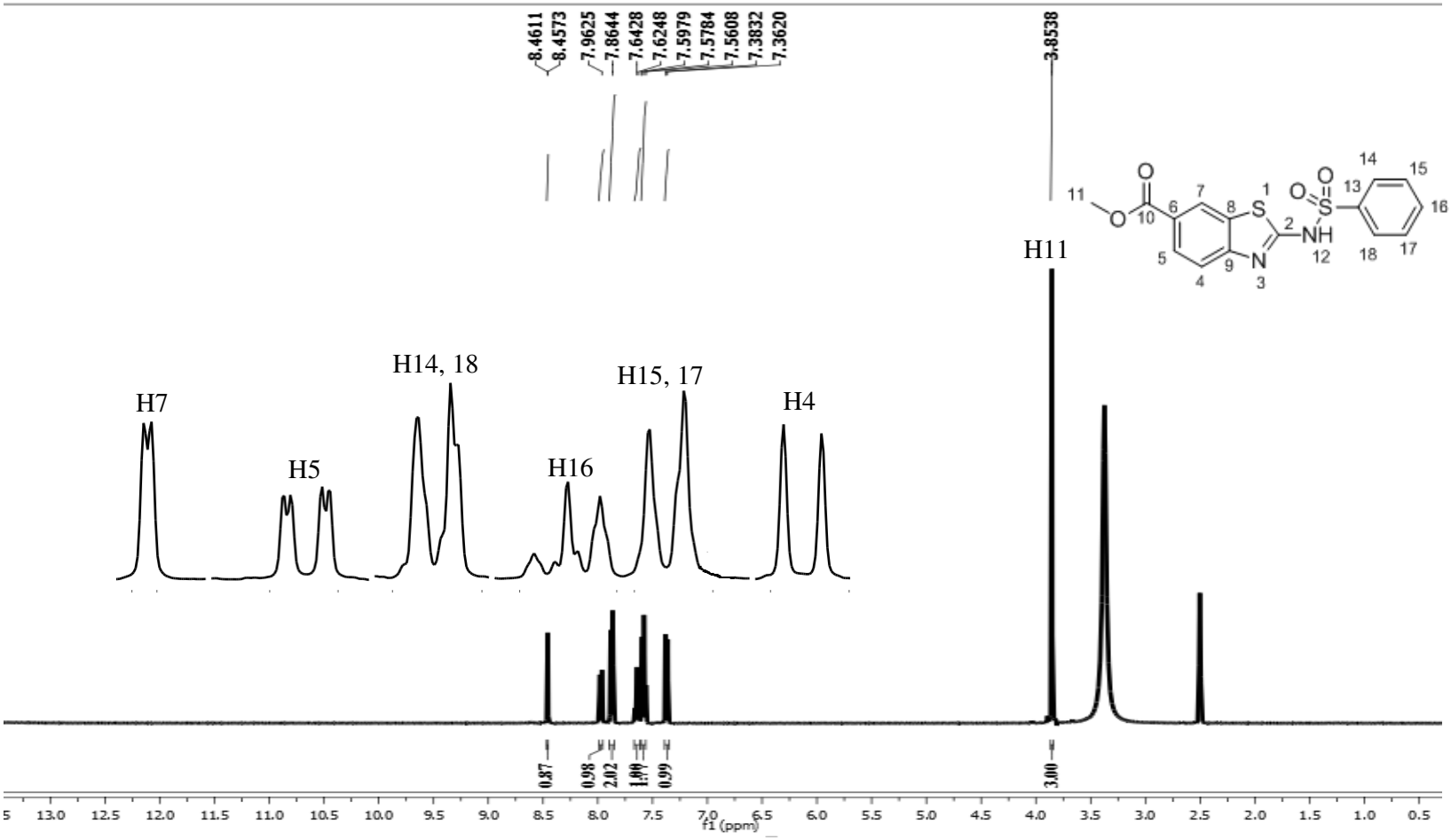

Figure 51: ^{1}H NMR spectrum of compound **64**.

4.3 Synthesis of 2-amino-1*H*-imidazole-5-carboxylate derivatives

Many methods have been reported in the literature for the synthesis of 2-amino[*H*]imidazole.[114-116] Although they are widely used for the formation of imidazoles bearing an amino group at position-2 and other groups at positions 4 and 5, none report a carbonyl substituent in these latter positions. Since a carboxylate moiety was important in our designed compounds, another method has been used which incorporated the substituent from the start.[117-120] Firstly, ethyl 4-methyl-1*H*-imidazole-5-carboxylate was treated under basic conditions with a diazonium salt previously prepared from sodium nitrite and a substituted aniline. The azo intermediate was then separated by extraction to give **135** and **136**. The amino group at position-2 was obtained after catalytic hydrogenation of the azo group by using platinum oxide IV (PtO_2) as a metal catalyst under 45 *psi* internal pressure. The crude product was then purified by crystallization to give ethyl 2-amino-4-methyl-1*H*-imidazole-5-carboxylate (**AIC**) in moderate yield (**Scheme 10**).

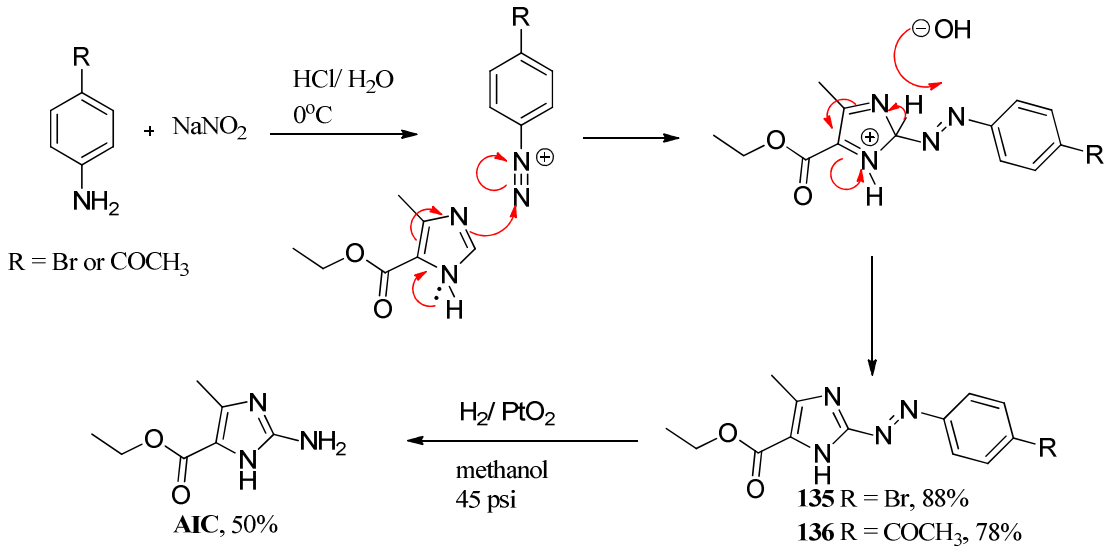

Scheme 10: Synthesis of **AIC** through the azo intermediate.

The ^{1}H NMR spectrum of compound **135** (**Figure 52**) showed the characteristic broad signal at δ 13.39 ppm that corresponds to the imidazole NH proton. The ethyl ester signals come as triplet/quartet signals at δ 1.31 and 4.27 ppm, with *J* coupling of 7.04 Hz. The singlet at δ 2.52 ppm corresponds to the methyl group at position-4 which is deshielded by the ring.

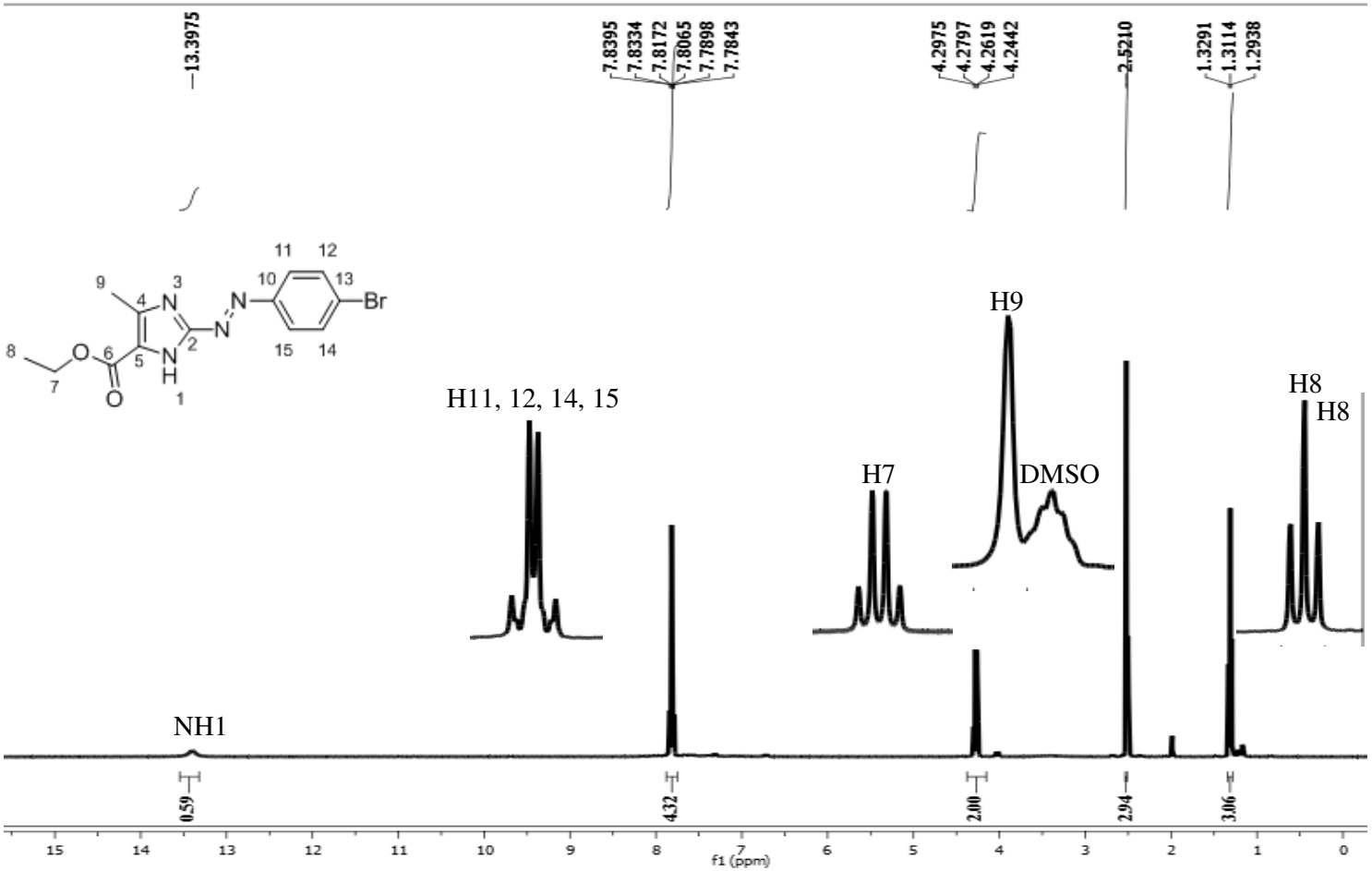

Figure 52: ^{1}H NMR spectrum of compound **135**.

The amide derivatives containing the 2-amino-1*H*-imidazole-5-carboxylate scaffold were synthesised by treating **AIC** with suitable acid chlorides under anhydrous conditions and the addition of TEA. The yields for this reaction as expected were moderate to good. The carboxylic acid derivatives were prepared by basic hydrolysis of the corresponding esters at room temperature. These compounds are shown in **Table 28**.

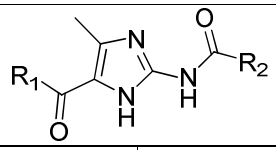

Compound	R_1	R_2	% yield
139	OC_2H_5	$(CH_2)_8CH_3$	52
140	OH	$(CH_2)_8CH_3$	62

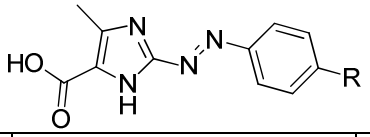

Compound	R	% yield
137	Br	38
138	COOH	30

Table 28: 2-amino-1*H*-imidazole-5-carboxylate derivatives.

4.4 Synthesis of 2-aminothiazole-5-carboxylate derivatives

The most practical and efficient method to synthesise the 2-aminothiazole-5-carboxylate scaffold was suggested by Barton and his group.[121] The reaction involves two steps; formation of the α-halo glycidic ester as the main intermediate (and β-halo-α-oxo ester as minor intermediate), followed by ring formation after addition of thiourea. The first step involves the Darzens reaction between an aldehyde and methyl dichloroacetate at 0˚C in diethyl ether in the presence of sodium methoxide as a strong base.[122] After washing with water, the diethyl ether was evaporated under vacuum to give the α-halo glycidic ester (**Scheme 11**). Since the α-halo glycidic ester is highly reactive, it was directly used for the second step without further purification. Position-4 of the target **ATC** scaffold is determined by the nature of the aldehyde used in this first step; for example a 4-phenyl substituted **ATC**

would use benzaldehyde, and a 4-phenethyl substituted **ATC** would use 3-phenylpropanal.

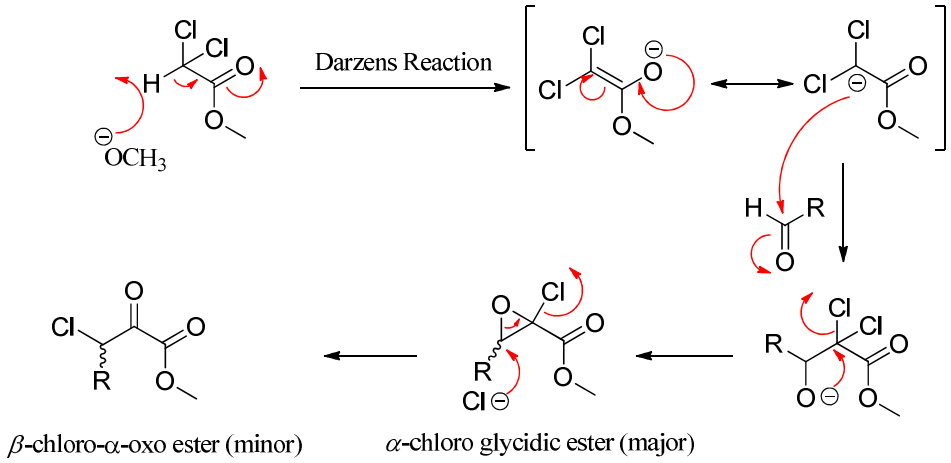

Scheme 11: Mechanism of the formation of *α*-chloroglycidic acid and *β*-chloro-oxo ester.

The second step involves the coupling between the *α*-chloroglycidic intermediate and thiourea in dry methanol to give the methyl 2-aminothiazole-5-carboxylate scaffold. The reaction proceeds *via* nucleophilic attack of the thiourea sulfur atom on the epoxide carbon which leads to epoxide ring opining and the formation of a new *α* -carbonyl moiety. Formation of the thiazole ring was achieved by subsequent nucleophilic attack of the thiourea amino group on the *α*-carbonyl carbon in a common Schiff's base reaction to form the thiazolidine ring. Two dehydration steps of the thiazolidine ring then restore the aromaticity of the thiazole ring (**Scheme 12**).

A number of different **ATC** scaffolds were prepared with different 4-substituents (**Table 29**) and were used in the synthesis of the 2-amido derivatives as described in **Section 4.1**.

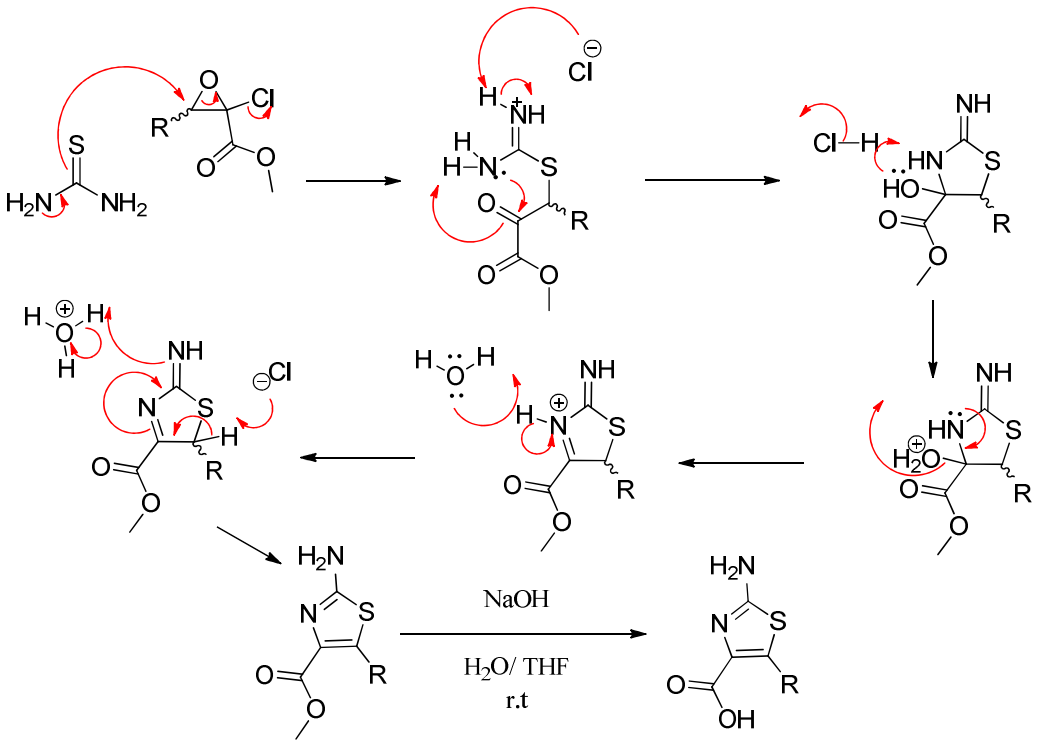

Scheme 12: Mechanism of thiazole ring formation by the coupling between α-chloroglycidic ester and thiourea, and the hydrolysis of ester to carboxylic acid.

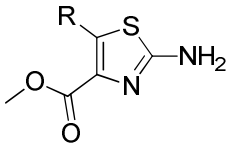		% yield
193	isopropyl	53
194	ethyl	29[†]
195	methyl	65
196	propyl	34
197	butyl	11[*]
198	phenyl	21[*]
199	benzyl	68
200	4-chlorophenyl	46[*]
201	4-methoxyphenyl	27[*]
202	phenyl$(CH_2)_2$	58

Table 29: **ATC** compounds used as precursors for the 2-aminothiazole-5-carboxylate derivatives

[†] Compounds prepared by another researcher

The structural elucidation of these compounds was performed by studying the ^{1}H and ^{13}C NMR spectra to confirm the formation of the thiazole ring. As an example, **Figure 53** illustrates the proton NMR of compound **199**, in which the benzylic proton (H6) appears as a singlet downfield at δ 4.33 ppm due to it being between two aromatic groups. The singlet at δ 3.74 ppm corresponds to the methyl ester protons (H14) and is shifted downfield due to the withdrawal effect of the oxygen atom. The presence of the amino group at position-2 is confirmed by the broad singlet at δ 7.04 ppm which is found in all the 2-aminothiazole-5-carboxylates from **Table 29**. A multiplet at δ 7.19-7.32 ppm represents the five phenyl protons.

For compound **199** (**Figure 54**), the ^{13}C NMR spectrum revealed that there is a carbon atom at δ 32.6 ppm which corresponds to the benzylic carbon directly attached to the thiazole ring. The characteristic signals at δ 137.3 and 140.6 ppm correspond to C4 and 5 in the thiazole ring. The highly deshielded signal at δ 163.2 ppm, which corresponds to C2, confirms the formation the thiazole since this atom is attached to two electronegative nitrogen atoms. Finally, the mostly deshielded signal at δ 165.3 ppm represents the carbonyl carbon (C13).

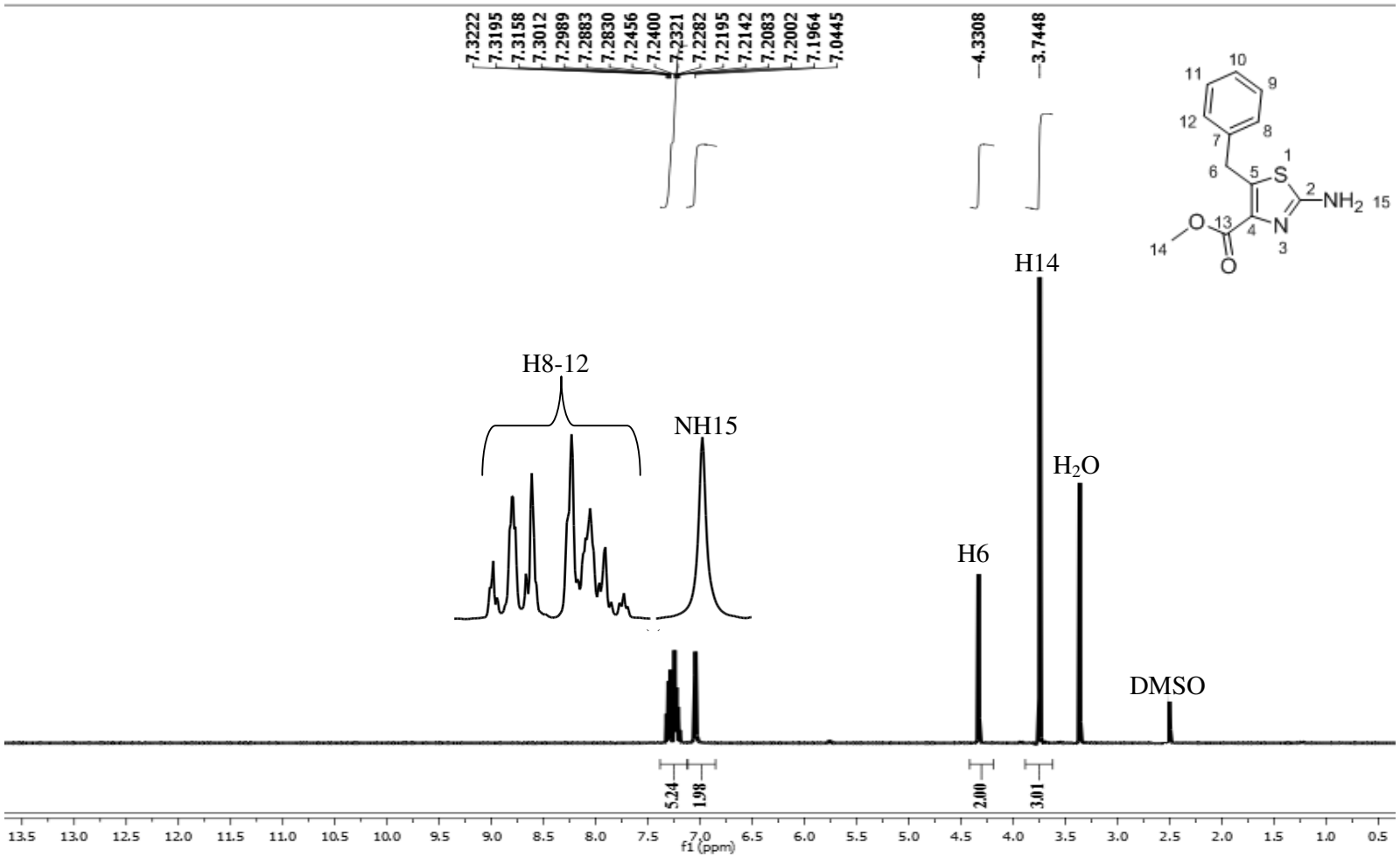

Figure 53: ^{1}H NMR spectrum of compound **199**.

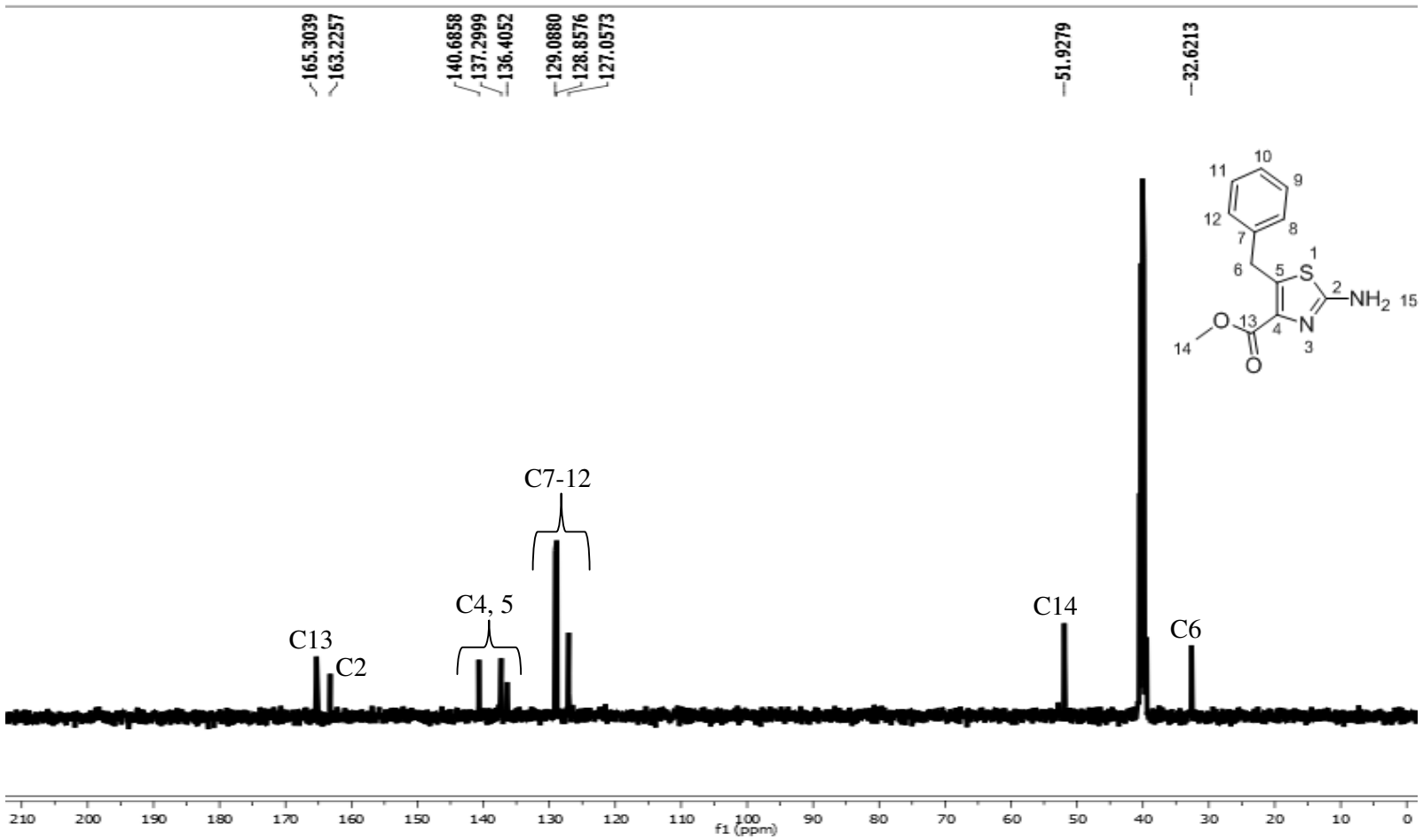

Figure 54: ^{13}C NMR spectrum of compound **199**.

These compounds were coupled with different acid chlorides using the method for the synthesis of 2-amino-1*H*-benzo[*d*]imidazole-5-carboxylate derivatives and the yields were moderate to good. A series of compounds with different groups ranging from simple aliphatic chains to unsubstituted and substituted aromatic rings were prepared, and then were hydrolysed to their carboxylic acids using base-catalysed hydrolysis (**Table 30**).

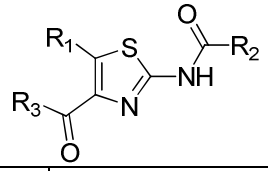

Compound	R_1	R_2	R_3	% yield
109	-(CH_2) phenyl	-$(CH_2)_8CH_3$	OCH_3	68
110	-(CH_2) phenyl	-$(CH_2)_8CH_3$	OH	58
111	isopropyl	-$(CH_2)_8CH_3$	OCH_3	70
112	isopropyl	-$(CH_2)_8CH_3$	OH	45
113	ethyl	-$(CH_2)_8CH_3$	OCH_3	59
114	ethyl	-$(CH_2)_8CH_3$	OH	52
115	n-propyl	-$(CH_2)_8CH_3$	OCH_3	65
116	n-propyl	-$(CH_2)_8CH_3$	OH	57
117	n-butyl	-$(CH_2)_8CH_3$	OCH_3	49
118	n-butyl	-$(CH_2)_8CH_3$	OH	62
119	4-chlorophenyl	-$(CH_2)_8CH_3$	OCH_3	39
120	4-chlorophenyl	-$(CH_2)_8CH_3$	OH	25
121	4-methoxyphenyl	-$(CH_2)_8CH_3$	OCH_3	43
122	4-methoxyphenyl	-$(CH_2)_8CH_3$	OH	65
123	benzyl	-$(CH_2)_8COOCH_3$	OCH_3	28
124	benzyl	-$(CH_2)_8COOH$	OH	68
141	isopropyl	-CH_2(4-methoxyphenyl)	OCH_3	76
142	isopropyl	-CH_2(4-methoxyphenyl)	OH	77
143	isopropyl	benzyl	OCH_3	57
144	isopropyl	benzyl	OH	43
145	isopropyl	-CH_2(3-methoxyphenyl)	OCH_3	64
146	isopropyl	-CH_2(3-methoxyphenyl)	OH	80
147	isopropyl	-CH_2(4-chlorophenyl)	OCH_3	69
148	isopropyl	-CH_2(4-chlorophenyl)	OH	73
149	benzyl	-CH_2(4-methoxyphenyl)	OCH_3	93
150	benzyl	-CH_2(4-methoxyphenyl)	OH	78
151	benzyl	-CH_2(3-methoxyphenyl)	OCH_3	96
152	benzyl	-CH_2(3-methoxyphenyl)	OH	89
153	benzyl	-CH_2(4-chlorophenyl)	OCH_3	92
154	benzyl	-CH_2(4-chlorophenyl)	OH	40

Table 30: 2-amidothiazole-5-carboxylate derivatives.

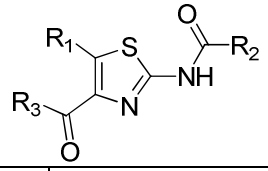

Compound	R_1	R_2	R_3	% yield
155	benzyl	-CH_2(4-nitrophenyl)	OCH_3	34
156	benzyl	-CH_2(4-nitrophenyl)	OH	40
157	benzyl	-CH_2(cyclohexyl)	OCH_3	83
158	benzyl	-CH_2(cyclohexyl)	OH	67
159	isopropyl	-CH_2(cyclohexyl)	OCH_3	56
160	isopropyl	-CH_2(cyclohexyl)	OH	87
161	ethyl	4-butoxyphenyl	OCH_3	41
162	ethyl	4-butoxyphenyl	OH	51
163	n-propyl	4-butoxyphenyl	OCH_3	45
164	n-propyl	4-butoxyphenyl	OH	73
165	n-butyl	4-butoxyphenyl	OCH_3	74
166	n-butyl	4-butoxyphenyl	OH	58
167	Phenyl	4-butoxyphenyl	OCH_3	34
168	phenyl	4-butoxyphenyl	OH	75
169	benzyl	4-chlorophenyl	OCH_3	51
170	benzyl	4-chlorophenyl	OH	77
171	isopropyl	4-methoxyphenyl	OCH_3	51
172	isopropyl	4-methoxyphenyl	OH	47
173	isopropyl	4-chlorophenyl	OCH_3	56

Table 30: continued...

The ^{1}H NMR spectrum of compound **164** (**Figure 55**) showed two superimposed triplets at δ 0.94 ppm that correspond to the terminal methyl groups of the butoxy and the propyl groups. The sextet signal at δ 1.43 ppm with *J* coupling of 7.48 Hz corresponds to H21 which is coupled to the adjacent five protons (H22 and 20). Two adjacent sextet signals appear at δ 1.61-1.75 ppm that represent the four protons of H7 and 20. The signal at δ 3.11 ppm is the methylene group at position-5 adjacent to the thiazole ring. The disappearance of the singlet at δ 3.6-3.9 ppm confirms the hydrolysis of the ester **163** to the corresponding acid **164**. The methylene triplet (H19) downfield at δ 4.06 ppm with *J* coupling of 6.6 Hz is coupled to the two protons at H20. The four phenyl protons appear as two doublet signals at δ 7.01 and 8.08 ppm with an *ortho* coupling of 8.76 Hz.

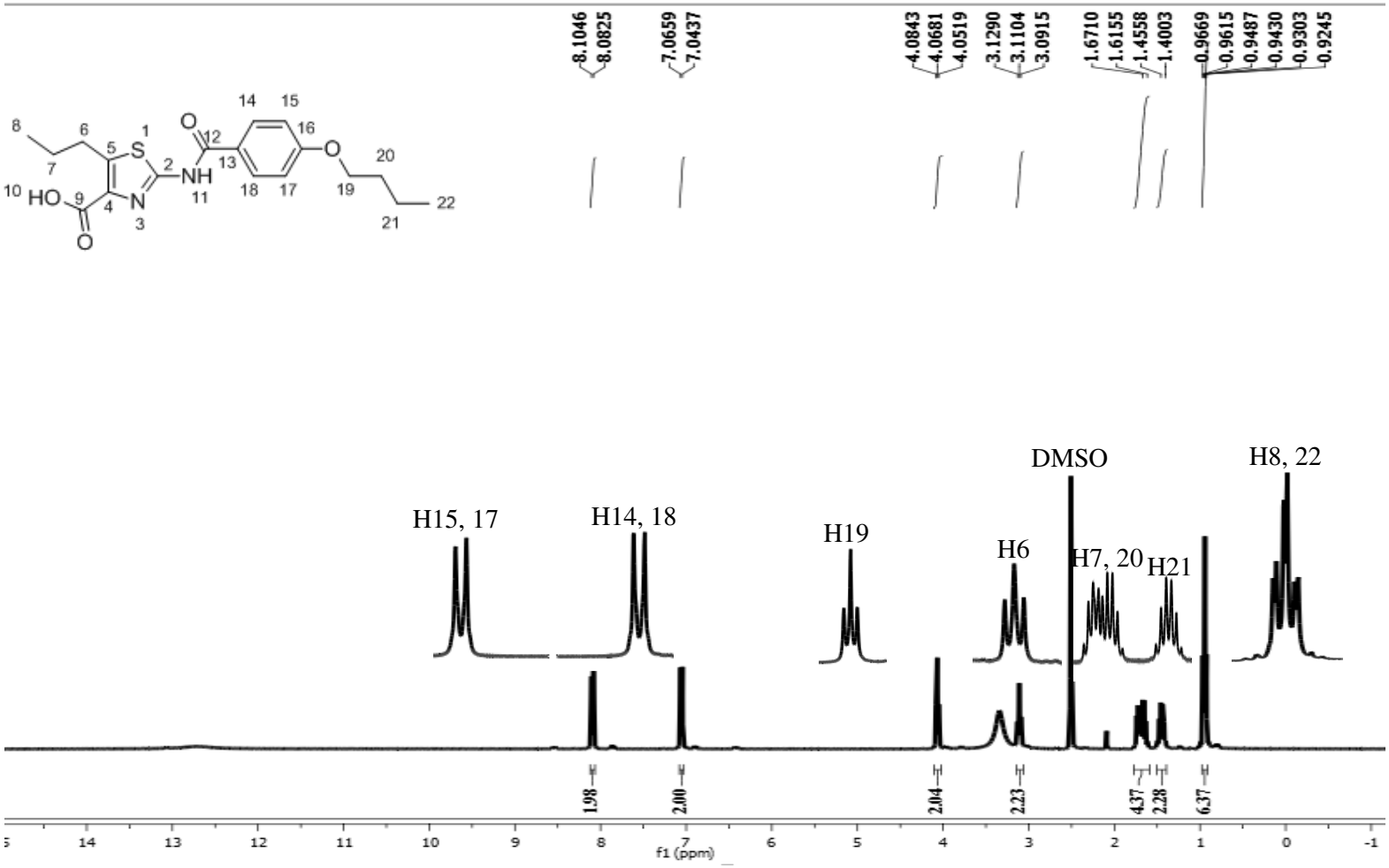

Figure 55: ^{1}H NMR spectrum of compound **164**.

For those acid chlorides not commercially available, oxalyl chloride was used to synthesise the acid chlorides from their corresponding carboxylic acids.[123, 124] This involved heating oxalyl chloride with the appropriate carboxylic acids in a dry solvent, followed by reaction with the 2-aminothiazole using the method previously described for the 2-amino-*1H*-benzo[*d*]imidazole-5-carboxylate library (**Scheme 13**).

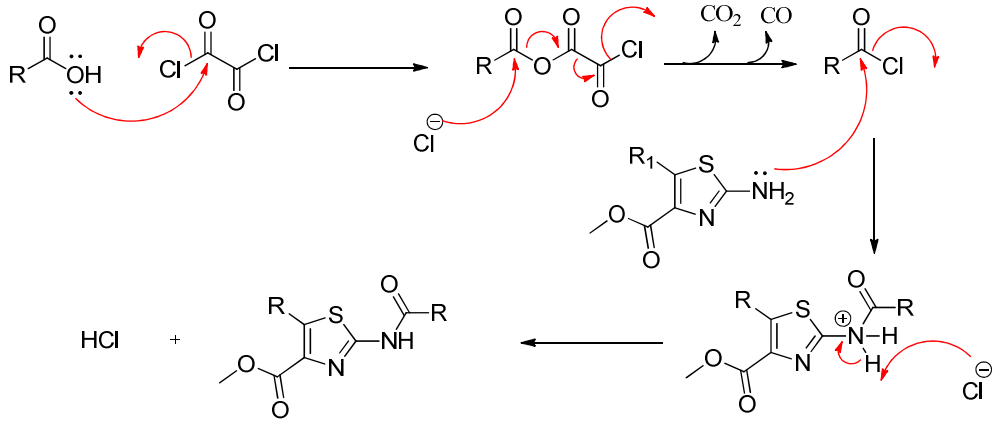

Scheme 13: General procedure for coupling of 2-aminothiazole and carboxylic acids through acid chloride intermediates.

4.5 Synthesis of thiazole-5-carboxamide derivatives

The most active **ATC** compounds, **19** and **27**, were also modified to the corresponding carboxamide. Aminolysis was used to convert the ester by dissolving in 7M ammonia or methylamine in methanol in the presence of potassium cyanide as a catalyst.[125] The solvent was then evaporated to dryness and the product was columned with a suitable solvent system to yield the primary and secondary amides. (**Table 31**).

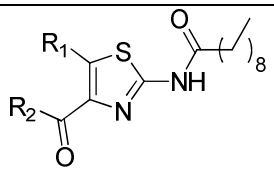

Compound	R_1	R_2	% yield
125	CH_3	NH_2	37
126	CH_3	$NHCH_3$	66
127	benzyl	NH_2	77
128	benzyl	$NHCH_3$	73

Table 31: thiazole-5-carboxamide derivatives.

The use of potassium cyanide in this reaction was to overcome the poor electrophilicity of the ester alkoxy group. The cyanide ion has nucleophilic properties which enable it to attack the ester carbonyl to form a reactive acyl cyanide intermediate, which in turn is displaced by the amino nucleophile to form the amide (**Scheme 14**).

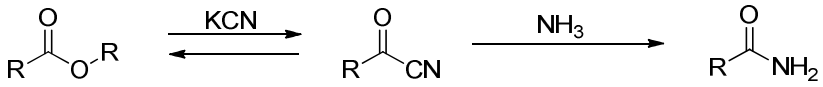

Scheme 14: Aminolysis of ester by using potassium cyanide as a catalyst.

4.6 Synthesis of indole and *β*-carboline containing derivatives

As mentioned in **Chapter Two**, to investigate the importance of the nitro group in **174** and **175**, compounds without nitro groups attached to the thiophene ring were synthesised. Tryptamine was coupled with thiophene-2-carboxylic acid using the propane phosphonic acid anhydride (T3P®) coupling method.[126] Compared with other modern coupling agents such as carbodiimides (DCC) and carbonyldiimidazole (CDI),[106] T3P® has low toxicity and produces purified products in high yield. The proposed mechanism for this reaction is shown in **Scheme 15**.

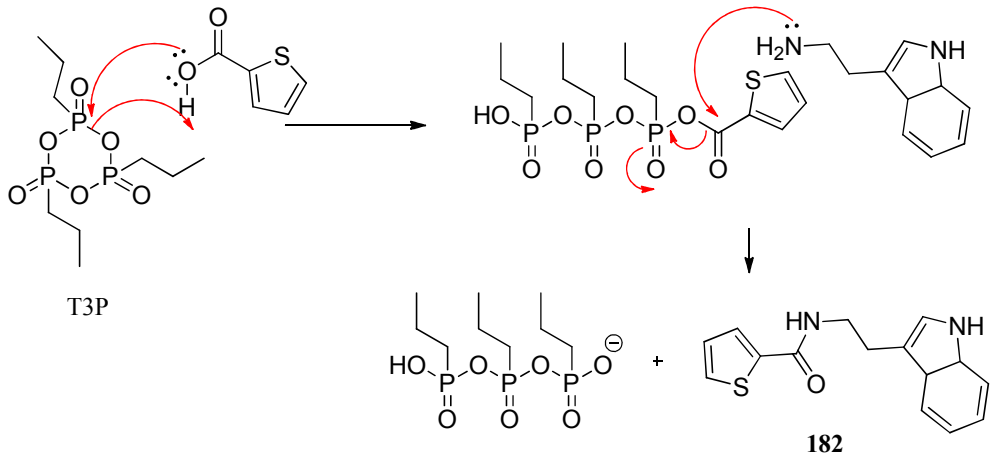

Scheme 15: Mechanism of coupling between tryptamine and carboxylic acids using T3P®.

The reaction proceeds in very good yield and products were obtained after they were precipitated by the addition of a saturated solution of sodium bicarbonate. In other

derivatives, the thiophene ring was replaced by benzene and thiazole rings; the same coupling method with T3P® was used for this purpose, and good yields were obtained after purification by crystallization or column chromatography.

Polar groups at position-5 of the indole ring were introduced by coupling 5-hydroxytryptamine and 5-methoxytryptamine with 2-nitrothiophene-5-carboxylic acid using T3P® to give **187** and **188** in moderate yields (**Table 32**).

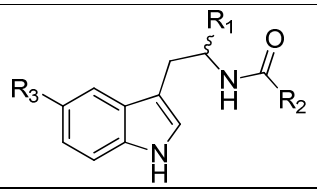

Compound	R_1	R_2	R_3	% yield
179	-(*S*)$COOCH_3$	2-aminothiophen-5-yl	H	67
180	H	2-aminothiophen-5-yl	H	82
190	-(*R*)$COOCH_3$	2-nitrothiophen-5-yl	H	92
181	-(*S*)$COOCH_3$	thiophene-5-yl	H	58
182	H	thiophene-5-yl	H	79
183	H	4-nitrophenyl	H	75
184	H	3-nitrophenyl	H	82
185	H	2-nitrophenyl	H	53
187	H	2-nitrothiophen-5-yl	OH	38
188	H	2-nitrothiophen-5-yl	OCH_3	78

Table 32: Indole derivatives.

To further investigate the importance of the nitro group for activity, it was reduced to amino group. There are many agents that can be used to reduce a nitro group, the most common being catalytic hydrogenation with either platinum oxide II or palladium/carbon as the metal catalysts.[123, 127-129] Although this method is commonly used, in this circumstance the yield was low. An alternative method involves iron reduction under acidic conditions, [130, 131]and compounds **174** and **175** were heated under reflux with iron powder in an ethanol/water mixture and acetic acid, followed by filtration through Kieselghur powder to remove the iron to give the amino derivatives **179** and **180** in good yields (**Scheme 16**). The actual mechanism for nitro reduction with iron metal in acetic acid is not known, but it is believed to be through radical transfer.[132]

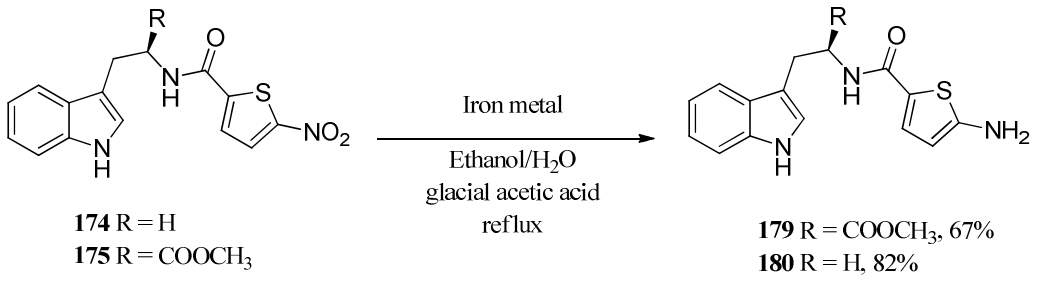

Scheme 16: Reduction of nitro group with iron metal in acetic acid aqueous solution.

The synthesis of the 1,2,3,4-tetrahydro-*β*-carboline scaffold as described in **Chapter Three** was carried out to rigidify the structure. Tetrahydrocarboline synthesis involves the Pictet-Spengler reaction in which tryptamine or *D*-tryptophan hydrochloride undergo ring closure after condensation with an aldehyde, with or without the presence of acid catalyst.[133, 134] The reaction proceeds *via* imine formation between the aliphatic amine and the formaldehyde followed by ring closure *via* nucleophilic attack of the indole double bond on the electrophilic iminium ion, with aromaticity restored by the action of sodium bicarbonate as a base to give compound **189** in low yield. Compound **189** was then coupled with 5-nitrothiophene-2-carboxylic acid using T3P® as the coupling agent to give compound **190** in 74% yield (**Scheme 17**).

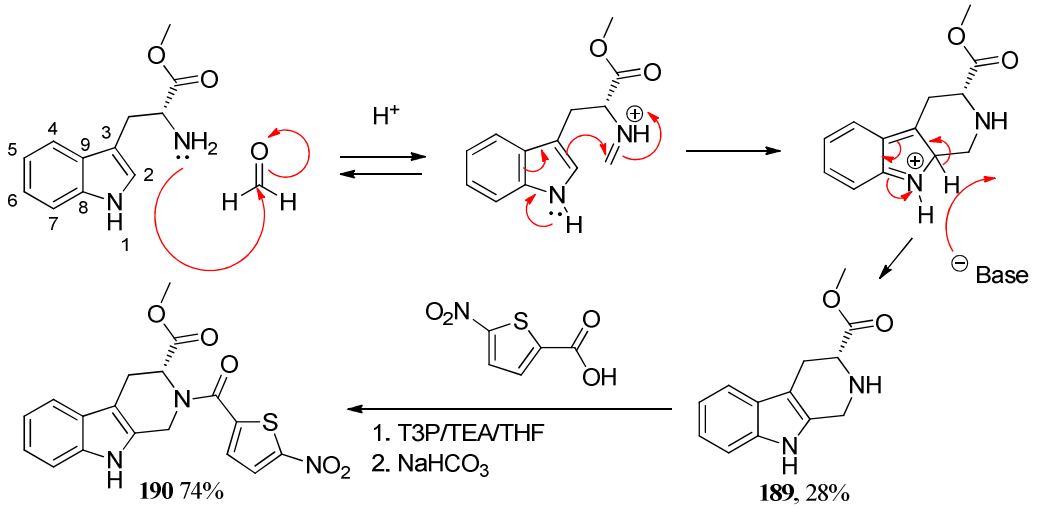

Scheme 17: 1,2,3,4-tetrahydro-*β*-carboline synthesis through Pictet-Spengler reaction.

The formation of the tetrahydrocarboline ring was confirmed using NMR spectroscopy (**Figure 56** and **57**). The absence of the singlet at δ 7.2-7.40 ppm for the proton at position-2 of *D*-tryptophan indole ring (**Scheme 17**) is the first evidence for cyclisation at carbon number 10. The multiplet at δ 2.73 ppm corresponds to one of the ethylene protons (H13), with the other as a doublet of doublets at δ 2.91 ppm with two *J* coupling; one is 6.4 Hz and represents the vicinal coupling with H12, and the other is 14.5 Hz which represents geminal coupling. This coupling pattern is due to the adjacent stereogenic carbon (C12) which makes the H13 protons non-equivalent. The methoxy protons appear as a singlet at δ 3.69 ppm. The single proton, H12 appears as a multiplet which is coupled to both non equivalent protons of H13 as well as the amino proton, NH11. The non equivalent methylene protons at position-2 of the indole appear as a doublet of doublets at δ 3.98 ppm with geminal coupling of 15.96 Hz. Regarding the aromatic protons of the indole, H6 coupled to both H7 and H5 appears as a superimposed doublet of doublets at δ 6.91 ppm with *J* coupling of 7.92 Hz. A superimposed doublet of doublets at δ 7.01 ppm correspond to H5, which is coupled with both H6 and H4 with a coupling constant of 7.92 Hz. The two doublets at δ 7.25 and 7.36 ppm correspond to H4 and H7 respectively with only *ortho* coupling apparent. Finally the singlet at δ 10.73 ppm represents the indole amino proton which is found in almost all our indole derivatives as well as the tetrahydrocarbolines.

The ^{13}C NMR spectrum also confirms the formation of the tetrahydrocarboline ring; a new signal at δ 41.91 ppm corresponds to the arbon atom (C10) after cyclisation. Peaks at δ 25.55, 52.18 and 55.75 represent C13, C15 and C12 respectively. C12 is the most deshielded since it is attached to both carbonyl and amino groups which are electron withdrawing. The aromatic carbons in this compound, as with the other indole derivatives, appear at δ 106.05-136.29 ppm with C8 and 9 being the most deshielded. The carbonyl carbon appears at δ 174.21 ppm, which is the most deshielded carbon in the structure.

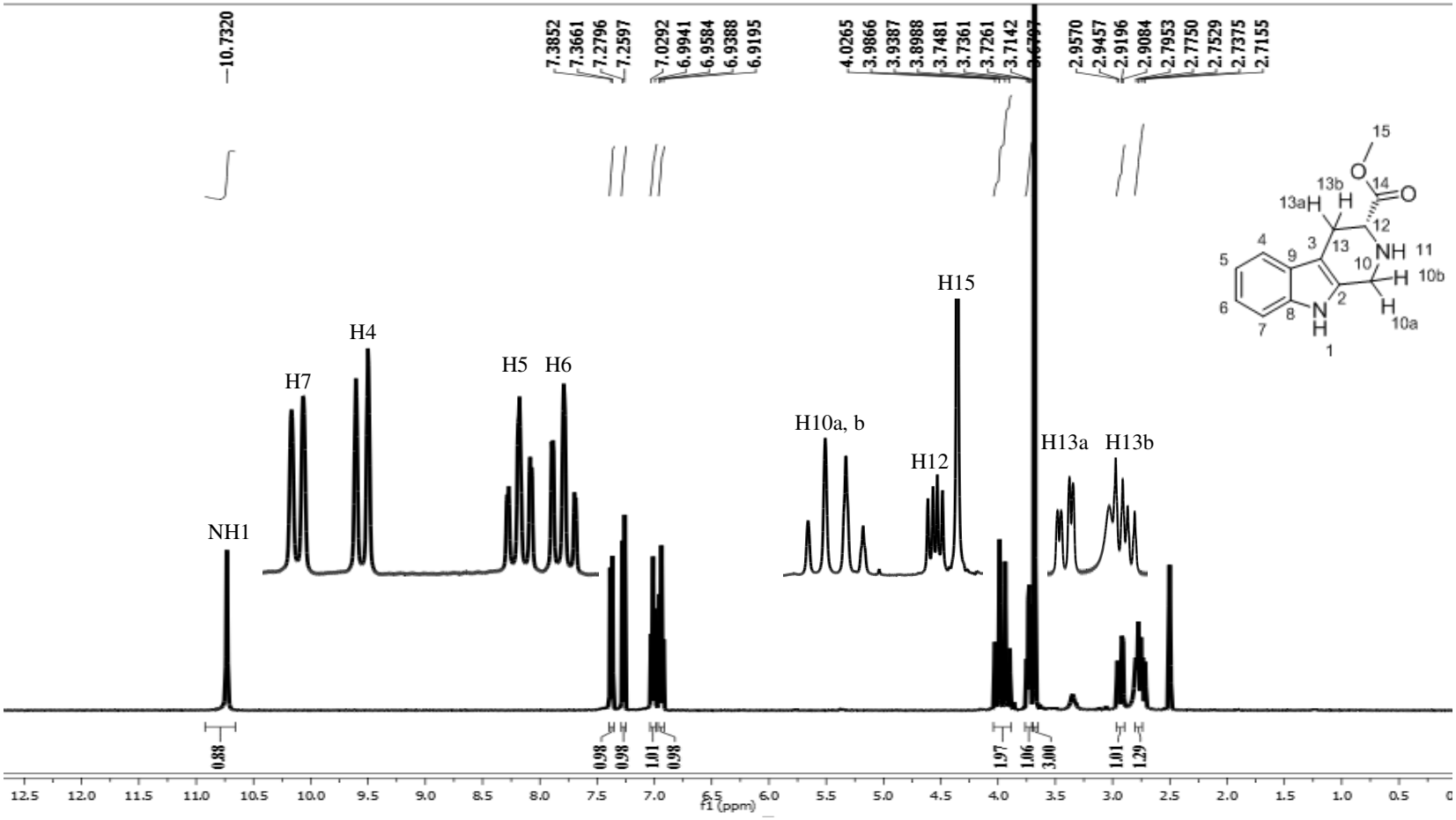

Figure 56: ^{1}H NMR spectrum of compound **189**.

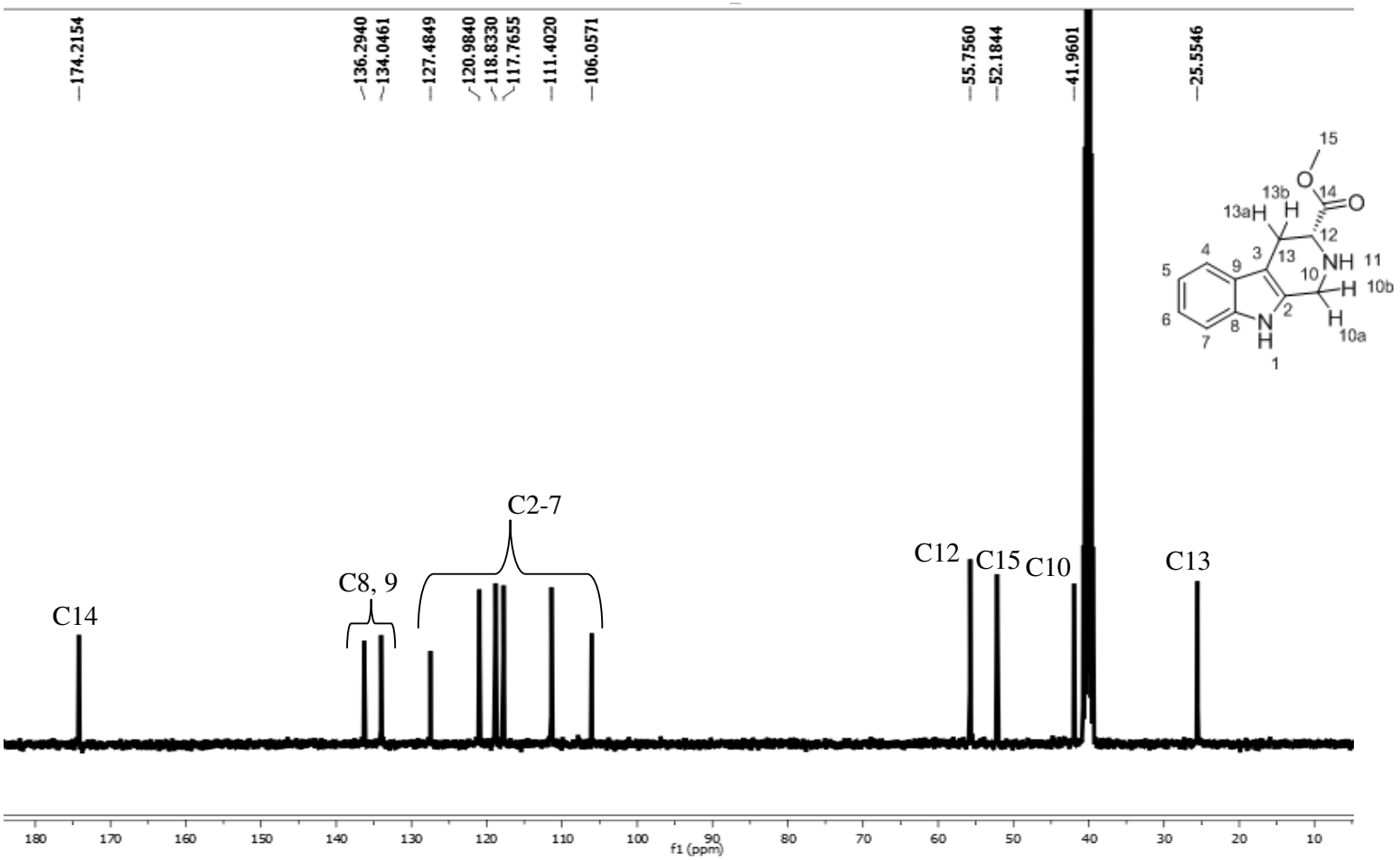

Figure 57: ^{13}C NMR spectrum of compound **189**.

The final synthesis of the hybrid compounds **191** and **192** involved coupling of **199** with 5-nitrothiophene-2-carboxylic acid using oxalyl chloride, followed by hydrolysis to the acid (**Scheme 18**).

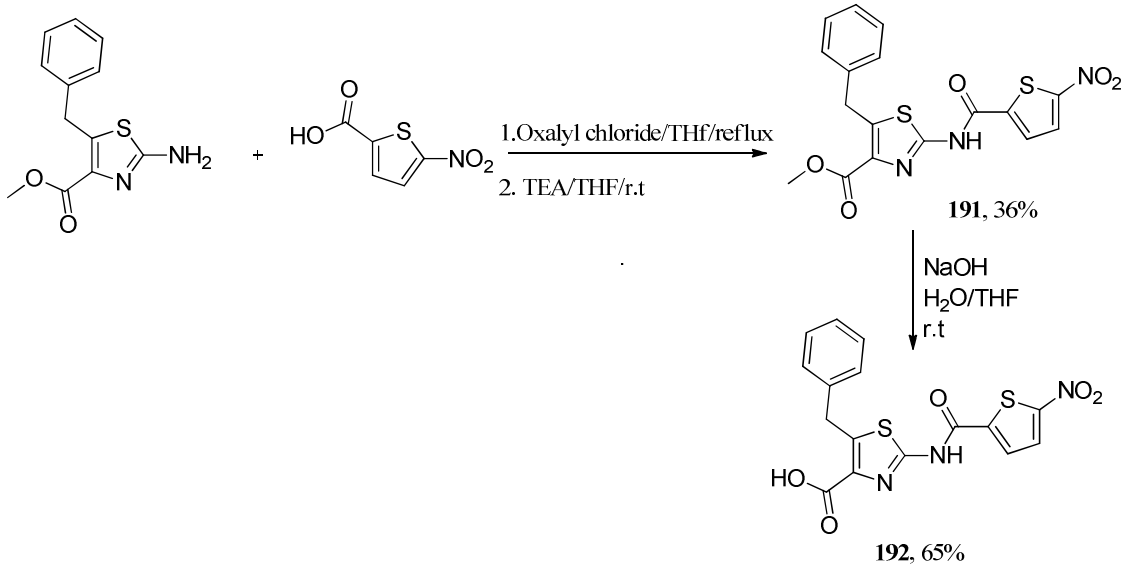

Scheme 18: compound **191** and **192** synthesis through T3P coupling.

The ^{1}H NMR spectrum for compound **191**(**Figure 58**) shows two singlets, one at δ 3.85 ppm, which corresponds to the methoxy protons, the other at δ 4.52 ppm which represents the deshielded benzylic protons. The thiophene protons are shifted downfield compared to the phenyl protons due to the presence of the electron-withdrawing nitro group and appear as one broad singlet at δ 8.20 ppm.

The disappearance of the methoxy signal in the spectrum for compound **192** (**Figure 59**) confirms that the hydrolysis of **191** was achieved. Moreover, the appearance of a broad signal at δ 13.30 ppm indicates the formation of the acid moiety at position-2.

In the ^{13}C NMR spectrum of **192** (**Figure 56**), the most characteristic feature is the disappearance of the methoxy signal at 52.6 ppm as well as the presence of deshielded signals at δ 140-143 ppm which represent C17-20 in the thiophene with the electron withdrawing nitro group.

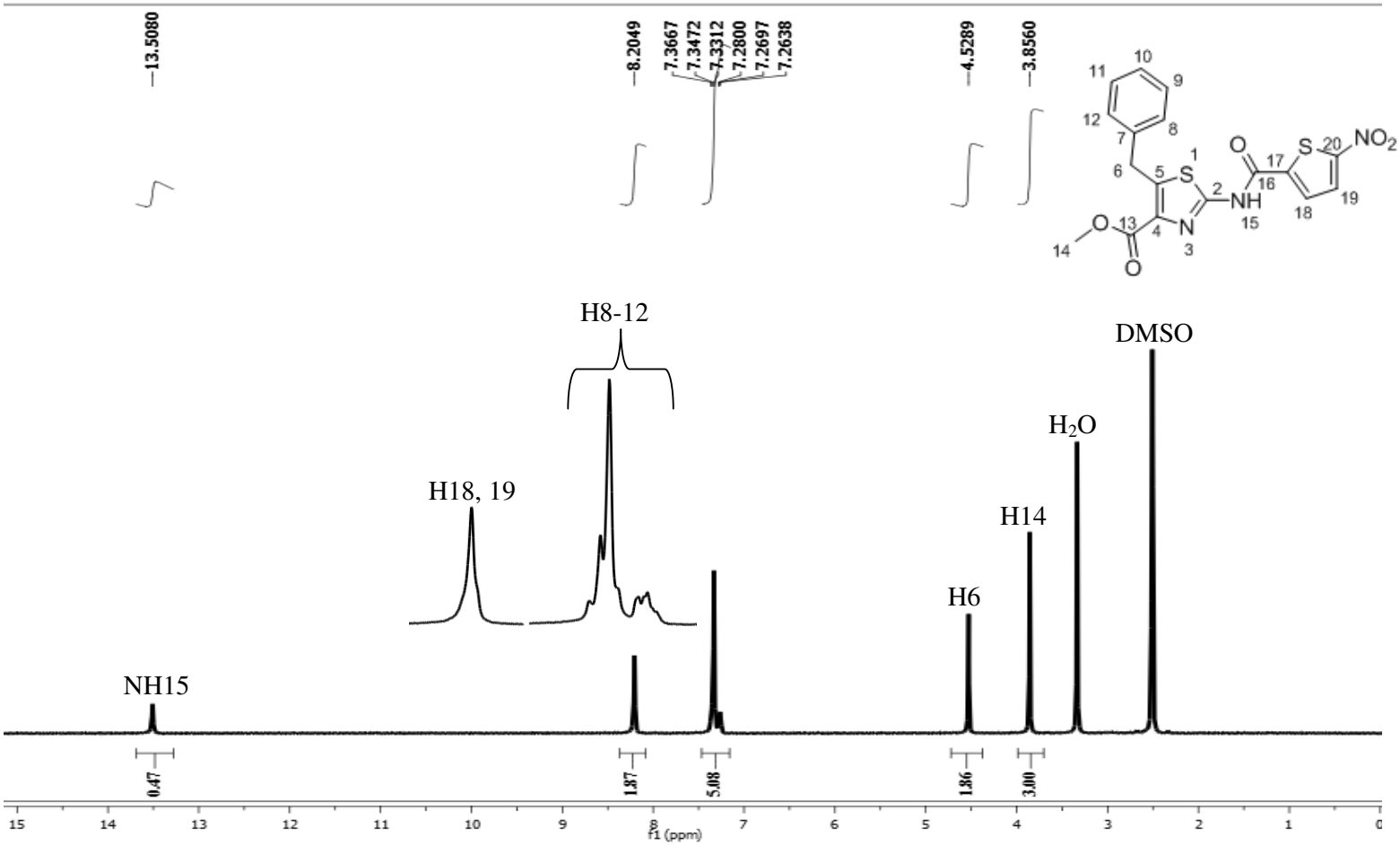

Figure 58: ^{1}H NMR spectrum of compound **191**.

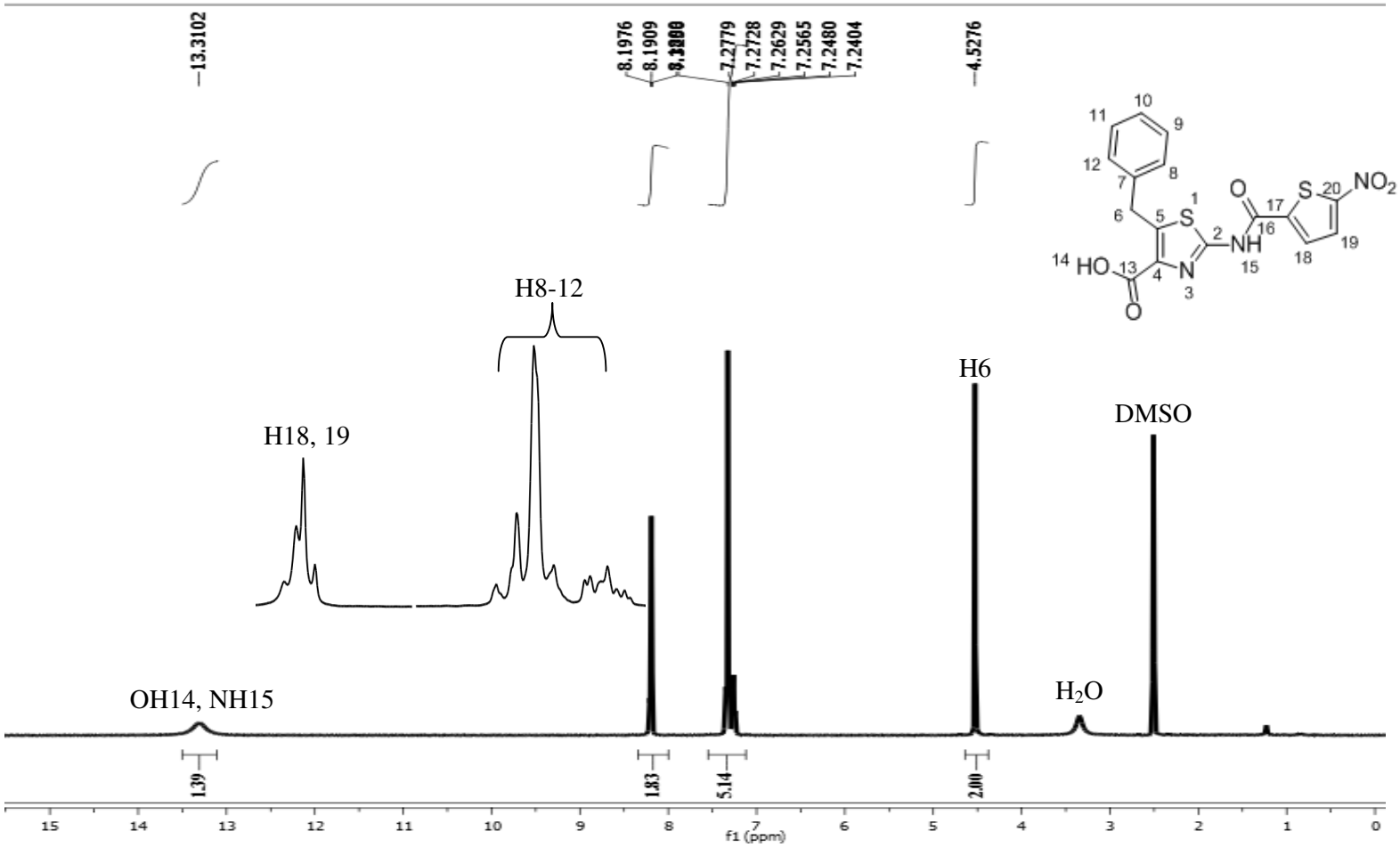

Figure 59: ^{1}H NMR spectrum of compound **192**.

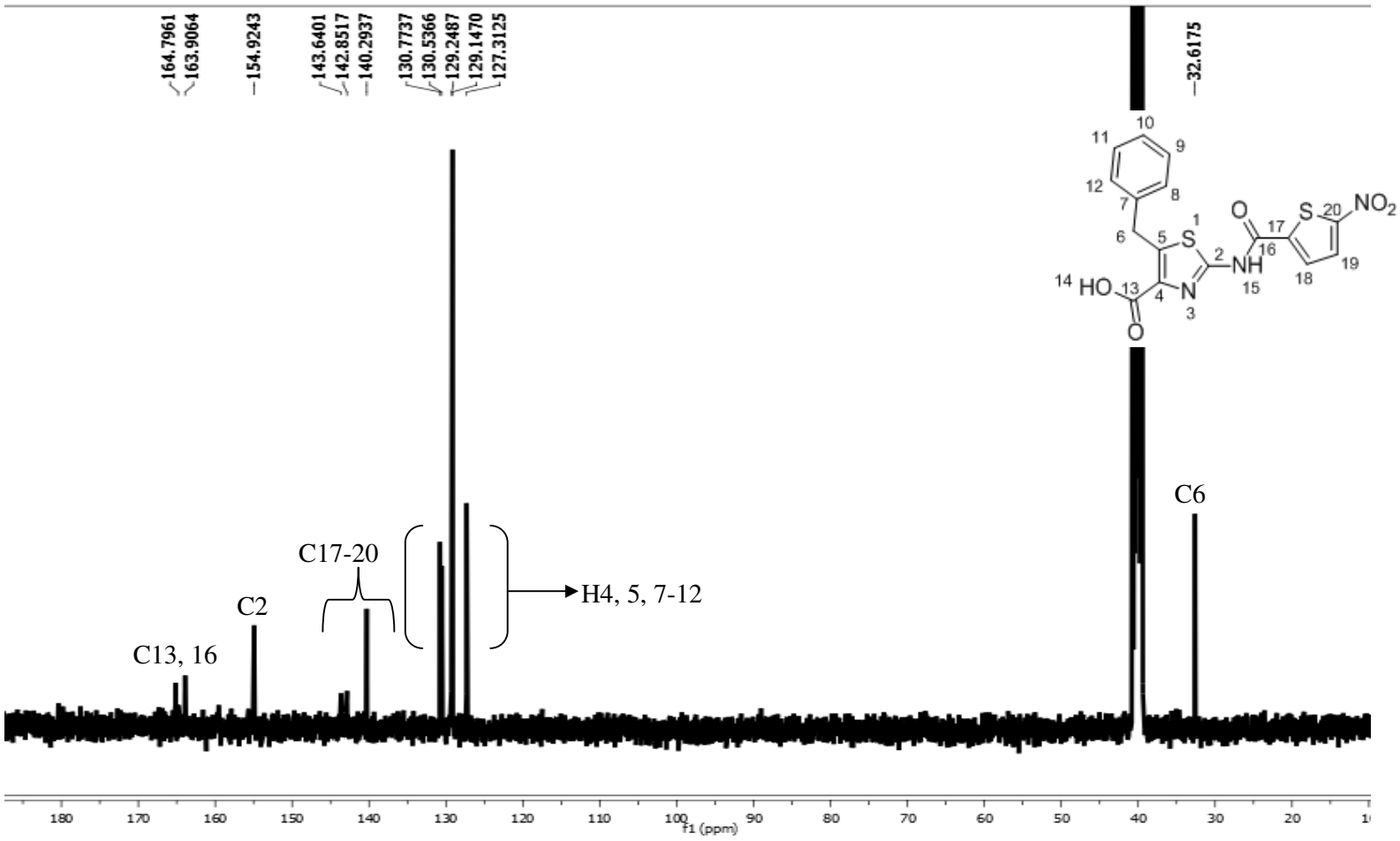

Figure 60: ^{13}C NMR spectrum of compound **192**.

4.7 Conclusions and future work

In an attempt to find new drug candidates for HAT, a 2-aminothiazole-4-carboxylate (**ATC)** library previously prepared in our laboratory was tested against *T.b. brucei.* The results obtained were promising with some compounds having MIC values of 1.9-0.78 μM (**Figure 61**).

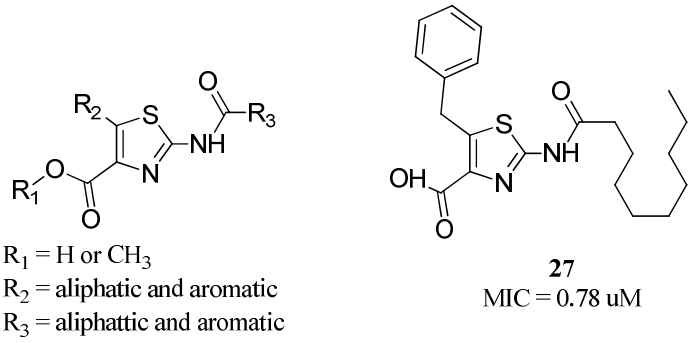

Figure 61: The structure of **ATC** main scaffold and the most active compound.

Ligand-based drug design was used to build the best common feature pharmacophore for the most active **ATC** compounds. This pharmacophore was then used to screen large commercially available chemical libraries to find possible hits, some of them showing moderate anti-trypanosomal activities and three were selected for further optimisation.

Five series of chemically diverse compounds were synthesised around benzimidazole, benzothiazole, imidazole, thiazole and indole scaffolds (**Figure 62**).

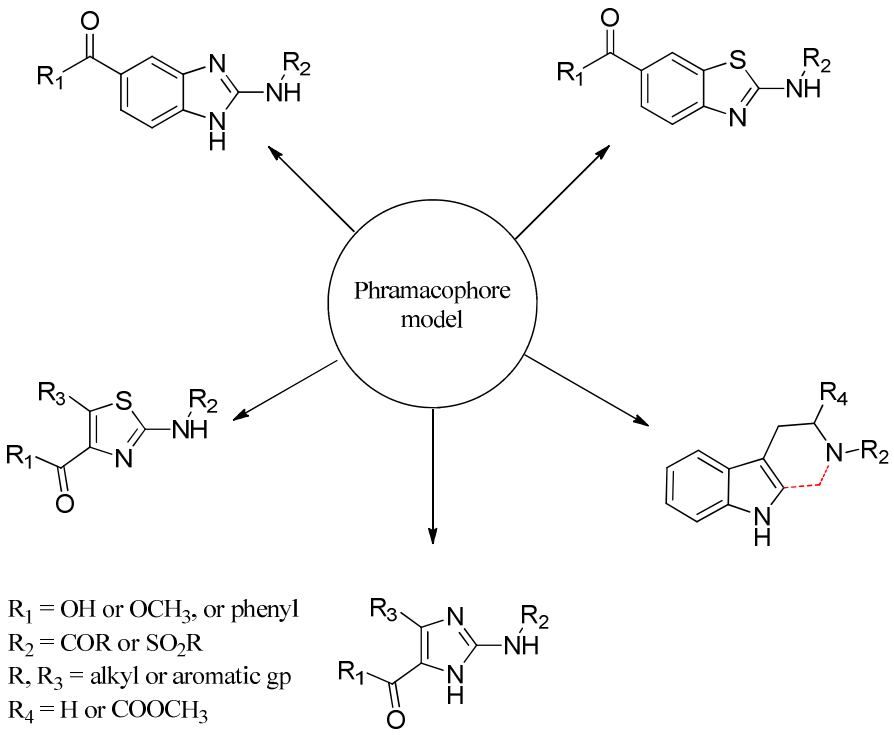

Figure 62: The five series synthesised based on the **ATC** pharmacophore model.

The *in vitro* results revealed that the thiazole compounds showed the best activities at MIC's as low as 195 nM for compound **192** and 490 nM for compound **164** (**Figure 63**).

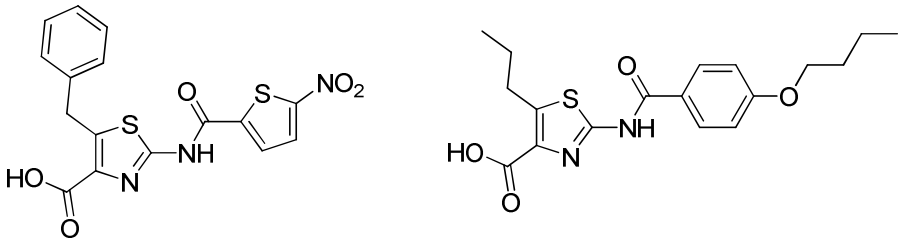

192
MIC = 195 nM

164
MIC = 490 nM

Figure 63: the most active compounds from the 2-aminothiazole-4-carboxylate library.

Derivatives from the other libraries had moderate to good activities in the range of 31.31-0.98 µM. Structure-activity relationship analysis for all these derivatives suggests that the thiazole ring was the optimum scaffold with a hydrophobic amide

group at position-2, another hydrophobic moiety, either aliphatic or aromatic at position-5 and a carboxylate group, specifically a carboxylic acid, at position-4 of the ring gave optimum activity. However, these relationships could not be transposed to other libraries where the core ring was not a thiazole.

The fact that most of the active compounds, especially **164** and **192**, did not show any signs of toxicity on the human normal cell lines, PNT2A, makes them promising leads for further development of new, safe and effective anti-trypanosomal agents.

To further study the pharmacodynamic and pharmacokinetic profile of these compounds, the most active ones are being tested in animal models infected with *T.b. brucei*, to determine both the *in vivo* efficacy and toxicity. The aim of this study is to find whether there is a relationship between the *in vitro* and *in vivo* activity, which can then be utilised to further improve the activity of our compounds.

Compounds **191** and **192** were among the most active compounds, and the nitrothiophene group appears to play a role in potency. This behaviour will be further investigated by establishing whether these compounds are substrates for the trypanosomal nitroreductase. Future plan in this circumstance will focus in trying to test these compounds on nitroheterocycle resistant strains which have the nitroreductase gene knock-out, as well as on NTR underexpressor and overexpressor strains.

Future work will focus on using these two compounds, along with compound **164**, as new leads for four new series of derivatives (**Figure 64**):

- In series A, the nitrothiophenyl carboxamide will be conserved and different groups will replace the benzyl group at position-5.
- In series B, different groups will replace the propyl group of compound **164** to find the best substituent to accompany the 4-butoxybenzamido group.
- In series C, the importance of the nitrothiophenyl carboxamide moiety will be further explored by replacement with other nitro heterocyclic rings such as nitroimidazole, nitrothiazole, nitrotriazole, nitrooxazole and nitrofuran. Also, the nitro group will be replaced by the CF_3 group, which has a similar electron-withdrawing capacity, but a different oxidative potential.

- In series D, the same nitroheterocycles will be used with the indole derivatives, and different substituents in the indole ring explored.

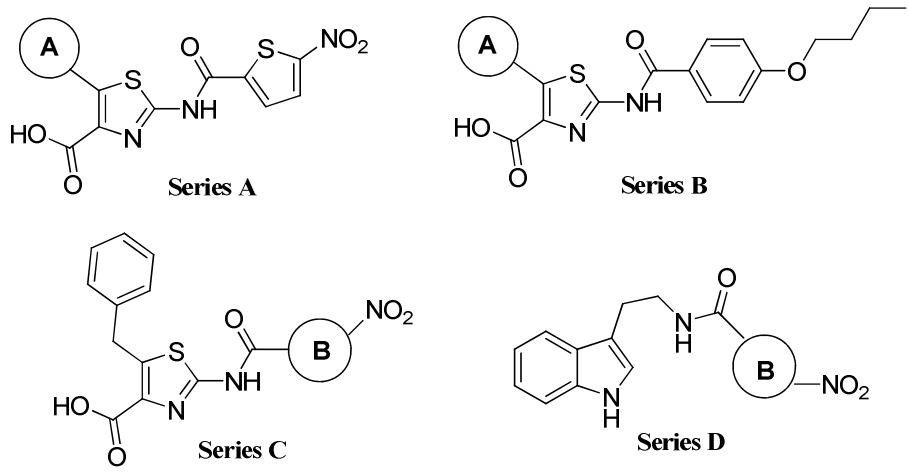

A = alkyl or aromatic (unsubstituted or substituted)
B = 1*H*-imidazole, 1,2,4-triazole, 1,3-oxazole, thiazole, furan, benzimidazole, benzothiazole or indole

Figure 64: The proposed derivatives for future work.

The proposed compounds in series A and B will be synthesised using the methods previously utilized to synthesise 2-aminothiazole-4-carboxylates. Once group A is introduced at position-5, the recommended nitrothiophenyl and 4-butoxybenzamido group can be added through the coupling with the amino group at position-2.

For the synthesis of series C and D, some of the nitro substituted heterocyclic rings such as 2-nitroimidazole-4-carboxylic acid, 2-nitrothiazole-5-carboxylic acid, 5-nitrofuran-2-carboxylic acid and 2-nitrobenzimidazole-5-carboxylic acid which are commercially available will be coupled with the suitable thiazoles using oxalyl chloride. Regarding the other nitroheterocycles which are not commercially available, the available amino derivatives will be oxidized to the recommended nitro intermediate by using oxone® (potassium peroxymonosulfate) as the oxidant,[135] followed by coupling with oxalyl chloride to give compounds of series C and D (**Scheme 19**).

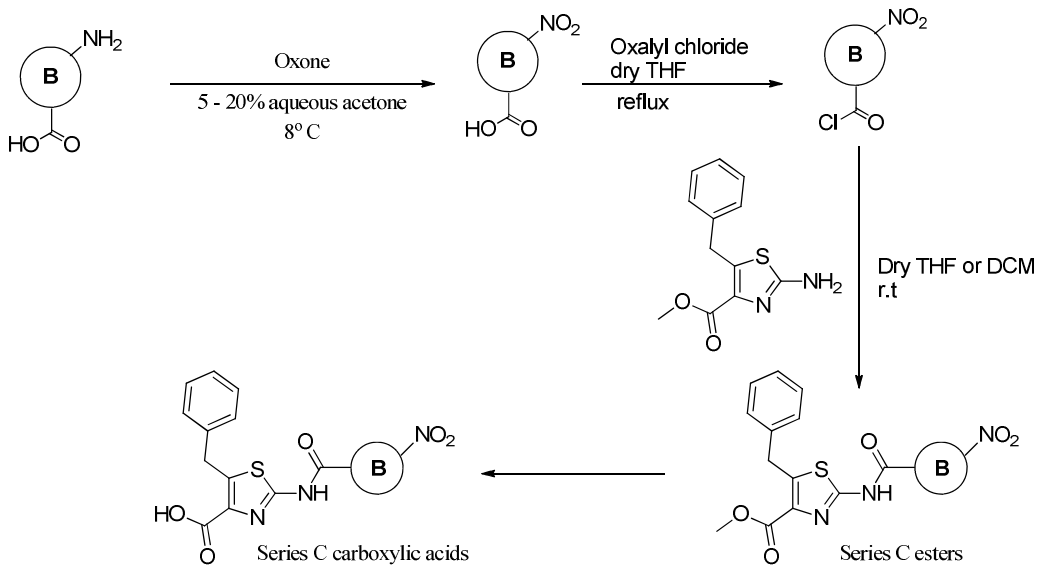

Scheme 19: Proposed synthesis of Series C compounds. For series D, the indole will be used in place of the ATC.

Chapter Five: Materials and methods

5.1 General experimental

Melting point determination

A Stuart Scientific Melting Point SMP1 apparatus was used for the melting point determinations with degrees Celsius (˚C) as the units.

Elemental analysis

Analysis was carried out on a Perkin Elmer 2400 Series II elemental analyser on 2-3mg of sample. The thermal conductivity for the combustion products, CO_2, N_2 and H_2O was measured to determine the levels of C, H and N in the sample. The level of sulfur was measured by titration with carium perchlorate solution.

Infrared Spectroscopy

Infrared spectra were run on Mattson Genesis Series FTIR spectrometers with samples prepared in KBr discs. The spectra were shown as transmittance output in frequencies expressed as ν_{max} in cm^{-1}.

Mass Spectroscopy

High resolution mass spectra (MS) were obtained on an Exactive® Thermo Scientific spectrometer using electrospry ionisation (ESI) in a Fourier transform (FT) analyser. Mass to charge ratio (m/z) are quoted for the molecular ions (M^+).

Nuclear magnetic resonance (NMR) spectroscopy

Proton nuclear magnetic resonance (^{1}H NMR) and carbon (^{13}C NMR) spectra were run on JEOL Lambda delta 400 (400MHz) spectrometers. Chemical shifts are stated in parts per million (ppm) and multiplicity indicated as a singlet (s), doublet (d), triplet (t), quartet (q), doublet of doublets (dd), pentet (p), sextet, septet, and multiplet (m), and broad peaks are denoted by letter (b) before the multiplicity symbol. Coupling constants (*J*) are quoted in hertz (Hz). Some of the amino protons especially in amido groups were missing due to solvent exchange.

5.2 Chemical synthesis

Synthesis of methyl 2-amino-1*H*-benzo[*d*]imidazole-5-carboxylate (70) as a general method for the synthesis of 2-amino-5-derivatized benzimidazoles (General procedure A):[100-103]

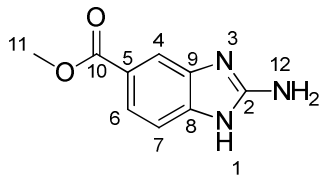

Methyl 3,4-diaminobenzenecarboxylate (1.5g, 9 mmol, 1eq) was suspended in 50 ml distilled H_2O to which 5M BrCN/ acetonitrile solution (2.2 ml, 11.2 mmol, 1.25 eq) was added drop wise. The mixture was stirred at room temperature for 24 hours, basified with Na_2CO_3 solution to pH 8 before extraction with ethyl acetate. The organic layer was separated, dried over $MgSO_4$, filtered and the solvent evaporated. The solid residue was crystallised from methanol/water to give **70** as pale yellow crystals (900 mg, 55%).

m.p: 190-191°C.[101]

^{1}H NMR (DMSO-*d*$_6$): 3.79 (s, 3H, **H11**), 6.55 (s, 2H, **NH12**), 7.15 (d, *J* = 8 Hz, 1H, **H7**), 7.58 (dd, *J* = 8, 1.32 Hz, 1H, **H6**), 7.70 (d, *J* = 1.32 Hz, 1H, **H4**), 10.97 (bs, 1H, **NH1**).

^{13}C NMR (DMSO-*d*$_6$): 52.08 (**C11**), 112.05-123.53 (**C4-7**), 134.49-140.41 (**C8, 9**), 155.41 (**C2**), 167.15 (**C10**).

FTMS-ESI: calculated for $C_9H_{10}N_3O_2$ (M+H) 192.0773, found 192.0768.

IR ν_{max} (cm^{-1}): 3562-3324 (aromatic N-H stretch), 1669 (ester C=O stretch).

Elemental analysis: calculated for ($C_9H_9N_3O_2$): C 56.54, H 4.74 and N 21.98, found for C 55.91, H 4.89 and N 21.63.

Synthesis of ethyl 2-((4-bromophenyl)diazenyl)-4-methyl-1*H*-imidazole-5-carboxylate (135) as a general method for the synthesis of ethyl 2-azaimidazole-5-carboxylate derivatives (General procedure B):[117-120]

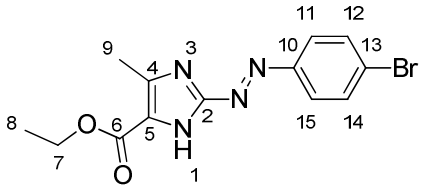

A cooled solution of sodium nitrite (1.38 g, 20 mmol, 1.1 eq) in 25 ml distilled water was gradually added to an ice-cooled solution of *p*-bromoaniline (3.44 g, 20 mmol, 1.1 eq) in 33 ml of 2.37 M HCl. The mixture was stirred at 0°C for 30 minutes and put to one side (this contains the diazonium salt). A solution of ethyl 4-methylimidazole-5-carboxylate (2 g, 18.2 mmol, 1 eq) and NaOH (2 g, 50 mmol, 2.74 eq) in 250 ml distilled water was then cooled in ice bath and added to 500 ml distilled water at pH 10 before adding the diazonium salt mixture with stirring over a 1 hour period. The mixture was stirred at 0°C for 4 hours upon which a dark orange precipitate were observed. The mixture was then extracted with three volumes of ethyl acetate, the combined ethyl acetate layers were dried over anhydrous $MgSO_4$, filtered and the solvent evaporated under vacuum to give **135** as dark orange crystals (4.3 g , 88%).

m.p: 178-179 °C (m.p).

^{1}H NMR (DMSO-*d*$_6$): 1.31 (t, *J* = 7 Hz, 3H, **H8**), 2.52 (s, 3H, **H9**), 4.27 (q, *J* = 7.48, 7.48 Hz, 2H, **H7**), 7.81 (m, 4H, **H11, 12, 14, 15**), 13.39 (bs, 1H, **NH1**).

^{13}C NMR (DMSO-*d*$_6$): 12.00 (**C8**), 34.87 (**C9**), 60.30 (**C7**), 124.85-133.36 (**C10-12, 14, 15**), 151.35 (**C4**), 152.80 (**C5**), 164.17 (**C13**), 164.90 (**C2**), 181.04 (**C6**).

FTMS-ESI: calculated for $C_{13}H_{15}BrN_4O_2$ (M+H) 337.0300, found 337.0293.

IR ν_{max} (cm^{-1}): 3065 (imidazole N-H stretch), 1703 (ester C=O stretch), 1450 (N=N stretch).

Elemental analysis: calculated for ($C_{13}H_{14}BrN_4O_2$): C 46.32, H 3.89 and N 16.62, found for C 46.01, H 3.75 and N 16.01.

Synthesis of 2-amino-1*H*-benzo[*d*]imidazole-5-carboxylic acid (74) as a general procedure for the hydrolysis of esters moiety into carboxylic acid derivatives (General procedure C):[104-106]

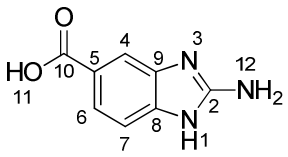

Compound **70** (1.0 g, 5.2 mmol, 1eq) was suspended in 20 ml distilled water, then 5.2 ml of a 1M NaOH solution was added. The mixture was stirred at room temperature for 20 minutes, followed by addition of 5 ml THF as a co solvent. The mixture was stirred for 24 hours, diluted with 50 ml water, acidified with 1M HCl to pH 4.5, and the precipitate collected by filtration to give **74** as a pink powder (750 mg, 81.5%).

m.p: 310 °C with decomposition.[101]

^{1}H NMR (DMSO-*d*$_6$): 6.54 (s, 2H, **H12**), 7.13 (d, *J* = 8 Hz, 1H, **H7**), 7.56 (d, *J* = 8 Hz, 1H, **H6**), 7.69 (s, 1H, **H4**), 11.90 (bs, 1H, **OH11**).

^{13}C NMR (DMSO-*d*$_6$): 104.97-122.38 (**C4-7**), 122.53 (**C8**), 122.68 (**C9**), 148.56 (**C2**), 169.25 (**C10**).

FTMS-ESI: calculated for $C_8H_8N_3O_2$ (M+H) 178.0617, found 178.0611.

IR ν_{max} (cm^{-1}): 3452 (1° amine N-H stretch), 3060 (carboxylic O-H stretch), 1692 (C=O stretch).

Elemental analysis: calculated for ($C_8H_7N_3O_2$): C 54.24, H 3.98 and N 23.72, found for C 53.74, H 4.29 and N 23.16.

Synthesis of methyl 2-acetamido-1*H*-benzo[*d*]imidazole-5-carboxylate (75) as a general method for amide formation from 2-aminobenzimidazole-5-carboxylate derivatives using acid chlorides (General procedure D):[136, 137]

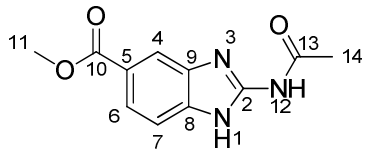

Compound **70** (0.5 g, 2.6 mmol, 1 eq) was dissolved in 100 ml dry THF, then 0.36 ml (5.6 mmol, 2 eq) of TEA was added and the mixture was stirred for 5 minutes. Acetyl chloride (0.41 g, 2.6 mmol, 1 eq) was added dropwise, and the reaction mixture stirred at room temperature for 24 hours. The solvent was evaporated to dryness and the solid residue was suspended in water and basified with NaOH solution to pH 8.0, then extracted with ethyl acetate twice, and the organic layer dried over magnesium sulfate, filtered, and evaporated under vacuum. The crude product was crystallised from hot methanol to give **75** as pale yellow crystals (400 mg, 70%).

m.p: 280°C.

^{1}H NMR (DMSO-*d*$_6$): 2.21 (s, 3H, **H14**), 3.88 (s, 3H, **H11**), 7.48 (bs, 1H, **H7**), 7.74 (d, *J* = 8.36, 1H, **H4**), 8.01 (bs, 1H, **H6**), 11.72 (s, 1H, **NH1**), 12.33 (bs, 1H, **NH12**).

^{13}C NMR (DMSO-*d*$_6$): 23.82 (**C14**), 52.40 (**C11**), 97.36-116.90 (**C4-7**), 122.86 (**C8**), 122.98 (**C9**), 149.34 (**C2**), 167.44 (**C13**), 170.45 (**C10**).

FTMS-ESI: calculated for $C_{11}H_{12}N_3O_3$ (M+H) 234.0879, found 234.0874.

IR ν_{max} (cm^{-1}): 3361 (amide N-H stretch), 1713 (ester C=O stretch), 1695 (amide C=O stretch).

Elemental analysis: calculated for ($C_{11}H_{11}N_3O_3$): C 56.65, H 4.75 and N 18.02, found for C 56.44, H 4.87 and N 18.49.

Synthesis of ethyl 2-acetamido-1*H*-benzo[*d*]imidazole-5-carboxylate (73) as a general method for amide formation from 2-aminobenzimidazole-5-carboxylate derivatives using acid anhydrides (General procedure E):[107, 108]

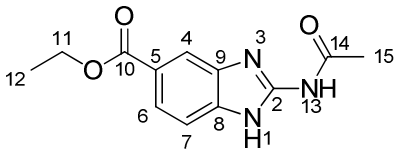

Compound **71** (1.0 g, 5.2 mmol, 1 eq) was dissolved in 100 ml dry THF, then 1 ml (15.6 mmol, 3 eq) of TEA added, and the reaction was cooled to 0°C. Acetic anhydride (0.62 g, 6 mmol, 1.15 eq) was added dropwise to the mixture, which was stirred at 0°C for 5 hours then overnight at room temperature. THF was evaporated under vacuum, and the residue suspended in water and neutralized with 1M HCl to pH 8, followed by extraction with ethyl acetate. The organic layer was separated and dried over anhydrous magnesium sulfate and evaporated to dryness. The solid residue was crystallised from hot ethyl acetate to give **73** as off-white powder (540 mg, 43%).

m.p: 309-310 °C.

^{1}H NMR (DMSO-*d*$_6$): 1.33 (t, *J* = 7.04 Hz, 3H, **H12**), 2.17 (s, 3H, **H15**), 4.29 (q, *J* = 7.04 Hz, 2H, **H11**), 7.48 (bs, 1H, **H7**), 7.73 (d, *J* = 8.36, 1H, **H6**), 8.13 (bs, 1H, **H4**), 11.70 (bs, 1H, **NH1**), 12.30 (bs, 1H, **NH13**).

^{13}C NMR (DMSO-*d*$_6$): 21.61 (**C12**), 27.25 (**C15**), 52.45 (**C11**), 115.07-120.98 (**C4-7**), 126.98 (**C8**), 130.87 (**C9**), 148.58 (**C2**), 167.10 (C**14**), 172.09 (C**10**).

FTMS-ESI: calculated $C_{12}H_{14}N_3O_3$ (M+H) 248.1035, found 248.1025.

IR ν_{max} (cm^{-1}): 3341 (amide N-H stretch), 1718 (ester C=O stretch), 1684 (amide C=O stretch).

Elemental analysis: calculated for ($C_{12}H_{13}N_3O_3$): C 58.29, H 5.3 and N 16.99, found for C 58.01, H 5.23 and N 16.67.

Synthesis of ethyl 2-(phenylsulfonamido)-1*H*-benzo[*d*]imidazole-5-carboxylate (97) as a general method for sulfonamide formation from the 2-aminobenzimidazole derivatives (General procedure F):[100]

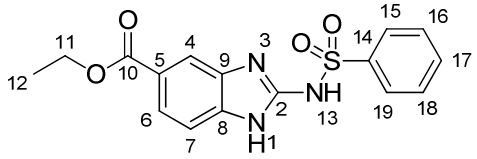

Compound **71** (1.0 g, 4.9 mmol, 1 eq) was dissolved in 100 ml dry DCM, followed by the addition of TEA (1.4 ml, 9.8 mmol, 3 eq), and the mixture cooled in ice bath. Benzenesulfonylchloride (1.04 g, 5.88 mmol, 1.2 eq) was added drop-wise and the mixture was stirred at room temperature for 5 hours. Solvent was removed by evaporation under vacuum then suspended in water and neutralized with 0.5M NaOH to pH 7.00, and extracted with chloroform. The organic layer was separated and dried over anhydrous magnesium sulfate, filtered and the solvent was evaporated to dryness. The solid residue was purified by flash chromatography using 5% methanol/chloroform to give **97** as shiny yellow crystals (800 g, 47%).

m.p: 150-151 °C.

^{1}H NMR (DMSO-*d*$_6$): 1.32 (t, *J* = 7.04, 7.48 Hz, 3H, **H12**), 4.29 (q, *J* = 7.04, 7.46 Hz, 2H, **H11**), 7.41 (bs, 1H, **NH1**), 7.69 (m, 3H, **H16-18**), 7.81 (m, 2H, **H15, 19**), 8.00 (d, *J* = 7.48 Hz, 1H, **H7**), 8.08 (d, *J* = 7.48 Hz, 1H, **H6**), 8.23 (s, 1H, **H4**).

^{13}C NMR (DMSO-*d*$_6$): 14.74 (**C12**), 61.12 (**C11**), 112.61-122.34 (**C4-7**), 127.27-136.20 (**C14-19**), 136.88 (**C8**), 143.40 (**C9**), 147.97 (**C2**), 154.92 (**C14**), 166.25 (**C10**).

FTMS-ESI: calculated for $C_{16}H_{16}N_3O_4S$ (M+H) 346.09, found 346.0858.

IR ν_{max} (cm^{-1}): 3449 (sulfonamide N-H stretch), 1711 (ester C=O stretch), 1342 (S=O stretch).

Elemental analysis: calculated for ($C_{16}H_{15}N_3O_4S$): C 55.64, H 4.38, N 12.17 and S 9.28, found for C 55.44, H 4.38, N 12.10 and S 8.86.

Synthesis of methyl 2-(4-chlorophenylsulfonamido)-1*H*-benzo[*d*]imidazole-5-carboxylate (98) as a general method for the synthesis of sulfonamide derivatives using pyridine as a solvent and a base (general procedure G):[109-111]

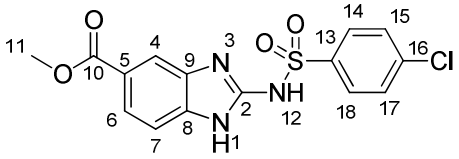

Compound **70** (0.20 g, 1.05 mmol, 1 eq) was dissolved in 10 ml dry pyridine, then warmed to 40 °C. 4-Chlorobensenesulfonylchloride was added, and the mixture was heated under reflux at 80 °C for 4 hours, and quenched in ice water. The pH was checked to be 6.70, and the mixture left to precipitate. The precipitate was collected by filtration then crystallised from hot ethyl acetate to give **98** as yellowish white needles (170 mg, 44%).

m.p: 230-232 °C.

^{1}H NMR (DMSO-d_6): 3.86 (s, 3H, **H11**), 7.22 (dd, *J* = 2.64, 8.36 Hz, 1H, **H7**), 7.62 (bs, 1H, **NH1**), 7.76 (dd, *J* = 2.64, 8.8 Hz, 2H, **H14, 18**), 7.82 (dd, *J* = 1.76, 6.6 Hz, 1H, **H6**), 8.02 (dd, *J* = 2.64, 8.8 Hz, 2H, **H15, 17**), 8.23 (s, 1H, **H4**).

^{13}C NMR (DMSO-d_6): 52.63 (**C11**), 113.45-122.17 (**C4-7**), 127.48-148.02 (**C8, 9, 13-15, 17, 18**), 154.83 (**C16**), 166.74 (**C10**).

FTMS-ESI: calculated for $C_{15}H_{13}ClN_3O_4S$ (M+H) 365.0237, found 365.0229.

IR ν_{max} (cm^{-1}): 3453 (sulfonamide N-H stretch), 1706 (ester C=O stretch), 1369 (S=O stretch).

Elemental analysis: calculated for ($C_{15}H_{12}ClN_3O_4S$): C 49.25, H 3.31, N 11.49 and S 8.77, found for C 48.91, H 3.34, N 11.27 and S 8.49.

Synthesis of methyl 2-amino-5-phenethylthiazole-4-carboxylate (202) as a general method for the synthesis of 2-aminothiazole-4-carbocylate derivatives (General procedure H):[121]

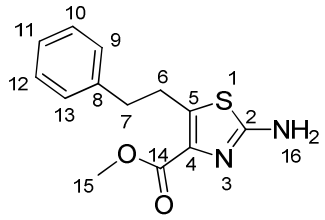

Methyl dichloroacetate (20 g, 0.14 mole, 1 eq) and 2-phenylacetaldehyde (28.15 g, 0.21 mol, 1.5 eq) were dissolved in dry ether (200 ml), stirred at 0 °C for 15 minutes upon which a solution of sodium methoxide (9.5 g, 0.175 mol, 1.25 eq) in 50 ml dry methanol was added dropwise. The mixture was stirred at 0 °C for 2 hours, then extracted two times with water, the organic layer was separated, dried over anhydrous magnesium sulfate, and filtered, the filtrate was evaporated to dryness, the pale yellow creamy residue (30 g, 0.125 mol, 1 eq) was dissolved in 150 ml dry methanol, then a solution of thiourea in methanol was added and the mixture heated under reflux for 5 hours. The solvent was evaporated to dryness, then the residue was suspended in water, basified with 1M NaOH to pH 8.5, after which it was extracted with ethyl acetate. The organic layer was separated, dried over $MgSO_4$, then evaporated to dryness. The oily residue was crystallised from ethyl acetate to give **202** as fine white crystals (18.5 g, 58%).

m.p: 134-135 °C.

^{1}H NMR (DMSO-d_6): 2.84 (t, *J* = 8 Hz, 2H, **H7**), 3.26 (t, *J* = 8 Hz, 2H, **H6**), 3.71 (s, 3H, **H15**), 7.10 (bs, 2H, **NH16**), 7.29 (m, 5H, **H9-13**).

^{13}C-NMR (DMSO-d_6): 28.81 (**C7**), 37.37 (**C6**), 51.85 (**C15**), 126.66-136.05 (**C8-13**), 137.48 (**C5**), 141.19 (**C4**), 162.90 (**C2**), 164.80 (**C14**).

FTMS-ESI: calculated for $C_{13}H_{15}N_2O_2S$ (M+H) 263.0854, found 263.0850.

IR ν_{max} (cm^{-1}): 3438-3404 (1°amine N-H stretch), 1686 (ester C=O stretch).

Elemental analysis: calculated for ($C_{13}H_{14}N_2O_2S$): C 59.52, H 5.38, N 10.68 and S 12.22, found for C 58.98, H 5.25, N 10.61 and S 12.01.

Synthesis of methyl 5-benzyl-2-(2-(4-nitrophenyl)acetamido)thiazole-4-carboxylate (155) as a general method for coupling between 2-aminothiazole derivatives and different carboxylic acids using oxalyl chloride (General procedure I):[123, 124]

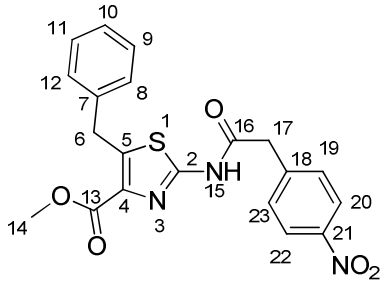

A solution of 4-nitrophenylacetic acid (500 mg, 2.76 mmol, 1 eq) and oxalyl chloride (3.35 g, 26.36 mmol, 9.55 eq) in 30 ml dry THF was heated under reflux for 2 hours. The solvent was evaporated to dryness to remove the excess oxalyl chloride, then residue was dissolved in 30 ml dry THF, cooled in an ice bath, and a solution of **199** (684 mg, 2.7 mmol, 1 eq) in 10 ml THF was added. The mixture was warmed to room temperature and stirred for 24 hours. The reaction was diluted with ethyl acetate, and then extracted three times with water, the organic layer was removed, dried over $MgSO_4$, then filtered and the filtrate was evaporated to dryness. The resultant residue was columned with a gradient 30% ethyl acetate/DCM to give **155** as white amorphous solid (380 mg, 33.5%).

m.p: 256-257 °C.

^{1}H NMR (DMSO-d_6): 3.82 (s, 3H, **H14**), 3.91 (s, 2H, **H6**), 4.46 (s, 2H, **H17**), 7.25 (m, 5H, **H8-12**), 7.55 (d, *J* = 8.32 Hz, 2H, **H19, 23**), 8.17 (d, *J* = 8.32 Hz, 2H, **H20, 22**), 12.78 (s, 1H, **NH15**).

^{13}C-NMR (DMSO-d_6): 32.47 (**C6**), 41.33 (**C17**), 52.25 (**C14**), 124.03-129.08 (**C7-12**), 129.21-140.16 (**C18-20, 22, 23**), 142.81 (**C5**), 143.09 (**C4**), 147.13 (**C2**), 154.95 (**21**), 163.25 (**C16**), 169.26 (**C13**).

FTMS-ESI: calculated for $C_{20}H_{18}N_3O_5S$ (M+H) 412.0967, found 412.0962.

IR ν_{max} (cm^{-1}): 3260-3224 (amide N-H stretch), 1710 (ester C=O stretch), 1687 (amide C=O stretch), 1545 (N=O stretch).

Elemental analysis: calculated for ($C_{20}H_{17}N_3O_5S$): 58.38, H 4.16 and N 10.21, found for C 58.15, H 4.05, and N 9.82.

Synthesis of N-(2-(1*H*-indol-3-yl)ethyl)thiophene-2-carboxamide (182) as a general method for coupling between tryptamine derivatives and carboxylic acids using propane phosphonic acid anhydride; T3P® (general procedure J):[126]

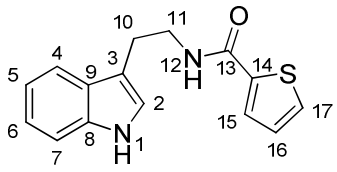

Tryptamine (300 mg, 1.87 mmol, 1 eq) and thiophene-2-carboxylic acid (289 mg, 2.26 mmol, 1.2 eq) were dissolved in 15 ml dry THF, then TEA (1.56 ml, 11.22 mmol, 6 eq) was added. The mixture was cooled in ice bath for 10 minutes, after which T3P (1.8 ml of 50% T3P solution in DMF, 2.83 mmol, 1.5 eq) was added and then warmed to room temperature and stirred for 24 hours. The solvent was evaporated to 1/3 its volume, then was poured into a saturated sodium bicarbonate solution (50 ml) and stirred for 24 hours. The precipitate formed was collected by filtration, dried in oven at 50 °C to give **182** as light brown crystals (280 mg, 53%).

m.p: 144-145 °C.

^{1}H NMR (DMSO-d_6): 2.94 (t, *J* = 7.88, 7.04 Hz, 2H, **H10**), 3.52 (q, *J* = 6.6, 7.04 Hz, 2H, **H11**), 6.98 (t, *J* = 7.84, 7.12 Hz, 1H, **H5**), 7.07 (t, *J* = 7.48, 7.44 Hz, 1H, **H6**), 7.14 (t, *J* = 7.38 Hz, 1H, **H16**), 7.18 (s, 1H, **H2**), 7.33 (d, *J* = 8.36 Hz, 1H, **H4**),

7.56 (d, *J* = 7.88 Hz, 1H, **H7**), 7.73 (m, 2H, **H15, 17**), 8.64 (t, *J* = 5.6, 5.28 Hz, 1H, **NH12**), 10.83 (s, 1H, **NH1**).

^{13}C-NMR (DMSO-*d*$_6$): 25.83 (**C10**), 40.70 (**C11**), 111.95-127.81 (**C2-7**), 128.35-136.80 (**C8, 9, 15-17**), 140.88 (**C14**), 161.61 (**C13**).

FTMS-ESI: calculated for $C_{15}H_{13}N_2OS$ (M-H) 269.0749, found 269.0754.

IR ν_{max} (cm^{-1}): 3367 (amide N-H stretch), 3288 (indole N-H stretch), 1592 (C=O stretch).

Elemental analysis: calculated for $C_{15}H_{14}N_2OS.H_2O$: C 62.88, H 5.59 and N 9.71, found for C 63.0, H 5.08 and N 9.42.

Synthesis of (S)-methyl 2-(5-aminothiophene-2-carboxamido)-3-(1*H*-indol-3-yl)propanoate (179) as a general procedure for the reduction of the nitro to the amino group (general procedure K):[130, 131]

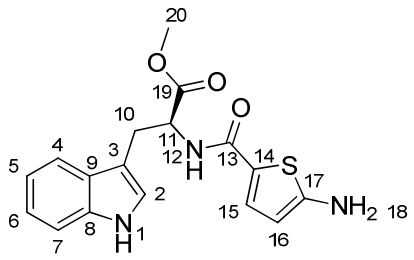

A solution of (*S*)-methyl 3-(1*H*-indol-3-yl)-2-(5-nitrothiophene-2-carboxamido)propanoate (**175**) (100 mg, 0.268 mmol, 1 eq) and glacial acetic acid (180.15 mg, 3 mmol, 11.2 eq) in 50 ml ethanol/water mixture (5:1) was heated to reflux, then metallic meshed iron (168 mg, 3 mmol, 11.2 eq) was added in portions. The mixture was heated at reflux for 30 minutes, diluted with water and then basified with saturated sodium carbonate solution to pH 8.00, after which it was extracted three times with ethyl acetate. The organic layer was separated, dried over $MgSO_4$, and then evaporated to dryness to give **179** as a dark brown powder (62 mg, 67.4%).

m.p: 94-96 °C.

^{1}H NMR (DMSO-d_6): 3.16 (m, 2H, **H10**), 4.57 (m, 1H, **H11**), 3.60 (s, 3H, **H20**), 6.28 (s, 2H, **NH18**), 6.98 (t, *J* = 7.68, 7.04 Hz, 1H, **H5**), 7.06 (t, *J* = 7.92, 7 Hz, 1H, **H6**), 7.17 (d, *J* = 2.2 Hz, 1H, **H2**), 7.31 (d, *J* = 7.88 Hz, 1H, **H15**), 7.38 (d, *J* = 7.66 Hz, 1H, **H4**), 7.52 (d, *J* = 7.92 Hz, 1H, **H7**), 8.17 (d, *J* = 7.92 Hz, 1H, **H16**), 10.85 (s, 1H, **NH1**).

^{13}C NMR (DMSO-d_6): 27.41 (**C10**), 52.35 (**C11**), 53.99 (**C20**), 104.32-121.52 (**C2-7**), 124.20-136.64 (**C8, 9, 14-16**), 160.89 (**C17**), 162.47 (**C13**), 173.56 (**C19**).

FTMS-ESI: calculated for $C_{17}H_{18}N_3O_3S$ (M+H) 344.1069, found 344.1063.

IR ν_{max} (cm^{-1}): 3409 (1° amine N-H stretch), 3338 (amide N-H stretch), 1730 (ester C=O stretch), 1617 (amide C=O stretch).

Elemental analysis: calculated for ($C_{17}H_{17}N_3O_3S$): C 59.46, H 4.99 and N 12.24, found for C 58.76, H 4.85 and N 11.99.

Synthesis of 2-decanamido-5-methylthiazole-4-carboxamide (125) as a general procedure for trans-amination of esters to amides (General procedure L):[125]

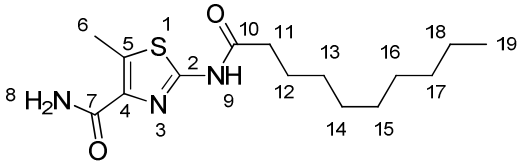

Methyl 2-decanamido-5-methylthiazole-4-carboxylate (**18**) (1.0 g, 3.1 mmol, 1 eq) and potassium cyanide (26 mg, 0.4 mmol, 0.1 eq) were dissolved in 5 ml of 7M ammonia in methanol in a closed tube, then heated at 60 °C for 72 hours. The solvent was evaporated to dryness, the residue was dissolved in DCM, and extracted with water, and the organic layer was separated, dried over $MgSO_4$ and filtered. The filtrate was evaporated to dryness, and the residue columned with 5% methanol/chloroform to give **125** as white crystals (350 mg, 36.4%).

m.p: 115-116 °C.

^{1}H NMR (DMSO-*d*$_6$): 0.84 (t, *J* = 5.72, 7.04 Hz, 3H, **H19**), 1.23 (bs, 12H, **H13-18**), 1.57 (p, *J* = 6.6, 7.48 Hz, 2H, **H12**), 2.40 (t, *J* = 7.48 Hz, 2H, **H11**), 2.60 (s, 3H, **H6**), 7.45 (s, 1H, **NH6**), 11.98 (s, 1H, **NH7**).

^{13}C NMR (DMSO-*d*$_6$): 12.16-31.84 (**C11-19**), 36.36 (**C6**), 133.03 (**C5**), 137.89 (**C4**), 153.55 (**C2**), 164.75 (**C7**), 172.26 (**C10**).

FTMS-ESI: calculated for $C_{15}H_{26}N_3O_2S$ (M+H) 312.1746, found 312.1741.

IR ν_{max} (cm^{-1}): 3471-3190 (amide N-H stretch), 1654 (1°Amide C=O stretch), 1653 (2°Amide C=O stretch).

Elemental analysis: calculated for ($C_{15}H_{25}N_3O_2S$): C 57.85, H 8.09, N 13.49 and S 10.30, found for C 57.99, H 8.43, N 13.00 and S 9.73.

Methyl 2-aminobenzo[*d*]thiazole-6-carboxylate (51):[138]

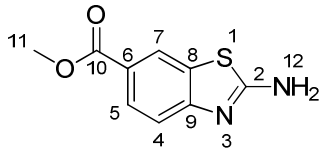

Methyl 4-aminobenzoate (2.0 g, 13.2 mmol, 1 eq) and potassium thiocyanate (5.13 g, 52.8 mmol, 4 eq) were dissolved in 100 ml glacial acetic acid, then a solution of bromine (2.10 g, 13.2 mmol, 1 eq) in 20 ml glacial acetic acid was added dropwise to the mixture. The mixture was stirred at room temperature for 48 hours, filtered, the precipitate dried, suspended in water then basified with 0.5M NaOH to pH 8.0, and extracted three times with ethyl acetate. The organic layer was removed, dried over anhydrous magnesium sulfate, then evaporated to dryness. The solid residue was crystallised from methanol to give **51** as bright yellow crystals (2.0 g, 73 %).

m.p: 240-240.5 °C.[66]

^{1}H NMR (DMSO-*d*$_6$): 3.82 (s, 3H, **H11**), 7.36 (d, *J* = 8.36 Hz, 1H, **H4**), 7.81 (dd, *J* = 1.76, 8.36 Hz, 1H, **H5**), 7.90 (s, 2H, **NH12**), 8.29 (d, *J* = 1.76 Hz, 1H, **H7**).

^{13}C NMR (DMSO-*d*$_6$): 52.43 (**C11**), 117.67-127.66 (**C4-7**), 131.71 (**C8**), 157.44 (**C9**), 166.74 (**C2**), 170.35 (**C10**).

FTMS-ESI: calculated for $C_9H_9N_2O_2S$ (M+H) 209.0385, found 209.0377.

IR ν_{max} (cm^{-1}): 3363 (1° amine N-H stretch), 1697 (ester C=O stretch).

Elemental analysis: calculated for ($C_9H_8N_2O_2S$): C 51.91, H 3.87, N 13.45 and S 15.40, found for C 51.31, H 4.03, N 13.24 and S 15.47.

2-Aminobenzo[*d*]thiazole-6-carboxylic acid (52):

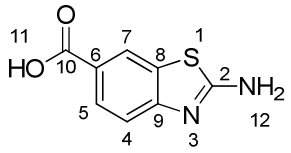

The title compound was obtained as pale yellow crystals using general procedure C (180 mg, 93%).

m.p: >300 °C.

^{1}H NMR (DMSO-*d*$_6$): 7.38 (d, *J* = 8.36 Hz, 1H, **H4**), 7.80 (dd, *J* = 1.32, 8.36 Hz, 1H, **H5**), 7.87 (s, 2H, **NH12**), 8.26 (d, *J* = 1.32 Hz, 1H, **H7**), 12.64 (bs, 1H, **OH11**).

^{3}C NMR (DMSO-*d*$_6$): 117.54-127.83 (**C4-7**), 131.52 (**C8**), 157.14 (**C9**), 167.78 (**C2**), 170.04 (**C10**).

FTMS-ESI: calculated $C_8H_7N_2O_2S$ (M+H) 195.0228, found 195.0221.

IR ν_{max} (cm^{-1}): 3409 (1° amine N-H stretch), 3163 (carboxylic O-H stretch), 1675 (carboxylic C=O stretch).

Elemental analysis: calculated for ($C_8H_6N_2O_2S$): C 49.47, H 3.11, N 14.42 and S 16.51, found for C 48.85, H 3.32, N 13.96 and S 16.41.

Methyl 2-decanamidobenzo[*d*]thiazole-6-carboxylate (53):

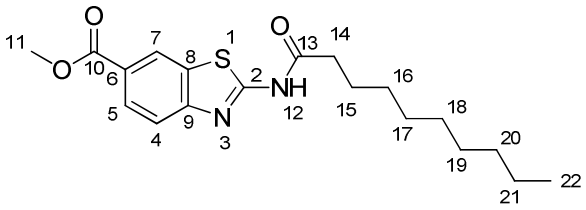

The title compound was obtained as shiny white flakes using general procedure D after column chromatography with 10% methanol/chloroform (280 mg, 54%).

m.p: 131-131.5 °C.

^{1}H NMR (DMSO-d_6): 0.84 (t, *J* = 6.6 Hz, 3H, **H22**), 1.23 (s, 12H, **H16-21**), 1.63 (m, 2H, **H15**), 2.50 (t, *J* = 7.04 Hz, 2H, **H14**), 3.87 (s, 3H, **H11**), 7.78 (d, *J* = 8.36 Hz, 1H, **H4**), 8.00 (dd, *J* = 1.32, 8.36 Hz, 1H, **H5**), 8.63 (d, *J* = 1.76 Hz, 1H, **H7**), 12.54 (bs, 1H, **NH12**).

^{13}C NMR (DMSO-d_6): 14.53-35.73 (**C14-22**), 52.71 (**C11**), 120.79-127.63 (**C4-7**), 132.31 (**C8**), 152.78 (**C9**), 162.00 (**C2**), 166.61 (**C13**), 173.33 (**C10**).

FTMS-ESI: calculated for $C_{19}H_{27}N_2O_3S$ (M+H) 363.1742, found 363.1731.

IR ν_{max} (cm^{-1}): 3265 (amide N-H stretch), 1702 (ester C=O stretch), 1697 (amide C=O stretch).

Elemental analysis: calculated for ($C_{19}H_{26}N_2O_3S$): C 62.96, H 7.23, N 7.73 and S 8.85, found C 62.52, H 7.38, N 7.66 and S 9.42.

2-Decanamidobenzo[*d*]thiazole-6-carboxylic acid (54):

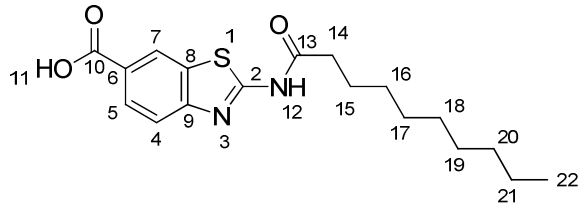

The title compound was obtained as a white fine powder using general procedure C (60 mg, 52%).

m.p: 290 °C (with decomposition).

^{1}H NMR (DMSO-d_6): 0.84 (t, *J* = 3.96, 7.04 Hz, 3H, **H22**), 1.24 (bs, 12H, **H16-21**), 1.62 (m, 2H, **H15**), 2.49 (bs, 2H, **H14**), 7.78 (d, *J* = 8.36 Hz, 1H, **H4**), 7.97 (dd, *J* = 8.36, 1.76 Hz, 1H, **H5**), 8.58 (s, 1H, **H7**), 12.51 (bs, 1H, **NH12**), 12.91 (bs, 1H, **OH11**).

^{13}C NMR (DMSO-d_6): 14.51-35.75 (**C14-22**), 120.64-134.21 (**C4-8**), 152.45 (**C9**), 161.90 (**C2**), 165.21 (**C13**), 173.30 (**C10**).

FTMS-ESI: calculated for $C_{18}H_{25}N_2O_3S$ (M+H) 349.1586, found 349.1576.

IR ν_{max} (cm^{-1}): 3444 (amide N-H stretch), 3149 (carboxylic O-H stretch), 1713 (carboxylic C=O stretch), 1675 (amide C=O stretch).

Elemental analysis: calculated for ($C_{18}H_{24}N_2O_3S$): C 62.04, H 6.94, N 8.04 and S 9.20, found for C 61.91, H 6.62, N 7.91 and S 8.75.

Methyl 2-heptanamidobenzo[d]thiazole-6-carboxylate (55):

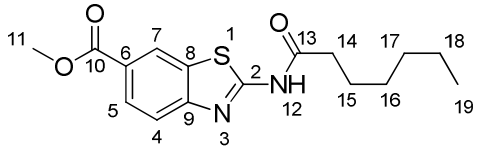

The title compound was obtained as white crystals using general procedure D after crystallization from hexane (150 mg, 48.8%).

m.p: 100-102°C.

^{1}H NMR (DMSO-d_6): 0.84 (m, 3H, **H19**), 1.26 (m, 6H, **H16-18**), 1.60 (p, *J* = 6.96, 7.36 Hz, 2H, **H15**), 2.18 (t, *J* = 7.36 Hz, 2H, **H14**), 3.89 (s, 3H, **H11**), 7.79 (d, *J* = 8.52 Hz, 1H, **H4**), 7.99 (dd, *J* = 8.48, 1.56 Hz, 1H, **H5**), 8.63 (d, *J* = 1.32, 1H, **H7**), 12.72 (s, 1H, **NH12**).

^{13}C NMR (DMSO-*d*$_6$): 14.35- 35.61 (**C14-19**), 52.59 (**C11**), 120.68-132.19 (**C4-8**), 152.12 (**C9**), 161.84 (**C2**), 166.49 (**C13**), 173.18 (**C10**).

FTMS-ESI: calculated for $C_{16}H_{21}N_2O_3S$ (M+H) 321.1273, found 321.1267.

IR ν_{max} (cm^{-1}): 3257 (amide N-H stretch), 1717 (ester C=O stretch), 1703 (amide C=O stretch).

Elemental analysis: calculated for ($C_{16}H_{20}N_2O_3S$): C 59.98, H 6.29 and N 8.74, found for C 59.49, H 6.43 and N 8.65.

2-Heptanamidobenzo[*d*]thiazole-6-carboxylic acid (56):

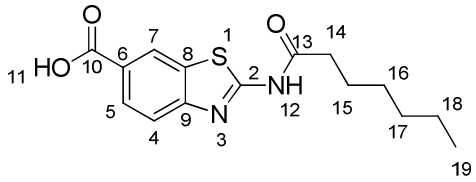

The title compound was obtained as a pink powder using general procedure C (50 mg, 65%).

m.p: >320 °C.

^{1}H NMR (DMSO-*d*$_6$): 0.84 (t, *J* = 6.6 Hz, 3H, **H19**), 1.27 (m. 6H, **H16-18**), 1.62 (p, *J* = 7.04 Hz, 2H, **H15**), 2.52 (m, 2H, **H14**), 7.76 (d, *J* = 8.36 Hz, 1H, **H4**), 7.98 (dd, *J* = 8.36, 1.32 Hz, 1H, **H5**), 8.59 (d, *J* = 0.88 Hz, 1H, **H7**), 12.52 (s, 1H, **NH12**), 12.95 (bs, 1H, **OH11**).

^{13}C NMR (DMSO-*d*$_6$): 14.50-35.72 (**C14-19**), 120.63-132.10 (**C4-8**), 152.46 (**C9**), 161.60 (**C2**), 167.67 (**C13**), 173.24 (**C10**).

FTMS-ESI: calculated for $C_{15}H_{19}N_2O_3S$ (M+H) 307.1116, found 307.1111.

IR ν_{max} (cm^{-1}): 3170 (amide N-H stretch), 3008 (carboxylic O-H stretch), 1707 (carboxylic C=O stretch), 1676 (amide C=O stretch).

Elemental analysis: calculated for ($C_{15}H_{18}N_2O_3S$): C 58.80, H 5.91 and N 9.14, found for C 59.30, H 6.17 and N 8.99.

Methyl 2-acetamidobenzo[*d*]thiazole-6-carboxylate (57):

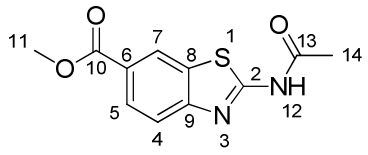

The title compound was obtained as pale yellow crystals using general procedure E after crystallization from ethyl acetate (150 mg, 62%).

m.p: 261-263 °C.

^{1}H NMR (DMSO-d_6): 2.22 (s, 3H, **H14**), 3.83 (s, 3H, **H11**), 7.79 (d, *J* = 8.8 Hz, 1H, **H4**), 7.98 (dd, *J* = 1.6, 8.8 Hz, 1H, **H5**), 8.62 (d, *J* = 1.6 Hz, 1H, **H7**), 12.55 (**NH12**).

^{13}C NMR (DMSO-d_6): 23.37 (**C14**), 52.72 (**C11**), 120.83-127.63 (**C4-8**), 152.71 (**C9**), 161.97 (**C2**), 166.60 (**C13**), 170.42 (**C10**).

FTMS-ESI: calculated for $C_{11}H_{11}N_2O_3S$ (M+H) 251.0490, found 251.0485.

IR ν_{max} (cm^{-1}): 3397 (amide N-H stretch), 1721 (ester C=O stretch), 1712 (amide C=O stretch).

Elemental analysis: calculated for ($C_{11}H_{10}N_2O_3S$): C 52.79, H 4.03 and N 11.19, found for C 52.61, H 4.21 and N 10.59.

Methyl 2-(methylsulfonamido)benzo[*d*]thiazole-6-carboxylate (58):

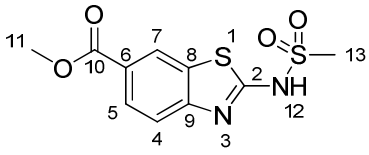

The title compound was obtained as white powder using general procedure F after column chromatography with 5% methanol/DCM (50 mg, 25%).

m.p: 286-288 °C.

^{1}H NMR (DMSO-*d*$_6$): 3.04 (s, 3H, **H13**), 3.86 (s, 3H, **H11**), 7.37 (d, *J* = 8.8 Hz, 1H, **H4**), 7.96 (dd, *J* = 8.8, 1.76 Hz, 1H, **H5**), 8.43 (d, *J* = 1.32 Hz, 1H, **H7**), 13.30 (**NH12**).

^{13}C NMR (DMSO-*d*$_6$): 41.63 (**C13**), 52.54 (**C11**), 113.00-129.06 (**C4-7**), 140.54 (**C8**), 140.65 (**C9**), 166.14 (**C2**), 167.91 (**C10**).

FTMS-ESI: calculated for $C_{10}H_{11}N_2O_4S_2$ (M+H) 287.0160, found 287.0155.

IR ν_{max} (cm^{-1}): 3421 (sulfonamide N-H stretch), 1714 (ester C=O stretch), 1442 (S=O stretch).

Elemental analysis: calculated for ($C_{10}H_{10}N_2O_4S_2$): C 41.71, H 3.52 and N 9.78, found for C 41.71, H 3.50 and N 9.69.

Methyl 2-(butylsulfonamido)benzo[*d*]thiazole-6-carboxylate (59):

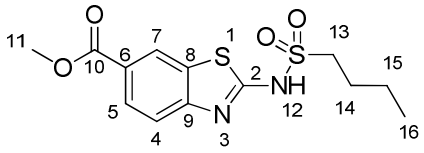

The title compound was obtained as white crystals using general procedure F after column chromatography with 5% methanol/DCM (40 mg, 15%).

m.p: 246-248 °C.

^{1}H NMR (DMSO-*d*$_6$): 0.88 (t, *J* = 7.04, 7.48 Hz, 3H, **H16**), 1.40 (sextet, *J* = 7.44, 7.48 Hz, 2H, **H15**), 1.66 (p, *J* = 5.72, 7.48 Hz, 2H, **H14**), 3.11 (t, *J* = 7.92, 7.48 Hz, 2H, **H13**), 3.85 (s, 3H, **H11**), 7.36 (d, *J* = 8.8 Hz, 1H, **H4**), 7.98 (dd, *J* = 8.8, 1.76 Hz, 1H, **H5**), 8.42 (d, *J* = 1.52 Hz, 1H, **H7**), 13.3 (bs, 1H, **NH12**).

^{13}C NMR (DMSO-d_6): 14.11-52.81 (**C13-16**), 53.28 (**C11**), 112.78-129.06 (**C4-7**), 140.21-140.95 (**C8, 9**), 163.68 (**C2**), 168.21 (**C10**).

FTMS-ESI: calculated for $C_{13}H_{17}N_2O_4S_2$ (M+H) 329.0630, found 329.0624.

IR ν_{max} (cm^{-1}): 3415 (sulfonamide N-H stretch), 1717 (ester C=O stretch), 1436 (S=O stretch).

Elemental analysis: calculated for ($C_{13}H_{16}N_2O_4S_2$): C 47.54, H 4.91 and N 8.53, found for C 47.15, H 4.78 and N 8.71.

Methyl 2-benzamidobenzo[*d*]thiazole-6-carboxylate (60):

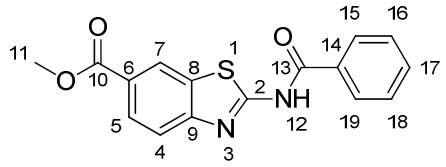

The title compound was obtained as white crystals using general procedure D after column chromatography with 20% ethyl acetate/hexane (200 mg, 60%).

m.p: 188-189 °C.

^{1}H NMR (DMSO-d_6): 3.89 (S, 3H, **H11**), 7.56 (t, *J* = 7.2 Hz, 2H, **H16, 18**), 7.68 (t, *J* = 7.24 Hz, 1H, **H17**), 7.85 (d, *J* = 8.8 Hz, 1H, **H4**), 8.04 (dd, *J* = 8.4, 2 Hz, 1H, **H5**), 8.14 (d, *J* = 7.2 Hz, 2H, **H15, 19**), 8.69 (d, *J* = 1.8 Hz, 1H, **H7**).13.1 (s, 1H, **NH12**).

^{13}C NMR (DMSO-d_6): 52.76 (**C11**), 124.50-134.21 (**C4-8, 15-19**), 142.36 (**C9**), 160.45 (**C2**), 166.82 (**C13**), 167.65 (**C10**).

FTMS-ESI: calculated for $C_{16}H_{13}N_2O_3S$ (M+H) 313.0647, found 313.0641.

IR ν_{max} (cm^{-1}): 3411 (amide N-H stretch), 1718 (ester C=O stretch), 1676 (amide C=O stretch).

Elemental analysis: calculated for ($C_{16}H_{12}N_2O_3S$): C 61.53, H 3.87 and N 8.97, found for C 61.52, H 3.93 and N 8.79.

Methyl 2-(4-nitrobenzamido)benzo[*d*]thiazole-6-carboxylate (61):

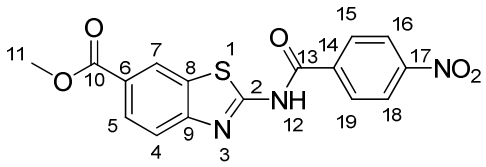

The title compound was obtained as white crystals using general procedure D (250 mg, 30%).

m.p: 320-321 °C.

^{1}H NMR (DMSO-d_6): 3.88 (s, 3H, **H11**), 7.82 (d, *J* = 8.32 Hz, 1H, **H4**), 8.02 (dd, *J* = 8.36, 1.76 Hz, 1H, **H5**), 8.36 (m, 4H, **H15, 16, 18, 19**), 8.66 (d, *J* = 1.32 Hz, 1H, **H7**).

^{13}C NMR (DMSO-d_6): 52.74 (**C11**), 124.20-130.54 (**C4-8, 14-16,18,19**), 145.12 (**C9**), 150.29 (**C17**), 163.54 (**C2**), 166.52 (**C13**), 166.59 (**C10**).

FTMS-ESI: calculated for $C_{16}H_{10}N_3O_5S$ (M-H) 356.0341, found 356.0346.

IR ν_{max} (cm^{-1}): 3257 (amide N-H stretch), 1698 (ester C=O stretch), 1624 (amide C=O stretch), 1588 (N=O stretch).

Elemental analysis: calculated for ($C_{16}H_{11}N_3O_5S$): C 53.78, H 3.10, N 11.76 and S 8.97, found for C 52.79, H 3.04, N 11.35 and S 8.71.

Methyl 2-(4-methoxybenzamido)benzo[*d*]thiazole-6-carboxylate (62):

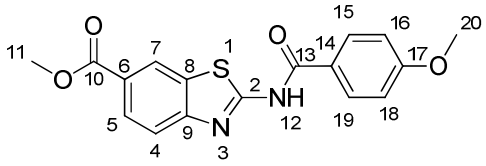

The title compound was obtained as light brown crystals using general procedure D after column chromatography with 1% methanol/chloroform (200 mg, 25 %).

m.p: 232-234 °C.

^{1}H NMR (DMSO-d_6): 3.86 (s, 3H, **H20**), 3.88 (s, 3H, **H11**), 7.09 (d, *J* = 8.8 Hz, 2H, **H15, 19**), 7.82 (d, *J* = 8.36 Hz, 1H, **H4**), 8.02 (dd, *J* = 8.36, 1.32 Hz, 1H , **H5**), 8.15 (d, *J* = 8.8 Hz, 2H, **H16, 18**), 8.67 (s, 1H, **H7**), 12.95 (s, 1H, **NH12**).

^{13}C NMR (DMSO-d_6): 52.72 (**C20**), 56.16 (**C11**), 114.58-127.66 (**C4-7**), 131.14-132.32 (**C8, 14-16, 18, 19**), 145.62 (**C9**), 152.65 (**C17**), 163.01-163.65 (**C2, 13**), 166.61 (**C10**).

FTMS-ESI: calculated for $C_{17}H_{15}N_2O_4S$ (M+H) 343.0753, found 343.0747.

IR ν_{max} (cm^{-1}): 3441 (amide N-H stretch), 1716 (ester C=O stretch), 1670 (amide C=O stretch), 1603 (N=O stretch).

Elemental analysis: calculated for ($C_{17}H_{14}N_2O_4S$): C 59.64, H 4.12 and N 7.18, found for C 59.08, H 4.10 and N 7.85.

Methyl 2-(4-chlorobenzamido)benzo[*d*]thiazole-6-carboxylate (63):

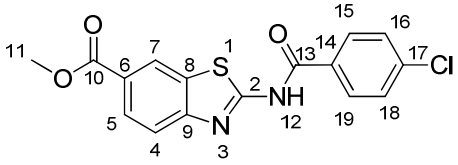

The title compound was obtained as white crystals using general procedure D (56 mg, 45%).

m.p: 224-225°C.

^{1}H NMR (DMSO-d_6): 3.88 (s, 3H, **H11**), 7.64 (d, *J* = 6.8 Hz, 2H, **H15, 19**), 7.86 (*J* = 6.8 Hz, 1H, **H4**), 8.03 (dd, *J* = 6.8, 1.2 Hz, 1H, **H5**), 8.14 (d, *J* = 6.8 Hz, 2H, **H16, 18**), 8.68 (s, 1H, **H7**), 13.19 (s, 1H, **NH12**).

^{13}C NMR (DMSO-d_6): 52.59 (**C11**), 124.35-127.59 (**C4-8**), 129.21 (**C14, 15, 19**), 130.77 (**C16-18**), 138.39 (**C9**), 160.57 (**C2**), 166.32-166.4 (**C13, 10**).

FTMS-ESI: calculated for $C_{16}H_{10}ClN_2O_3S$ (M-H) 345.0101, found 345.0107.

IR ν_{max} (cm^{-1}): 3305 (amide N-H stretch), 1701 (ester C=O stretch), 1676 (amide C=O stretch), 1271 (C-Cl stretch).

Elemental analysis: calculated for ($C_{16}H_{11}ClN_2O_3S$): C 55.41, H 3.20, and N 8.08, found for C 54.92, H 3.01 and N 7.64.

Methyl 2-(phenylsulfonamido)benzo[*d*]thiazole-6-carboxylate (64):

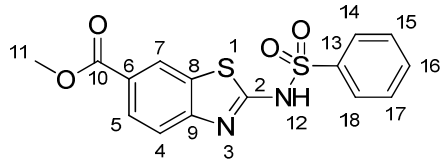

The title compound was obtained as light brown crystals using general procedure G (250 mg, 55%).

m.p: 258-259 °C.

^{1}H NMR (DMSO-d_6): 3.85 (s, 3H, **H11**), 7.38 (d, *J* = 8.36 Hz, 1H, **H4**), 7.57 (d, *J* = 7.38 Hz, 2H, **H15, 17**), 7.62 (t, *J* = 7.28 Hz, 1H, **H16**), 7.86 (d, *J* = 7.20 Hz, 2H, **H14, 18**), 7.96 (dd, *J* = 8.36, 1.32 Hz, 1H, **H5**), 8.45 (d, *J* = 1.36 Hz, 1H, **H7**).

^{13}C NMR (DMSO-d_6): 52.72 (**C11**), 113.15-125.92 (**C4-7**), 126.29-129.21 (**C14-18**), 133.07 (**C8**), 140.57 (**C13**), 142.14 (**C9**), 163.97 (**C2**), 168.42 (**C10**).

FTMS-ESI: calculated for $C_{15}H_{13}N_2O_4S_2$ (M+H) 349.0317, found 349.0311.

IR ν_{max} (cm^{-1}): 3442 (sulfonamide N-H stretch), 1714 (ester C=O stretch), 1440 (S=O stretch).

Elemental analysis: calculated for ($C_{15}H_{12}N_2O_4S_2$): C 51.71, H 3.47, N 8.04 and S 18.41, found for C 51.40, H 3.21, N 7.79 and S 18.01.

2-(Phenylsulfonamido)benzo[*d*]thiazole-6-carboxylic acid (65):[113]

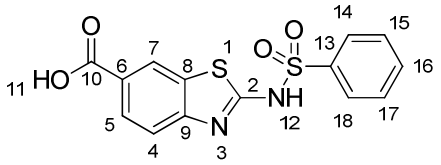

Compound **64** (100 mg, 0.3 mmol, 1 eq) was suspended in 30 ml water, then lithium hydroxide monohydrate (110 mg, 2.6 mmol, 5 eq) was added, and the mixture stirred at room temperature for 4 hours. The mixture was diluted with 100 ml water, then acidified with 1M HCl to pH 4.00, and the precipitate was filtered and dried at room temperature to give **65** (45 mg, 45%).

m.p: 320-321°C.

^{1}H NMR (DMSO-d_6): 7.33 (d, *J* = 8.4 Hz, 1H, **H4**), 7.55-7.64 (m, 3H, **H15-17**), 7.85 (d, *J* = 5.92 Hz, 2H, **H14, 18**), 7.93 (dd, *J* = 1.08, 8.40 Hz, 1H, **H5**), 8.40 (d, *J* = 0.84 Hz, 1H, **H7**), 13.03 (s, 1H, **NH12**), 13.43 (bs, 1H, **OH11**).

^{13}C NMR (DMSO-d_6): 113.16-125.85 (**C4-7**), 126.38-129.29 (**C14-18**), 133.16 (**C8**), 140.51 (**C13**), 142.27 (**C9**), 163.13 (**C2**), 168.56 (**C10**).

FTMS-ESI: calculated for $C_{14}H_{11}N_2O_4S_2$ (M+H) 335.0160, found 335.0155.

IR ν_{max} (cm^{-1}): 3434 (sulfonamide N-H stretch), 3095 (carboxylic O-H stretch), 1685 (carboxylic C=O stretch), 1322 (S=O stretch).

Elemental analysis: calculated for ($C_{14}H_{10}N_2O_4S_2$): C 50.29, H 3.01 and N 8.38, found for C 50.43, H 3.19 and N 7.63.

Methyl 2-(4-methoxyphenylsulfonamido)benzo[*d*]thiazole-6-carboxylate (66):

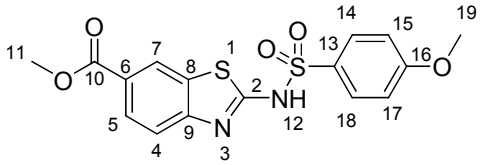

The title compound was obtained as a brown powder using general procedure G after column chromatography with 10% methanol/chloroform (60 mg, 22%).

m.p: 228-229 °C.

^{1}H NMR (DMSO-*d*$_6$): 3.80 (s, 3H, **H19**), 3.86 (s, 3H, **H11**), 7.08 (d, *J* = 9.04 Hz, 2H, **H14, 18**), 7.35 (d, *J* = 8.8 Hz, 1H, **H4**), 7.79 (d, *J* = 8.8 Hz, 2H, **H15, 17**), 7.96 (dd, *J* = 1.76, 8.40 Hz, 1H, **H5**), 8.45 (d, *J* = 1.76 Hz, 1H, **H7**), 13.41 (bs, 1H, **NH12**).

^{13}C NMR (DMSO-*d*$_6$): 52.84 (**C19**), 56.21 (**C11**), 114. -125.96 (**C4-7**), 128.60 - 129.14 (**C13-15, 17, 18**), 133.93 (**C8**), 140.71 (**C9**), 162.89 (**C2**), 166.10 (**C16**), 168.01 (**C10**).

FTMS-ESI: calculated for $C_{16}H_{15}N_2O_5S_2$ (M+H) 379.0422, found 379.0417.

IR ν_{max} (cm^{-1}): 3421 (sulfonamide N-H stretch), 1719 (ester C=O stretch), 1433 (S=O stretch).

Elemental analysis: calculated for ($C_{16}H_{14}N_2O_5S_2$): C 51.71, H 3.47, N 8.04 and S 18.41, found for C 51.45, H 3.68, N 7.41 and S 18.59.

Methyl 2-(4-nitrophenylsulfonamido)benzo[*d*]thiazole-6-carboxylate (67):

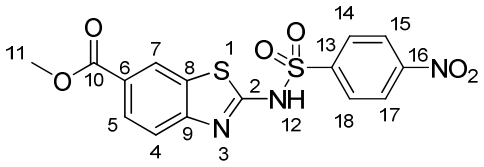

The title compound was obtained as dark brown crystals using general procedure G after column chromatography with 10% methanol/chloroform (40 mg, 14%).

m.p: 190-192 °C.

^{1}H NMR (DMSO-*d*$_6$): 3.87 (s, 3H, **H11**), 7.40 (d, *J* = 8.36 Hz, 1H, **H4**), 8.00 (dd, *J* = 8.36, 1.76 Hz, 1H, **H5**), 8.10 (d, *J* = 8.8 Hz, 2H, **H14, 18**), 8.39 (d, *J* = 8.8 Hz, 2H, **H15, 17**), 8.50 (d, *J* = 1.76 Hz, 1H, **H7**).

^{13}C NMR (DMSO-d_6): 56.81 (**C11**), 117.88-125.96 (**C4-7**), 128.-133.93 (**C8, 13-15, 17, 18**), 140.71 (**C9**), 162.89 (**C16**), 166.10 (**C2**), 168.01 (**C10**).

FTMS-ESI: calculated for $C_{15}H_{10}N_3O_6S_2$ (M-H) 392.0011, found 392.0016.

IR ν_{max} (cm^{-1}): 3410 (sulfonamide N-H stretch), 1689 (ester C=O stretch), 1540 (N=O stretch), 1322 (S=O stretch).

Elemental analysis: calculated for ($C_{15}H_{11}N_3O_6S_2$): C 45.80, H 2.82 and N 10.68, found for C 46.69, H 2.94 and N 11.04.

Methyl 2-(4-chlorophenylsulfonamido)benzo[*d*]thiazole-6-carboxylate (68):

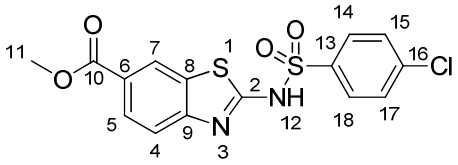

The title compound was obtained as pale yellow crystals using general procedure G (95 mg, 35%).

m.p: 262-263°C.

^{1}H NMR (DMSO-d_6): 3.86 (s, 3H, **H11**), 7.36 (d, *J* = 6 Hz, 1H, **H4**), 7.64 (d, *J* = 6.8 Hz, 2H, **H14, 18**), 7.86 (d, *J* = 6.8 Hz, 2H, **H15, 17**), 7.97 (dd, *J* = 1.2, 6 Hz, 1H, **H5**), 8.47 (d, *J* = 1.2 Hz, 1H, **H7**), 13.45 (bs, 1H, **NH12**).

^{13}C NMR (DMSO-d_6): 52.72 (**C11**), 118.28-125.95 (**C4-7**), 128.27-129.32 (**C13-15, 17, 18**), 139.21 (**C8**), 140.82 (**C9**), 141.02 (**C16**), 164.52 (**C2**), 169.56 (**C10**).

FTMS-ESI: calculated for $C_{16}H_{10}ClN_2O_4S_2$ (M-H) 380.9771, found 380.9776.

IR ν_{max} (cm^{-1}): 3421 (sulfonamide N-H stretch), 1716 (ester C=O stretch), 1435 (S=O stretch).

methyl 2-(4-methylphenylsulfonamido)benzo[*d*]thiazole-6-carboxylate (69):

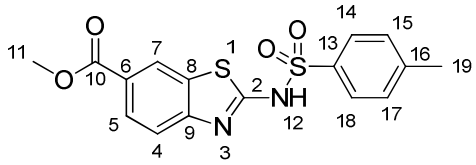

The title compound was obtained as a white powder using general procedure G (60 mg, 43%).

m.p: 254-256°C.

^{1}H NMR (DMSO-d_6): 2.36 (s, 3H, **H19**), 3.85 (s, 3H, **H11**), 7.35-7.38 (m, 3H, **H4, 14, 18**), 7.74 (d, *J* = 8 Hz, 2H, **H15, 17**), 7.96 (dd, *J* = 7.45, 1.75 Hz, 1H, **H5**), 8.45 (d, *J* = 1.70 Hz, 1H, **H7**), 13.50 (bs, 1H, **NH12**).

^{13}C NMR (DMSO-d_6): 21.43 (**C19**), 52.71 (**C11**), 118.13-125.98 (**C4-7**), 126.36-139.54 (**C8, 9, 13-18**), 165.99 (**C2**), 168.22 (**C10**).

FTMS-ESI: calculated for $C_{16}H_{13}N_2O_4S_2$ (M-H) 361.0317, found 361.0328.

IR ν_{max} (cm^{-1}): 3452 (sulfonamide N-H stretch), 1716 (ester C=O stretch), 1434 (S=O stretch).

Ethyl 2-amino-1*H*-benzo[*d*]imidazole-5-carboxylate (71):

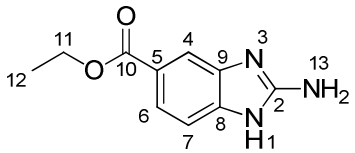

The title compounds was obtained as pale yellow crystals using general procedure A after crystallization from ethanol/water (800 mg, 76%).

m.p: 162-162.8 °C.

^{1}H NMR (DMSO-*d*$_6$): 1.31 (t, *J* = 6.8, 7.04 Hz, 3H, **H12**), 4.27 (q, *J* = 7.04, 7.48 Hz, 2H, **H11**), 6.58 (bs, 2H, **NH13**), 7.13 (d, *J* = 8.36 Hz, 1H, **H7**), 7.57 (dd, *J* = 8.36, 1.76 Hz, 1H, **H6**), 7.71 (d, *J* = 1.76 Hz, 1H, **H4**), 10.98 (bs, 1H, **NH1**).

^{13}C NMR (DMSO-*d*$_6$): 14.90 (**C12**), 60.48 (**C11**), 112.24-120.59 (**C4-7**), 132.32-137.54 (**C8, 9**), 157.94 (**C2**), 167.22 (**C10**).

IR ν_{max} (cm^{-1}): 3458 (1° amine N-H stretch), 1668 (ester C=O stretch).

FTMS-ESI: calculated for $C_{10}H_{12}N_3O_2$ (M+H) 206.093, found 206.0923.

Elemental analysis: calculated for ($C_{10}H_{11}N_3O_2$): C 58.53, H 5.4 and N 20.48, Found for C 58.01; H 5.2 and N 19.9

2-Amino-5-phenylcarbonylbenzimidazole (72):

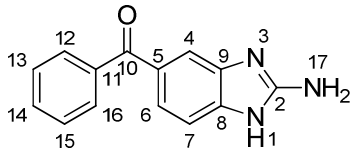

The title compound was obtained as a pale yellow powder using general procedure A (3.2 g, 94.9%).

m.p: 186-186.4 °C.[129]

^{1}H NMR (DMSO-*d*$_6$): 6.64 (bs, 2H, **NH17**), 7.19 (d, *J* = 7.9 Hz, 1H, **H7**), 7.41 (d, *J* = 7.9 Hz, 1H, **H6**), 7.53 (m, 3H, **H4, 13, 15**), 7.61 (t, *J* = 7.48, 1H, **H14**), 7.68 (d, *J* = 7.48 Hz, 2H, **H12,16**), 10.99 (bs, 1H, **NH1**).

^{13}C NMR (DMSO-*d*$_6$): 121.32-124.54 (**C4-7**), 128.7-129.6 (**C11-16**), 130.5 (**C8**), 131.9 (**C9**), 159.6 (**C2**), 196.93 (**C10**).

FTMS-ESI: calculated for $C_{14}H_{12}N_3O$ (M+H) 238.098, found 238.0976.

IR ν_{max} (cm^{-1}): 3456 (amide N-H stretch), 1651 (keto C=O stretch).

Elemental analysis: calculated for ($C_{14}H_{11}N_3O$): C 70.87, H 4.67 and N 17.71, found for C 70.44, H 4.83 and N 17.94.

***N*-(5-Benzoyl-1*H*-benzo[*d*]imidazol-2-yl)acetamide (76):**

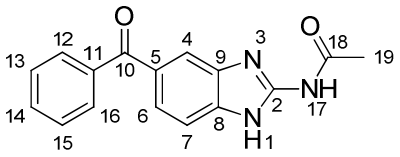

The title compound was obtained as fine pink crystals using general procedure E after crystallization from ethyl acetate/hexane (350 mg, 71%).

m.p: 210-211 °C.

^{1}H NMR (DMSO-d_6): 2.18 (s, 3H, **H19**), 7.19 (m, 1H, **H7**), 7.32 (m, 1H, **H6**), 7.59 (m, 5H, **H12-16**), 7.72 (s, 1H, **H4**), 11.74 (bs, 1H, **NH1**), 12.31 (bs, 1H, **NH17**).

^{13}C NMR (DMSO-d_6): 21.63 (**C19**), 123.90-128.19 (**C4-7**), 128.79-128.90 (**C11-16**), 129.65-131.92 (**C8, 9**), 149.57 (**C2**), 172.64 (**C18**), 196.21 (**C10**).

FTMS-ESI: calculated for $C_{16}H_{14}N_3O_2$ (M+H) 280.11, found 280.1074.

IR ν_{max} (cm^{-1}): 3351 (amide N-H stretch), 1690 (ester C=O stretch), 1629 (amide C=O stretch).

Elemental analysis: calculated for ($C_{16}H_{13}N_3O_2$): C 68.81, H 4.69 and N 15.05, found for C 68.92, H 4.88 and N 15.33.

***N*-(5-Benzoyl-1*H*-benzo[*d*]imidazol-2-yl)benzamide (77):**

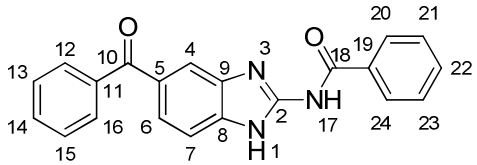

The title compound was obtained as pale yellow crystals using general procedure D after crystallization from ethyl acetate/ether (400 mg, 59%).

m.p: 198-199 °C.

^{1}H NMR (DMSO-*d*$_6$): 7.49-7.66 (m, 8H, **H13-15, 20-23**), 7.73 (d, *J* = 6.6 Hz, **H7**), 7.93 (bs, 1H, **H6**), 7.96 (s, 1H, **H4**), 8.13 (d, *J* = 7.04 Hz, 2H, **H12, 16**), 12.62 (bs, 2H, **NH1, NH17**).

^{13}C NMR (DMSO-*d*$_6$): 124.58-129.95 (**C4-7, 11-16**), 130.79-139.45 (**C8, 9, 19-24**), 145.86 (**C2**), 167.90 (**C18**), 196.17 (**C10**).

FTMS-ESI: calculated for $C_{21}H_{16}N_3O_2$ (M+H) 342.1243, found 342.1238.

IR ν_{max} (cm^{-1}): 3366 (amide N-H stretch), 1676 (keto C=O stretch), 1653 (amide C=O stretch).

Elemental analysis: calculated for ($C_{21}H_{15}N_3O_2$): C 73.89, H 4.43 and N 12.30, found for C 73.67, H 4.12 and N 11.96.

Methyl 2-decanamido-1*H*-benzo[*d*]imidazole-5-carboxylate (78):

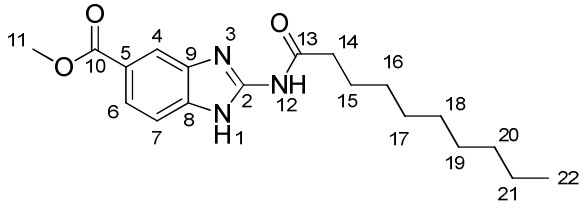

The title compound was obtained as shiny colourless flakes using general procedure D after crystallization from ethyl acetate (1.27 g, 71%).

m.p: 190-191°C.

^{1}H NMR (DMSO-*d*$_6$): 0.84 (m, 3H, **H22**), 1.22 (bs, 12H, **H16-21**), 1.45 (m, 2H, **H15**), 2.18 (t, *J* = 7.44 Hz, 2H, **H14**), 3.79 (s, 3H, **H11**), 6.59 (bs, 1H, **NH1**), 7.12 (d, *J* = 7.92 Hz, 1H, **H7**), 7.56 (dd, *J* = 1.32, 7.88 Hz, 1H, **H6**), 7.69 (d, *J* = 1.32 Hz, 1H, **H4**).

^{13}C NMR (DMSO-d_6): 14.52-35.96 (**C14-22**), 52.39 (**C11**), 112.10-122.28 (**C4-7**), 123.41-126.65 (**C8, 9**), 151.31 (**C2**), 167.44 (**C13**), 173.34 (**C10**).

FTMS-ESI: calculated for $C_{19}H_{27}N_3O_3$ (M+H) 346.2131, found 346.2118.

IR ν_{max} (cm^{-1}): 3348 (amide N-H stretch), 1702 (ester C=O stretch), 1654 (amide C=O stretch).

Elemental analysis: calculated for ($C_{19}H_{26}N_3O_3$): C 66.06, H 7.88 and N 12.16, found C 64.96, H 7.81 and N 11.81.

2-Decanamido-1*H*-benzo[*d*]imidazole-5-carboxylic acid (79):

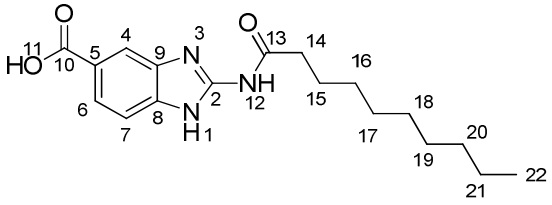

The title compound was obtained as a pink powder using general procedure C (400 mg, 83.3%).

m.p: 201-202 °C.

^{1}H NMR (DMSO-d_6): 0.83 (t, *J* = 7.04 Hz, 3H, **H22**), 1.23 (bs, 12H, **H16-21**), 1.47 (bs, 2H, **H15**), 2.18 (t, *J* = 7.44 Hz, 2H, **H14**), 6.53 (bs, 1H, **NH1**), 7.11 (d, *J* = 7.92 Hz, 1H, **H7**), 7.57 (d, *J* = 8.06 Hz, 1H, **H6**), 7.69 (s, 1H, **H4**).

^{13}C NMR (DMSO-d_6): 14.53-35.96 (**C14-22**), 104.82-122.27 (**C4-7**), 139.45-148.44 (**C8, 9**), 157.83 (**C2**), 169.24 (**C13**), 173.27 (**C10**).

FTMS-ESI: calculated for $C_{18}H_{26}N_3O_3$ (M+H) 332.4173, found 332.4160.

IR ν_{max} (cm^{-1}): 3325 (amide N-H stretch), 3080 (carboxylic O-H stretch), 1687 (carboxylic C=O stretch), 1690 (amide C=O stretch).

Elemental analysis: calculated for ($C_{18}H_{25}N_3O_3$): C 65.23, H 7.60 and N 12.68, found for C 64.87; H 8.20 and N 11.40.

Methyl 2-propionamido-1*H*-benzo[*d*]imidazole-5-carboxylate (80):

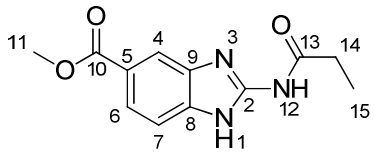

The title compound was obtained as fine white crystals using general procedure D after crystallization from ethyl acetate/hexane (580 mg, 45%).

m.p: 250-250.5 °C.

^{1}H NMR (DMSO-d_6): 1.12 (t, *J* = 7.48 Hz, 3H, **H15**), 2.49 (q, *J* = 7.48, 7.46 Hz, 2H, **H14**), 3.84 (s, 3H, **H11**), 7.47 (bs, 1H, **H7**), 7.36 (d, *J* = 8.36 Hz, 1H, **H6**), 8.12 (bs, 1H, **H4**), 11.67 (bs, 1H, **NH1**), 12.37 (bs, 1H, **NH12**).

^{13}C NMR (DMSO-d_6): 9.65 (**C15**), 29.32 (**C14**), 52.36 (**C11**), 115.31-123.19 (**C4-7**), 142.21-149.11 (**C8, 9**), 158.44 (**C2**), 167.45 (**C13**), 174.06 (**C10**).

FTMS-ESI: calculated for $C_{12}H_{14}N_3O_3$ (M+H) 248.1035, found 248.1031.

IR ν_{max} (cm^{-1}): 3348 (amide N-H stretch), 1707 (ester C=O), 1697 (amide C=O stretch).

Elemental analysis: calculated for ($C_{12}H_{13}N_3O_3$): C 58.29, H 5.3 and N 16.99, found for C 57.98, H 5.39 and N 16.71.

2-Propionamido-1*H*-benzo[*d*]imidazole-5-carboxylic acid (81):

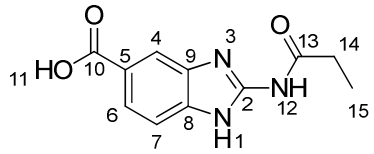

The title compound was obtained as a pink powder using general procedure C (85 mg, 61%).

m.p: 263 °C (with decomposition).

^{1}H NMR (DMSO-d_6): 1.12 (t, *J* = 7.52 Hz, 3H, **H15**), 2.46 (q, *J* = 7.52 Hz, 2H, **H14**), 7.45 (bs, 1H, **H7**), 7.72 (dd, *J* = 8.36, 1.48 Hz, **H6**), 8.09 (bs, 1H, **H4**), 11.65 (bs, 1H, **NH1**), 12.33 (bs, 2H, **NH12, OH11**).

^{13}C NMR (DMSO-d_6): 107.59-121.56 (**C4-7**), 123.56-136.77 (**C8, 9**), 140.59 (**C2**), 168.55 (**C13**), 174.02 (**C10**).

FTMS-ESI: calculated for $C_{11}H_{12}N_3O_3$ (M+H) 234.0879, found 234.0873.

IR ν_{max} (cm^{-1}): 3274 (amide N-H stretch), 3063 (carboxylic O-H stretch), 1701 (carboxylic C=O stretch), 1693 (amide C=O stretch).

Elemental analysis: calculated for ($C_{11}H_{11}N_3O_3$): C 45.90, H 4.95 and N 22.94, found C 47.39, H 4.89 and N 18.95.

Methyl 2-(2-phenylacetamido)-1*H*-benzo[*d*]imidazole-5-carboxylate (82):

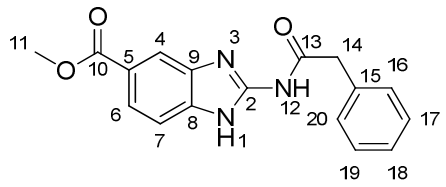

The title compound was obtained as fine white crystals using general procedure D after crystallization from ethyl acetate (660 mg, 60%).

m.p: 238-239 °C.

^{1}H NMR (DMSO-d_6): 3.78 (s, 2H, **H14**), 3.84 (s, 3H, **H11**), 7.27 (t, *J* = 7.48 Hz, 1H, **H18**), 7.37 (m, 4H, **H16,17,19,20**), 7.51 (bs, 1H, **H7**), 7.74 (d, *J* = 8.36 Hz, 1H, **H6**), 8.09 (bs, 1H, **H4**), 12.00 (bs, 1H, **NH1**), 12.38 (bs, 1H, **NH12**).

^{13}C NMR (DMSO-d_6): 42.84 (**C14**), 52.41 (**C11**), 122.89-123.18 (**C4-7**), 123.24-127.42 (**C8, 9**), 128.98-129.81 (**C15-20**), 145.54 (**C2**), 167.40 (**C13**), 171.17 (**C10**).

FTMS-ESI: calculated for $C_{17}H_{16}N_3O_3$ (M+H) 310.1192, found 310.1187.

IR ν_{max} (cm^{-1}): 3337 (amide N-H stretch), 1704 (ester C=O stretch), 1644 (amide C=O stretch).

Elemental analysis: calculated for ($C_{17}H_{15}N_3O_3$): C 66.01, H 4.89 and N 13.58, found for C 65.87, H 4.79 and N 13.51.

2-(2-Phenylacetamido)-1*H*-benzo[*d*]imidazole-5-carboxylic acid (83):

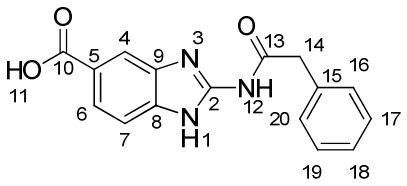

The title compound was obtained as a white powder using general procedure C (45 mg, 57%).

m.p: 306-307 °C.

^{1}H NMR (DMSO-d_6): 3.79 (s, 2H, **H14**), 7.26 (m, 1H, **H18**), 7.32-7.39 (m, 4H, **H16, 17, 19, 20**), 7.46 (d, *J* = 8.36 Hz, 1H, **H7**), 7.72 (dd, *J* = 8.36, 1.32 Hz, 1H, **H6**), 8.04 (bs, 1H, **H4**), 12.01 (bs, 1H, **NH12**), 12.36 (bs, 1H, **OH11**).

^{13}C NMR (DMSO-d_6): 40.28 (**C14**), 120.41-129.80 (**C4-7, 15-20**), 132.54-135.58 (**C8, 9**), 148.35 (**C2**), 168.52 (**C13**), 171.15 (**C10**).

FTMS-ESI: calculated for $C_{16}H_{14}N_3O_3$ (M+H) 296.1035, found 296.10297.

IR ν_{max} (cm^{-1}): 3376 (amide N-H stretch), 2921 (carboxylic O-H stretch), 1684 (carboxylic C=O stretch), 1636 (amide C=O stretch).

Elemental analysis: calculated for ($C_{16}H_{13}N_3O_3$): C 65.08, H 4.44 and N 14.23, found for C 65.37, H 3.88 and N 14.12.

Ethyl 2-hexanamido-1*H*-benzo[*d*]imidazole-5-carboxylate (84):

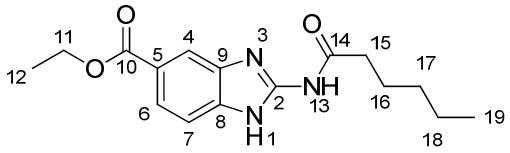

The title compound was obtained as fine off-white crystals using general procedure D after crystallization from methanol/water (620 mg, 42%).

m.p: 209-210 °C.

^{1}H NMR (DMSO-d_6): 0.87 (m, 3H, **H19**), 1.32 (m, 7H, **H12, 17, 18**), 1.62 (t, *J* = 7.04 Hz, 2H, **H16**), 2.44 (t, *J* = 7.48 Hz, 2H, **H15**), 4.29 (q, *J* = 7.16, 7.08 Hz, 2H, **H11**), 7.48 (bs, 1H, **H7**), 7.73 (d, *J* = 8.36 Hz, 1H, **H6**), 8.11 (bs, 1H, **H4**), 11.69 (bs, 1H, **NH1**), 12.38 (bs, 1H, **NH13**).

^{13}C NMR (DMSO-d_6): 14.41-35.92 (**C12, 15-19**), 60.86 (**C11**), 113.70-122.56 (**C4-7**), 126.65-132.84 (**C8, 9**), 145.19 (**C2**), 166.93 (**C14**), 173.38 (**C10**).

FTMS-ESI: calculated for $C_{16}H_{22}N_3O_3$ (M+H) 304.1661, found 304.1700.

IR ν_{max} (cm^{-1}): 3346 (amide N-H stretch), 1689 (ester C=O stretch), 1645 (amide C=O stretch).

Elemental analysis: calculated for ($C_{16}H_{21}N_3O_3$): C 63.35, H 6.98 and N 13.85, found for C 63.24, H 7.10 and N 13.70.

2-Hexanamido-1*H*-benzo[*d*]imidazole-5-carboxylic acid (85):

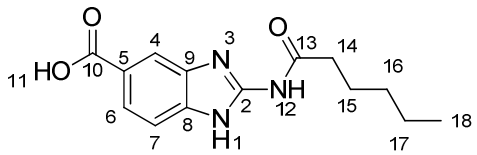

The title compound was obtained as light brown flakes using general procedure C (90mg, 40%).

m.p: 262-263 °C.

^{1}H NMR (DMSO-d_6): 0.88 (m, 3H, **H18**), 1.32 (m, 4H, **H16, 17**), 1.63 (m, 2H, **H15**), 2.43 (t, *J* = 7.36 Hz, 2H, **H14**), 7.46 (bs, 1H, **H7**), 7.72 (d, *J* = 8.36 Hz, 1H, **H6**), 8.02 (bs, 1H, **H4**), 11.66 (s, 1H, **NH1**), 12.36 (bs, 2H, **NH12, OH11**).

^{13}C NMR (DMSO-d_6): 14.4-35.94 (**C14-18**), 115.78-125.54 (**C4-7**), 136.23 (**C8, 9**), 153.21 (**C2**), 168.42 (**C13**), 173.34 (**C10**).

FTMS-ESI: calculated for $C_{14}H_{18}N_3O_3$ (M+H) 276.1348, found 276.1339.

IR ν_{max} (cm^{-1}): 3222 (amide N-H stretch), 3075 (carboxylic O-H stretch), 1690 (carboxylic C=O stretch), 1640 (amide C=O stretch).

Elemental analysis: calculated for ($C_{14}H_{17}N_3O_3$): C 61.08, H 6.22 and N 15.26, found for C 59.71, H 6.21 and N 15.76.

***N*-(5-Benzoyl-1*H*-benzo[*d*]imidazol-2-yl)decanamide (86):**

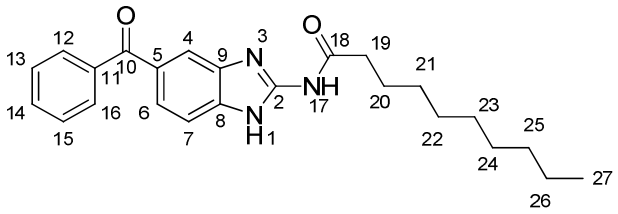

The title compound was obtained as fine white crystals using general procedure D after crystallization from ethyl acetate (760 mg, 90%).

m.p: 163-164°C.

^{1}H NMR (DMSO-d_6): 0.84 (t, *J* = 5.28, 7.04 Hz, 3H, **H27**), 1.24 (bs, 12H, **H21-26**), 1.62 (m, 2H, **H20**), 2.45 (t, *J* = 7.44 Hz, 2H, **H19**), 7.55-7.62 (m, 5H, **H12-16**), 7.72 (m, 2H, **H6, 7**), 7.96 (bs, 1H, **H4**), 11.71 (bs, 1H, **NH1**), 12.35 (bs, 1H, **NH17**).

^{13}C NMR (DMSO-d_6): 14.50-35.99 (**C19-27**), 111.96-123.75 (**C4-7**), 128.-129.88 (**C11-16**), 132.35-145.25 (**C8, 9**), 149.90 (**C2**), 167.36 (**C18**), 173.43 (**C10**).

FTMS-ESI: calculated for $C_{24}H_{30}N_3O_2$ (M+H) 392.2338, found 392.2331.

IR ν_{max} (cm^{-1}): 3323 (amide N-H stretch), 1702 (carboxylic C=O stretch), 1635 (amide C=O stretch).

Elemental analysis: calculated for ($C_{24}H_{29}N_3O_2$): C 73.63, H 7.47 and N 10.73, found for C 73.20, H 7.54 and N 10.66.

Methyl 2-benzamido-1*H*-benzo[*d*]imidazole-5-carboxylate (87):

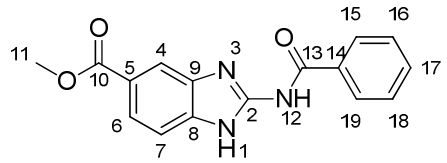

The title compound was obtained as a fine white powder using general procedure D after crystallization from DCM/ether (480 mg, 62%).

m.p: 178-178.5 °C.

^{1}H NMR (DMSO-d_6): 3.87 (s, 3H, **H11**), 7.55 (m, 5H, **H15-19**), 7.78 (d, *J* = 7.48 Hz, 1H, **H7**), 7.93 (d, *J* = 7.48 Hz, 1H, **H6**), 8.13 (m, 1H, **H4**), 12.63 (bs, 1H, **NH12**).

^{13}C NMR (DMSO-d_6): 61.13 (**C11**), 112.54-122.66 (**C4-7**), 125.32-136.13 (**C14-19**), 136.86 (**C8, 9**), 153.60 (**C2**), 163.99 (**C13**), 166.24 (**C10**).

FTMS-ESI: calculated for $C_{16}H_{13}N_3O_3$ (M+H) 296.1305, found 296.2901.

IR ν_{max} (cm^{-1}): 3302 (amide N-H stretch), 1712 (ester C=O stretch), 1687 (amide C=O stretch).

Elemental analysis: calculated for ($C_{16}H_{12}N_3O_3$): C 65.08, H 4.44 and N 14.23, found for C 67.08, H 4.25 and N 10.28.

2-Benzamido-1*H*-benzo[*d*]imidazole-5-carboxylic acid (88):

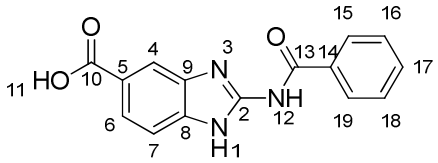

The title compound was obtained as light brown flakes using general procedure D (90 mg, 64%).

m.p: >300 °C.

^{1}H NMR (DMSO-d_6): 7.56 (m, 3H, **H16, 17, 18**), 7.64 (d, *J* = 7.48 Hz, 1H, **H7**), 7.80 (dd, *J* = 1.32 Hz, 7.36 Hz, 1H, **H6**), 8.10 (s, 1H, **H4**), 8.15 (d, *J* = 7.48 Hz, 2H, **H15, 19**), 12.54 (bs, 2H, **NH12, OH11**).

^{13}C NMR (DMSO-d_6): 123.5-124.3 (**C4-7**), 128.7-129.70 (**C14-19**), 132.9-133.7 (**C8, 9**), 150.5 (**C2**), 166.8 (**C13**), 168.3 (**C10**).

FTMS-ESI: calculated for $C_{15}H_{11}N_3O_3$ (M+H) 282.0879; found 282.0870.

IR ν_{max} (cm^{-1}): 3469-3303 (amide N-H stretch), 3056 (carboxylic O-H stretch), 1674 (carboxylic C=O stretch), 1654 (amide C=O stretch).

Elemental analysis: calculated for ($C_{15}H_{10}N_3O_3$): C 64.05, H 3.94 and N 14.92, found for C 63.18, H 4.07 and N 13.95.

***N*-(5-Benzoyl-1*H*-benzo[*d*]imidazol-2-yl)-4-chlorobenzamide (89):**

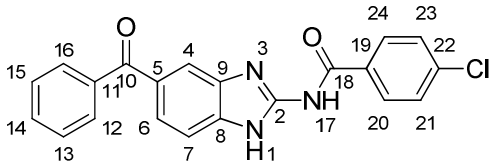

The title compound was obtained as fine white crystals using general procedure D after crystallization from methanol (250 mg, 54%).

m.p: 239-239.5 °C.

^{1}H NMR (DMSO-*d*$_6$): 7.55-7.68 (m, 7H, **H6, 7, 12-16**), 7.75 (d, *J* = 7.04 Hz, 2H, **H24, 20**), 7.91 (s, 1H, **H4**), 8.14 (d, *J* = 7.04 Hz, 2H, **H21, 23**), 12.61 (bs, 1H, **NH17**).

^{13}C NMR (DMSO-*d*$_6$): 124.69-128.32 (**C4-7**), 130.74-137.69 (**C8, 9, 11-16, 19-24**), 138.70 (**C22**), 145.75 (**C2**), 171.2 (**C18**), 195.97 (**C10**).

FTMS-ESI: calculated for $C_{21}H_{14}ClN_3O_2$ (M+H) 376.0853, found 376.0844.

IR ν_{max} (cm^{-1}): 3351 (amide N-H stretch), 1685 (keto C=O stretch), 1631 (amide C=O stretch).

Elemental analysis: calculated for ($C_{21}H_{13}ClN_3O_2$): C 67.12, H 3.75 and N 11.18, found for C 66.03, H 3.57 and N 10.45.

***N*-(5-Benzoyl-1*H*-benzo[*d*]imidazol-2-yl)heptanamide (90):**

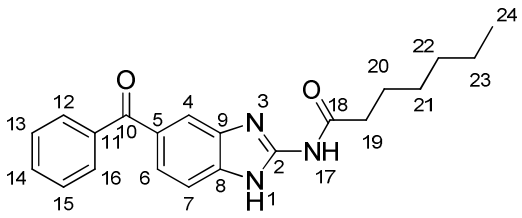

The title compound was obtained as pale yellow crystals using general procedure D (170 mg, 61%).

m.p: 189-189.5 °C.

^{1}H NMR (DMSO-*d*$_6$): 0.87 (t, *J* = 6.6 Hz, 3H, **H24**), 1.29 (bs, 6H, **H21-23**), 1.63 (m, 2H, **H20**), 2.46 (t, *J* = 7.44 Hz, 2H, **H19**), 7.63 (m, 7H, **H6, 7, 12-16**), 7.96 (bs, 1H, **H4**), 11.72 (bs, 1H, **NH1**), 12.36 (bs, 1H, **NH17**).

^{13}C NMR (DMSO-*d*$_6$): 14.30-35.90 (**C19-24**), 111.32-124.40 (**C4-7**), 124.4-141.21 (**C8 9, 11-16**), 150.42 (**C2**), 173.3 (**C18**), 194.53 (**C10**).

FTMS-ESI: calculated for $C_{21}H_{24}N_3O_2$ (M+H) 350.1869, found 350.1859.

IR ν_{max} (cm^{-1}): 3350 (amide N-H stretch), 1700 (ester C=O stretch), 1636 (amide C=O stretch).

Elemental analysis: calculated for ($C_{21}H_{23}N_3O_2$): C 72.18, H 6.63 and N 12.03, found for C 71.62, H 5.90 and N 11.33.

***N*-(5-Benzoyl-1*H*-benzo[*d*]imidazol-2-yl)-4-methylbenzamide (91):**

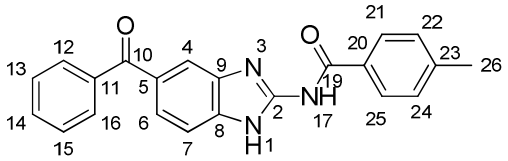

The title compound was obtained as fine white crystals using general procedure D after column chromatography with 20% ethyl acetate/petroleum ether (60 mg, 20%).

m.p: 250-251 °C.

^{1}H NMR (DMSO-d_6): 2.40 (s, 3H, **H26**), 7.37 (d, *J* = 8.36 Hz, 2H, **H22, 24**), 7.61 (m, 5H, **H6, 7, 13-15**), 7.73 (d, *J* = 7.04 Hz, 2H, **H12, 16**), 7.93 (s, 1H, **H4**), 8.06 (d, *J* = 8.23 Hz, 2H, **H21, 25**), 12.60 (bs, 1H, **NH17**).

^{13}C NMR (DMSO-d_6): 21.68 (**C26**), 124.50-132.47 (**C4-7, 11-16**), 138.93-143.43 (**C8, 9, 20-25**), 150.65 (**C2**), 168.20 (**C19**), 196.15 (**C10**).

FTMS-ESI: calculated for $C_{22}H_{18}N_3O_2S$ (M+H) 356.1393, found 356.138.

IR ν_{max} (cm^{-1}): 3312 (amide N-H stretch), 1695 (keto C=O stretch), 1675 (amide C=O stretch).

Elemental analysis: calculated for ($C_{22}H_{17}N_3O_2S$): C 74.35, H 4.82 and N 11.82, found for C 73.58, H 4.84 and N 11.13.

Methyl 2-(4-methylbenzamido)-1*H*-benzo[*d*]imidazole-5-carboxylate (92):

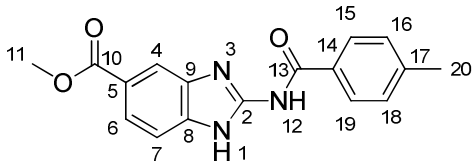

The title compound was obtained as a light brown powder using general procedure D (50 mg, 35%).

m.p: 210-212 °C.

^{1}H NMR (DMSO-d_6): 2.40 (s, 3H, **H20**), 3.86 (s, 3H, **H11**), 7.35 (d, *J* = 7.92 Hz, 2H, **H16, 18**), 7.54 (d, *J* = 8.36 Hz, 1H, **H7**), 7.80 (d, *J* = 8.36 Hz, 1H, **H6**), 8.04 (d, *J* = 7.92 Hz, 2H, **H15, 19**), 8.11 (s, 1H, **H4**), 12.50 (bs, 1H, **NH12**).

^{13}C NMR (DMSO-d_6): 21.68 (**C20**), 52.45 (**C11**), 116.16-129.90 (**C4-7, 14-19**), 143.43-143.60 (**C8, 9**), 150.13 (**C2**), 167.39 (**C13**), 167.87 (**C10**).

FTMS-ESI: calculated for $C_{17}H_{16}N_3O_3$ (M+H) 310.1186, found 310.1175.

IR ν_{max} (cm^{-1}): 3283 (amide N-H stretch), 1711 (ester C=O stretch), 1675 (amide C=O stretch).

Elemental analysis: calculated for ($C_{17}H_{15}N_3O_3$): C 66.01, H 4.89 and N 13.58, found for C 65.67, H 5.03 and N 12.97.

***N*-(5-Benzoyl-1*H*-benzo[*d*]imidazol-2-yl)-4-methoxybenzamide (93):**

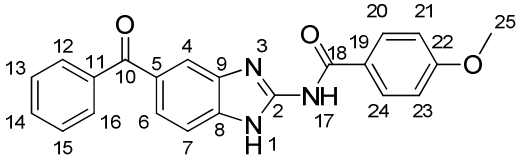

The title compound was obtained as white crystals using general procedure D after crystallization from ethyl acetate/hexane (200 mg, 67%).

m.p: 160-161 °C.

^{1}H NMR (DMSO-d_6): 3.86 (s, 3H, **H25**), 7.10 (d, *J* = 8.8 Hz, 2H, **H20, 24**), 7.57 (m, 7H, **H6, 7, 12-16**), 7.95 (bs, 1H, **H4**), 8.14 (d *J* = 8.8 Hz, 2H, **H21, 23**), 12.54 (bs, 1H, **NH17**).

^{13}C NMR (DMSO-d_6): 56.11 (**C25**), 114.42-124.47 (**C4-7**), 125.15-138.96 (**C8, 9, 11-16, 19-21, 23, 24**), 148.32 (**C2**), 163.33-165.36 (**C18, 22**), 195.95 (**C10**).

FTMS-ESI: calculated for $C_{22}H_{19}N_3O_3$ (M+H) 372.1348, found 372.1340.

IR ν_{max} (cm^{-1}): 3322 (sulfonamide N-H stretch), 1675(keto C=O stretch), 1649 (amide C=O stretch).

Elemental analysis: calculated for ($C_{22}H_{18}N_3O_3$): C 70.96, H 4.87 and N 11.28, found for C 70.24, H 4.32 and N 10.85.

***N*-(5-Benzoyl-1*H*-benzo[*d*]imidazol-2-yl)-4-nitrobenzamide (94):**

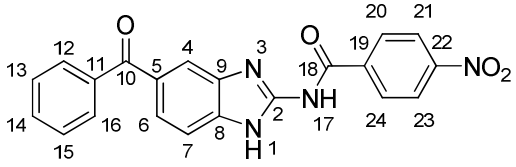

The title compound was obtained as yellow crystals using general procedure D after crystallization from ethyl acetate/hexane (300 mg, 62%).

m.p: 295 °C (with decomposition).

^{1}H NMR (DMSO-d_6): 7.57 (m, 3H, **H13-15**), 7.65 (m, 2H, **H6, 7**), 7.74 (d, *J* = 7.92 Hz, 2H, **H12, 16**), 7.89 (s, 1H, **H4**), 8.35 (bs, 4H, **H20, 21, 23, 24**), 12.85 (bs, 1H, **NH17**).

^{13}C NMR (DMSO-d_6): 115.65-124.05 (**C4-7**), 125.98-132.90 (**C11-16, 19-21, 23, 24**), 138.61-139.90 (**C8, 9**), 147.85 (**C2**), 149.92 (**C22**), 168.42 (**C18**), 195.92 (**C10**).

FTMS-ESI: calculated for $C_{21}H_{15}N_4O_4$ (M+H) 387.1088, found 387.1081.

IR ν_{max} (cm^{-1}): 3334 (amide N-H stretch), 1687 (keto C=O stretch), 1665 (amide C=O stretch), 1632 (N=O stretch).

Elemental analysis: calculated for ($C_{21}H_{14}N_4O_4$): C 65.28, H 3.65 and N 14.50, found for C 65.87, H 3.47 and N 13.78.

Methyl 2-(4-nitrobenzamido)-1*H*-benzo[*d*]imidazole-5-carboxylate (95):

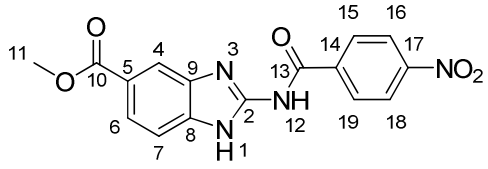

The title compound was obtained as fine white crystals using general procedure D after crystallization from ethyl acetate/hexane (80 mg, 40%).

m.p: 300-301°C.

^{1}H NMR (DMSO-d_6): 3.85 (s, 3H, **H11**), 7.52 (d, *J* = 8.36 Hz, 1H, **H7**), 7.81 (d, *J* = 8.32 Hz, 1H, **H6)**, 8.06 (s, 1H, **H4**), 8.35 (bs, 4H, **H15, 16, 18, 19**), 12.77 (bs, 1H, **NH12**).

^{13}C NMR (DMSO-d_6): 52.58 (**C11**), 124.05-145.38 (**C4-9, 14-16, 18, 19**), 147.54 (**C2**), 149.91 (**C17**), 167.04 (**C13**), 169.95 (**C10**).

FTMS-ESI: calculated for $C_{16}H_{13}N_4O_5$ (M+H) 341.0880, found 341.0875.

IR ν_{max} (cm^{-1}): 3316 (amide N-H stretch), 1708 (ester C=O stretch), 1674 (amide C=O stretch), 1621 (N=O stretch).

Elemental analysis: calculated for ($C_{16}H_{12}N_4O_5$): C 56.47, H 3.55 and N 16.46, found for C 56.25, H 3.24 and N 16.08.

Methyl 2-(4-methoxybenzamido)-1*H*-benzo[*d*]imidazole-5-carboxylate (96):

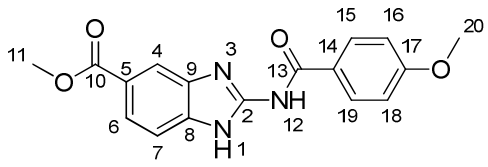

The title compound was obtained as a white powder using general procedure D after crystallization from methanol (120 mg, 42%).

m.p: 194-195 °C.

^{1}H NMR (DMSO-d_6): 3.70 (s, 3H, **H20**), 3.89 (s, 3H, **H11**), 7.03 (m, 1H, **H7**), 7.13 (d, *J* = 8.36 Hz, 2H, **H15, 19**), 7.26 (d, *J* = 8.36 Hz, 1H, **H6**), 7.40 (s, 1H, **H4**), 7.74 (d, *J* = 8.8 Hz, 2H, **H16, 18**).

^{13}C NMR (DMSO-d_6): 52.21 (**C20**), 56.23 (**C11**), 113.75-125.87 (**C4-7**), 130.83-148.65 (**C8, 9, 14-16, 18, 19**), 151.22 (**C2**), 166.76 (**C17**), 168.69 (**C20**), 169.32 (**C10**).

FTMS-ESI: calculated for $C_{17}H_{16}N_3O_4$ (M+H) 326.1141, found 326.1147.

IR ν_{max} (cm^{-1}): 3444 (amide N-H stretch), 1709 (ester C=O stretch), 1678 (amide C=O stretch).

Elemental analysis: calculated for ($C_{17}H_{15}N_3O_4$): C 62.76, H 4.65 and N 12.92, found for C 62.33, H 4.09 and N 12.78.

Methyl 2-(4-methoxyphenylsulfonamido)-1*H*-benzo[*d*]imidazole-5-carboxylate (99):

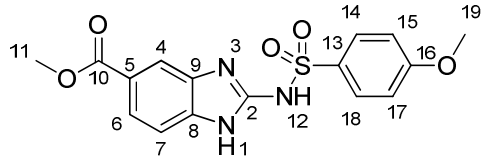

The title compound was obtained as off-white crystals using general procedure G after crystallization from DCM/ether (700 mg, 75%).

m.p: 190-190.5 °C.

^{1}H NMR (DMSO-*d*$_6$): 3.80 (s, 3H, **H19**), 3.86 (s, 3H, **H11**), 7.18 (m. 2H, **H14, 18**), 7.68 (m, 2H, **H15, 17**), 7.80 (d, *J* = 8.36 Hz, 1H, **H7**), 7.94 (dd, *J* = 1.32, 8.8, 1H, **H6**), 8.24 (bs, 1H, **H4**).

^{13}C NMR (DMSO-*d*$_6$): 52.60 (**C19**), 56.54 (**C11**), 115.89-121.94 (**C4-7**), 134.31-148.01 (**C8, 9, 13-15, 17, 18**), 153.74 (**C2**), 155.02 (**C16**), 166.82 (**C10**).

FTMS-ESI: calculated for $C_{16}H_{15}N_3O_5S$ (M+H) 362.0811, found 362.0801.

IR ν_{max} (cm^{-1}): 3452 (sulfonamide N-H stretch), 1708 (ester C=O stretch), 1369 (S=O stretch).

Elemental analysis: calculated for ($C_{16}H_{14}N_3O_5S$): C 53.18, H 4.18, N 11.63 and S 8.87, found for C 52.82, H 4.15, N 11.51 and S 8.38.

***N*-(5-Benzoyl-1*H*-benzo[*d*]imidazol-2-yl)benzenesulfonamide (100):**

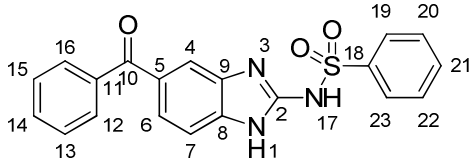

The title compound was obtained as light brown crystals using general procedure F after crystallization from ethyl acetate/hexane (180 mg, 60%).

m.p: 200-200.5 °C.

^{1}H NMR (DMSO-*d*$_6$): 7.47 (m, 2H, **H6, 7**), 7.60 (m, 3H, **H13-15**), 7.71 (m, 5H, **H12, 16, 20-22**), 7.82 (m, 1H, **H4**), 8.01 (d, *J* = 7.48 Hz, 1H, **H19**), 8.14 (d, *J* = 8.36 Hz, 1H, **H23**), 12.62 (bs, 1H, **NH17**).

^{13}C NMR (DMSO-*d*$_6$): 112.35-123.53 (**C4-7**), 125.94-153.58 (**C8, 9, 11-16, 18-23**), 155.02 (**C2**), 195.81 (**C10**).

FTMS-ESI: calculated for $C_{21}H_{14}ClN_3O_2$ (M+H) 378.0912, found 378.0898.

IR ν_{max} (cm^{-1}): 3464 (sulfonamide N-H stretch), 1672 (keto C=O stretch), 1376 (S=O stretch).

Elemental analysis: calculated for ($C_{21}H_{13}ClN_3O_2$): C 63.65, H 4.01, N 11.13, and S 8.50, found for C 63.74, H 4.28, N 10.84, and S 8.32.

***N*-(5-Benzoyl-1*H*-benzo[*d*]imidazol-2-yl)-4-nitrobenzenesulfonamide (101):**

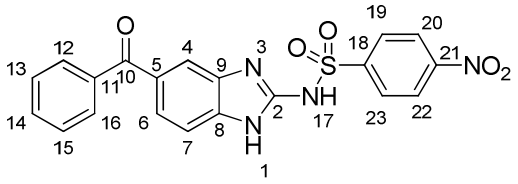

The title compound was obtained as pale yellow crystals using general procedure G after crystallization from ethyl acetate/DCM (280 mg, 62%).

m.p: >300°C.

^{1}H NMR (DMSO-d_6): 7.62 (m, 7H, **H6, 7, 12-16**), 8.10 (bs, 1H, **H4**), 8.27 (d, *J* = 9.24 Hz, 1H, **H19**), 8.39 (d, *J* = 9.24 Hz, 1H, **H23**), 8.49 (d, *J* = 10.08 Hz, 2H, **H20, 22**).

^{13}C NMR (DMSO-d_6): 112.41-123.69 (**C4-7**), 125.90-147.86 (**C8, 9, 11-16, 18-20, 22, 23**), 153.37 (**C2**), 154.77 (**C21**), 195.76 (**C10**).

FTMS-ESI: calculated for $C_{20}H_{15}N_4O_5S$ (M+H) 423.0763, found 423.0754.

IR ν_{max} (cm^{-1}): 3456 (sulfonamide N-H stretch), 1670 (keto C=O stretch), 1648 (N=O stretch), 1348 (S=O stretch).

Elemental analysis: calculated for ($C_{20}H_{14}N_4O_5S$): C 56.73, H 3.57, N 13.23 and S 7.57, found for C 57.31, H 4.03, N 13.24 and S 7.09.

Methyl 2-(5-(dimethylamino)naphthalene-1-sulfonamido)-1*H*-benzo[*d*]imidazole-5-carboxylate (102):

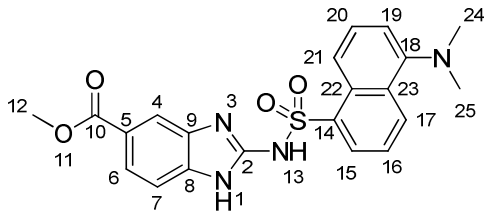

The title compound was obtained as bright orange crystals using general procedure F after column chromatography with 10% methanol/chloroform (200 mg, 45%).

m.p: 100-100.5 °C.

^{1}H NMR (DMSO-d_6): 2.77 (s, 6H, **H24, 25**), 3.81 (s, 3H, **H12**), 7.23 (m, 1H, **H7**), 7.42 (bs, 1H, **H6**), 7.58 (m, 3H, **H19-21**), 7.75 (m, 1H, **H17**), 8.08 (m, 1H, **H4**), 8.31 (m, 2H, **H16**), 8.57 (d, *J* = 8.36 Hz, **NH1**).

^{13}C NMR (DMSO-d_6): 45.58 (**C24, 25**), 52.72 (**C12**), 111.77-128.32 (**C4-7**), 130.43-144.82 (**C8,9, 14-23**) , 152.19 (**C2**), 166.36 (**C10**).

FTMS-ESI: calculated for $C_{21}H_{21}N_4O_4$ (M+H) 425.1284, found 425.1271.

IR ν_{max} (cm^{-1}): 3448 (sulfonamide N-H stretch), 1716 (ester C=O stretch), 1363 (S=O stretch).

Elemental analysis: calculated for ($C_{21}H_{20}N_4O_4$): C 59.42, H 4.75, N 13.20 and S 7.55, found for C 60.07, H 4.39, N 12.46 and S 7.31.

Methyl 2-(4-methylphenylsulfonamido)-1*H*-benzo[*d*]imidazole-5-carboxylate (103):

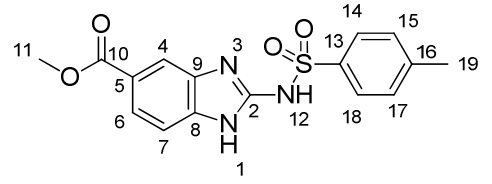

The title compound was obtained as a light brown powder using general procedure G after column chromatography with 20% ethyl acetate/hexane (170 mg, 58%).

m.p: 185-186 °C.

^{1}H NMR (DMSO-*d*$_6$): 2.33 (s, 3H, **H19**), 3.81 (s, 3H, **H11**), 7.18 (d, *J* = 8.32 Hz, 1H, **H7**), 7.46 (d, *J*= 7.92 Hz, 2H, **H15, 17**), 7.57 (bs, 1H, **NH12**), 7.77 (d, *J* = 8.36 Hz, 1H, **H6**), 7.87 (d, *J* = 8.36 Hz, 2H, **H14, 18**), 8.22 (s, 1H, **H4**).

^{13}C NMR (DMSO-*d*$_6$): 21.35 (**C19**), 52.84 (**C11**), 111.86-134.22 (**C4-7, 14-18**), 138.39-145.97 (**C8, 9**), 152.26 (**C2**), 166.42 (**C10**).

FTMS-ESI: calculated for $C_{16}H_{14}N_3O_4S$ (M-H) 344.0705, found 344.0711.

IR ν_{max} (cm^{-1}): 3428 (amide N-H stretch), 1710 (ester C=O stretch), 1372 (S=O stretch).

Elemental analysis: calculated for ($C_{16}H_{15}N_3O_4S$): C 55.64, H 4.38, N 12.17 and S 9.28, found for C 55.45, H 4.40, N 12.07 and S 9.05.

***N*-(5-Benzoyl-1*H*-benzo[*d*]imidazol-2-yl)-4-methylbenzenesulfonamide (104):**

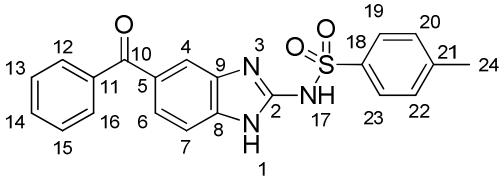

The title compound was obtained as a white powder using general procedure G after crystallization from ethyl acetate/hexane (150 mg, 45%).

m.p: 192-193 °C.

^{1}H NMR (DMSO-*d*$_6$): 2.37 (s, 3H, **H24**), 7.24 (d, *J* = 7.92 Hz, 1H, **H7**), 7.30 (m, 1H, **H14**), 7.50-7.79 (m, 10H, **H12, 13, 15, 16, 19, 20, 22, 23, NH1, NH17**), 7.90 (d, *J* = 8.36 Hz, 1H, **H6**), 8.04 (d, *J* = 1.32 Hz, 1H, **H4**).

^{13}C NMR (DMSO-*d*$_6$): 21.71 (**C24**), 114.29-130.32 (**C4-7, 11-16**), 133.90-147.38 (C**8, 9, 18-23**), 155.17 (**C2**), 195.19 (**C10**).

FTMS-ESI: calculated for $C_{21}H_{17}N_3O_3S$ (M+H) 392.1063, found 392.1063.

IR ν_{max} (cm^{-1}): 3443 (sulfonamide N-H stretch), 1653 (keto C=O stretch), 1376 (S=O stretch)

Elemental analysis: calculated for ($C_{21}H_{16}N_3O_3S$): C 64.43, H 4.38, N 10.73 and S 8.19, found for C 63.85, H 4.32, N 10.24 and S 8.39.

Methyl 2-(butylsulfonamido)-1*H*-benzo[*d*]imidazole-5-carboxylate (105):

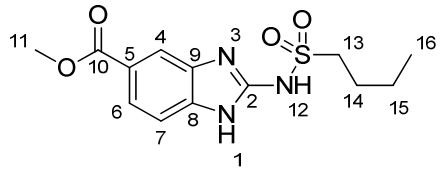

The title compound was obtained as yelow crystals using general procedure F after crystallization from ether (50 mg, 35%).

m.p: 150-152 °C.

^{1}H NMR (DMSO-d_6): 0.78 (m, 3H, **H16**), 1.27 (m, 2H, **H15**), 1.51 (m, 2H, **H14**), 3.70 (t, 2H, *J* = 8 Hz, **H13**), 3.84 (s, 3H, **H11**), 7.30 (d, *J* = 8.4 Hz, 1H, **H7**), 7.82 (dd, *J* = 8.4, 1.6 Hz, 1H, **H6**), 8.08 (d, *J* = 1.2 Hz, 1H, **H4**), 8.62 (s, 1H, **NH1**), 12.75 (bs, 1H, **NH12**).

^{13}C NMR (DMSO-d_6): 13.69-24.83 (**C14-16**), 52.69 (**C13**), 53.30 (**C11**), 113.12-126.74 (**C4-7**), 139.65-147.49 (**C8, 9**), 155.06 (**C2**), 166.78 (**C10**).

FTMS-ESI: calculated $C_{17}H_{15}N_2O_4S$ (M+H) 312.1010, found 312.1013.

IR ν_{max} (cm^{-1}): 3459 (sulfonamide N-H stretch), 1709 (ester C=O stretch), 1371 (S=O stretch).

Elemental analysis: calculated for ($C_{17}H_{14}N_2O_4S$): C 50.15, H 5.50 and N 13.50, found for C 49.08, H 5.64 and N 12.93.

***N*-(5-Benzoyl-1*H*-benzo[*d*]imidazol-2-yl)-5-(dimethylamino)naphthalene-1-sulfonamide (106):**

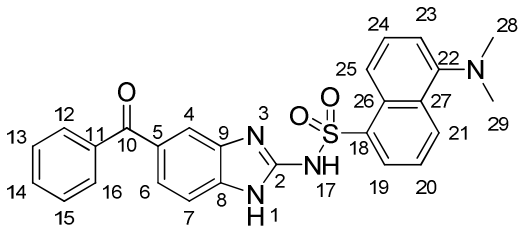

The title compound was obtained as shiny orange crystals using general procedure F after column chromatography with 10% methanol/chloroform (300 mg, 55%).

m.p: 102-104 °C.

^{1}H NMR (DMSO-d_6): 2.78 (d, *J* = 3.52 Hz, 6H, **H28, 29**), 7.25 (t, *J* = 8.08 Hz, 1H, **H14**), 7.45 (d, *J* = 7.28 Hz, 1H, **H7**), 7.58 (m, 10H, **H12, 13, 15, 16, 19-21, 23-25**), 8.31 (bs, 1H, **H6**), 8.60 (m, 1H, **H4**).

^{13}C NMR (DMSO-d_6): 45.43 (**C27, 28**), 112.03-123.31 (**C4-7**), 124.89-152.52 (**C8, 9, 18-27**), 153.79 (C**2**), 195.75 (**C10**).

FTMS-ESI: calculated for $C_{26}H_{23}N_4O_3S$ (M+H) 471.1485, found 471.1479.

IR ν_{max} (cm^{-1}): 3448 (sulfonamide N-H stretch), 1642 (keto C=O stretch), 1362 (S=O stretch).

Elemental analysis: calculated for ($C_{26}H_{22}N_4O_3S$): C 66.43, H 4.71 and N 11.91, found for C 65.43, H 5.01 and N 11.49.

Methyl 2-(4-nitrophenylsulfonamido)-1*H*-benzo[*d*]imidazole-5-carboxylate (107):

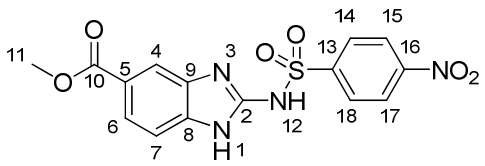

The title compound was obtained as yellow fine crystals using general procedure F after crystallization from ethyl acetate/DCM (250 mg, 42%).

m.p: 226-228 °C (m.p).

^{1}H NMR (DMSO-*d*$_6$): 3.85 (s, 3H, **H11**), 7.50 (bs, 1H, **NH12**), 7.69 (d, *J* = 8.8 Hz, 1H, **H7**), 7.84 (d, *J* = 8.8 Hz, 1H, **H6**), 8.26 (d, *J* = 9.24 Hz, 2H, **H14, 18**), 8.45 (m, 3H, **H4, 15, 17**).

^{13}C NMR (DMSO-*d*$_6$): 52.66 (**C11**), 112.69-122.35 (**C4-7**), 124.88-141.56 (C**13-15, 17, 18**), 142.53-148.03 (**C8, 9**), 151.97 (**C2**), 154.72 (**C16**), 166.71 (**C10**).

FTMS-ESI: calculated for $C_{15}H_{13}N_4O_6S$ (M+H) 377.0550, found 377.05423.

IR ν_{max} (cm^{-1}): 3437 (sulfonamide N-H stretch), 1714 (ester C=O stretch), 1667 (N=O stretch), 1349 (S=O stretch).

Elemental analysis: calculated for ($C_{15}H_{12}N_4O_6S$): C 47.87, H 3.21, N 14.89 and S 8.52, found for C 47.67, H 2.80, N 14.68 and S 8.41.

Methyl 2-(3-nitrophenylsulfonamido)-1*H*-benzo[*d*]imidazole-5-carboxylate (108):

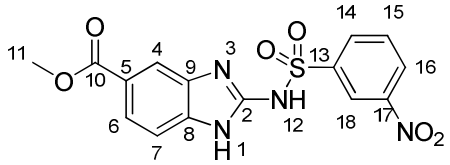

The title compound was obtained as orange crystals using general procedure G after crystallization from ethyl acetate (630 mg, 60%).

m.p: 198-199 °C.

^{1}H NMR (DMSO-*d*$_6$): 3.82 (s, 3H, **H11**), 7.54 (s, **NH17**), 7.71 (m, 2H, **H6, 7**), 7.83 (m, 1H, **H4**), 7.96 (dd, *J* = 5.28, 2.6 Hz, 1H, **H18**), 8.56 (m, 2H, **H14, 15**), 8.79 (dd, *J* = 9.01, 2.45 Hz, 1H, **H16**).

^{13}C NMR (DMSO-d_6): 52.66 (**C11**), 112.65-129.54 (**C4-7**), 133.21-148.86 (**C8, 9, 13-16, 18**), 153.42 (**C2**), 154.67 (**C17**), 166.70 (**C10**).

FTMS-ESI: calculated for $C_{15}H_{13}N_4O_6S$ (M+H) 377.05503, found 377.05518.

IR ν_{max} (cm^{-1}): 3436 (sulfonamide N-H stretch), 1717 (ester C=O stretch), 1667 (N=O stretch), 1346 (S=O stretch).

Elemental analysis: calculated for ($C_{15}H_{12}N_4O_6S$): C 47.87, H 3.21, N 14.89 and S 8.52, found for C 48.12, H 3.34, N 14.34 and S 7.90.

Methyl 2-decanamido-5-(2-phenylethyl) thiazole-4-carboxylate (109):

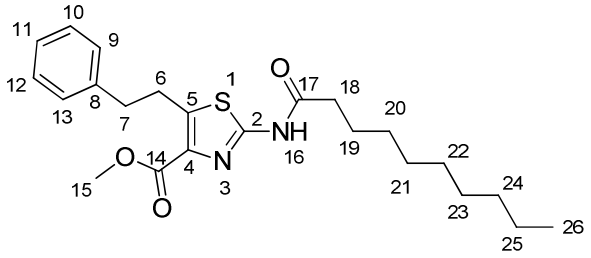

The title compound was obtained as white flakes using general procedure D after column chromatography with 6% methanol/chloroform (2.5 g, 68%).

m.p: 90-91 °C.

^{1}H NMR (DMSO-d_6): 0.85 (t, *J* = 7.04, 6.6 Hz, 3H, **H26**), 1.23 (bs, 12H, **H20-25**), 1.57 (m, 2H, **H19**), 2.37 (t, *J* = 7.48 Hz, 2H, **H18**), 2.90 (t, *J* = 7.48 Hz, 2H, **H7**), 3.37 (t, 2H, *J* = 7.92, 7.48 Hz, **H6**), 3.78 (s, 3H, **H15**), 7.23 (m, 5H, **H9-13**), 12.32 (s, 1H, **NH16**).

^{13}C NMR (DMSO-d_6): 14.53-31.83 (**C18-26**), 35.21 (**C7**), 37.52 (**C6**), 52.14 (**C15**), 126.72- 135.12 (**C8-13**), 141.02 (**C5**), 142.32 (**C4**), 154.21 (**C2**), 163.25 (**C17**), 172.31 (**C14**).

FTMS-ESI: calculated $C_{23}H_{33}N_2O_3S$ (M+H) 417.2212, found 417.220.

IR ν_{max} (cm^{-1}): 3273.1 (amide N-H stretch), 1724.6 (ester C=O stretch), 1691.2 (amide C=O stretch).

Elemental analysis: calculated for ($C_{23}H_{32}N_2O_3S$): C 66.31, H 7.74, N 6.72 and S 7.70, found for C 66.49, H 7.88, N 6.72 and S 7.78.

2-Decanamido-5-(2-phenethyl)thiazole-4-carboxylic acid (110):

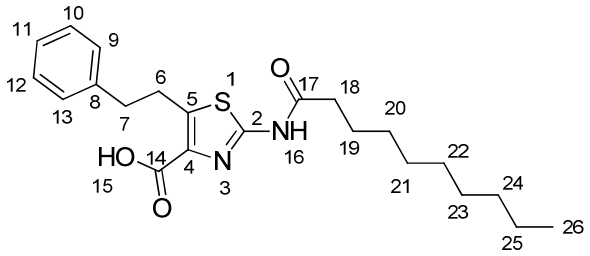

The title compound was obtained as a white powder using the general procedure C (92 mg, 58%).

m.p: 122-124 °C.

^{1}H NMR (DMSO-*d*$_6$): 0.84 (t, *J* = 7.04, 6.16 Hz, 3H, **H26**), 1.23 (bs, 12H, **H20-25**), 1.58 (m, 2H, **H19**), 2.37 (t, *J* = 7.48, 7.04 Hz, 2H, **H18**), 2.90 (t, *J* = 7.48, 7.92 Hz, 2H, **H7**), 3.38 (t, *J* = 7.92, 7.48 Hz, 2H, **H6**), 7.23 (m, 5H, **H9-13**), 12.25 (s, 1H, **NH16**), 12.78 (bs, 1H, **OH15**).

^{13}C NMR (DMSO-*d*$_6$): 14.52-31.84 (**C18-C26**), 35.38 (**C7**), 37.37 (**C6**), 126.68-137.58 (**C8-13**), 141.22 (**C5**), 141.53 (**C4**), 154.08 (**C2**), 164.09 (**C17**), 172.22 (**C14**).

FTMS-ESI: calculated $C_{22}H_{31}N_2O_3S$ (M+H) 403.2055, found 403.2050.

IR ν_{max} (cm^{-1}): 3197.6 (amide N-H stretch), 2937 (carboxylic O-H stretch), 1695 (carboxylic C=O stretch), 1667.8 (amide C=O stretch).

Elemental analysis: calculated for ($C_{22}H_{30}N_2O_3S$): C 65.64, H 7.51, N 6.96 and S 7.97, found for C 65.64, H 7.57, N 6.87 and S 7.82.

Methyl 2-decanamido-5-isopropylthiazole-4-carboxylate (111):

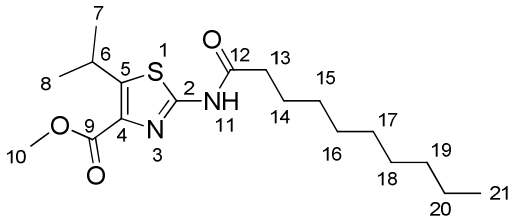

The title compound was obtained as light yellow crystals using general procedure D after column chromatography with 10% ethyl acetate/DCM (320 mg, 70%).

m.p: 62-63 °C.

^{1}H NMR (DMSO-d_6): 0.84 (t, *J* = 6.6, 7.04 Hz, 3H, **H21**), 1.26 (m, 18H, **H7, 8, 15-20**), 1.57 (bs, 2H, **H14**), 2.37 (t, *J* = 7.48 Hz, 2H, **H13**), 3.78 (s, 3H, **H10**), 3.97 (m, 1H, **H6**), 12.32 (s, 1H, **NH11**).

^{13}C NMR (DMSO-d_6): 14.50-29.22 (**C14-21**), 29.37 (**C7, 8**), 31.38 (**C6**), 35.38 (**C13**), 52.13 (**C10**), 133.94 (**C5**), 150.98 (**C4**), 154.22 (**C2**), 162.98 (**C12**), 172.30 (**C9**).

FTMS-ESI: calculated for $C_{18}H_{31}N_2O_3S$ (M+H) 355.2055, found 355.2046.

IR ν_{max} (cm^{-1}): 3275 (amide N-H stretch), 1723 (ester C=O stretch), 1695 (amide C=O stretch).

Elemental analysis: calculated for ($C_{18}H_{30}N_2O_3S$): C 60.98, H 8.53, N 7.90 and S 9.04, found for C 61.06, H 8.93, N 7.75 and S 8.99.

2-Decanamido-5-isopropylthiazole-4-carboxylic acid (112):

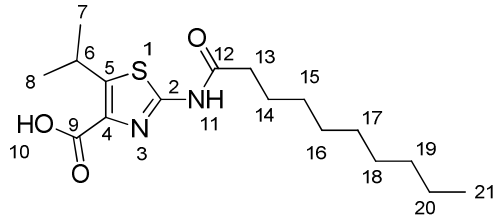

The title compound was obtained as pink flakes using general procedure C (90 mg, 45%).

m.p: 96-97 °C.

^{1}H NMR (DMSO-*d*$_6$): 0.84 (t, *J* = 5.92, 7.28 Hz, 3H, **H21**), 1.24 (m, 18H, **H7, 8, 15-20**), 1.56 (m, 2H, **H14**), 2.36 (t, *J* = 7.04, 7.48 Hz, 2H, **H13**), 4.02 (m, 1H, **H6**), 12.4 (s, 1H, **NH11**), 12.75 (bs, 1H, **OH10**).

^{13}C NMR (DMSO-*d*$_6$): 14.51-29.22 (**C14-21**), 29.37-31.82 (**C7, 8**), 35.36 (**C6**), 135.24 (**C5**), 150.08 (**C5**), 153.83 (**C2**), 164.17 (**C12**), 172.21 (**C9**).

FTMS-ESI: calculated $C_{17}H_{29}N_2O_3S$ (M+H) 341.1899, found 341.1893.

IR ν_{max} (cm^{-1}): 3433 (amide N-H stretch), 3087 (carboxylic O-H stretch), 1697 (carboxylic C=O stretch), 1668 (amide C=O stretch).

Elemental analysis: calculated for ($C_{17}H_{28}N_2O_3S$): C 59.97, H 8.29, N 8.23 and S 9.42, found for C 60.40, H 8.50, N 8.10, and S 8.93.

Methyl 5-ethyl-2-decanamidothiazole-4-carboxylate (113):

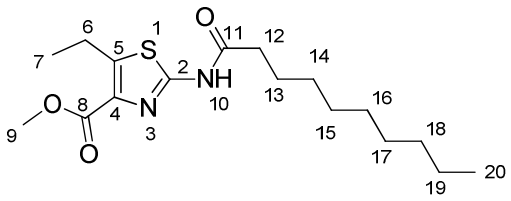

The title compound was obtained as a light brown powder using general procedure D after column chromatography with 15% ethyl acetate/DCM (180 mg, 59%).

m.p: 60-61 °C.

^{1}H NMR (DMSO-*d*$_6$): 0.84 (t, *J* = 6.6 Hz, 3H, **H20**), 1.23 (m, 15H, **H7, 14-19**), 1.57 (t, *J* = 6.36, 7.14 Hz, 2H, **H13**), 2.38 (t, *J* = 7.48 Hz, 2H, **H12**), 3.11 (q, *J* = 7.48, 7.48 Hz, 2H, **H6**), 3.78, (s, 3H, **H9**), 12.32 (s, 1H, **NH10**).

^{13}C NMR (DMSO-d_6): 14.51-29.38 (**C7, 13-20**), 31.82 (**C6**), 35.38 (**C12**), 52.11 (**C9**), 134.64 (**C5**), 145.13 (**C4**), 154.22 (**C2**), 162.94 (**C11**), 172.32 (**C8**).

FTMS-ESI: calculated for $C_{17}H_{29}N_2O_3S$ (M+H) 341.1899, found 341.1893.

IR ν_{max} (cm^{-1}): 3271 (amide N-H stretch), 1723.9 (ester C=O stretch), 1694 (amide C=O stretch).

Elemental analysis: calculated for ($C_{17}H_{28}N_2O_3S$): C 59.97, H 8.29, N 8.23 and S 9.42, found for C 60.31, H 8.56, N 7.77 and S 9.26.

5-Ethyl-2-decanamidothiazole-4-carboxylic acid (114):

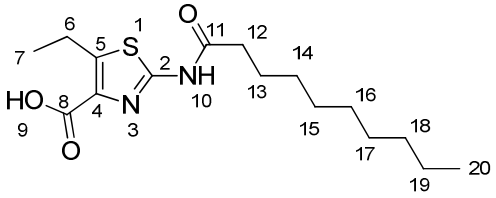

The title compound was obtained as a light yellow powder using the general procedure C (65 mg, 52%).

m.p: 120-121 °C.

^{1}H NMR (DMSO-d_6): 0.83 (t, *J* = 6.16, 7.04 Hz, 3H, **H20**), 1.20 (m, 15H, **H7, 14-19**), 1.56 (m, 2H, **H13**), 2.37 (t, *J* = 7.48 Hz, 2H, **H12**), 3.09 (q, *J* = 7.48, 7.44 Hz, 2H, **H6**), 12.23 (s, 1H, **NH10**), 12.71 (bs, 1H, **OH9**).

^{13}C NMR (DMSO-d_6): 14.51-29.38 (**C7, 13-20**), 31.82 (**C6**), 35.36 (**C12**), 135.84 (**C5**), 144.32 (**C4**), 153.82 (**C2**), 164.08 (**11**), 172.24 (**C8**).

FTMS-ESI: calculated for $C_{16}H_{27}N_2O_3S$ (M+H) 327.1742, found 327.1737.

IR ν_{max} (cm^{-1}): 3423-3192 (amide N-H stretch), 2947 (1696 (carboxylic C=O stretch), 1668 (amide C=O stretch).

Elemental analysis: calculated for ($C_{16}H_{26}N_2O_3S$): C 58.87, H 8.03, N 8.58 and S 9.82, found for C 59.03, H 8.03, N 8.55 and S 9.86.

Methyl 2-decanamido-5-(2-propyl) thiazole-4-carboxylate (115):

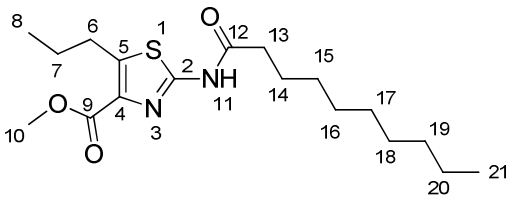

The title compound was obtained as white crystals using general procedure D after column chromatography with 10% ethyl acetate/DCM (180 mg, 65%).

m.p: 42-43 °C.

^{1}H NMR (DMSO-d_6): 0.85 (m, 3H, **H21**), 0.91 (t, *J* = 7.04 Hz, 3H, **H8**), 1.23 (bs, 12H, **H15-20**), 1.59 (m, 4H, **H7, 14**), 2.37 (t, *J* = 7.48 Hz, 2H, **H13**), 3.06 (t, *J* = 7.04, 7.92 Hz, 2H, **H6**), 3.77 (s, 3H, **H10**), 12.32 (s, 1H, **NH11**).

^{13}C NMR (DMSO-d_6): 14.13-29.38 (**C7, 8, 14-20**), 31.83 (**C6**), 35.38 (**C13**), 52.10 (**C10**), 135.2 (**C5**), 143.18 (**C4**), 154.36 (**C2**), 168.32 (**C12**), 172.33 (**C9**).

FTMS-ESI: calculated for $C_{18}H_{31}N_2O_3S$ (M+H) 355.2055, found 355.2050.

IR ν_{max} (cm^{-1}): 3168 (amide N-H stretch), 1719 (ester C=O stretch), 1695 (amide C=O stretch).

Elemental analysis: calculated for ($C_{18}H_{30}N_2O_3S$): C 60.98, H 8.53, N 7.90 and S 9.04, found for C 61.01, H 9.06, N 7.44 and S 8.96.

2-Decanamido-5-(2-propyl) thiazole-4-carboxylic acid (116):

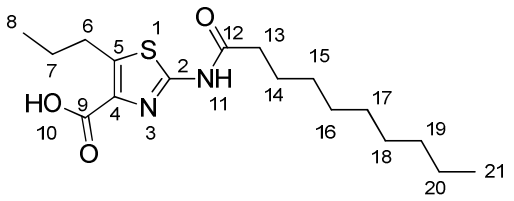

The title compound was obtained as a brown powder using general procedure C (80 mg, 57%).

m.p: 132-133 °C.

^{1}H NMR (DMSO-*d*$_6$): 0.84 (m, 3H, **H21**), 0.91 (t, *J* = 7.04, 7.44 Hz, 3H, **H8**), 1.23 (bs, 12H, **H15-20**), 1.58 (m, 4H, **H7, 14**), 2.37 (t, *J* = 7.04, 7.48 Hz, 2H, **H13**), 3.05 (t, *J* = 7.48 Hz, 2H, **H6**), 12.23 (s, 1H, **NH11**), 12.75 (bs, 1H, **OH10**).

^{13}C NMR (DMSO-*d*$_6$): 14.14-29.37 (**C7, 8, 14-21**), 31.82 (**C6**), 35.36 (**C13**), 136.36 (**C5**), 142.30 (**C4**), 153.95 (**C2**), 164.13 (**C12**), 172.24 (**C9**).

FTMS-ESI: calculated for $C_{17}H_{29}N_2O_3S$ (M+H) 341.1899, found 341.1893.

IR ν_{max} (cm^{-1}): 3189.2 (amide N-H stretch), 2957 (carboxylic O-H stretch), 1691 (carboxylic C=O stretch), 1665 (amide C=O stretch).

Elemental analysis: calculated for ($C_{17}H_{28}N_2O_3S$): C 59.97, H 8.29, N 8.23 and S 9.42, found for C 59.91, H 8.38, N 8.01 and S 9.24.

Methyl 5-butyl-2-decanamidothiazole-4-carboxylate (117):

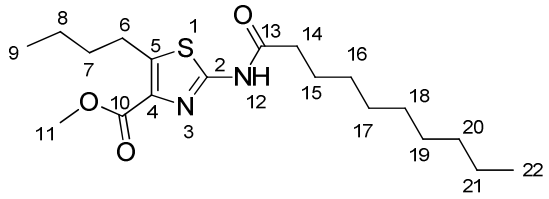

The title compound was obtained as a yellow thick oil using general procedure D after column chromatography with 15% ethyl acetate/DCM (180 mg, 49%).

^{1}H NMR (DMSO-*d*$_6$): 0.87 (m, 6H, **H9, 22**), 1.23 (m, 14H, **H8, 16-21**), 1.58 (m, 4H, **H7, 15**), 2.37 (t, *J* = 7.8Hz, 2H, **H6**), 3.09 (t, *J* = 8.0 Hz, 2H, **H14**), 3.77 (s, 3H, **H11**), 12.32 (s, 1H, **NH12**).

^{13}C NMR (DMSO-*d*$_6$): 14.15-31.82 (**C7-9, 15-22**), 33.68 (**C6**), 35.38 (**C14**), 52.09 (**C11**), 135.02 (**C5**), 143.45 (**C4**), 154.45 (**C2**), 162.98 (**C13**), 172.31 (**C10**).

FTMS-ESI: calculated for $C_{19}H_{33}N_2O_3S$ (M+H) 369.2212, found 369.2206.

IR ν_{max} (cm^{-1}): 3420 (amide N-H stretch), 1701 (ester C=O stretch), 1685 (amide C=O stretch).

Elemental analysis: calculated for ($C_{19}H_{32}N_2O_3S$): C 61.92, H 8.75 and N 7.60, found for C 62.48, H 8.72 and N 7.70.

5-Butyl-2-decanamidothiazole-4-carboxylic acid (118):

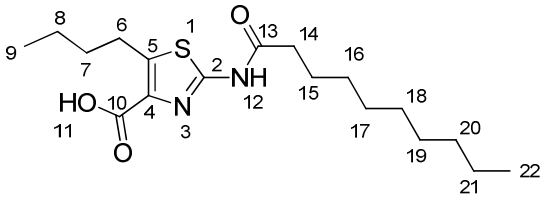

The title compound was obtained as white flakes using general procedure C (48 mg, 62%).

m.p: 108-109 °C.

^{1}H NMR (DMSO-d_6): 0.87 (m, 6H, **H9, 22**), 1.29 (m, 14H, **H8, 16-21**), 1.57 (m, 4H, **H7, 15**), 2.37 (t, *J* = 6.8, 7.72 Hz, 2H, **H6**), 3.09 (t, *J* = 7.04, 7.88 Hz, 2H, **H14**), 12.27 (bs, 1H, **NH12**), 12.78 (bs, 1H, **OH11**).

^{13}C NMR (DMSO-d_6): 14.19-31.83 (**C7-9, 15-22**), 33.78 (**C6**), 35.38 (**C14**), 135.02 (**C5**), 143.45 (**C4**), 153.91 (**C2**), 164.18 (**C13**), 172.23 (**C10**).

FTMS-ESI: calculated for $C_{18}H_{31}N_2O_3S$ (M+H) 355.2055, found 355.2050.

IR ν_{max} (cm^{-1}): 3193 (amide N-H stretch), 2987 (carboxylic O-H stretch), 1695 (carboxylic C=O stretch), 1666 (amide C=O stretch).

Elemental analysis: calculated for ($C_{18}H_{30}N_2O_3S$): C 60.62, H 6.43 and N 7.44, found for C 59.93, H 5.79 and N 7.07.

Methyl 5-(4-chlorophenyl)-2-decanamidothiazole-4-carboxylate (119):

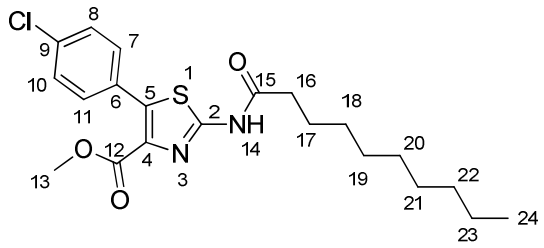

The title compound was obtained as white crystals using general procedure D after column chromatography with 20% ethyl acetate/hexane (78 mg, 39%).

m.p: 64-66°C.

^{1}H NMR (DMSO-d_6): 0.85 (t, *J* = 7.04 Hz, 3H, **H24**), 1.24 (bs, 12H, **H18-23**), 1.59 (p, *J* = 7.04, 6.6 Hz, 2H, **H17**), 2.43 (t, *J* = 7.04 Hz, 2H, **H16**), 3.69 (s, 3H, **H13**), 7.51 (m, 4H, **H7, 8, 10, 11**), 12.65 (bs, 1H, **NH14**).

^{13}C NMR (DMSO-d_6): 14.53-35.42 (**C16-24**), 52.31 (**C13**), 128.88 (**C7, 11**), 129.83 (**C6**), 132.12 (**C8, 10**), 134.40 (**C9**), 135.21 (**C5**), 136.65 (**C4**), 156.19 (**C2**), 162.63 (**C15**), 172.72 (**C12**).

FTMS-ESI: calculated for $C_{21}H_{26}ClN_2O_3S$ (M-H) 421.1353, found 421.1358.

IR ν_{max} (cm^{-1}): 3271 (amide N-H stretch), 1729 (ester C=O stretch), 1695 (amide C=O stretch).

Elemental analysis: calculated for ($C_{21}H_{27}ClN_2O_3S$): C 59.63, H 6.43 and N 6.61, found for C 59.33, H 6.03 and N 6.42.

5-(4-Chlorophenyl)-2-decanamidothiazole-4-carboxylic acid (120):

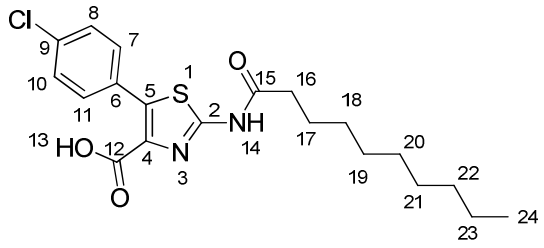

The title compound was obtained as a light brown gum using general procedure C (45 mg, 25%).

^{1}H NMR (DMSO-*d*$_6$): 0.83 (t, *J* = 7.14 Hz, 3H, **H24**), 1.26 (bs, 12H, **H18-23**), 1.48 (m, 2H, **H17**), 2.43 (t, *J* = 7.48 Hz, 2H, **H16**), 7.68 (m, 4H, **H7, 8, 10, 11**), 12.65-12.87 (bs, 2H, **OH13, NH14**).

^{13}C NMR (DMSO-*d*$_6$): 15.13-35.74 (**C16-24**), 127.48- 134.68 (**C6-11**), 136.21 (**C5**), 149.88 (**C4**), 155.64 (**C2**), 163.53 (**C15**), 169.72 (**C12**).

FTMS-ESI: calculated for $C_{20}H_{24}ClN_2O_3S$ (M-H) 407.1196, found 407.1190.

IR ν_{max} (cm^{-1}): 3379 (amide N-H stretch), 2987 (carboxylic O-H stretch), 1712 (carboxylic C=O stretch), 1687 (amide C=O stretch).

Elemental analysis: calculated for ($C_{20}H_{25}ClN_2O_3S$): C 56.26, H 6.37 and N 6.56, found for C 55.98, H 6.03 and N 6.18.

Methyl 2-decanamido-5-(4-methoxyphenyl)thiazole-4-carboxylate (121):

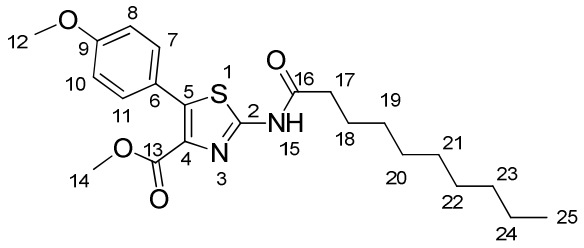

The title compound was obtained as white crystals using general procedure D after column chromatography with 50% ethyl acetate/hexane (100 mg, 43%).

m.p: 88-90 °C.

^{1}H NMR (DMSO-*d*$_6$): 0.83 (t, *J* = 6.84 Hz, 3H, **H25**), 1.23 (bs, 12H, **H19-24**), 1.58 (m, 2H, **H18**), 2.41 (t, *J* = 7.48 Hz, 2H, **H17**), 3.67 (s, 3H, **H12**), 3.79 (s, 3H, **H14**), 6.97 (d, *J* = 8.8 Hz, 2H, **H7, 11**), 7.41 (d, *J* = 8.8 Hz, 2H, **H8, 10**), 12.46 (s, 1H, **NH15**).

^{13}C NMR (DMSO-d_6): 14.52-35.38 (**C17-25**), 52.15 (**C12**), 55.80 (**C14**), 114.32-131.64 (**C6-8, 10, 11**), 139.14 (**C5**), 145.40 (**C4**), 155.22 (**C2**), 157.32 (**C9**), 162.89 (**C16**), 172.55 (**C13**).

FTMS-ESI: calculated for $C_{22}H_{29}N_2O_4S$ (M-H) 417.1848, found 417.1853.

IR ν_{max} (cm^{-1}): 3255 (amide N-H stretch), 1709 (ester C=O stretch), 1690 (amide C=O stretch).

Elemental analysis: calculated for ($C_{22}H_{30}N_2O_4S$): C 63.13, H 7.22 and N 6.69, found for C 63.41, H 6.87 and N 6.39.

2-Decanamido-5-(4-methoxyphenyl)thiazole-4-carboxylic acid (122):

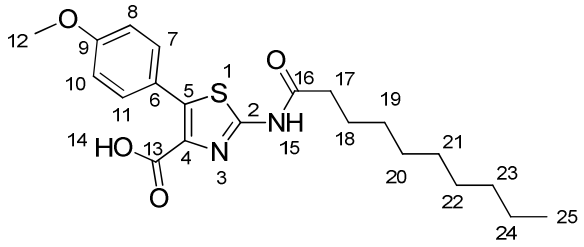

The title compound was obtained as a pale yellow powder using general procedure C (56 mg, 65%).

m.p: 210-212 °C.

^{1}H NMR (DMSO-d_6): 0.84 (m, 3H, **H25**), 1.24 (bs, 12H, **H19-24**), 1.58 (m, 2H, **H18**), 2.42 (t, *J* = 7.2 Hz, 2H, **H17**), 3.79 (s, 3H, **H12**), 6.99 (d, *J* = 8.8, 2H, **H7, 11**), 7.44 (d, *J* = 8.8, 2H, **H 8, 10**), 12.41 (s, 1H, **NH15**), 12.68 (bs, 1H, **OH14**).

^{13}C NMR (DMSO-d_6): 14.52-35.37 (**C17-25**), 55.78 (**C12**), 114.25-135.61 (**C6-8, 10, 11**), 137.98 (**C5**), 145.10 (**C4**), 155.05 (**C2**), 158.58 (**C9**), 164.0 (**C16**), 172.47 (**C13**).

FTMS-ESI: calculated for $C_{21}H_{29}N_2O_4S$ (M+H) 405.1848, found 405.1842.

IR ν_{max} (cm^{-1}): 3460 (amide N-H stretch), 3180 (carboxylic O-H stretch), 1694 (carboxylic C=O stretch), 1674 (amide C=O stretch).

Elemental analysis: calculated for ($C_{21}H_{28}N_2O_4S$): C 62.35, H 6.98, N 6.93 and S 7.93, found for C 62.28, H 6.91, N 6.20 and S 7.60.

Methyl 5-benzyl-2-(10-methoxy-10-oxodecanamido)thiazole-4-carboxylate (123):

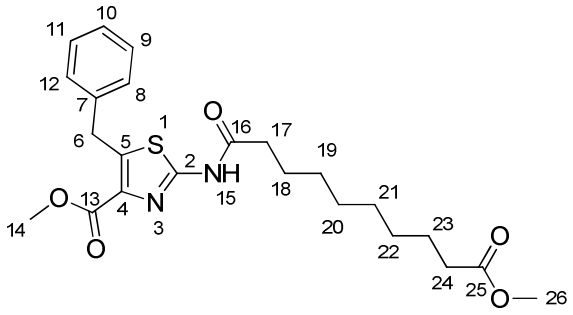

The title compound was obtained as an orange powder using general procedure D after crystallization from ethyl acetate/hexane (500 mg, 28%).

m.p: 88-89 °C.

^{1}H NMR (DMSO-d_6): 1.2 (bs, 8H, **H19-22**), 1.48 (m, 4H, **H18, 23**), 2.26 (t, *J* = 7.36 Hz, 2H, **H17**), 2.35 (t, *J* = 7.36 Hz, 2H, **H24**), 3.56 (s, 3H, **H26**), 3.81 (s, 3H, **H14**), 4.46 (s, 2H, **H6**), 7.29 (m, 5H, **H8-12**), 12.35 (s, 1H, **NH15**).

^{13}C NMR (DMSO-d_6): 24.95-33.79 (**C17-24**), 35.31 (**C6**), 51.71 (**C26**), 52.25 (**C14**), 127.25-135.11 (**C7-12**), 140.23 (**C5**), 142.37 (**C4**), 155.10 (**C2**), 163.07 (**C16**), 172.38 (**C25**), 173.93 (**C13**).

FTMS-ESI: calculated for $C_{23}H_{31}N_2O_5S$ (M+H) 447.1954, found 447.1951.

IR ν_{max} (cm^{-1}): 3229 (amide N-H stretch), 1728-1710 (2 ester C=O stretch), 1695 (amide C=O stretch).

Elemental analysis: calculated for ($C_{23}H_{30}N_2O_5S$): C 61.09, H 6.52, N 6.48 and S 7.41, found for C 61.60, H 6.77, N 6.24 and S 7.14.

5-Benzyl-2-(9-carboxynonanamido)thiazole-4-carboxylic acid (124):

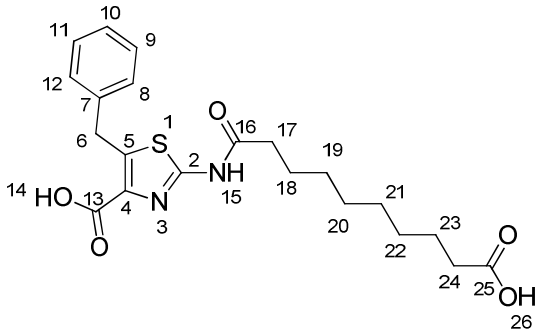

The title compound was obtained as an orange powder using general procedure C (160 mg, 68.3%).

m.p: 174-175 °C.

^{1}H NMR (DMSO-d_6): 1.22 (bs, 8H, **H19-22**), 1.46 (m, 2H, **H18**), 1.53 (m, 2H, **H23**), 2.17 (t, *J* = 7.36 Hz, 2H, **H17**), 2.35 (t, *J* = 7.36 Hz, 2H, **H24**), 4.47 (s, 2H, **H6**), 7.26 (m, 5H, **H8-12**), 12.27 (**NH15**), 12.36 (bs, 2H, **OH14, 26**).

^{13}C NMR (DMSO-d_6): 25.02-34.20 (**C17-24**), 35.31 (**C6**), 127.17-136.39 (**C7-12**), 140.52 (**C5**), 141.53 (**C4**), 154.75 (**C2**), 164.23 (**C16**), 172.31 (**C25**), 175.08 (**C13**).

FTMS-ESI: calculated for $C_{21}H_{27}N_2O_5S$ (M+H) 419.1641, found 419.1638.

IR ν_{max} (cm^{-1}): 3186 (amide N-H stretch), 3065 (carboxylic O=-H stretch), 1701-1698 (2 carboxylic C=O stretch), 1675 (amide C=O stretch).

Elemental analysis: calculated for ($C_{21}H_{26}N_2O_5S$): C 59.39, H 5.98, H 6.93 and S 7.93, found for C 59.46, H 6.14, N 6.75 and S 7.52.

2-Decanamido-*N*,5-dimethylthiazole-4-carboxamide (126):

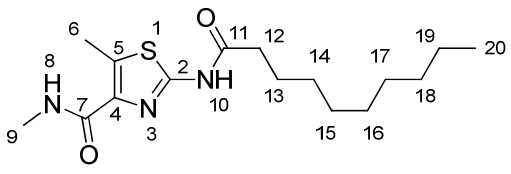

The title compound was obtained as yellow crystals using general procedure L after column chromatography with 25% ethyl acetate/hexane (300 mg, 66%).

m.p: 60-62 °C.

^{1}H NMR (DMSO-d_6): 0.85 (t, *J* = 6.6, 7.04 Hz, 3H, **H20**), 1.23 (bs, 12H, **H14-19**), 1.46 (p, *J* = 7.48, 6.6 Hz, 2H, **H13**), 2.02 (t, *J* = 7.48 Hz, 2H, **H12**), 2.49 (s, 3H, **H6**), 2.60 (s, 3H, **H9**), 7.67 (s, 1H, **NH8**), 12.01 (s, 1H, **NH10**).

^{13}C NMR (DMSO-d_6): 12.29-31.29 (**C6, 12-20**), 35.38 (**C9**), 126.96 (**C5**), 138.85 (**C4**), 153.46 (**C2**), 164.07 (**C11**), 173.04 (**C7**).

FTMS-ESI: calculated for $C_{16}H_{26}N_3O_2S$ (M-H) 324.1746, found 324.1751.

IR ν_{max} (cm^{-1}): 3393-3299 (amide N-H stretch), 1654-1637 (2 Amide C=O stretch).

Elemental analysis: calculated for ($C_{16}H_{27}N_3O_2S$): C 59.04, H 8.36, N 12.91 and S 9.85, found for C 59.26, H 8.52, N 12.98 and S 9.84.

5-Benzyl-2-decanamidothiazole-4-carboxamide (127):

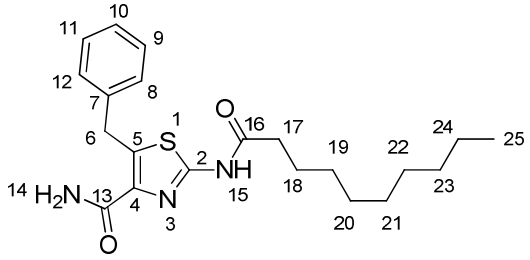

The title compound was obtained as white crystals using general procedure L after column chromatography with 10% methanol/chloroform (180 mg, 77.3%).

m.p: 68-70 °C.

^{1}H NMR (DMSO-d_6): 0.83 (t, *J* = 6.6 Hz, 3H, **H25**), 1.22 (bs, 12H, **H19-24**), 1.53 (p, *J* = 7.04, 6.6 Hz, 2H, **H18**), 2.38 (t, *J* = 7.04 Hz, 2H, **H17**), 4.53 (s, 2H, **H6**), 7.16 (m, 1H, **H10**), 7.28 (m, 4H, **H8, 9, 11, 12**), 7.29 (s, 1H, **NH14**), 12.03 (s, 1H, **NH15**).

^{13}C NMR (DMSO-*d*$_6$): 14.51-31.90 (**C17-25**), 35.25 (**C6**), 127.03-137.64 (**C7-12**), 137.73 (**C5**), 140.97 (**C4**), 154.62 (**C2**), 164.73 (**C16**), 172.36 (**C13**).

FTMS-ESI: calculated for $C_{21}H_{30}N_3O_2S$ (M+H) 388.2059, found 388.2053.

IR ν_{max} (cm^{-1}): 3467-3178 (amide N-H stretch), 1696-1660 (2 amide C=O stretch).

Elemental analysis: calculated for ($C_{21}H_{29}N_3O_2S$): C 65.08, H 7.54, N 10.84 and S 8.27, found for C 65.41, H 7.68, N 10.94 and S 8.49.

5-Benzyl-2-decanamido-*N*-methylthiazole-4-carboxamide (128):

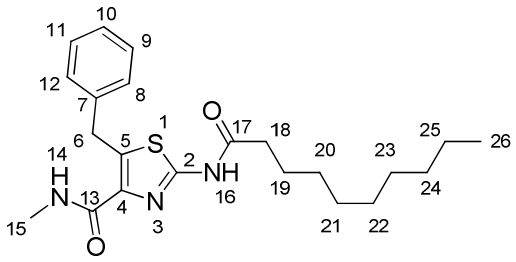

The title compound was obtained as a white powder using general procedure L after column chromatography with 25% ethyl acetate/hexane (500 mg, 73.5%)

m.p: 82-83 °C.

^{1}H NMR (DMSO-*d*$_6$): 0.84 (t, *J* = 6.16, 7.04 Hz, 3H, **H26**), 1.22 (bs, 12H, **H20-25**), 1.54 (m, 2H, **H19**), 2.39 (t, *J* = 7.48 Hz, 2H, **H18**), 2.80 (d, *J* = 4.84 Hz, 3H, **H15**), 4.53 (s, 2H, **H6**), 7.21-7.28 (m, 5H, **H8-12**), 7.77 (s, 1H, **NH14**), 11.99 (s, 1H, **NH16**).

^{13}C NMR (DMSO-*d*$_6$): 14.51- 31.90 (**C18-26**), 35.23 (**C6**), 37.02 (**C15**), 127.01-136.78 (**C7-12**), 137.65 (**C5**), 140.99 (**C4**), 154.77 (**C2**), 163.24 (**C17**), 172.40 (**C13**).

FTMS-ESI: calculated for $C_{22}H_{30}N_3O_2S$ (M-H) 400.2059, found 400.2064.

IR ν_{max} (cm^{-1}): 3428-3178 (amide N-H stretch), 1678-1635 (2 amide C=O stretch).

Elemental analysis: calculated for ($C_{22}H_{31}N_3O_2S$): C 65.80, H 7.78, N 10.46 and S 7.98, found for C 66.32, H 8.43, N 9.92 and S 7.29.

Methyl 4-decanamidobenzoate (129):

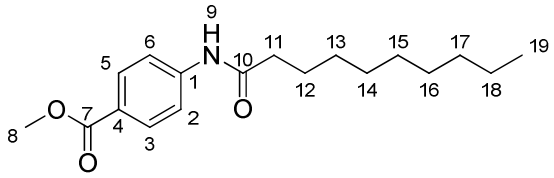

The title compound was obtained as shiny white flakes using general procedure D after crystallization from ethyl acetate (3.4 g, 85%).

m.p: 76-77 °C.

^{1}H NMR (DMSO-d_6): 0.84 (t, *J* = 7.04 Hz, 3H, **H19**), 1.26 (m, 12H, **H13-18**), 1.58 (p, *J* = 4.84, 7.48 Hz, 2H, **H12**), 2.32 (t, *J* = 7.48 Hz, 2H, **H11**), 3.81(s, 3H, **H8**), 7.71 (d, *J* = 8.8, 2H, **H2, 6**), 7.88 (d, *J* = 8.8 Hz, 2H, **H3, 5**), 10.19 (s, 1H, **NH9**).

^{13}C NMR (DMSO-d_6): 14.49-37.06 (**C11-19**), 52.38 (**C8**), 118.88-130.79 (**C2-6**), 144.30 (**C1**), 166.39 (**C10**), 172.45 (**C7**).

FTMS-ESI: calculated for $C_{18}H_{28}NO_3$ (M+H) 306.2069, found 306.2058.

IR ν_{max} (cm^{-1}): 3341 (amide N-H stretch), 1710 (ester C=O stretch), 1681 (amide C=O stretch).

Elemental analysis: calculated for ($C_{18}H_{27}NO_3$): C 70.79, H 8.91 and N 4.59, found for C 69.83, H 8.90 and N 4.65.

4-Decanamidobenzoic acid (130):

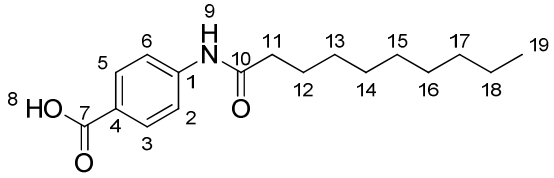

The title compound was obtained as a fine white powder using general procedure C (570 mg, 85%).

m.p: 234-235 °C.

^{1}H NMR (DMSO-*d*$_6$): 0.84 (t, *J* = 7.04 Hz, 3H, **H19**), 1.23 (m, 12H, **H13-18**), 1.58 (p, *J* = 6.6 Hz, 2H, **H12**), 2.32 (t, *J* = 7.48, 7 Hz, 2H, **H11**), 7.69 (d, *J* = 8.76 Hz, 2H, **H2, 6**), 7.85 (d, *J* = 8.76 Hz, 2H, **H3, 5**), 10.19 (s, 1H, **NH9**), 12.66 (s, 1H, **OH8**).

^{13}C NMR (DMSO-*d*$_6$): 14.51-37.05 (**C11-19**), 118.76-130.90 (**C2-6**), 144.35 (**C1**), 167.50 (**C10**), 172.40 (**C7**).

FTMS-ESI: calculated for $C_{17}H_{26}NO_3$ (M+H) 292.1913, found 292.1907.

IR ν_{max} (cm^{-1}): 3323 (amide N-H stretch), 2987 (carboxylic O-H stretch), 1702 (carboxylic C=O stretch), 1667 (amide C=O stretch).

Elemental analysis: calculated for ($C_{17}H_{25}NO_3$): C 70.07, H 8.65 and N 4.58, found for C 69.68, H 8.31 and N 4.09.

Methyl 3-decanamidobenzoate (131):

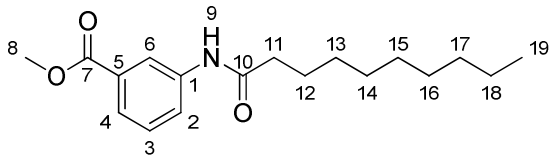

The title compound was obtained as pink flakes using general procedure D after crystallization from ethyl acetate/ether (2.8 g, 70%).

m.p: 52-53 °C (m.p).

^{1}H NMR (DMSO-*d*$_6$): 0.84 (t, *J* = 6.16, 7.04 Hz, 3H, **H19**), 1.26 (m, 12H, **H13-18**), 1.58 (p, *J* = 6.72, 7.04 Hz, 2H, **H12**), 2.30 (t, *J* = 7, 7.48 Hz, 2H, **H11**), 3.84 (s, 3H, **H8**), 7.43 (t, *J* = 7.88, 7.92 Hz, 1H, **H3**), 7.62 (d, *J* = 7.88 Hz, 1H, **H2**), 7.84 (dd, *J* = 7.92, 0.68 Hz, 1H, **H4**), 8.27 (s, 1H, **H6**), 10.09 (s, 1H, **NH9**).

^{13}C NMR (DMSO-*d*$_6$): 14.05-36.95 (**C11-19**), 52.71 (**C8**), 120.03-130.58 (**C2-6**), 140.26 (**C1**), 166.68 (**C10**), 172.16 (**C7**).

FTMS-ESI: calculated for $C_{18}H_{28}N_2O_3$ (M+H) 306.2069, found 306.2064.

IR ν_{max} (cm^{-1}): 3289 (amide N-H stretch), 1720 (ester C=O stretch), 1655 (amide C=O stretch).

Elemental analysis: calculated for ($C_{18}H_{27}N_2O_3$): C 70.79, H 8.91 and N 4.59, found for C 71.02, H 9.07 and N 4.77.

3-Decanamidobenzoic acid (132):

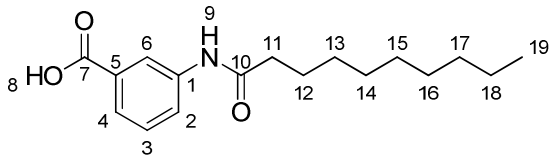

The title compound was obtained as a pink powder using general procedure C (660 mg, 98 %).

m.p: 204-205 °C.

^{1}H NMR (DMSO-*d*$_6$): 0.84 (t, *J* = 5.28, 7.48 Hz, 3H, **H19**), 1.27 (m, 12H, **H13-18**), 1.58 (m, 2H, **H12**), 2.30 (t, *J* = 7.44, 7.04 Hz, 2H, **H11**), 7.40 (t, *J* = 7.92 Hz, 1H, **H3**), 7.60 (d, *J* = 7.48 Hz, 1H, **H2**), 7.80 (d, *J* = 7.92 Hz, 1H, **H4**), 8.23 (s, 1H, **H6**), 10.06 (s, 1H, **NH9**).

^{13}C NMR (DMSO-*d*$_6$): 14.5-36.95 (**C11-19**), 120.30-131.76 (**C2-6**), 140.11 (**C1**), 167.76 (**C10**), 172.10 (**C7**).

FTMS-ESI: Calculated for $C_{17}H_{26}NO_3$ (M+H) 292.1913, found 292.1907.

IR ν_{max} (cm^{-1}): 3290 (amide N-H stretch), 2956 (carboxylic O-H stretch), 1690 (carboxylic C=O stretch), 1657 (amide C=O stretch).

Elemental analysis: calculated for ($C_{17}H_{25}NO_3$) C 70.07, H 8.65 and N 4.58, found for C 68.51, H 8.54 and N 4.58.

Methyl 2-decanamidobenzoate (133):

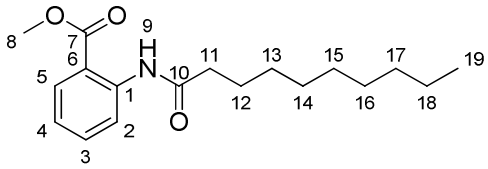

The title compound was obtained as a pale orange semisolid using general procedure D after crystallization from ether/hexane (3.0 g, 75%).

^{1}H NMR (DMSO-*d*$_6$): 0.84 (t, *J* = 4.84, 7.04 Hz, 3H, **H19**), 1.23 (bs, 12H, **H13-18**), 1.58 (p, *J* = 6.84, 7.04 Hz, 2H, **H12**), 2.36 (t, *J* = 7.04 Hz, 2H, **H11**), 3.94 (s, 3H, **H8**), 7.16 (t, *J* = 7.92, 7.48 Hz, 1H, **H4**), 7.58 (t, *J* = 7.32, 8.36 Hz, 1H, **H3**), 7.89 (d, *J* = 7.92 Hz, **H5**), 8.30 (d, *J* = 8.38 Hz, 1H, **H2**), 10.60 (s, 1H, **NH9**).

^{13}C NMR (DMSO-*d*$_6$): 14.49-37.77 (**C11-19**), 52.92 (**C8**), 117.86-134.51 (**C2-6**), 140.41 (**C1**), 168.21 (**C10**), 171.85 (**C7**).

FTMS-ESI: calculated for $C_{18}H_{28}N_2O_3$ (M+H) 306.2069, found 306.2064.

IR ν_{max} (cm^{-1}): 3302 (amide N-H stretch), 1701 (ester C=O stretch), 1691 (amide C=O stretch).

Elemental analysis: calculated for ($C_{18}H_{27}N_2O_3$): C 70.79, H 8.91 and N 4.59, found for C 70.86, H 9.52 and N 3.91.

2-Decanamidobenzoic acid (134):

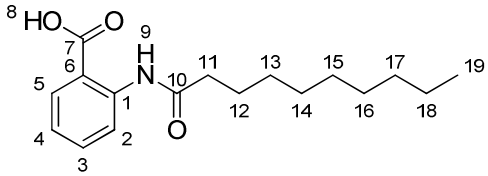

The title compound was obtained as a white powder using general procedure C (250 mg, 67%).

m.p: 60-61 °C.

^{1}H NMR (DMSO-d_6): 0.85 (m, 3H, **H19**), 1.23 (bs, 12H, **H13-18**), 1.28 (p, *J* = 7.04, 7.40 Hz, 2H, **H12**), 2.36 (t, *J* = 7.40 Hz, 2H, **H11**), 7.14 (t, *J* = 8.12, 7.38 Hz, 1H, **H4**), 7.55 (t, *J* = 7.04, 7.48 Hz, 1H, **H3**), 7.96 (d, *J* = 7.88 Hz, 1H, **H5**), 8.49 (d, *J* = 7.48 Hz, 1H, **H2**), 11.14 (s, 1H, **NH9**), 13.21 (bs, 1H, **OH8**).

^{13}C NMR (DMSO-d_6): 14.50-38.14 (**C11-19**), 116.77-134.61 (**C2-6**), 141.53 (**C1**), 170.15 (**C10**), 171.85 (**C7**).

FTMS-ESI: calculated for $C_{17}H_{26}NO_3$ (M+H) 292.1913, found 292.1907.

IR ν_{max} (cm^{-1}): 3335 (amide N-H stretch), 3007 (carboxylic O-H stretch), 1707 (carboxylic C=O stretch), 1683 (amide C=O stretch).

Elemental analysis: calculated for ($C_{17}H_{25}NO_3$): C 70.07, H 8.65 and N 4.58, found for C 70.23, H 9.06 and N 4.95.

(*E*)-Ethyl 2-((4-(methoxycarbonyl)phenyl)diazenyl)-4-methyl-1*H*-imidazole-5-carboxylate (136):

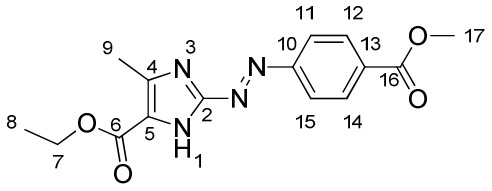

The title compound was obtained as dark orange crystals using general procedure B after crystallization from ethyl acetate/hexane (3.27 g, 78%).

m.p: 181-181.5°C.

^{1}H NMR (DMSO-d_6): 1.31 (t, *J* = 7.04 Hz, 3H, **H8**), 2.53 (s, 3H, **H9**), 3.89 (s, 3H, **H17**), 4.28 (q, *J* = 7.04 Hz, 2H, **H7**), 7.94 (d, *J* = 8.36 Hz, 2H, **H11, 15**), 8.15 (d, *J* = 8.36 Hz, 2H, **H12, 14**), 13.49 (bs, 1H, **NH1**).

^{13}C NMR (DMSO-d_6): 11.79 (**C8**), 14.85 (**C9**), 53.02 (**C17**), 60.32 (**C7**), 123.12-132.31 (**C10-15**), 139.54 (**C4**), 142.89 (**C5**), 155.01 (**C2**), 163.28 (**C16**), 166.10 (**C6**).

FTMS-ESI: calculated for $C_{15}H_{17}N_4O_4$ (M+H) 317.1250, found 317.1243.

IR ν_{max} (cm^{-1}): 3423 (imidazole N-H stretch), 1723-1706 (2 ester C=O stretch), 1421 (N=N stretch).

Elemental analysis: calculated for ($C_{15}H_{16}N_4O_4$): C 56.96, H 5.10 and N 17.71, found for C 56.86, H 5.04 and N 17.45.

(*E*)-2-((4-Bromophenyl)diazenyl)-4-methyl-1*H*-imidazole-5-carboxylic acid (137):

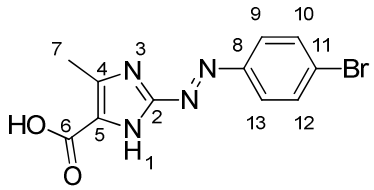

The title compound was obtained as a yellow powder using genral procedure C (200 mg, 38%).

m.p: 260°C (with decomposition).

^{1}H NMR (DMSO-d_6): 2.49 (s, 3H, **H7**), 7.75 (m, 4H, **H9, 10, 12, 13**), 12.56 (bs, 1H, **OH14**).

^{13}C NMR (DMSO-d_6): 19.11 (**C7**), 123.44-127.12 (**C8-13**), 133.02 (**C4**), 138.06 (**C5**), 167.77 (**C6**).

FTMS-ESI: calculated for $C_{11}H_{10}N_4O_2$ (M+H) 308.9987, found 308.9979.

IR ν_{max} (cm^{-1}): 3421 (imidazole N-H stretch), 3102 (carboxylic O-H stretch), 1683 (ester C=O stretch), 1442 (N=N stretch).

Elemental analysis: calculated for ($C_{11}H_9N_4O_2$): C 42.60, H 3.25 and N 18.07, found C 42.10, H 2.98 and N 18.43.

(*E*)-4-((5-(Ethoxycarbonyl)-4-methyl-1*H*-imidazol-2-yl)diazenyl)benzoic acid (138):

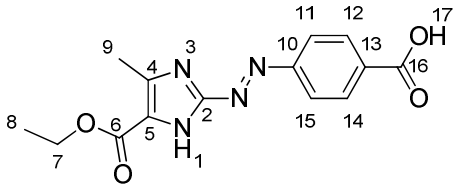

The title compound was obtained as yellow crystals using general procedure C (90 mg, 30%).

m.p: 250 °C (with decomposition).

^{1}H NMR (DMSO-*d*$_6$): 1.31 (t, *J* = 7.04 Hz, 3H, **H8**), 2.51 (s, 3H, **H9**), 4.25 (q, *J* = 7.04 Hz, 2H, **H7**), 7.78 (d, *J* = 7.92 Hz, 2H, **H11, 15**), 8.05 (d, *J* = 7.92 Hz, 2H, **H12, 14**), 13.5 (bs, 1H, **OH17**).

^{13}C NMR (DMSO-*d*$_6$): 12.30 (**C9**), 14.91 (**C8**), 60.31 (**C7**), 122.19-131.12 (**C10-15**), 142.56 (**C4**), 153.13 (**C5**), 163.51 (**C16**), 169.15 (**C6**).

FTMS-ESI: calculated for $C_{14}H_{15}N_4O_4$ (M+H) 303.1093, found 303.1090.

IR ν_{max} (cm^{-1}): 3397 (imidazole N-H stretch), 3085 (carboxylic O-H stretch), 1703 (ester C=O stretch), 1685 (carboxylic C=O stretch), 1510 (N=N stretch).

Elemental analysis: calculated for ($C_{14}H_{14}N_4O_4$): C 55.63, H 4.67 and N 18.53, found for C 55.21, H 4.21 and N 17.90.

Ethyl 2-amino-4-methyl-1*H*-imidazole-5-carboxylate (AIC): [139]

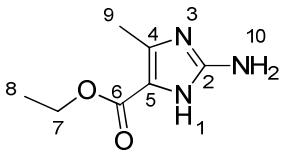

Compound **135** (2.0 g, 6.0 mmol, 1 eq) was dissolved in absolute ethanol, then platinum oxide IV (1.0 g, 4.30 mmol, 0.7 eq) was added, upon which the mixture

was hydrogenated under 50 psi overnight. The catalyst was removed through a layer of Kieselghur powder and the filtrate was evaporated to dryness. The residue was dissolved in water and basified with 0.5M NaOH to pH 7.5, then extracted three times with ether, the water layer removed and basified to pH 10.5, followed by extraction with ethyl acetate. The organic layer was separated and dried over anhydrous magnesium sulfate then evaporated under vacuum to give light brown flakes (500 g, 50%).

m.p: 199.0-199.5 °C.

^{1}H NMR (DMSO-*d*$_6$): 1.24 (t, *J* = 7.04 Hz, 3H, **H8**), 2.49 (s, 3H, **H9**), 4.13 (q, *J* = 7, 7.04 Hz, 2H, **H7**), 5.58 (bs, 2H, **NH10**), 10.52 (bs, 1H, **NH1**).

^{13}C NMR (DMSO-*d*$_6$): 15.05 (**C8, 9**), 59.30 (**C7**), 127.26 (**C4**), 134.04 (**C5**), 136.23 (**C2**), 165.71 (**C6**).

FTMS-ESI: calculated for $C_7H_{12}N_3O_2$ (M+H) 170.093, found 170.0924.

IR ν_{max} (cm^{-1}): 3444 (1° amine N-H stretch), 3342 (imidazole N-H stretch), 1668 (ester C=O stretch).

Elemental analysis: calculated for ($C_7H_{11}N_3O_2$): C 49.40, H 6.55 and N 24.69, found for C 50.07, H 6.72 and N 25.32.

Ethyl 2-decanamido-4-methyl-1*H*-imidazole-5-carboxylate (139):

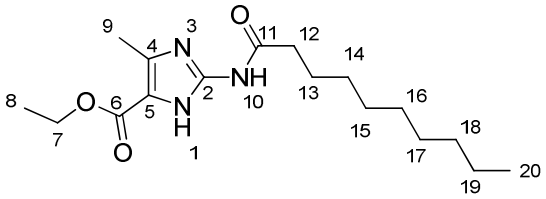

The title compound was obtained as white crystals using general procedure D after column chromatography with 50% ethyl acetate/hexane (300 mg, 52%).

m.p: 112-113 °C.

^{1}H NMR (DMSO-*d*$_6$): 0.84 (t, *J* = 6.6 Hz, 3H, **H20**), 1.23 (bs, 15H, **H8, 14-19**), 1.56 (p, *J* = 6.6 Hz, 2H, **H13**), 2.29 (q, *J* = 6.6, 7.48 Hz, 2H, **H12**), 2.40 (s, 3H, **H9**), 4.13 (q, *J* = 7.04, 7.04 Hz, 2H, **H7**), 11.14 (s, 1H, **NH1**), 11.96 (s, 1H, **NH10**).

^{13}C NMR (DMSO-*d*$_6$): 11.34-35.56 (**C8, 9, 12-20**), 59.40 (**C7**), 132.77 (**C4**), 140.00 (**C5**), 152.32 (**C2**), 163.74 (**C11**), 171.94 (**C6**).

FTMS-ESI: calculated for $C_{17}H_{30}N_3O_3$ (M+H) 324.2287, found 324.2282.

IR ν_{max} (cm^{-1}): 3296 (amide N-H stretch), 1720 (ester C=O stretch), 1661 (amide C=O stretch).

Elemental analysis: calculated for ($C_{17}H_{29}N_3O_3$) C 63.13, H 9.04 and N 12.99, found for C 63.29, H 8.73 and N 12.41.

2-Decanamido-4-methyl-1*H*-imidazole-5-carboxylic acid (140):

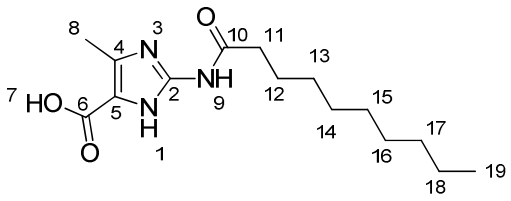

The title compound was obtained as white flakes using general procedure C (56 mg, 62%).

m.p: 210-211 °C.

^{1}H NMR (DMSO-*d*$_6$): 0.83 (t, *J* = 6.76 Hz, 3H, **H19**), 1.24 (bs, 12H, **H13-17**), 1.57 (m, 2H, **H12**), 2.32 (bs, 2H, **H11**), 2.40 (s, 3H, **H8**), 11.09 (bs, 1H, **NH1**), 11.98 (bs, 1H, **OH7**).

^{13}C NMR (DMSO-*d*$_6$): 10.05-35.06 (**C8, 11-19**), 134.12 (**C4**), 144.32 (**C5**), 151.49 (**C2**), 166.86 (**C10**), 171.87 (**C6**).

FTMS-ESI: calculated for $C_{15}H_{24}N_3O_3$ (M-H) 294.1818, found 294.1823.

IR ν_{max} (cm^{-1}): 3403 (amide N-H stretch), 1714 (carboxylic C=O stretch), 1694 (amide C=O stretch).

Elemental analysis: calculated for ($C_{15}H_{25}N_3O_3$): C 60.99, H 8.53 and N 14.23, found for C 60.45, H 8.96 and for N 14.22.

2-Amino-5-phenethylthiazole-4-carboxylic acid (202a):

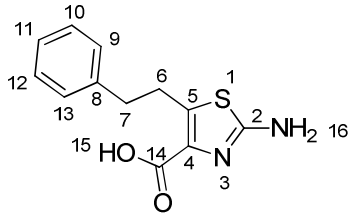

The title compound was obtained as an off-white powder using general procedure C (140 mg, 54%).

m.p: 156-157 °C.

H^1 NMR (DMSO-d_6): 2.83 (t, *J* = 7.48, 7.88 Hz, 2H, **H7**), 3.27 (t, *J* = 7.48, 7.92 Hz, 2H, **H6**), 6.99 (bs, 2H, **NH16**), 7.22 (m, 5H, **H9-13**), 12.35 (bs, 1H, **OH15**).

^{13}C NMR (DMSO-d_6): 28.80 (**C7**), 37.46 (**C6**), 126.61-136.31 (**C8-13**), 137.83 (**C5**), 141.35 (**C4**), 154.24 (**C2**), 164.47 (**C14**).

FTMS-ESI: calculated for $C_{12}H_{13}N_2O_2S$ (M+H) 249.0698, found 249.0692.

IR ν_{max} (cm^{-1}): 3401 (1° amine N-H stretch), 3196 (carboxylic O-H stretch), 1677 (carboxylic C=O stretch).

Elemental analysis: calculated for ($C_{12}H_{12}N_2O_2S$): C 58.05, H 4.87, N 11.28 and S 12.91, found for C 54.66, H 4.82, N 9.66 and S 10.92.

Methyl 5-isopropyl-2-(2-(4-methoxyphenyl)acetamido)thiazole-4-carboxylate (141):

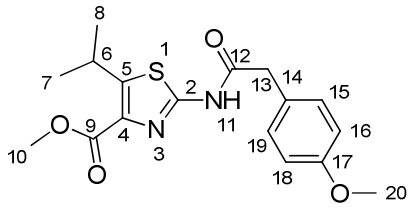

The title compound was obtained as white crystals using general procedure D after crystallization from DCM/hexane (250 mg, 76%).

m.p: 138-139 °C.

^{1}H NMR (DMSO-*d*$_6$): 1.25 (d, *J* = 7.04 Hz, 6H, **H7, 8**), 3.63 (s, 2H, **H14**), 3.72 (s, 3H, **H20**), 3.79 (s, 3H, **H10**), 3.98 (septet, *J* = 7.01, 6.6 Hz, 1H, **H6**), 6.87 (d, *J* = 8.36 Hz, 2H, **H15, 19**), 7.22 (d, *J* = 8.36 Hz, 2H, **H16, 18**), 12.58 (s, 1H, **NH11**).

^{13}C NMR (DMSO-*d*$_6$): 25.13-27.46 (**C6-8**), 41.39 (**C13**), 52.18 (**C20**), 55.60 (**C10**), 114.42-130.74 (**C14-16, 18, 19**), 134.02 (**C5**), 151.22 (**C4**), 154.23 (**C2**), 158.81 (**C17**), 162.94 (**C12**), 170.52 (**C9**).

FTMS-ESI: calculated for $C_{17}H_{22}N_2O_4S$ (M+H) 349.1222, found 349.1217.

IR ν_{max} (cm^{-1}): 3280 (amide N-H stretch), 1724 (ester C=O stretch), 1691 (amide C=O stretch).

Elemental analysis: calculated for ($C_{17}H_{21}N_2O_4S$): C 58.60, H 5.79, N 8.04 and S 9.20, found for C 58.94, H 5.79, N 7.91 and S 9.12.

5-Isopropyl-2-(2-(4-methoxyphenyl)acetamido)thiazole-4-carboxylic acid (142):

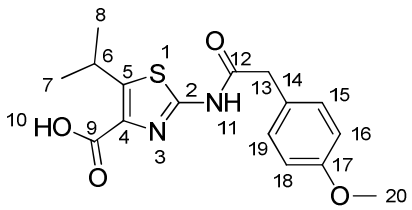

The title compound was obtained as a pale yellow powder using general procedure C (75 mg, 77.4%).

m.p: 219-220 °C.

^{1}H NMR (DMSO-*d*$_6$): 1.24 (d, *J* = 7.04 Hz, 6H, **H7, 8**), 3.64 (s, 2H, **H13**), 3.72 (s, 3H, **H20**), 4.02 (septet, *J* = 6.6, 7.04 Hz, 1H, **H6**), 6.87 (d, *J* = 8.36 Hz, 2H, **H15, 19**), 7.25 (d, *J* = 8.36 Hz, 2H, **H16, 18**), 12.51 (s, 1H, **NH11**), 12.79 (bs, 1H, **OH10**).

^{13}C NMR (DMSO-*d*$_6$): 25.25-27.41 (**C6-8**), 41.39 (**C13**), 55.60 (**C20**), 114.42 - 130.74 (**C14, 15, 16, 18, 19**), 135.26 (**C5**), 150.86 (**C4**), 153.86 (**C17**), 164.11 (**C12**), 170.46 (**C9**).

FTMS-ESI: calculated for $C_{16}H_{19}N_2O_4S$ (M+H) 335.1066, found 335.1060.

IR ν_{max} (cm^{-1}): 3426 (amide N-H stretch), 2954 (carboxylic O-H stretch), 1695 (carboxylic C=O stretch), 1670 (amide C=O stretch).

Elemental analysis: calculated for ($C_{16}H_{18}N_2O_4S$): C 57.47, H 5.43, N 8.38 and S 9.59, found for C 56.98, H 5.23, N 7.48 and S 9.09.

Methyl 5-isopropyl-2-(2-phenylacetamido)thiazole-4-carboxylate (143):

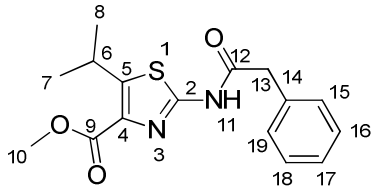

The title compound was obtained as a light brown powder using general procedure D after column chromatography with 10% ethyl acetate/DCM (180 mg, 57%).

m.p: 154-156 °C.

^{1}H NMR (DMSO-*d*$_6$): 1.26 (d, *J* = 7.04, 6H, **H7, 8**), 3.72 (s, 2H, **H13**), 3.79 (s, 3H, **H10**), 3.96 (septet, *J* = 7.04, 6.56 Hz, 1H, **H6**), 7.25 (m, 1H, **H17**), 7.31 (m, 4H, **H15, 16, 18, 19**), 12.64 (s, 1H, **NH11**).

^{13}C NMR (DMSO-*d*$_6$): 25.14-31.28 (**C6-8**), 42.26 (**C14**), 52.19 (**C10**), 127.44-129.73 (**C14-19**), 135.35 (**C5**), 151.28 (**C4**), 154.18 (**C2**), 162.18 (**C12**), 170.20 (**C9**).

FTMS-ESI: calculated for $C_{16}H_{17}N_2O_3S$ (M-H) 317.0960, found 317.0965.

IR ν_{max} (cm^{-1}): 3270 (amide N-H stretch), 1717 (ester C=O stretch), 1695 (amide C=O stretch).

Elemental analysis: calculated for ($C_{16}H_{18}N_2O_3S$): C 60.36, H 5.70, N 8.80 and S 10.07, found for C 60.17, H 5.49, N 8.97 and S 9.54.

5-Isopropyl-2-(2-phenylacetamido)thiazole-4-carboxylic acid (144):

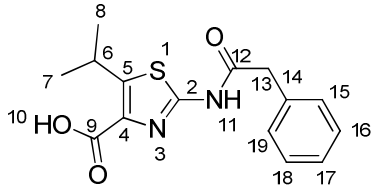

The title compound was obtained as a white powder using general procedure C (45 mg, 43%).

m.p: 252 °C (with decomposition).

^{1}H NMR (DMSO-*d*$_6$): 1.23 (d, *J* = 6.6 Hz, 6H, **H7, 8**), 3.72 (s, 2H, **H13**), 4.00 (p, *J* = 6.6, 7.04 Hz, 1H, **H6**), 7.24 (m, 1H, **H17**), 7.33 (m, 4H, **H15, 16, 18, 19**), 12.57 (s, 1H, **NH11**), 12.79 (s, 1H, **OH10**).

^{13}C NMR (DMSO-*d*$_6$): 25.25-27.42 (**C6-8**), 42.25 (**C13**), 127.42-129.71 (**C14-19**), 135.27 (**C5**), 150.47 (**C4**), 153.81 (**C2**), 164.10 (**C12**), 170.12 (**C9**).

FTMS-ESI: calculated for $C_{15}H_{17}N_2O_3S$ (M+H) 305.0960, found 305.0954.

IR ν_{max} (cm^{-1}): 3435 (amide N-H stretch), 3058 (carboxylic O-H stretch), 1696 (carboxylic C=O stretch), 1670 (amide C=O stretch).

Elemental analysis: calculated for ($C_{15}H_{16}N_2O_3S$): C 59.19, H 5.30, N 9.20 and S 10.54, found for C 58.67, H 5.00, N 8.46 and S 10.10.

Methyl 5-isopropyl-2-(2-(3-methoxyphenyl)acetamido)thiazole-4-carboxylate (145):

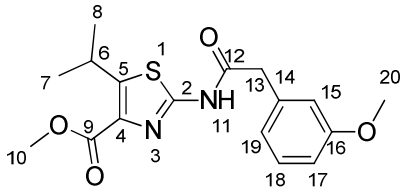

The title compound was obtained as light brown crystals using general procedure D after column chromatography with 10% ethyl acetate/hexane (220 mg, 64%).

m.p: 118-119 °C.

^{1}H NMR (DMSO-*d*$_6$): 1.26 (d, *J* = 6.6 Hz, 6H, **H7, 8**), 3.63 (s, 2H, **H13**), 3.73 (s, 3H, **H20**), 3.79 (s, 3H, **H10**), 3.97 (septet, *J* = 7.04, 6.56 Hz, 1H, **H6**), 6.87 (m, 3H, **H15, 17, 19**), 7.23 (t, *J* = 7.92, 7.48 Hz, 1H, **H18**), 12.63 (s, 1H, **NH11**).

^{13}C NMR (DMSO-*d*$_6$): 25.15-27.49 (**C6**), 42.33 (**C13**), 52.23 (**C20**), 55.55 (**C10**), 112.86-134.06 (**C14, 15, 17-19**), 136.72 (**C5**), 151.30 (**C4**), 154.17 (**C2**), 159.81 (**C16**), 162.95 (**C12**), 170.06 (**C9**).

FTMS-ESI: calculated for $C_{17}H_{19}N_2O_4S$ (M-H) 347.1066, found 347.1071.

IR ν_{max} (cm^{-1}): 3275 (amide N-H stretch), 1720 (ester C=O stretch), 1690 (amide C=O stretch).

Elemental analysis: calculated for ($C_{17}H_{20}N_2O_4S$): C 58.60, H 5.79 and N 8.04, found for C 58.78, H 5.80 and N 7.87.

5-Isopropyl-2-(2-(3-methoxyphenyl)acetamido)thiazole-4-carboxylic acid (146):

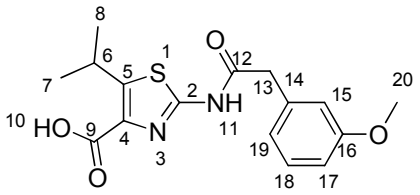

The title compound was obtained as yellow flakes using general procedure C (78 mg, 80.5%).

m.p: 222-224 °C.

^{1}H NMR (DMSO-d_6): 1.25 (d, *J* = 7.04 Hz, 6H, **H7, 8**), 3.68 (s, 2H, **H13**), 3.74 (s, 3H, **H20**), 4.00 (septet, *J* = 7.04, 6.6 Hz, 1H, **H6**), 6.84-6.90 (m, 3H, **H15, 17, 19**), 7.23 (t, *J* = 7.92 Hz, 1H, **H18**), 12.55 (s, 1H, **NH11**), 12.81 (s, 1H, **OH10**).

^{13}C NMR (DMSO-d_6): 25.25-27.42 (**C6-8**), 42.31 (**C13**), 55.56 (**C20**), 112.82-136.81 (**C5, 14, 15, 17-19**), 150.48 (**C4**), 153.81 (**C2**), 159.81 (**C16**), 164.10 (**C12**), 169.98 (**C9**).

FTMS-ESI: calculated for $C_{16}H_{19}N_2O_4S$ (M+H) 335.1066, found 335.1060.

IR ν_{max} (cm^{-1}): 3432 (amide N-H stretch), 2967 (carboxylic O-H stretch), 1695 (carboxylic C=O stretch), 1669 (amide C=O stretch).

Elemental analysis: calculated for ($C_{16}H_{18}N_2O_4S$): C 57.47, H 5.43, N 8.38 and S 9.59, found for C 57.16, H 5.36, N 7.87 and S 9.05.

Methyl 2-(2-(4-chlorophenyl)acetamido)-5-isopropylthiazole-4-carboxylate (147):

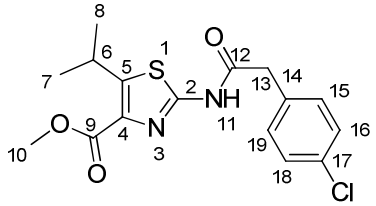

The title compound was obtained as transparent crystals using general procedure D after crystallization from DCM/hexane (240 mg, 69%).

m.p: 206-207 °C.

^{1}H NMR (DMSO-d_6): 1.26 (d, *J* = 7.04 Hz, 6H, **H7, 8**), 3.74 (s, 2H, **H13**), 3.79 (s, 3H, **H10**), 3.96 (septet, *J* = 7.04, 6.56 Hz, 1H, **H6**), 7.32 (d, *J* = 8.36 Hz, 2H, **H15, 19**), 7.40 (d, *J* = 8.36 Hz, 2H, **H16, 18**), 12.65 (s, 1H, **NH11**).

^{13}C NMR (DMSO-d_6): 25.13-27.48 (**C6-8**), 42.31 (**C13**), 52.20 (**C10**), 128.93-132.20 (**C14-16, 18, 19**), 134.06 (**C5**), 144.30 (**C17**), 151.31 (**C4**), 154.12 (**C2**), 162.91 (**C12**), 169.86 (**C9**).

FTMS-ESI: calculated for $C_{16}H_{16}ClN_2O_3S$ (M-H) 351.0570, found 351.0574.

IR ν_{max} (cm^{-1}): 3261 (amide N-H stretch), 1715 (ester C=O stretch), 1694 (amide C=O stretch).

Elemental analysis: calculated for ($C_{16}H_{17}ClN_2O_3S$): C 54.46, H 4.86 and N 7.94, found for C 54.51, H 4.95 and N 8.12.

2-(2-(4-Chlorophenyl)acetamido)-5-isopropylthiazole-4-carboxylic acid (148):

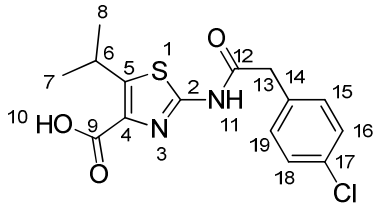

The title compound was obtained as light brown crystals using general procedure C (70 mg, 73%).

m.p: 238-239 °C.

^{1}H NMR (DMSO-d_6): 1.23 (d, *J* = 6.6Hz, 6H, **H7, 8**), 3.74 (s, 2H, **H13**), 4.02 (septet, *J* = 6.6, 7.04, 6.6 Hz, 1H, **H6**), 7.34 (d, *J* = 8.8 Hz, 2H, **H15, 19**), 7.38 (d, *J* = 8.8 Hz, 2H, **H16, 18**), 12.59 (s, 1H, **NH11**), 12.81 (s, 1H, **OH10**).

^{13}C NMR (DMSO-*d*$_6$): 25.25-27.41 (**C6-8**), 41.4 (**C13**), 128.92-132.17 (**C14-16, 18, 19**), 134.41 (**C5**), 145.30 (**C17**), 150.51 (**C4**), 153.75 (**C2**), 164.08 (**C12**), 169.79 (**C9**).

FTMS-ESI: calculated for $C_{15}H_{16}ClN_2O_3S$ (M+H) 339.0570, found 339.0565.

IR ν_{max} (cm^{-1}): 3430 (amide N-H stretch), 3191 (carboxylic O-H stretch), 1698 (carboxylic C=O stretch), 1669 (amide C=O stretch).

Elemental analysis: calculated for ($C_{15}H_{15}ClN_2O_3S$): C 53.17, H 4.46, N 8.27 and S 9.46, found for C 52.97, H 3.92, N 8.26 and S 8.94.

Methyl 5-benzyl-2-(2-(4-methoxyphenyl)acetamido)thiazole-4-carboxylate (149):

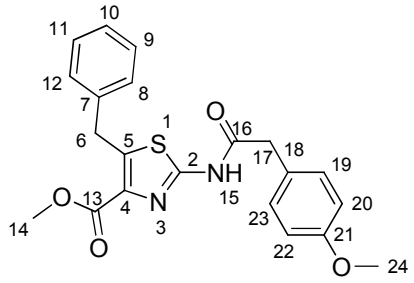

The title compound was obtained as pink fine crystals using general procedure D after crystallization from DCM/hexane (300 mg, 93%).

m.p: 180-182 °C.

^{1}H NMR (DMSO-*d*$_6$): 3.62 (s, 2H, **H17**), 3.71 (s, 3H, **H24**), 3.81 (s, 3H, **H14**), 4.45 (s, 2H, **H6**), 6.85 (d, *J* = 7.48, 2H, **H19, 23**), 7.19-7.28 (m, 7H, **H8-12, 20, 22**), 12.62 (s, 1H, **NH15**).

^{13}C NMR (DMSO-*d*$_6$): 32.45 (**C17**), 41.32 (**C6**), 52.29 (**C24**), 55.59 (**C14**), 114.40 -127.25 (**C7-12**), 129.07-135.22 (**C18-20, 22, 23**), 140.19 (**C5**), 142.59 (**C4**), 155.12 (**C2**), 158.79 (**C21**), 163.02 (**C16**), 170.61 (**C13**).

FTMS-ESI: calculated for $C_{21}H_{19}N_2O_4S$ (M-H) 395.1066, found 395.1071.

IR ν_{max} (cm^{-1}): 3439 (amide N-H stretch), 1723 (ester C=O stretch), 1696 (amide C=O stretch).

Elemental analysis: calculated for ($C_{21}H_{20}N_2O_4S$): C 63.62, H 5.08, N 7.07 and S 8.09, found for C 63.39, H 5.11, N 7.09 and S 7.89.

5-Benzyl-2-(2-(4-methoxyphenyl)acetamido)thiazole-4-carboxylic acid (150):

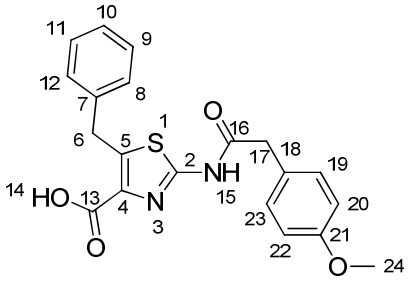

The title compound was obtained as yellowish flakes using general procedure C (75 mg, 78.5%).

m.p: 240 °C (with decomposition).

^{1}H NMR (DMSO-d_6): 3.63 (s, 2H, **H17**), 3.71 (s, 3H, **H24**), 4.46 (s, 2H, **H6**), 6.85 (d, *J* = 8.8 Hz, 2H, **H19, 23**), 7.19 (d, *J* = 8.8 Hz, 2H, **H20, 22**), 7.28 (m, 5H, **H8-12**), 12.55 (s, 1H, **NH15**), 12.93 (s, 1H, **OH14**).

^{13}C NMR (DMSO-d_6): 32.50 (**C6**), 41.23 (**C17**), 55.59 (**C24**), 114.39-129.04 (**C7-12**), 129.16-136.49 (**C18-20, 22, 23**), 140.46 (**C5**), 141.77 (**C4**), 154.77 (**C2**), 158.78 (**C21**), 164.17 (**C16**), 170.55 (**C13**).

FTMS-ESI: calculated for $C_{20}H_{17}N_2O_4S$ (M-H) 381.0909, found 381.0913.

IR ν_{max} (cm^{-1}): 3446 (amide N-H stretch), 3186 (carboxylic O-H stretch), 1696 (carboxylic C=O stretch), 1664 (amide C=O stretch).

Elemental analysis: calculated for ($C_{20}H_{18}N_2O_4S$): C 62.81, H 4.74, N 7.33 and S 8.38, found for C 62.61, H 4.52, N 7.96 and S 8.02.

Methyl 5-benzyl-2-(2-(3-methoxyphenyl)acetamido)thiazole-4-carboxylate (151):

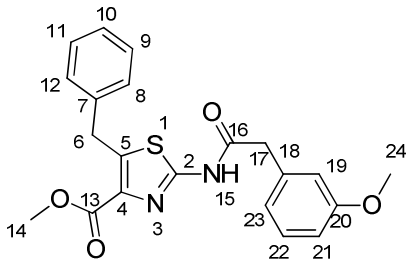

The title compound was obtained as white crystals using general procedure D after recrystallization from DCM/hexane (310 mg, 96%).

m.p: 165-166 °C.

^{1}H NMR (DMSO-*d*$_6$): 3.66 (s, 2H, **H17**), 3.72 (s, 3H, **H24**), 3.81 (s, 3H, **H14**), 4.46 (s, 2H, **H6**), 6.83 (m, 3H, **H9-11**), 7.25 (m, 6H, **H8, 12, 19, 21-23**), 12.65 (s, 1H, **NH15**).

^{13}C NMR (DMSO-*d*$_6$): 32.47 (**C6**), 42.25 (**C17**), 52.29 (**C24**), 55.54 (**C14**), 112.86-127.27 (**C7-12**), 129.08-136.62 (**C18, 19, 21-23**), 140.17 (**C5**), 142.66 (**C4**), 155.07 (**C2**), 159.79 (**C20**), 163.03 (**C16**), 170.15 (**C13**).

FTMS-ESI: calculated for $C_{21}H_{19}N_2O_4S$ (M-H) 395.1066, found 395.1076.

IR ν_{max} (cm^{-1}): 3273 (amide N-H stretch), 1712 (ester C=O stretch), 1690 (amide C=O stretch).

Elemental analysis: calculated for ($C_{21}H_{20}N_2O_4S$): C 63.62, H 5.08, N 7.07 and S 8.09, found for C 63.55, H 4.98, N 6.45 and S 7.56.

5-Benzyl-2-(2-(3-methoxyphenyl)acetamido)thiazole-4-carboxylic acid (152):

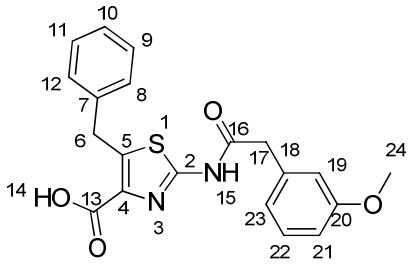

The title compound was obtained as a white powder using general procedure C (85 mg, 89%).

m.p: 240-241 °C.

^{1}H NMR (DMSO-d_6): 3.66 (s, 2H, **H17**), 3.74 (s, 3H, **H24**), 4.46 (s, 2H, **H6**), 6.84 (m, 3H, **H9-11**), 7.25 (m, 6H, **H8, 12, 19, 21-23**), 12.59 (s, 1H, **NH15**), 12.95 (s, 1H, **OH14**).

^{13}C NMR (DMSO-d_6): 32.50 (**C6**), 42.23 (**C17**), 55.54 (**C24**), 112.83-127.18 (**C7-12**), 129.05-136.69 (**C18, 19, 21-23**), 140.45 (**C5**), 141.84 (**C4**), 154.72 (**C2**), 159.79 (**C20**), 164.17 (**C16**), 170.06 (**C13**).

FTMS-ESI: calculated for $C_{20}H_{17}N_2O_4S$ (M+H) 383.1066, found 383.1063.

IR ν_{max} (cm^{-1}): 3422 (amide N-H stretch), 3185 (carboxylic O-H stretch), 1696 (carboxylic C=O stretch), 1664 (amide C=O stretch).

Elemental analysis: calculated for ($C_{20}H_{16}N_2O_4S$): C 62.81, H 4.74, N 7.33 and S 8.38, found for C 63.11, H 4.84, N 6.96 and S 7.96.

Methyl 5-benzyl-2-(2-(4-chlorophenyl)acetamido)thiazole-4-carboxylate (153):

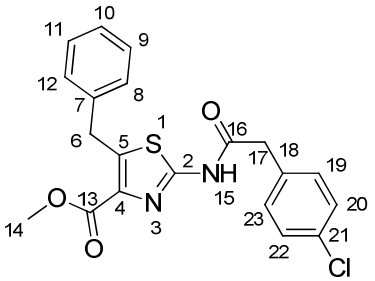

The title compound was obtained as a white amorphous solid using general procedure D after crystallization from DCM/Hexane (300 mg, 92.6%).

m.p: 229-230 °C.

^{1}H NMR (DMSO-d_6): 3.72 (s, 2H, **H17**), 3.81 (s, 3H, **H14**), 4.46 (s, 2H, **H6**), 7.28 (m, 7H, **H8-12, 19, 23**), 7.36 (m, 2H, **H20, 22**), 12.68 (s, 1H, **NH15**).

^{13}C NMR (DMSO-d_6): 32.47 (**C6**), 41.33 (**C17**), 52.31 (**C14**), 127.26-129.08 (**C7-12**), 129.21-135.24 (**C18-23**), 140.16 (**C5**), 142.70 (**C4**), 155.02 (**C2**), 163.01 (**C16**), 169.95 (**C13**).

FTMS-ESI: calculated for $C_{20}H_{18}ClN_2O_3S$ (M+H) 401.0727, found 401.0721.

IR ν_{max} (cm^{-1}): 3267 (amide N-H stretch), 1710 (ester C=O stretch), 1688 (amide C=O stretch).

Elemental analysis: calculated for ($C_{20}H_{17}ClN_2O_3S$): C 59.92, H 4.27 and N 6.99, found for C 60.69, H 4.99 and N 7.01.

5-Benzyl-2-(2-(4-chlorophenyl)acetamido)thiazole-4-carboxylic acid (154):

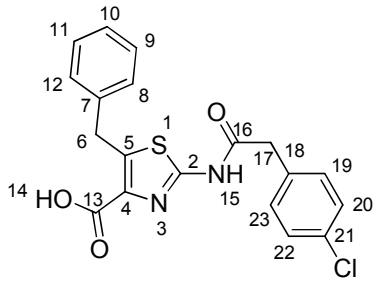

The title compound was obtained as a white powder using general procedure C (50 mg, 40%).

m.p: 260-261 °C.

^{1}H NMR (DMSO-d_6): 3.71 (s, 2H, **H17**), 4.46 (s, 2H, **H6**), 7.24 (m, 7H, **H8-12, 19, 23**), 7.36 (m, 2H, **H20, 22**), 12.61 (s, 1H, **NH15**), 12.94 (1H, **OH14**).

^{13}C NMR (DMSO-d_6): 32.51 (**C6**), 41.33 (**C17**), 127.19-129.05 (**C7-12**), 129.17--136.51 (**C18-23**), 140.45 (**C5**), 141.89 (**C4**), 154.66 (**C2**), 164.15 (**C16**), 169.87 (**C13**).

FTMS-ESI: calculated for $C_{19}H_{14}ClN_2O_3S$ (M-H) 385.0414, found 385.0419.

IR ν_{max} (cm^{-1}): 3434 (amide N-H stretch), 3190 (carboxylic O-H stretch), 1700 (carboxylic C=O stretch), 1654 (amide C=O stretch).

Elemental analysis: calculated for ($C_{19}H_{15}ClN_2O_3S$): C 58.99, H 3.91 and N 7.24, found for C 58.16, H 3.82 and N 7.10.

5-Benzyl-2-(2-(4-nitrophenyl)acetamido)thiazole-4-carboxylic acid (156):

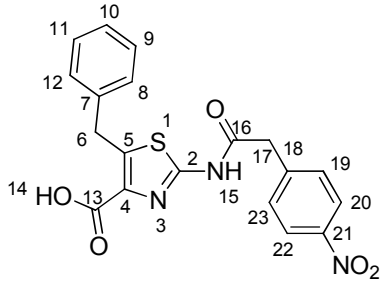

The title compound was obtained as a brown powder using general procedure C (30 mg, 40%).

m.p: 220 °C (with decomposition).

^{1}H NMR (DMSO-d_6): 3.91 (s, 2H, **H17**), 4.46 (s, 2H, **H6**), 7.26 (m, 5H, **H8-12**), 7.56 (d, *J* = 8.32 Hz, 2H, **H19, 23**), 8.17 (d, *J* = 8.32 Hz, 2H, **H20, 22**), 12.71 (s, 1H, **NH15**), 12.97 (bs, 1H, **OH14**).

^{13}C NMR (DMSO-d_6): 32.53 (**C6**), 41.05 (**C17**), 124.03-129.18 (**C7-12**), 129.32-132.96 (**C18-20, 22, 23**), 140.45-141.54 (**C4, 5**), 143.20 (**C21**), 159.85 (**C2**), 162.08 (**C16**), 169.19 (**C13**)

FTMS-ESI: calculated for $C_{19}H_{16}N_3O_5S$ (M+H) 398.0811, found 398.0852.

IR ν_{max} (cm^{-1}): 3442 (amide N-H stretch), 3189 (carboxylic O-H stretch), 1696 (carboxylic C=O stretch), 1675 (amide C=O stretch), 1559 (N=O stretch).

Elemental analysis: calculated for ($C_{19}H_{15}N_3O_5S$): C 57.42, H 3.80 and N 10.57, found for C 57.43, H 3.79 and N 10.48.

Methyl 5-benzyl-2-(2-cyclohexylacetamido)thiazole-4-carboxylate (157):

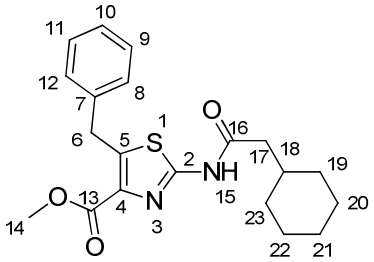

The title compound was obtained as an off-white powder using general procedure D after crystallization from hexane (250 mg, 82.9%).

m.p: 100-101 °C.

^{1}H NMR (DMSO-d_6): 0.90 (m, 2H, **H21**), 1.16-1.61 (m, 8H, **H19, 20, 22, 23**), 1.71 (m, 1H, **H18**), 2.24 (d, *J* = 7.04 Hz, 2H, **H17**), 3.81 (s, 3H, **H14**), 4.46 (s, 2H, **H6**), 7.30 (m, 5H, **H8-12**), 12.37 (s, 1H, **NH15**).

^{13}C NMR (DMSO-d_6): 26.07-32.87 (**C18-23**), 35.18 (**C17**), 43.05 (**C6**), 52.25 (**C14**), 127.26-135.12 (**C7-12**), 140.22 (**C5**), 142.41 (**C4**), 155.0 (**C2**), 163.08 (**C16**), 171.59 (**C13**).

FTMS-ESI: calculated for $C_{20}H_{25}N_2O_3S$ (M+H) 373.1586, found 373.1581.

IR ν_{max} (cm^{-1}): 3266 (amide N-H stretch), 1716 (ester C=O stretch), 1684 (amide C=O stretch).

Elemental analysis: calculated for ($C_{20}H_{24}N_2O_3S$): C 64.49, H 6.49 and N 7.52, found for C 64.36, H 6.27 and N 7.39.

5-Benzyl-2-(2-cyclohexylacetamido)thiazole-4-carboxylic acid (158):

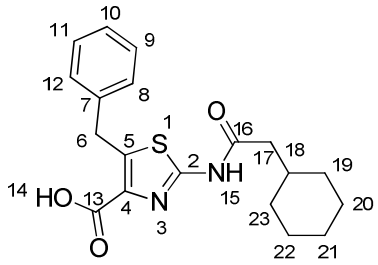

The title compound was obtained as a white powder using general procedure C (65 mg, 67.2%).

m.p: 260-261 °C.

^{1}H NMR (DMSO-d_6): 0.90 (m, 2H, **H21**), 1.13-1.59 (bs, 8H, **H19, 20, 22, 23**), 1.70 (bs, 1H, **H18**), 2.24 (d, *J* = 6.6 Hz, 2H, **H17**), 4.47 (s, 2H, **H6**), 7.30 (m, 5H, **H8-12**), 12.29 (s, 1H, **NH15**), 12.90 (s, 1H, **OH14**).

^{13}C NMR (DMSO-d_6): 26.07-33.09 (**C18-23**), 35.21 (C**17**), 43.03 (**C6**), 127.18-136.36 (**C7-12**), 140.50 (**C5**), 141.56 (**C4**), 154.67 (**C2**), 164.20 (**C16**), 171.53 (**C13**).

FTMS-ESI: calculated for $C_{19}H_{23}N_2O_3S$ (M+H) 359.1429, found 359.1424.

IR ν_{max} (cm^{-1}): 3427 (amide N-H stretch), 3186 (carboxylic O-H stretch), 1696 (carboxylic C=O stretch), 1665 (amide C=O stretch).

Elemental analysis: calculated for ($C_{19}H_{22}N_2O_3S$) C 63.66, H 6.19 and N 7.82, found for C 63.79, H 6.46 and N 7.78.

Methyl 2-(2-cyclohexylacetamido)-5-isopropylthiazole-4-carboxylate (159):

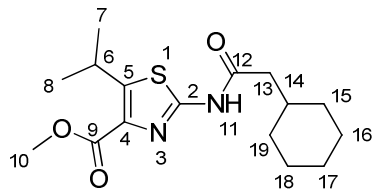

The title compound was obtained as white crystals using general procedure D and after crystallization from hexane (180 mg, 56%).

m.p: 130-132 °C.

^{1}H NMR (DMSO-*d*$_6$): 0.95 (m, 2H, **H17**), 1.18 (m, 4H, **H16, 18**), 1.26 (d, *J* = 7.04 Hz, 6H, **H7, 8**), 1.62 (m, 4H, **H15, 19**), 1.74 (m, 1H, **H14**), 2.28 (d, *J* = 7.04 Hz, 2H, **H13**), 3.78 (s, 3H, **H10**), 3.97 (septet, *J* = 6.4, 7.2 Hz, 1H, **H6**), 12.34 (s, 1H, **NH11**),

^{13}C NMR (DMSO-*d*$_6$): 25.15 (**C7, 8**), 26.10-32.89 (**C14-19**), 35.26 (**C6**), 43.09 (**C13**), 52.14 (**C10**), 133.98 (**C5**), 151.01 (**C4**), 154.11 (**C2**), 162.98 (**C12**), 171.52 (**C9**).

FTMS-ESI: calculated for $C_{16}H_{23}N_2O_3S$ (M-H) 323.1429, found 323.1434.

IR ν_{max} (cm^{-1}): 3427 (amide N-H stretch), 1723 (ester C=O stretch), 1687 (amide C=O stretch).

Elemental analysis: calculated for ($C_{16}H_{24}N_2O_3S$): C 59.23, H 7.46 and N 8.54, found for C 59.38, H 7.60 and N 8.54.

2-(2-Cyclohexylacetamido)-5-isopropylthiazole-4-carboxylic acid (160):

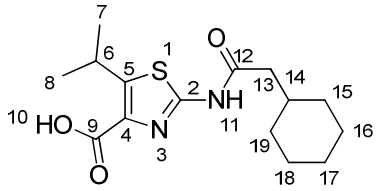

The title compound was obtained as a white powder using general procedure C (75 mg, 87.3%).

m.p: 220-221 °C.

^{1}H NMR (DMSO-*d*$_6$): 0.93 (m, 2H, **H17**), 1.15 (m, 4H, **H16, 18**), 1.25 (d, *J* = 6.6 Hz, 6H, **H7, 8**), 1.62 (m, 4H, **H15, 19**), 1.76 (m, 1H, **H14**), 2.28 (d, *J* = 7.48 Hz, 2H,

H13), 4.02 (septet, *J* = 7.04, 6.6, 7.04 Hz, 1H, **H6**), 12.25 (s, 1H, **NH11**), 12.77 (s, 1H, **OH10**).

^{13}C NMR (DMSO-*d*$_6$): 25.27 (**C7, 8**), 26.10-32.90 (**C14-19**), 35.30 (**C6**), 43.09 (**C13**), 135.19 (**C5**), 150.17 (**C4**), 153.73 (**C2**), 164.15 (**C12**), 171.45 (**C9**).

FTMS-ESI: calculated for $C_{15}H_{23}N_2O_3S$ (M+H) 311.1429, found 311.1428.

IR ν_{max} (cm^{-1}): 3435 (amide N-H stretch), 3190 (carboxylic O-H stretch), 1697 (carboxylic C=O stretch), 1671 (amide C=O stretch).

Elemental analysis: calculated for ($C_{15}H_{22}N_2O_3S$): C 58.04, H 7.14 and N 9.02, found for C 57.96, H 6.79 and N 8.75.

Methyl 2-(4-butoxybenzamido)-5-ethylthiazole-4-carboxylate (161):

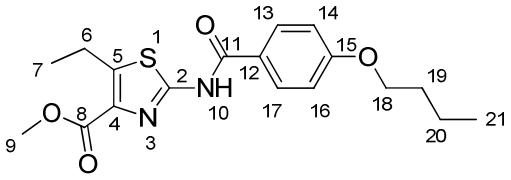

The title compound was obtained as a white powder using general procedure D after column chromatography with 20% ethyl acetate/hexane (160 mg, 41.2%).

m.p: 140-141 °C.

^{1}H NMR (DMSO-*d*$_6$): 0.93 (t, *J* = 7.48 Hz, 3H, **H21**), 1.26 (t, *J* = 7.48 Hz, 3H, **H7**), 1.42 (sextet, *J* = 7.48, 7.92, 7 Hz, 2H, **H20**), 1.71 (pentet, *J* = 6.6, 7.92 Hz, 2H, **H19**), 3.13 (q, *J* = 7.48, 7.48 Hz, 2H, **H6**), 3.81 (s, 3H, **H9**), 4.05 (t, *J* = 7.48, 2H, **H18**), 7.03 (d, *J* = 8.8 Hz, 2H, **H13, 17**), 8.08 (d, *J* = 8.8 Hz, 2H, **H14, 16**), 12.73 (s, 1H, **NH10**).

^{13}C NMR (DMSO-*d*$_6$): 14.22-20.45 (**C7, 19-21**), 31.14 (**C6**), 52.07 (**C9**), 68.12 (**C18**), 114.88-130.82 (**C12-14, 16, 17**), 134.88 (**C5**), 145.51 (**C4**), 155.10 (**C2**), 162.87 (**C15**), 162.99 (**C11**), 165.23 (**C8**).

FTMS-ESI: calculated for $C_{18}H_{21}N_2O_4S$ (M+H) 361.1222, found 361.1227.

IR ν_{max} (cm^{-1}): 3156 (amide N-H stretch), 1721 (ester C=O stretch), 1656 (amide C=O stretch).

Elemental analysis: calculated for ($C_{18}H_{20}N_2O_4S$): C 59.85, H 6.12 and N 7.73, found C 59.64, H 6.10 and N 7.56.

2-(4-Butoxybenzamido)-5-ethylthiazole-4-carboxylic acid (162):

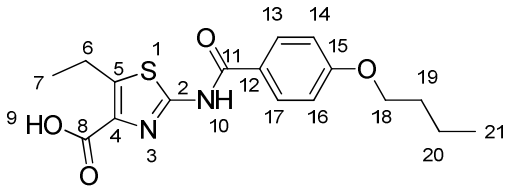

The title compound was obtained as a light brown powder using general procedure C (50 mg, 51%).

m.p: 262 °C (with decomposition).

^{1}H NMR (DMSO-d_6): 0.93 (t, *J* = 7.48 Hz, 3H, **H21**), 1.26 (t, *J* = 7.48 Hz, 3H, **H7**), 1.44 (m, 2H, **H20**), 1.71 (m, 2H, **H19**), 3.14 (m, 2H, **H6**), 4.05 (m, 2H, **H18**), 7.03 (d, *J* = 8 Hz, 2H, **H13, 17**), 8.02 (d, *J* = 8 Hz, 2H, **H14, 16**), 12.74 (s, 1H, **NH10**).

^{13}C NMR (DMSO-d_6): 14.23-20.51 (**C7, 19-21**), 31.14 (**C6**), 68.11 (**C18**), 114.85-130.81 (**C12-14, 16, 17**), 136.12 (**C5**), 144.65 (**C4**), 154.73 (**C2**), 162.81 (**C18**), 164.14 (**C11**), 165.20 (**C8**).

FTMS-ESI: calculated for $C_{17}H_{21}N_2O_4S$ (M+H) 349.1222, found 349.1226.

IR ν_{max} (cm^{-1}): 3435 (amide N-H stretch), 3181 (carboxylic O-H stretch), 1669 (carboxylic C=O stretch), 1606 (amide C=O stretch).

Elemental analysis: calculated for ($C_{17}H_{20}N_2O_4S$): C 58.60, H 5.79 and N 8.04, found for C 58.77, H 5.70 and N 7.72.

Methyl 2-(4-butoxybenzamido)-5-propylthiazole-4-carboxylate (163):

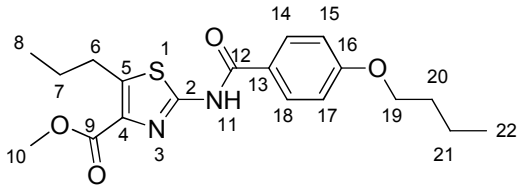

The title compound was obtained as a white powder using general procedure D after column chromatography with 20% ethyl acetate/hexane (170 mg, 45%).

m.p: 102-104 °C.

^{1}H NMR (DMSO-d_6): 0.94 (m, 6H, **H8, 22**), 1.42 (sextet, *J* = 7.48, 8, 7.48 Hz, 2H, **H21**), 1.69 (m, 4H, **H7, 20**), 3.10 (t, *J* = 7.24, 7.72 Hz, 2H, **H6**), 3.79 (s, 3H, **H10**), 4.07 (t, *J* = 6.6, 6.16 Hz, 2H, **H19**), 7.03 (d, *J* = 8.8 Hz, 2H, **H14, 18**), 8.10 (d, *J* = 8.8 Hz, 2H, **H15, 17**), 12.79 (bs, 1H, **NH11**).

^{13}C NMR (DMSO-d_6): 14.19-28.62 (**C7, 8, 20-22**), 31.17 (**C6**), 51.97 (**C10**), 68.08 (**C19**), 114.77-131.62 (**C13-15, 17, 18**), 134.05 (**C5**), 135.27 (**C4**), 148.18 (**C2**), 162.52 (**C16**), 162.62 (**C12**), 163.16 (**C9**).

FTMS-ESI: calculated for $C_{19}H_{25}N_2O_4S$ (M+H) 377.1535, found 377.1531.

IR ν_{max} (cm^{-1}): 3436 (amide N-H stretch), 1725 (ester C=O stretch), 1655 (amide C=O stretch).

Elemental analysis: calculated for ($C_{19}H_{24}N_2O_4S$): C 60.62, H 6.43 and N 7.44, found for C 60.61, H 6.22 and N 7.69.

2-(4-Butoxybenzamido)-5-propylthiazole-4-carboxylic acid (164):

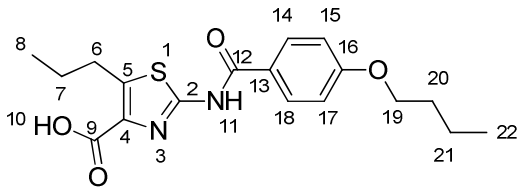

The title compound was obtained as a light brown powder using general procedure C after crystallization from methanol (70 mg, 73%).

m.p: 280 °C (with decomposition).

^{1}H NMR (DMSO-*d*$_6$): 0.94 (dt, *J* = 7.28, 7.48, 2.16 Hz, 6H, **H8, 22**), 1.45 (sextet, *J* = 7.48, 7.48 Hz, 2H, **H21**), 1.69 (m, 4H, **H7, 20**), 3.11 (t, *J* = 7.48 Hz, 2H, **H6**), 4.06 (t, *J* = 6.6 Hz, 2H, **H19**), 7.04 (d, *J* = 8.76 Hz, 2H, **H14, 18**), 8.08 (d, *J* = 8.76 Hz, 2H, **H15, 17**), 12.75 (bs, 2H, **NH11, OH10**).

^{13}C NMR (DMSO-*d*$_6$): 14.19-19.24 (**C7, 8, 20-22**), 31.15 (**C6**), 68.12 (**C19**), 114.86-130.82 (**C13-15, 17, 18**), 136.38 (**C5**), 142.38 (**C4**), 154.92 (**C2**), 162.80 (**C16**), 164.20 (**C12**), 165.28 (**C9**).

FTMS-ESI: calculated for $C_{18}H_{23}N_2O_4S$ (M+H) 363.1379, found 363.1373.

IR ν_{max} (cm^{-1}): 3435 (amide N-H stretch), 3190 (carboxylic O-H stretch), 1665 (carboxylic C=O stretch), 1607 (amide C=O stretch).

Elemental analysis: calculated for ($C_{18}H_{22}N_2O_4S$): C 59.65, H 6.12 and N 7.73, found for C 59.10, H 5.93 and N 7.4.

Methyl 2-(4-butoxybenzamido)-5-butylthiazole-4-carboxylate (165):

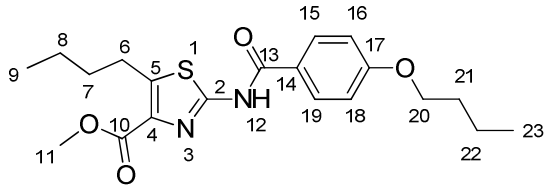

The title compound was obtained as a white powder using general procedure D after column chromatography with 20% ethyl acetate/hexane (270 mg, 74.4%).

m.p: 73-74 °C.

^{1}H NMR (DMSO-*d*$_6$): 0.93 (m, 6H, **H9, 23**), 1.33 (sextet, *J* = 7.56, 7.44, 7.24 Hz, 2H, **H8**), 1.45 (sextet, *J* = 7.36, 7.6, 7.52 Hz, **H22**), 1.62 (p, *J* = 7.32, 7.6, 7.32 Hz, 2H, **H21**), 1.72 (p, *J* = 6.64, 7.24, 7.70 Hz, 2H, **H7**), 3.13 (t, *J* = 7.48, 7.68 Hz, 2H,

H6), 3.81 (s, 3H, **H11**), 4.06 (t, *J* = 7.32 Hz, 2H, **H20**), 7.06 (d, *J* = 8.88 Hz, 2H, **H15, 19**), 8.08 (d, *J* = 8.84 Hz, 2H, **H16, 18**), 12.69 (s, 1H, **NH12**).

^{13}C NMR (DMSO-*d*$_6$): 14.18-31.15 (**C7-9, 21-23**), 33.68 (**C6**), 52.06 (**C11**), 68.14 (**C20**), 114.90-130.83 (**C14-16, 18, 19**), 135.29 (**C5**), 143.85 (**C4**), 155.22 (**C2**), 162.88 (**C17**), 163.04 (**C13**), 165.25 (**C10**).

FTMS-ESI: calculated for $C_{20}H_{25}N_2O_4S$ (M-H) 389.1535, found 389.1540.

IR ν_{max} (cm^{-1}): 3453 (amide N-H stretch), 1716 (ester C=O stretch), 1668 (amide C=O stretch).

Elemental analysis: calculated for ($C_{20}H_{26}N_2O_4S$) C 61.52, H 6.71 and N 7.17, found for C 61.36, H 7.02 and N 6.93.

2-(4-Butoxybenzamido)-5-butylthiazole-4-carboxylic acid (166):

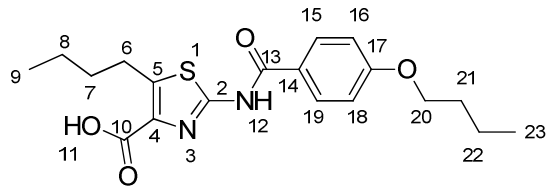

The title compound was obtained as a white powder using general procedure C (56 mg, 58.2%).

m.p: 275 °C (with decomposition)

^{1}H NMR (DMSO-*d*$_6$): 0.93 (m, 6H, **H9, 23**), 1.37 (sextet, *J* = 4.4, 7.92, 7.04 Hz, 2H, **H8**), 1.45 (sextet, *J* = 7.04, 7.48, 7.48 Hz, 2H, **H22**), 1.62 (p, *J* = 7.48, 7.48 Hz, 2H, **H21**), 1.72 (p, *J* = 6.6, 7.04, 7.92 Hz, 2H, **H7**), 3.13 (t, *J* = 7.48 Hz, 2H, **H6**), 4.06 (t, *J* = 6.6 Hz, 2H, **H20**), 7.04 (d, *J* = 8.76 Hz, 2H, **H15, 19**), 8.10 (d, *J* = 8.76 Hz, 2H, **H16, 18**), 12.65 (bs, 1H, **NH12**), 12.77 (bs, 1H, **OH11**).

^{13}C NMR (DMSO-*d*$_6$): 14.24-31.32 (**C7-9, 21-23**), 32.22 (**C6**), 68.12 (**C20**), 114.88-130.82 (**C14-16, 18, 19**), 136.53 (**C5**), 142.91 (**C4**), 157.78 (**C2**), 162.45 (**C17**), 164.18 (**C13**), 165.52 (**C10**).

FTMS-ESI: calculated for $C_{19}H_{25}N_2O_4S$ (M+H) 377.1535, found 377.1530.

IR ν_{max} (cm^{-1}): 3441 (amide N-H stretch), 3186 (carboxylic O-H stretch), 1669 (amide C=O stretch), 1657 (carboxylic C=O stretch).

Elemental analysis: calculated for ($C_{19}H_{24}N_2O_4S$): C 60.62, H 6.43 and N 7.44, found for C 60.31, H 6.14 and N 7.19.

Methyl 2-(4-butoxybenzamido)-5-phenylthiazole-4-carboxylate (167):

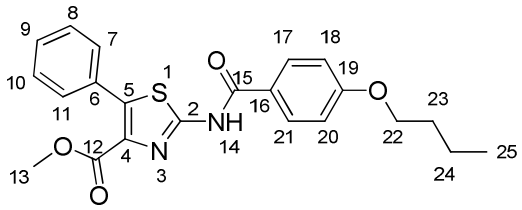

The title compound was obtained as a light brown powder using general procedure D after column chromatography with 20% ethyl acetate/hexane (120 mg, 34.4%).

m.p: 95-96 °C.

^{1}H NMR (DMSO-d_6): 0.94 (t, *J* = 7.04, 7.48 Hz, 3H, **H25**), 1.45 (sextet, *J* = 7.04, 7.48 Hz, 2H, **H24**), 1.72 (p, *J* = 6.6, 7.04 Hz, 2H, **H23**), 3.70 (s, 3H, **H13**), 4.07 (t, *J* = 6.16 Hz, 2H, **H22**), 7.07 (d, *J* = 8.36 Hz, 2H, **H17, 21**), 7.44 (bs, 3H, **H8-10**), 7.52 (bs, 2H, **H7, 11**), 8.11 (*J* = 8.36 Hz, 2H, **H18, 20**), 12.90 (s, 1H, **NH14**).

^{13}C NMR (DMSO-d_6): 14.24-31.15 (**C23-25**), 52.19 (**C13**), 68.16 (**C22**), 114.94-130.29 (**C6-11**), 130.93-131.89 (**C16-18, 20, 21**), 135.01 (**C5**), 139.14 (**C4**), 157.11 (**C2**), 162.90 (**C19**), 165.52 (**C15**), 175.30 (**C12**).

FTMS-ESI: calculated for $C_{22}H_{23}N_2O_4S$ (M+H) 411.1379, found 411.1378.

IR ν_{max} (cm^{-1}): 3468 (amide N-H stretch), 1718 (ester C=O stretch), 1668 (amide C=O stretch).

Elemental analysis: calculated for ($C_{22}H_{22}N_2O_4S$): C 64.37, H 5.40 and N 6.82, found for C 64.32, H 5.34 and N 6.31.

2-(4-Butoxybenzamido)-5-phenylthiazole-4-carboxylic acid (168):

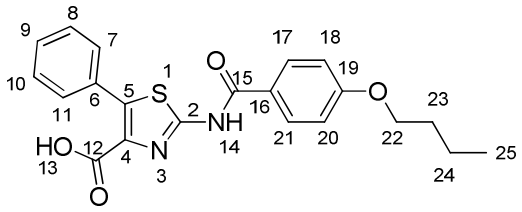

The title compound was obtained as a light brown powder using general procedure C (62 mg, 75%).

m.p: 241-243°C.

^{1}H NMR (DMSO-*d*$_6$): 0.94 (t, *J* = 7.04, 7.48 Hz, 3H, **H25**), 1.44 (sextet, *J* = 7.48, 7.48, 7.04 Hz, 2H, **H24**), 1.73 (p, *J* = 7.04, 7.48 Hz, 2H, **H23**), 4.08 (q, *J* = 6, 6.76 Hz, 2H, **H22**), 7.06 (d, *J* = 8.8 Hz, 2H, **H17, 21**), 7.43 (m, 3H, **H8-10**), 7.52 (d, *J* = 7.04 Hz, 2H, **H7, 11**), 8.12 (d, *J* =8.36 Hz, 2H, **H18, 20**), 12.85 (s, 1H, **NH14**).

^{13}C NMR (DMSO-*d*$_6$): 14.24-31.52 (**C23-25**), 68.16 (**C22**), 114.95-131.34 (**C6-11, 16-18, 20, 21**), 137.21 (**C5**), 138.54 (**C4**), 156.67 (**C2**), 162.97 (**C19**), 164.03 (**C15**), 166.54 (**C12**).

FTMS-ESI: calculated for $C_{21}H_{21}N_2O_4S$ (M+H) 397.1222, found 397.1217.

IR ν_{max} (cm^{-1}): 3179 (amide N-H stretch), 2957 (carboxylic O-H stretch), 1676 (carboxylic C=O stretch), 1652 (amide C=O stretch).

Elemental analysis: calculated for ($C_{21}H_{20}N_2O_4S.2H_2O$): C 58.32, H 5.58 and N 6.48, found for C 58.31, H 5.28 and N 6.35.

Methyl 5-benzyl-2-(4-chlorobenzamido)thiazole-4-carboxylate (169):

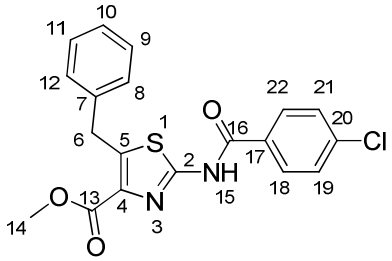

The title compound was obtained as white crystals using general procedure D after column chromatography with chloroform (160 mg, 51.3%).

m.p: 224-226 °C.

^{1}H NMR (DMSO-d_6): 3.84 (s, 3H, **H14**), 4.52 (s, 2H, **H6**), 7.25 (m, 1H, **H10**), 7.34 (m, 4H, **H8, 9, 11, 12**), 7.60 (dd, *J* = 7.04, 1.76 Hz, 2H, **H18, 22**), 8.07 (dd, *J* = 6.98, 2.2 Hz, 2H, **H19, 21**), 13.01 (s, 1H, **NH15**).

^{13}C NMR (DMSO-d_6): 32.50 (**C6**), 52.27 (**C14**), 127.31-135.49 (**C7-12, 17-19, 21, 22**), 138.28 (**C5**), 140.20 (**C4**), 143.09 (**C20**), 155.71 (**C2**), 163.05 (**C16**), 165.02 (**C13**).

FTMS-ESI: calculated for $C_{19}H_{14}ClN_2O_3S$ (M-H) 385.0414, found 385.0419.

IR ν_{max} (cm^{-1}): 3447-3063 (amide N-H stretch), 1720 (ester C=O stretch), 1666 (amide C=O stretch).

Elemental analysis: calculated for ($C_{19}H_{15}ClN_2O_3S$): C 58.99, H 3.91 and N 9.16, found for C 59.80, H 3.77 and N 8.72.

5-Benzyl-2-(4-chlorobenzamido)thiazole-4-carboxylic acid (170):

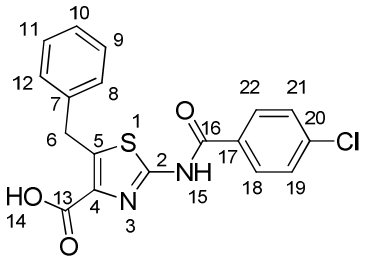

The title compound was obtained as a white powder using general procedure C (75 mg, 77.4%).

m.p: 305 °C (with decomposition).

^{1}H NMR (DMSO-d_6): 4.52 (s, 2H, **H6**), 7.24 (m, 1H, **H10**), 7.32 (m, 4H, **H8, 9, 11, 12**), 7.59 (d, *J* = 8.36 Hz, 2H, **H18, 22**), 8.08 (d, *J* = 8.36 Hz, 2H, **H19, 21**). 12.99 (bs, 2H, **NH15, OH14**).

^{13}C NMR (DMSO-d_6): 32.56 (**C6**), 127.23-136.77 (**C7-12, 17-19, 21, 22**), 138.21 (**C5**), 140.49 (**C4**), 142.18 (**C20**), 155.39 (**C2**), 164.18 (**C16**), 165.0 (**C13**).

FTMS-ESI: calculated for $C_{18}H_{14}ClN_2O_3S$ (M+H) 373.0414, found 373.0408.

IR ν_{max} (cm^{-1}): 3418-3189 (amide N-H stretch), 3062 (carboxylic O-H stretch), 1674 (carboxylic C=O stretch), 1596 (amide C=O stretch).

Elemental analysis: calculated for $C_{18}H_{13}ClN_2O_3S.H_2O$: C 55.31, H 3.87 and N 7.17, found for C 55.35, H 3.72 and N 6.87.

Methyl 5-isopropyl-2-(4-methoxybenzamido)thiazole-4-carboxylate (171):

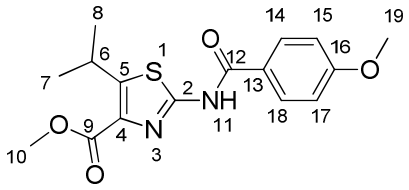

The title compound was obtained as a pale yellow powder using general procedure D after column chromatography with 20 % ethyl acetate/hexane (160 mg, 50.7%).

m.p: 82-83 °C.

^{1}H NMR (DMSO-d_6): 1.32 (d, *J* = 6.6 Hz, 6H, **H7, 8**), 3.81 (s, 3H, **H19**), 3.84 (s, 3H, **H10**), 4.02 (m, 1H, **H6**), 7.08 (d, *J* = 8.8 Hz, 2H, **H14, 18**), 8.12 (d, *J* = 8.8 Hz, 2H, **H15, 17**), 12.69 (s, 1H, **NH11**).

^{13}C NMR (DMSO-d_6): 25.19-27.51 (**C6-8**), 52.32 (**C19**), 56.23 (**C10**), 114.52-130.82 (**C13-15, 17, 18**), 134.21 (**C5**), 151.36 (**C4**), 155.11 (**C2**), 163.04 (**C16**), 163.40 (**C12**), 165.24 (**C9**).

FTMS-ESI: calculated for $C_{16}H_{19}N_2O_4S$ (M+H) 335.1066, found 335.1061.

IR ν_{max} (cm^{-1}): 3211 (amide N-H stretch), 1721 (ester C=O stretch), 1667 (amide C=O stretch).

Elemental analysis: calculated for ($C_{16}H_{18}N_2O_4S$): C 57.47, H 4.43 and N 8.38, found for C 57.14, H 5.27 and N 8.43.

5-Isopropyl-2-(4-methoxybenzamido)thiazole-4-carboxylic acid (172):

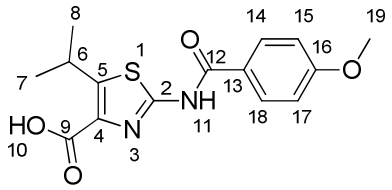

The title compound was obtained as white flakes using general procedure C (45 mg, 46.9%).

m.p: 250 °C (with decomposition).

^{1}H NMR (DMSO-d_6): 1.29 (d, *J* = 7.04 Hz, 6H, **H7, 8**), 3.84 (s, 3H, **H19**), 4.07 (septet, *J* = 6.6, 7.08, 7 Hz, 1H, **H6**), 7.08 (d, *J* = 8.76 Hz, 2H, **H14, 18**), 8.12 (d, *J* = 8.8 Hz, 2H, **H15, 17**), 12.66 (bs, 1H, **NH11**), 12.81 (bs, 1H, **OH10**).

^{13}C NMR (DMSO-d_6): 25.19-27.51 (**C6-8**), 56.10 (**C19**), 114.49-130.81 (**C13-15, 17, 18**), 135.46 (**C5**), 150.48 (**C4**), 154.75 (**C2**), 163.34 (**C16**), 164.21 (**C12**), 165.21 (**C9**).

FTMS-ESI: calculated for $C_{15}H_{17}N_2O_4S$ (M+H) 321.0909, found 321.0902.

IR ν_{max} (cm^{-1}): 3419-3190 (amide N-H stretch), 2962 (carboxylic O-H stretch), 1671 (carboxylic C=O stretch), 1647 (amide C=O stretch).

Elemental analysis: calculated for ($C_{15}H_{16}N_2O_4S$): C 56.24, H 5.03 and N 8.74, found for C 55.94, H 4.98 and N 8.39.

Methyl 2-(4-chlorobenzamido)-5-isopropylthiazole-4-carboxylate (173):

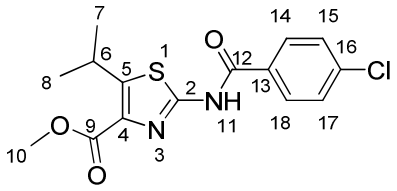

The title compound was obtained as a white powder using general procedure D after column chromatography with chloroform (160 mg, 55.6%).

m.p: 142-144 °C.

^{1}H NMR (DMSO-*d*$_6$): 1.32 (d, *J* = 6.96 Hz, 6H, **H7, 8**), 3.81 (s, 3H, **H10**), 4.02 (septet, *J* = 6.6, 6.96 Hz, 1H, **H6**), 7.63 (d, *J* = 8.8 Hz, 2H, **H14, 18**), 8.10 (d, *J* = 8.8 Hz, 2H, **H15, 17**).

^{13}C NMR (DMSO-*d*$_6$): 25.19-27.55 (**C6-8**), 52.16 (**C10**), 129.33-130.85 (**C13-15, 17, 18**), 141.27 (**C16**), 143.71 (**C5**), 162.49 (**C2**), 165.01 (**C12**), 175.39 (**C9**).

FTMS-ESI: calculated for $C_{15}H_{14}ClN_2O_3S$ (M-H) 337.0414, found 337.0419.

IR ν_{max} (cm^{-1}): 3400-3244 (amide N-H stretch), 1721 (ester C=O stretch), 1670 (amide C=O stretch), 1325 (C-Cl stretch).

Elemental analysis: calculated for ($C_{15}H_{15}ClN_2O_3S$): C 53.17, H 4.46 and N 8.27, found for C 52.88, H 4.21 and N 7.93.

***N*-(2-(1*H*-Indol-3-yl)ethyl)-5-aminothiophene-2-carboxamide (180):**

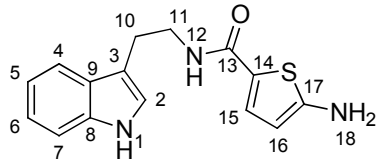

The title compound was obtained as a dark brown powder using general procedure K (75 mg, 82.2%).

m.p: 190-191 °C.

^{1}H NMR (DMSO-*d*$_6$): 2.87 (t, *J* = 7.94 Hz, 2H, **H10**), 3.43 (q, *J* = 6.64, 8.01 Hz, 2H, **H11**), 6.17 (bs, 2H, **NH18**), 6.97 (m, *J* = 6.96 Hz, 1H, **H5**), 7.04 (t, *J* = 6.96, 8.08 Hz, 1H, **H6**), 7.15 (d, *J* = 2.04 Hz, 1H, **H2**), 7.25 (d, *J* = 5.96 Hz, 1H, **H15**), 7.32 (m, 2H, **H4, 16**), 7.55 (d, *J* = 7.96 Hz, 1H, **H7**), 8.03 (m, 1H, **NH12**), 10.80 (s, 1H, **NH1**).

^{13}C NMR (DMSO-*d*$_6$): 26.19 (**C10**), 31.27 (**C11**), 104.30-123.09 (**C2-7**), 127.-129.35 (**C8, 9**), 136.79-150.05 (**C14-17**), 162.42 (**C13**).

FTMS-ESI: calculated for $C_{15}H_{16}N_3OS$ (M+H) 286.1014, found 286.10086.

IR ν_{max} (cm^{-1}): 3407 (amide N-H stretch), 3295 (indole N-H stretch), 1610 (amide C=O stretch).

Elemental analysis: calculated for ($C_{15}H_{15}N_3OS$): C 63.13, H 5.30 and N 14.73, found for C 62.86, H 5.62 and N 13.62.

(*S*)-methyl 3-(1*H*-indol-3-yl)-2-(thiophene-2-carboxamido)propanoate (181):

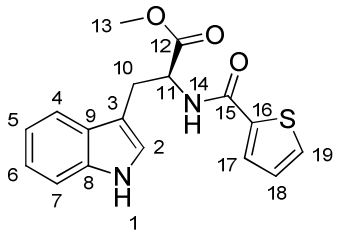

The title compound was obtained as orange crystals using general procedure J (180 mg, 57.5%).

m.p: 78-80 °C.

^{1}H NMR (DMSO-*d*$_6$): 3.19-3.26 (m, 2H, **H10**), 3.63 (s, 3H, **H13**), 4.65 (m, 1H, **H11**), 6.98 (t, *J* = 7.92 Hz, 1H, **H5**), 7.06 (t, *J* = 7.04, 7.92 Hz, 1H, **H6**), 7.15 (t, *J* = 4.84, 3.88 Hz, 1H, **H18**), 7.19 (d, *J* = 2.2 Hz, 1H, **H2**), 7.32 (d, *J* = 7.92 Hz, 1H, **H4**), 7.55 (d, *J* = 7.92 Hz, 1H, **H7**), 7.76 (d, *J* = 5.04 Hz, 1H, **H17**), 7.84 (d, *J* = 3.96 Hz, 1H, **H19**), 8.84 (d, *J* = 7.88 Hz, 1H, **NH14**), 10.85 (s, 1H, **NH1**).

^{13}C NMR (DMSO-*d*$_6$): 27.26 (**C10**), 52.53 (**C11**), 54.23 (**C13**), 110.40-124.22 (**C2-7**), 127.59-128.49 (**C8, 9**), 129.31-139.65 (**C16-19**), 161.78 (**C15**), 172.99 (**C12**).

FTMS-ESI: calculated for $C_{17}H_{15}N_2O_3S$ (M-H) 327.0803, found 327.0808.

IR ν_{max} (cm^{-1}): 3401 (amide N-H stretch), 3310 (indole N-H stretch), 1735 (ester C=O stretch), 1635 (amide C=O stretch).

Elemental analysis: calculated for ($C_{17}H_{16}N_2O_3S$): C 62.18, H 4.91 and N 8.53, found for C 62.54, H 5.09 and N 8.31.

***N*-(2-(1*H*-Indol-3-yl)ethyl)-4-nitrobenzamide (183):**

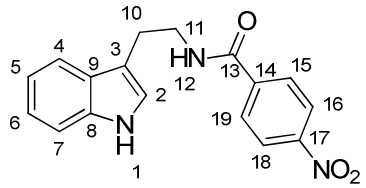

The title compound was obtained as a bright orange powder using general procedure D (290 mg, 75%).

m.p: 192-193 °C.

^{1}H NMR (DMSO-*d*$_6$): 2.97 (t, *J* = 7.48, 7.44 Hz, 2H, **H10**), 3.58 (q, *J* = 6.6, 7.44 Hz, 2H, **H11**), 6.98 (t, *J* = 7.48 Hz, 1H, **H5**), 7.06 (t, *J* = 7.04, 7.88 Hz, 1H, **H6**), 7.19 (d, *J* = 1.32 Hz, 1H, **H2**), 7.33 (d, *J* = 7.92 Hz, 1H, **H4**), 7.58 (d, *J* = 7.44 Hz, 1H, **H7**), 8.08 (d, *J* = 8.8 Hz, 2H, **H15, 19**), 8.30 (d, *J* = 8.8 Hz, 2H, **H16, 18**), 8.94 (t, *J* = 4.84, 5.72 Hz, 1H, **NH12**), 10.81 (s, 1H, **NH1**).

^{13}C NMR (DMSO-*d*$_6$): 25.54 (**C10**), 41.32 (**C11**), 111.95-123.24 (**C2-7**), 124.08 - 140.90 (**C8, 9, 14-16, 18, 19**), 149.51 (**C17**), 165.04 (**C13**).

FTMS-ESI: calculated for $C_{17}H_{14}N_3O_3$ (M-H) 308.1035, found 308.1040.

IR ν_{max} (cm^{-1}): 3434 (amide N-H stretch), 3271 (indole N-H stretch), 1653 (amide C=O stretch), 1601 (N=O stretch).

Elemental analysis: calculated for ($C_{17}H_{15}N_3O_3$): C 66.01, H 4.89 and N 13.58, found for C 65.80, H 4.97 and N 13.88.

***N*-(2-(1*H*-Indol-3-yl)ethyl)-3-nitrobenzamide (184):**

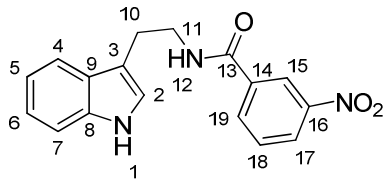

The title compound was obtained as an orange powder using general procedure D (317 mg, 82.2%).

m.p: 140-141 °C.

^{1}H NMR (DMSO-d_6): 2.98 (t, *J* = 7.48, 7.04 Hz, 2H, **H10**), 3.59 (q, *J* = 7.0, 6.16, 7.04 Hz, 2H, **H11**), 6.98 (t, *J* = 7.04 Hz, 1H, **H5**), 7.06 (t, *J* = 7.88, 7.04 Hz, 1H, **H6**), 7.19 (d, *J* = 0.88Hz, 1H, **H2**), 7.33 (d, *J* = 7.48 Hz, 1H, **H4**), 7.59 (d, *J* = 7.88 Hz, 1H, **H7**), 7.78 (t, *J* = 7.92 Hz, 1H, **H18**), 8.30 (d, *J* = 8.36 Hz, 1H, **H19**), 8.36 (d, *J* = 8.36 Hz, 1H, **H17**), 8.65 (s, 1H, **H15**), 9.00 (t, *J* = 5.72, 5.28 Hz, 1H, **NH12**), 10.82 (s, 1H, **NH1**).

^{13}C NMR (DMSO-d_6): 25.56 (**C10**), 41.02 (**C11**), 111.96-122.45 (**C2-7**), 126.31 - 130.67 (**C8, 9**), 134.20-136.82 (**C14, 15, 17-19**), 153.43 (**C16**), 164.53 (**C13**).

FTMS-ESI: calculated for $C_{17}H_{16}N_3O_3$ (M+H) 310.1192, found 310.1186.

IR ν_{max} (cm^{-1}): 3410 (amide N-H stretch), 3281 (indole N-H stretch), 1650 (amide C=O stretch), 1517 (N=O stretch).

Elemental analysis: calculated for ($C_{17}H_{15}N_3O_3$): C 66.01, H 4.89 and N 13.58, found for C 65.56, H 4.82 and N 13.34.

***N*-(2-(1*H*-Indol-3-yl)ethyl)-2-nitrobenzamide (185):**

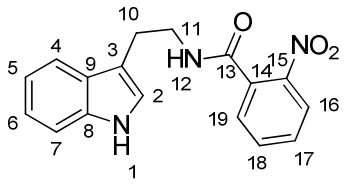

The title compound was obtained as orange crystals using general procedure D after column chromatography with 5% methanol/DCM (200 mg, 53%).

m.p: 63-64 °C.

^{1}H NMR (DMSO-*d*$_6$): 2.94 (t, *J* = 7.44, 7.04 Hz, 2H, **H10**), 3.51 (q, *J* = 7.04, 6.6 Hz, 2H, **H11**), 6.99 (t, *J* = 7.92, 7.04 Hz, 1H, **H5**), 7.09 (t, *J* = 8.32, 7.04 Hz, 1H, **H6**), 7.21 (d, *J* = 1.8 Hz, 1H, **H2**), 7.35 (d, *J* = 7.92 Hz, 1H, **H4**), 7.56 (m, 2H, **H7, 19**), 7.67 (t, *J* = 7.76, 7.64 Hz, 1H, **H18**), 7.76 (t, *J* = 7.78 Hz, 1H, **H17**), 8.01 (d, *J* = 7.85 Hz, 1H, **H16**), 8.79 (t, *J* = 5.28 Hz, 1H, **NH12**), 10.83 (s, 1H, **NH1**).

^{13}C NMR (DMSO-*d*$_6$): 25.32 (**C10**), 41.03 (**C11**), 101.87-118.80 (**C2-7**), 123.34-147.72 (**C14, 16-19**), 153.09 (**C15**), 165.88 (**C13**).

FTMS-ESI: calculated for $C_{17}H_{14}N_3O_3$ (M-H) 308.1035, found 308.1040.

IR ν_{max} (cm^{-1}): 3399 (amide N-H stretch), 3277 (indole N-H stretch), 1645 (amide C=O stretch), 1527 (N=O stretch).

Elemental analysis: calculated for ($C_{17}H_{15}N_3O_3$): C 66.01, H 4.89 and N 13.58, found for C 65.72, H 4.83 and N 13.3.

(*R*)-Methyl 3-(1*H*-indol-3-yl)-2-(5-nitrothiophene-2-carboxamido)propanoate (186):

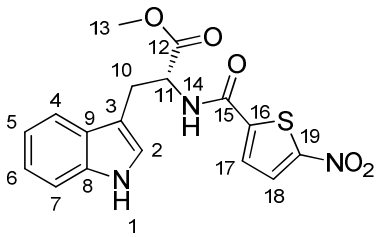

The title compound was obtained as a bright yellow powder using general procedure J (270 mg, 92%).

m.p: 94-95 °C.

^{1}H NMR (DMSO-*d*$_6$): 3.20-3.28 (m, 2H, **H10**), 3.65 (s, 3H, **H13**), 4.68 (m, 1H, **H11**), 6.96 (t, *J* = 7.92, 7.04 Hz, 1H, **H5**), 7.06 (t, *J* = 7.04, 7.88 Hz, 1H, **H6**), 7.19 (d, *J* = 2.16 Hz, 1H, **H2**), 7.34 (d, *J* = 8.02 Hz, 1H, **H4**), 7.54 (d, *J* = 7.92 Hz, 1H, **H7**), 7.89 (d, *J* = 4.4 Hz, 1H, **H17**), 8.13 (d, *J* = 4.4 Hz, 1H, **H18**), 9.40 (d, *J* = 6.48 Hz, 1H, **NH14**), 10.86 (s, 1H, **NH1**).

^{13}C NMR (DMSO-*d*$_6$): 27.18 (**C10**), 52.72 (**C11**), 54.57 (**C13**), 110.08-127.54 (**C2-7**), 128.60-145.78 (**C8, 9, 16-18**), 153.77 (**C19**), 160.24 (**C15**), 172.37 (**C12**).

FTMS-ESI: calculated for $C_{17}H_{14}N_2O_5S$ (M-H) 372.0654, found 372.0659.

IR ν_{max} (cm^{-1}): 3560 (amide N-H stretch), 3415 (indole N-H stretch), 1725 (ester C=O stretch), 1649 (amide C=O stretch), 1544 (N=O stretch).

Elemental analysis: calculated for $C_{17}H_{15}N_2O_5S.H_2O$: C 51.17, H 4.38 and N 10.74, found for C 51.13, H 4.08 and N 10.72.

***N*-(2-(5-Hydroxy-1*H*-indol-3-yl)ethyl)-5-nitrothiophene-2-carboxamide (187):**

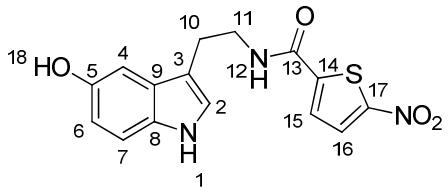

The title compound was obtained as an orange powder using general procedure J (100 mg, 38.4%).

m.p: 110-112 °C.

^{1}H NMR (DMSO-*d*$_6$): 2.86 (t, *J* = 7.48 Hz, 2H, **H10**), 3.51 (q, *J* = 6.6, 7.48 Hz, 2H, **H11**), 6.60 (dd, *J* = 2.2, 8.36 Hz, 1H, **H6**), 6.86 (d, *J* = 2.2 Hz, 1H, **H4**), 7.07 (d, *J* =

1.32 Hz, 1H, **H2**), 7.11 (d, *J* = 8.38 Hz, 1H, **H7**), 7.79 (d, *J* = 4.4 Hz, 1H, **H15**), 8.15 (d, *J* = 4.4 Hz, 1H, **H16**), 8.63 (bs, 1H, **OH18**), 9.13 (t, *J* = 5.28, 5.72 Hz, 1H, **NH12**), 10.52 (s, 1H, **NH1**).

^{13}C NMR (DMSO-*d*$_6$): 25.66 (**C10**), 41.32 (**C11**), 102.74-127.66 (**C2-4, 6, 7**), 128.41-147.34 (**C8, 9, 14-16**), 150.82 (**C17**), 153.32 (**C5**), 159.93 (**C13**).

FTMS-ESI: calculated for $C_{15}H_{12}N_3O_4S$ (M-H) 330.0549, found 330.0554.

IR ν_{max} (cm^{-1}): 3428 (amide N-H stretch), 3329 (indole N-H stretch), 3029 (O-H stretch), 1618 (amide C=O stretch), 1567 (N=O stretch).

Elemental analysis: calculated for ($C_{15}H_{13}N_3O_4S$): C 54.37, H 3.95 and N 12.68, found for C 53.93, H 4.01 and N 12.24.

***N*-(2-(5-Methoxy-1*H*-indol-3-yl)ethyl)-5-nitrothiophene-2-carboxamide (188):**

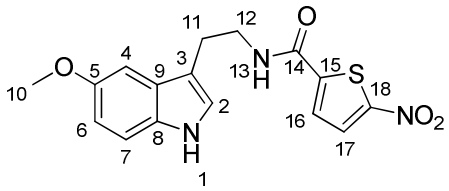

The title compound was obtained as dark orange crystals using general procedure J (200 mg, 77.8%).

m.p: 154-155 °C.

^{1}H NMR (DMSO-*d*$_6$): 2.93 (t, *J* = 7.48 Hz, 2H, **H11**), 3.54 (q, *J* = 6.6, 7.48 Hz, 2H, **H12**), 3.72 (s, 3H, **H10**), 6.72 (dd, *J* = 2.64, 8.8 Hz, 1H, **H6**), 7.03 (d, *J* = 2.2 Hz, **H4**), 7.14 (d, *J* = 2.2 Hz, 1H, **H2**), 7.24 (d, *J* = 8.8 Hz, 1H, **H7**), 7.78 (d, *J* = 4.44 Hz, 1H, **H16**), 8.14 (d, *J* = 4.44 Hz, 1H, **H17**), 9.13 (t, *J* = 6.32 Hz, 1H, **NH13**), 10.68 (s, 1H, **NH1**).

^{13}C NMR (DMSO-*d*$_6$): 25.48 (**C11**), 41.23 (**C12**), 55.83 (**C10**), 100.59-124.02 (**C2-4, 6, 7**), 127.65-147.34 (**C8, 9, 15-17**), 153.32 (**C18**), 153.58 (**C5**), 159.96 (**C14**).

FTMS-ESI: calculated for $C_{16}H_{16}N_3O_4S$ (M+H) 346.0862, found 346.0856.

IR ν_{max} (cm^{-1}): 3405 (amide N-H stretch), 3287 (indole N-H stretch), 1649 (amide C=O stretch), 1545 (N=O stretch).

Elemental analysis: calculated for ($C_{16}H_{15}N_3O_4S$): C 55.64, H 4.38 and N 12.17, found for C 54.85, H 4.34 and N 11.74.

(*R*)-Methyl 2,3,4,9-tetrahydro-1H-pyrido[3,4-b]indole-3-carboxylate (189):

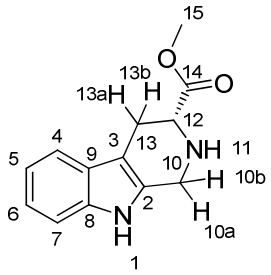

Formaldehyde (1.02 ml of a 37% water solution, 12.6 mmol, 1.6 eq) was added to a solution of *D*-tryptophan methyl ester hydrochloride (2.0 g, 7.8 mmol, 1 eq) in methanol (20 ml) and water (1 ml), and the mixture stirred for 4 hours. Saturated sodium bicarbonate (50 ml) was added to the mixture and a precipitate formed immediately. The mixture was stirred overnight at room temperature to facilitate the precipitation of the product. The precipitate was collected by filtration, then columned with gradient 5% methanol/DCM to give **189** as a light yellow powder (510 mg, 28%).

m.p: 136-137 °C.

^{1}H NMR (DMSO-d_6): 2.75 (m, 1H, **H13a**), 2.94 (dd, *J* = 4.4, 14.96 Hz, 1H, **H13b**), 3.68 (s, 3H, **H15**), 3.74 (m, 1H, **H12**), 3.94 (dd, *J* = 15.96 Hz, 2H, **H10a, H10b**), 6.93 (t, *J* = 7.92, 7 Hz, 1H, **H5**), 7.01 (t, *J* = 7.92, 7.48 Hz, 1H, **H6**), 7.26 (d, *J* = 7.92 Hz, 1H, **H4**), 7.38 (d, *J* = 7.48 Hz, 1H, **H7**), 10.73 (s, 1H, **NH1**).

^{13}C NMR (DMSO-d_6): 25.55 (**C13**), 41.96 (**C10**), 52.19 (**C15**), 55.76 (**C12**), 106.06-127.49 (**C2-7**), 134.05-136.29 (**C8, 9**), 174.22 (**C14**).

FTMS-ESI: calculated for $C_{13}H_{13}N_2O_2$ (M-H) 229.0977, found 229.0982.

IR ν_{max} (cm^{-1}): 3328 (indole N-H stretch), 3180 (aliphatic N-H stretch), 1733 (ester C=O stretch).

Elemental analysis: calculated for ($C_{13}H_{14}N_2O_2$): C 67.81, H 6.13 and N 12.10, found for C 67.76, H 6.12 and N 12.10.

(*R*)-Methyl 2-(5-nitrothiophene-2-carbonyl)-2,3,4,9-tetrahydro-1*H*-pyrido[3,4-*b*]indole-3-carboxylate (190):

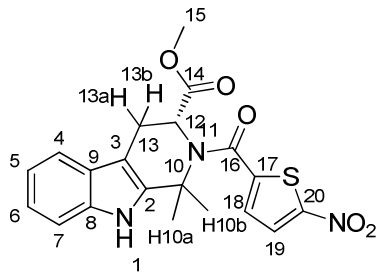

The title compound was obtained as bright yellow crystals using general procedure J (330 mg, 74%).

m.p: 202-204 °C.

^{1}H NMR (DMSO-d_6): 3.10 (bs, 1H, **H13a**), 3.23 (m, 1H, **H13b**), 3.36 (bs, 2H, **H10**), 3.60 (bs, 3H, **H15**), 4.15 (m, 1H, **H12**), 6.97 (t, *J* = 7.44 Hz, 1H, **H5**), 7.08 (t, *J* = 7.24 Hz, 1H, **H6**), 7.31 (m, 1H, **H4**), 7.48 (d, *J* = 7.36 Hz, 1H, **H7**), 8.15 (m, 2H, **H18, 19**), 10.83 (bs, 1H, **NH1**).

^{13}C NMR (DMSO-d_6): 35.20 (**C13**), 41.24 (**C10**), 53.30 (**C15**), 55.82 (**C12**), 105.14-126.69 (**C2-7**), 126.98-136.82 (**C8, 9, 17-19**), 154.32 (**C20**), 169.21 (**C16**), 171.06 (**C14**).

FTMS-ESI: calculated for $C_{18}H_{14}N_3O_5S$ (M-H) 384.0654, found 384.0659.

IR ν_{max} (cm^{-1}): 3366 (indole N-H stretch), 1726 (ester C=O stretch), 1645 (amide C=O stretch), 1601 (nitro N=O stretch).

Elemental analysis: calculated for ($C_{18}H_{15}N_3O_5S$): C 56.10, H 3.92 and N 10.90, found for C 56.37, H 3.91 and N 10.52.

Methyl 5-benzyl-2-(5-nitrothiophene-2-carboxamido)thiazole-4-carboxylate (191):

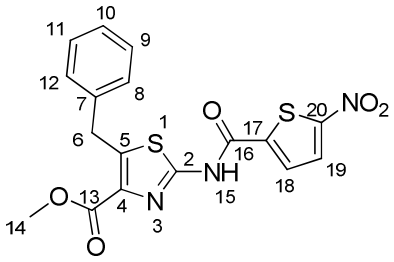

The title compound was obtained as fine orange crystals using general procedure I after column chromatography with 20 % ethyl acetate/hexane (210 mg, 35.3%).

m.p: 210 °C.

^{1}H NMR (DMSO-d_6): 3.85 (s, 3H, **H14**), 4.52 (s, 2H, **H6**), 7.26 (m, 1H, **H10**), 7.33 (m, 4H, **H8, 9, 11, 12**), 8.20 (bs, 2H, **H18, 19**), 13.50 (s, 1H, **NH15**).

^{13}C NMR (DMSO-d_6): 32.32 (**C6**), 52.23 (**C14**), 127.38-129.28 (**C7-12**), 130.60-130.85 (**C4, 5**), 138.18-140.06 (**C18-20**), 155.01 (**C2**), 162.23 (**C16**), 165.32 (**C13**).

FTMS-ESI: calculated for $C_{17}H_{14}N_3O_5S_2$ (M+H) 404.0375, found 404.0369.

IR ν_{max} (cm^{-1}): 3428 (amide N-H stretch), 1725 (ester C=O stretch), 1698 (amide C=O stretch), 1568 (N=O stretch).

Elemental analysis: calculated for ($C_{17}H_{13}N_3O_5S_2$): C 50.61, H 3.25 and N 10.42, found for C 49.97, H 3.52 and N 10.13.

5-Benzyl-2-(5-nitrothiophene-2-carboxamido)thiazole-4-carboxylic acid (192):

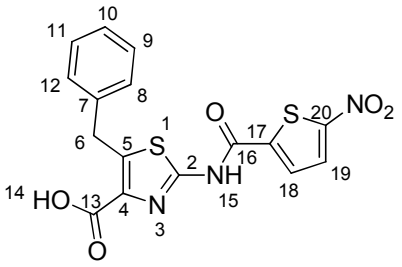

The title compound was obtained as an orange powder using general procedure C (60 mg, 65%).

m.p: 260 °C.

^{1}H NMR (DMSO-d_6): 4.52 (s, 2H, **H6**), 7.25 (m, 1H, **H10**), 7.30-7.36 (m, 4H, **H8, 9, 11, 12**), 8.19 (m, 2H, **H18, 19**), 13.31 (bs, 2H, **OH14, NH15**).

^{13}C NMR (DMSO-d_6): 31.45 (**C6**), 127.31-129.65 (**C7-12**), 130.77-131.35 (**C4, 5**), 140.29-143.64 (**C18-20**), 154.92 (**C2**), 163.91 (**C16**), 164.79 (**C13**).

FTMS-ESI: calculated for $C_{16}H_{12}N_3O_5S_2$ (M+H) 390.0218, found 390.0213.

IR ν_{max} (cm^{-1}): 3181 (amide N-H stretch), 3026 (carboxylic O-H stretch), 1675 (carboxylic C=O stretch), 1668 (amide C=O stretch), 1568 (N=O stretch).

Elemental analysis: calculated for ($C_{16}H_{11}N_3O_5S_2$): C 49.35, H 2.85 and N 10.79, found for C 48.84, H 2.68 and N 10.72

5.3 Biological evaluation

5.3.1 Instruments

Fluorescence Intensity measurement

1420 Multilabel Counter (WallacVictor®) was used for the measurement of the Alamar Blue intensity in the 96 well assay plates at 530 nm excitation and 590 nm emission wave lengths. The test plates were incubated at 37°C and under 5% CO_2

humidified atmosphere in Forma® incubator. The required volume of Alamar Blue® was added to the wells by using RDX Microtiter Dispensing System (DYNEX®).

5.3.2 Solvents and reagents

Solvents for preparation of compound stock solutions

DMSO obtained from Sigma Aldrich, UK was used for dissolving all compounds to prepare stock solutions for the assay.

Culture medium for *T. brucei*

HMI-9 medium was obtained from Invitrogen.

5.3.3 Parasite and cell lines

Trypanosoma brucei brucei

T.b. brucei was obtained from Prof. Mike Barrett (University of Glasgow) in the blood stream form (Strain 427)

Cell line

The normal human epithelial cell line PNT2A (normal prostatic cells) was used.

5.4 Biological assay procedures

5.4.1 *In vitro* Alamar Blue assay of *T.b. brucei* S427

Initially, all compounds were assessed at a concentration of 250 μM. Compounds that inhibited ≥ 90% were assessed to obtain the minimum inhibitory concentrations (MICs).

5.4.1.1 Initial screening

All compounds were prepared as 25 mM DMSO stock solutions and stored in glass vials for evaluation. HMI-9 medium was used for *Trypanosoma* subcultures and compound dilutions.

T.b. brucei parasites were removed from the -80°C cryostorage, reactivated by warming to 37°C in a water bath, subcultured by taking 1 ml from the stock broth, diluted with 5 ml HMI-9 medium in a filter-cap flask and incubated at 37°C under a humidified 5% CO_2 atmosphere for 24 hours. The resultant subculture was checked at 400X magnification to ensure that the parasites were viable.

To columns 2-11 of the 96-well flat bottomed Microtiter plates, 2 µl from each compound stock solution was placed in a separate well, and 98µl HMI-9 medium added. To column 1, 100 µl HMI-9 medium was added in addition to 80 µl to column 12 (**Figure 65**).

	1	2	3	4	5	6	7	8	9	10	11	12
A												
B												
C												
D												
E												
F												
G												
H												

Figure 65: 96-well plate format.

The Trypanosoma inoculum for the assay ($3x10^4$ cell/ml) was prepared by diluting 1.8 ml of the subculture broth (contains $1x10^6$ cells/ml measured by using haematocytometer slide) to 60 ml with HMI-9 medium. 100 µl from the Trypanosoma suspension was added to all wells in the plate except well A1 which was the –ve control (background) to indicate contamination. To column 12, 20 µl of suramin solution from a dilution series (10, 5, 2.5, 1.25, 0.625, 0.31, 0.15 and 0.078 µM) was added and the plate was incubated at 37°C in 5% CO_2 humidified atmosphere for 48 hours.

20 µl of Alamar Blue solution was added to all wells in the plate by using the RDX Microtiter dispensing system (DYNEX®) and the plate incubated under the same conditions for 20 hours. To measure the % of growth compared to the control (well A1), a 1420 Multilabel Counter (Wallace Victor®), in fluorescence mode with wavelengths set at 530 nm for excitation and 590 nm for emission, was used to measure fluorescence. The data obtained was transferred to an excel worksheet to manually calculate the % growth using the equation below.

$$\%\ of\ Control = \frac{A\ [Compound] - A\ [Background]}{A\ [-ve\ Control] - A\ [Background]}\ X\ 100\%$$

Equation 1: calculation of the % of control based on the fluorescence intensity: A represents the intensity reading from the counter as relative fluorescence units (rfus).

Compounds with % of control ≤ 10% were considered active and were taken forward for MIC determination.

5.4.1.2 MIC determination

The micro-dilution method was applied using 96 well plates to obtain MIC values for 3 compounds in duplicate per plate as illustrated in **Figure 66**.

	1	2	3	4	5	6	7	8	9	10	11	12
A	-ve control	Compound 1	→									Suramin 1.0µM
B	+ve control	Compound 1 duplicate	→									Suramin 0.5µM
C	+ve control	Compound 2	→									Suramin 0.25µM
D	+ve control	Compound 2 duplicate	→									Suramin 0.125µM
E	+ve control	Compound 3	→									Suramin 0.0625µM
F	+ve control	Compound 3 duplicate	→									Suramin 0.0313µM
G	+ve control	DMSO	→									Suramin 0.0151µM
H	+ve control	DMSO duplicate	→									Suramin 0.0078µM

Figure 66: The microplate map for the MIC determination assay: -ve control (well contains HMI-9 medium and Alamar Blue dye), +ve control (wells contain HMI-9 medium + Trypanosoma suspension + Alamar Blue dye), the arrows indicate the 1:1 serial dilutions of the compounds starting from column 2 to column 11.

Active compounds from the initial screening were prepared in 25 mM stock solutions, from which 2 µl was inoculated into wells A2 and B2 for the first compound in duplicate; the same was done for the second compounds and placed in wells C2 and D2. The third compound was inoculated into wells E2 and F2. 2 µl of DMSO was placed into wells G2 and H2 to study the effect of using different concentration of DMSO on the Trypanosomal growth. To column 2, 198 µl of HMI-9 medium was added. For columns 1, and 3 to 11, 100 µl HMI-9 medium was inoculated whereas in column 12, 80 µl was added. 1:1 serial dilution was performed by transferring 100 µl from column 2 to 3, and then from column 3 to 4. The same 1:1 dilution was performed for columns 4 to 11. At the end of this process, the final concentration for the compounds moving from column 2 to 11 were 125, 62.5, 31.25, 15.6, 7.8, 3.9, 1.9, 0.97, 0.49, and 0.24 µM respectively. In column 12, a dilution series of suramin was obtained to generate a range of concentrations from 10-0.078 µM. Trypanosoma suspension was prepared as mentioned before and 100 µl was added to all the wells. The incubation was then performed for 24 hours, after which the same steps applied in the initial screening method were used to add the 20 µl Alamar Blue solution to read the plates.

Equation 1 was used to measure the % of control growth compared to the background. The concentration at which 90% or more growth inhibition compared to the control was considered as the MIC for that particular compound.

5.4.2 Host toxicity assay

The compounds at a final concentration of 100µM in Dublicco's modified eagle medium (DMEM) were tested for cytotoxicity against the normal cell line PNT2A (normal prostatic cells). The seeding densities were 0.5 x 10^4 per well for PNT2A cells. The assays were conducted in 96 well microplates with incubation at 37°C (humidified 5% CO_2 atmosphere) for a period of 48 hours prior to the addition of Alamar blue. After a further 20 hours incubation, fluorescence was detected using a Wallac Victor 2 multilabel plate reader (excitation 560nm and emission 590nm) and % of control values were calculated.

5.4.3 *In vivo* anti-trypanosomal testing of compound 164, 191 and 192's

5.4.3.1 *In vivo* testing of acute toxicity

Separate female adult mice (obtained from Harlan Laboratories UK Ltd) were injected intraperitoneally with 1 mg kg^{-1} (0.2 mL) of **164**, **191** and **192** respectively. Mice were then observed and weighed daily for three consecutive days for signs of acute toxicity (i.e. continual staunching, laboured breathing, shivers & tremors) and/or 25% body weight loss. Compound doses were increased accordingly at the end of every 3-day observation if the lower threshold proved to be non-toxic: 10 mg kg^{-1} and 50 mg kg^{-1}. The highest tolerable dose of each test compound would be determined and used subsequently in the *in vivo* efficacy experiment.

5.4.3.2 *In vivo* anti-trypanosomal testing

Five groups of mice (three mice per group) were inoculated with *T.b. brucei* 427 wild-type. Each inoculum consisted of 2 x 10^4 parasites per animal (i.e. 200 µL of 1 x 10^5 cells mL^{-1}) which was administered via intraperitoneal (i/p) injection. The mice were treated on day 3 post-infection with four different types of treatments: Pentamidine (4 mg kg^{-1}), **164** (50 mg kg^{-1}), **191** (50 mg kg^{-1}) and **192** (50 mg kg^{-1}) and one group was left untreated as the negative control. Each treatment was prepared fresh and administered via i/p injection with a volume of 200 µL. The treatments were repeated on a daily basis for another three days. Parasitaemia level of each animal was monitored daily via microscopic observations of subsequent blood smears.

5.5 Pharmacophore model study

5.5.1 Data selection

A set of 10 compounds containing the most active was selected from the **ATC** library to serve as the "Training set" for pharmacophore generation. To test and validate the selectivity of the generated pharmacophores, a test set composed of the remaining **ATC** compounds for which activities were known was screened.

5.5.2 Conformation generation

Before running the pharmacophore generation and subsequent screening, the Conformation Generation Protocol in Discovery Studio (Accelrys®), version 2.5.5 was used to generate the best and the lowest energy conformers for both the training and test set. Conformers (255 maximum) were generated for each molecule using "BEST" method, and minimised using the CHARMm minimization forcefield. All other parameters of the protocol were set to their default value.

5.5.3 Feature mapping of the training set

Feature mapping of the minimised training set was carried out using default parameters of the Feature Mapping Protocol Discovery Studio (Accelrys®); version 2.5.5 to find accessible features in these compounds to be fed later into the Pharmacophore Generation Protocol. The obtained features included hydrogen bond acceptors, hydrogen bond donors, hydrophobic, hydrophobic-aromatic, hydrophobic-aliphatic, positive ionisable, negative ionisable, positively charged, negatively charged and ring aromatic groups.

5.5.4 Common feature pharmacophore generation (HipHop® protocol)

This protocol was applied to generate a maximum of 10 hypothetical pharmacophores to represent the key features of the training compounds, based on the output of the Feature Mapping Protocol. The protocol used was the common feature pharmacophore generation; HipHop® generation function, from Discovery Studio (Accelrys®), version 2.5.5. The features identified from the feature mapping were hydrogen bond donor, hydrogen bond acceptor, hydrophobic, negative ionisable and ring aromatic. The default parameters from this protocol were used, with the exception of the maximum pharmacophore to be generated, which was set to 10, the maximum features to miss is one; and the Principal Number parameter (which specifies the reference ligands) was set to 2 for compounds **24**, **27** and **28** which ensures that all chemical features in these compounds will be considered in building the hypothesis. The rest of the compounds were given a value of 1 for their Principal Number, which means the protocol will consider these ligands as moderately active. Finally, the MaxOmitFeat was set to 1, which means all the features except one must be mapped. The experiment resulted in 10 pharmacophores

arranged according to a ranking score. The number and types of features along with the ranking score for each hypothesis are given in **Table 33**.

CPU time = 159 s System time = 0 s

	Features	Rank	Direct Hit	Partial Hit	Max Fit
01	HHAAAAA	157.003	0111111111	1000000000	7
02	RHHDAAA	154.209	0111111111	1000000000	7
03	HHDAAAA	152.574	0111111111	1000000000	7
04	HHAAAAA	151.652	0111111111	1000000000	7
05	HHAAAAA	150.270	0111111111	1000000000	7
06	HHDAAAA	148.254	0111111111	1000000000	7
07	NHHAAA	140.691	0111111111	1000000000	6
08	NHHAAA	138.562	0111111111	1000000000	6
09	RNHHDA	137.825	0111111111	1000000000	6
10	RHDAAA	137.809	1111111111	0000000000	6

Table 33: Ranking of the generated 10 pharmacophore hypothesis: H refers to hydrophobic group, A to hydrogen bond acceptor, D hydrogen bond donor, N to negative ionisable and R to aromatic ring

5.5.5 Common feature pharmacophore generation (HipHopRefine® protocol)

This protocol was used to improve the selectivity of the best pharmacophore hypothesis obtained from the HipHop® experiment by adding excluded volumes to an input pharmacophore. The algorithm identifies areas of space that are occupied by inactive ligands and strategically places excluded volumes in these regions to reduce the number of false positives that can map the pharmacophore. The protocol used was the Steric Refinement with excluded volumes (HipHopRefine®) from Discovery Studio (Accelrys®), version 2.5.5. The input pharmacophore was the best one from the HipHop experiment, the input active ligands were the training set, and the input inactive ligands were selected from those that were totally inactive and structurally diverse (three compounds). The default parameters were used except for maximum excluded volumes, which were set to 100.

5.5.6 Ligand pharmacophore mapping of the test set

This was applied as a validation step to test the selectivity of the generated hypothesis. The ligand pharmacophore mapping protocol from Discovery Studio (Accelrys®), version 2.5.5 was used, the input database was the test set, and the input pharmacophore was the most selective one with the two additional features. The default parameters were used in this experiment except the following: the fitting method used was "Rigid", the MaxOmitFeat was set to zero, and only the best mapped compounds were saved. Ten compounds were retrieved and their fit values (describing how closely the chemical features of the compounds map the pharmacophore features) were obtained. The highest fit value is equal to the maximum number of pharmacophore features which is 10 and the minimum should be zero when there is no mapping at all.

Ten molecules of the test set were retrieved of which 9 were among the most active compounds based on an MIC of 7.8 μM as the cut-off value. This highlights the high selectivity of this pharmacophore.

Appendix A

The published work on **ATC** compounds:

OPEN ACCESS Freely available online PLoS one

Identification of 2-Aminothiazole-4-Carboxylate Derivatives Active against *Mycobacterium tuberculosis* $H_{37}R_v$ and the β-Ketoacyl-ACP Synthase mtFabH

Qosay Al-Balas[1], Nahoum G. Anthony[1], Bilal Al-Jaidi[1], Amani Alnimr[2], Grainne Abbott[3], Alistair K. Brown[4], Rebecca C. Taylor[4], Gurdyal S. Besra[4], Timothy D. McHugh[2], Stephen H. Gillespie[2], Blair F. Johnston[1], Simon P. Mackay[1], Geoffrey D. Coxon[1]*

1 Strathclyde Institute of Pharmacy and Biomedical Sciences, University of Strathclyde, Glasgow, United Kingdom, 2 Department of Infection, University College London, London, United Kingdom, 3 Strathclyde Innovations in Drug Research, Glasgow, United Kingdom, 4 School of Biosciences, University of Birmingham, Edgebaston, Birmingham, United Kingdom

Abstract

Background: Tuberculosis (TB) is a disease which kills two million people every year and infects approximately over one-third of the world's population. The difficulty in managing tuberculosis is the prolonged treatment duration, the emergence of drug resistance and co-infection with HIV/AIDS. Tuberculosis control requires new drugs that act at novel drug targets to help combat resistant forms of *Mycobacterium tuberculosis* and reduce treatment duration.

Methodology/Principal Findings: Our approach was to modify the naturally occurring and synthetically challenging antibiotic thiolactomycin (TLM) to the more tractable 2-aminothiazole-4-carboxylate scaffold to generate compounds that mimic TLM's novel mode of action. We report here the identification of a series of compounds possessing excellent activity against *M. tuberculosis* $H_{37}R_v$ and, dissociatively, against the β-ketacyl synthase enzyme mtFabH which is targeted by TLM. Specfically, methyl 2-amino-5-benzylthiazole-4-carboxylate was found to inhibit *M. tuberculosis* $H_{37}R_v$ with an MIC of 0.06 µg/ml (240 nM), but showed no activity against mtFabH, whereas methyl 2-(2-bromoacetamido)-5-(3-chlorophenyl)thiazole-4-carboxylate inhibited mtFabH with an IC_{50} of 0.95±0.05 µg/ml (2.43±0.13 µM) but was not active against the whole cell organism.

Conclusions/Significance: These findings clearly identify the 2-aminothiazole-4-carboxylate scaffold as a promising new template towards the discovery of a new class of anti-tubercular agents.

Citation: Al-Balas Q, Anthony NG, Al-Jaidi B, Alnimr A, Abbott G, et al. (2009) Identification of 2-Aminothiazole-4-Carboxylate Derivatives Active against *Mycobacterium tuberculosis* $H_{37}R_v$ and the β-Ketoacyl-ACP Synthase mtFabH. PLoS ONE 4(5): e5617. doi:10.1371/journal.pone.0005617

Editor: Matthew H. Todd, University of Sydney, Australia

Received October 16, 2008; **Accepted** April 21, 2009; **Published** May 19, 2009

Funding: The authors have no support or funding to report.

Competing Interests: The authors have declared that no competing interests exist.

* E-mail: geoff.coxon@strath.ac.uk

Appendix B

The **ATC** full library activity on Trypanosoma parasite and their toxicity on human normal fibroblast (HS27):

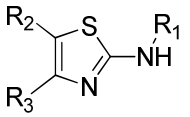

R_1	R_2	R_3	***T.b. bruci*** **MIC**	Cytotoxicity against HS27 (% control)
H	CH_3	$COOCH_3$	>250	100
H	CH_3	COOH	>250	101
-$COCH_3$	CH_3	$COOCH_3$	>250	96
-$COCH_3$	CH_3	COOH	>250	98
-COC_2H_5	CH_3	$COOCH_3$	>250	93
-$CO(CH_2)_2CH_3$	CH_3	$COOCH_3$	>250	85
-$CO(CH_2)_4CH_3$	CH_3	$COOCH_3$	>250	89
-$CO(CH_2)_6CH_3$	CH_3	$COOCH_3$	>250	87
-$CO(CH_2)_{14}CH_3$	CH_3	$COOCH_3$	>250	97
-CO(cyclopropyl)	CH_3	$COOCH_3$	>250	96
-CO(cyclopropyl)	CH_3	COOH	>250	94
-CO(2-acetyloxy)ethyl	CH_3	$COOCH_3$	>250	91
-CO(4-nitrophenyl)	CH_3	$COOCH_3$	>250	94
-CO(4-butoxyphenyl)	CH_3	$COOCH_3$	>250	87
-CO(4-methoxyphenyl)	CH_3	$COOCH_3$	250	78
-CO(3-Pyrrolyl)	CH_3	$COOCH_3$	250	86
-CO(4-Pyridyl)	CH_3	$COOCH_3$	>250	99
-CO[2,4-dichlorophenyl(oxymethyl)]	CH_3	$COOCH_3$	>250	70
H	CH_2CH_3	$COOCH_3$	>250	100
H	CH_2CH_3	COOH	>250	97
-CO(cyclopropyl)	CH_2CH_3	$COOCH_3$	>250	86
-CO(cyclopropyl)	CH_2CH_3	COOH	>250	97
H	$CH_2CH_2CH_3$	$COOCH_3$	>250	93
H	$CH_2CH_2CH_3$	COOH	>250	98
-CO(cyclopropyl)	$CH_2CH_2CH_3$	$COOCH_3$	>250	87
-CO(cyclopropyl)	$CH_2CH_2CH_3$	COOH	>250	100
H	$CH(CH_2)_2$	$COOCH_3$	>250	100
H	$CH(CH_2)_2$	COOH	>250	97
-CO(cyclopropyl)	$CH(CH_2)_2$	$COOCH_3$	125	83
-CO(cyclopropyl)	$CH(CH_2)_2$	COOH	125	95
H	$CH_2CH_2CH_2CH_3$	$COOCH_3$	>250	91
H	$CH_2CH_2CH_2CH_3$	COOH	>250	99
-CO(cyclopropyl)	$CH_2CH_2CH_2CH_3$	$COOCH_3$	62.5	74
-CO(cyclopropyl)	$CH_2CH_2CH_2CH_3$	COOH	31.3	97
H	benzyl	$COOCH_3$	>250	81
H	benzyl	COOH	>250	92
-COC_2H_5	benzyl	$COOCH_3$	>250	97

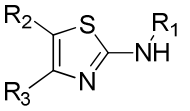

R_1	R_2	R_3	***T.b. bruci* MIC**	Cytotoxicity against HS27 (% control)
$-CO(CH_2)_5CH_3$	benzyl	$COOCH_3$	>250	108
-CO(cyclopropyl)	benzyl	$COOCH_3$	250	102
-CO(benzyl)	benzyl	$COOCH_3$	>250	85
-CO(4-nitrophenyl)	benzyl	$COOCH_3$	>250	97
-CO(2-carboxyethyl)	benzyl	$COOCH_3$	>250	102
-CO(2-carboxyethyl)	benzyl	COOH	>250	99
-CO[2-(2-carboxyphenyl)phenyl]	benzyl	$COOCH_3$	>250	136
-CO(2-carboxyetheneyl)	benzyl	$COOCH_3$	>250	110
-CO(2-carboxyetheneyl)	benzyl	COOH	>250	106
bromoacetyl	benzyl	$COOCH_3$	31.3	95
bromoacetyl	benzyl	COOH	1.0	112
H	phenyl	$COOCH_3$	>250	83
H	phenyl	COOH	>250	92
$-COCH_2CH_3$	phenyl	$COOCH_3$	>250	86
$-COCH_2CH_3$	phenyl	COOH	>250	102
-CO(cyclopropyl)	phenyl	COOH	>250	103
bromoacetyl	phenyl	$COOCH_3$	31.3	83
bromoacetyl	phenyl	COOH	31.3	93
bromoacetyl	3-chlorophenyl	$COOCH_3$	62.5	82
bromoacetyl	3-chlorophenyl	COOH	62.5	97
$-COC_2H_5$	3-chlorophenyl	$COOCH_3$	>250	78
$-COC_2H_5$	3-chlorophenyl	COOH	>250	98
$-COCH_3$	3-chlorophenyl	$COOCH_3$	>250	85
$-COCH_3$	3-chlorophenyl	COOH	>250	99
H	4-chlorophenyl	$COOCH_3$	>250	102
bromoacetyl	4-chlorophenyl	$COOCH_3$	62.5	99
-CO(cyclopropyl)	4-chlorophenyl	$COOCH_3$	31.3	96
-CO(cyclopropyl)	4-chlorophenyl	COOH	15.6	110
H	4-methoxyphenyl	$COOCH_3$	>250	94
bromoacetyl	4-methoxyphenyl	$COOCH_3$	31.3	94
-CO(cyclopropyl)	4-methoxyphenyl	$COOCH_3$	125	91
-CO(cyclopropyl)	4-methoxyphenyl	COOH	62.5	106
H	2-naphthyl	$COOCH_3$	>250	98
H	$COOC_2H_5$	CH_3	>250	98
H	COOH	CH_3	>250	90
bromoacetyl	$COOC_2H_5$	CH_3	31.3	89
$-COC_2H_5$	$COOC_2H_5$	CH_3	125	87
$-COC_2H_5$	COOH	CH_3	>250	83
$-COCH_3$	$COOC_2H_5$	CH_3	250	83
$-COCH_3$	COOH	CH_3	>250	89
-CO(cyclopropyl)	$COOC_2H_5$	CH_3	125	91
-CO(cyclopropyl)	COOH	CH_3	>250	85
H	$COOC_2H_5$	CH_2CH_3	>250	90

Chapter Six: References

1. WHO *Human African Trypanosomiasis: better treatment opportunity*; Geneva, Switzerland, 2009.
2. Welburn, S. C.; Fèvre, E. M.; Coleman, P. G.; Odiit, M.; Maudlin, I., Sleeping sickness: A tale of two diseases. *Trends in Parasitology* **2001,** *17* (1), 19-24.
3. Courtin, D.; Berthier, D.; Theventon, S.; Dayo, G.-K.; Garcia, A.; Bucheton, B., Host genetics in African Trypanosomiasis. *Infections, Genetics and Evolution* **2008,** *8*, 229-238.
4. Fe`vre, E. M.; Wissmann, B. v.; Welburn, S. C.; Lutumba, P., The burden of Human African Trypanosomiasis. *PLoS Neglected Tropical Diseases* **2008,** *2* (12), 333-370.
5. Brun, R.; Blum, J.; Chappuis, F.; Burri, C., Human African Trypanosomiasis. *The Lancet* **2010,** *375*, 148-159.
6. Barrett, M.; Boykin, D.; Brun, R.; Tidwell, R., Human African Trypanosomiasis: pharmacological re-engagement with a neglected disease. *British Journal of Pharmacology* **2007,** *152*, 1155-1171.
7. Krafsur, E. S., Tsetse flies: Genetics, evolution, and role as vectors. *Infections, Genetics and Evolution* **2009,** *9*, 124-141.
8. Barrett, M. P.; Burchmore, R. J.; Stich, A.; Lazzari, J. O.; Frasch, A. C.; Cazzulo, J. J.; Krishna, S., The Trypanosomiasis. *The Lancet* **2003,** *362*, 1462-1480.
9. Lee, S. H.; Stephens, J. L.; Englund, P. T., A fatty acid synthesis mechanism specialized for parasitism. *Nature Reviews* **2007,** *5*, 287-297.
10. Kennedy, P. G. E., Human African Trypanosomiasis of the CNS: current issues and challenges. *Journal of Clinical Invistigations* **2004,** *113*, 496-504.
11. Simo, G.; Asonganyi, T.; Nkinin, S. W.; Njiokou, F.; Herder, S., High prevalence of *Trypanosoma brucei gambiense* group 1 in pigs from the Fontem sleeping sickness focus in Cameroon. *Vet. Parasit.* **2006,** *139*, 57-66.
12. Penchenier, L.; Grebaut, P.; Njokou, F.; Eboo Eyenga, V.; Buscher, P., Evaluation of LATEX/*T.b.gambiense* for mass screening of *Trypanosoma brucei gambiense* sleeping sickness in central Africa. *Acta Tropica* **2003,** *85*, 31-37.

13. WHO *Control and surveillance of African trypanosomiasis*; World Health Organization Geneva, 1998.
14. Tarleton, R. L., New approaches in vaccine development for parasitic infections. *Cellular Microbiology* **2005,** *7* (10), 1379-1386.
15. Dumonteil, E., DNA vaccines against protozoan parasites: advances and challenges. *Journal of Biomedicine and Biotechnology* **2007**, 1-11.
16. Barrett, M. P., The fall and rise of sleeping sickness. *The Lancet* **2006,** *367*, 1377-1378.
17. WHO *WHO Programme to elimenate sleeping sickness-building a global alliance*; World Health Organisation: Geneva, 2002.
18. Docambo, R.; Moreno, S. N., Current chemotherapy of Human African Trypanosomiasis *Parasit. Res.* **2003,** *90*, S10-13.
19. Hanau, S.; Rippa, M.; Bertelli, M.; Dallocchio, F.; Barrett, M. P., 6-Phosphogluconate dehydrogenase from Trypanosoma brucei: Kinetic analysis and inhibition by trypanocidal drugs. *Europ. J. Bioch.* **1996,** *240*, 592-599.
20. Sanderson, L., Pentamidine movement across the murine blood-brain and blood-cerebrospinal fluid barriers: Effect of trypanosome infection, combination therapy, P-glycoprotein, and multidrug resistance-associated protein. *Journal of Pharmacology and Experimental Therapeutics* **2009,** *329*, 967-977.
21. Croft, S. L., Pharmacological approaches to antitrypanosomal chemotherapy. *Memorias do Instituto Oswaldo Cruz* **1999,** *94* (2), 215-220.
22. Gehrig, S.; Efferth, T., Development of drug resistance in *Trypanosoma brucei rhodesiense* and *Trypanosoma brucei gambiense*. Treatment of Human African Trypanosomiasis with natural products. *International journal of molecular medicine* **2008,** *22*, 411-419.
23. Carter, N. S.; Berger, B. J.; Fairlamb, A. H., Uptake of diamidine drugs by the P2 nucleoside transporter in melarsen-sensitive and-resistant *Trypanosoma brucei brucei*. *J. Biol. Chem.* **1995,** *270*, 28153-28157.
24. Peppin, J.; Milford, F., Treatment of Human African Trypanosomiasis. *Advances in Parasitology* **1994,** *33*, 1-47.

25. Nok, A. J., Arsenicals (melarsoprol), pentamidine and suramin in the treatment of Human African Trypanosomiasis. *Parasit. Res.* **2003,** *90*, 71-79.
26. Fairlamb, A. H.; Henderson, G. B.; Bacchi, C. J.; A., C., In vivo effects of difluoromethylornithine on trypanothione and polyamine levels in blood-stream forms of *Trypanosoma brucei*. *Molecular Biochem. Parasit.* **1987,** *24* 185-191.
27. Chappuis, F.; Udayraj, N.; Stietenroth, K.; Meussen, A.; Bovier, P. A., Eflornithine is safer than melarsoprol for the treatment of second-stage *Trypanosoma brucei gambiense* Human African Trypanosomiasis. *Clinical Infectious Diseases* **2005,** *41*, 748-51.
28. Legros, D., Treatment of Human African Trypanosomiasis: present situation and needs for research and development. *Lancet Infectious Diseases 2* **2002**, 437-440.
29. Willert, E. K.; Phillips, M. A., Regulated expression of an essential allosteric activator of polyamine biosynthesis in African trypanosomes. *PLoS Pathogens* **2008,** *4*, e1000183.
30. Wilkinson, S. R.; Kelly, J. M., Trypanocidal drugs: Mechanisms, resistance and new targets. *Expert Reviews in Molecular Medicine* **2009,** *11* (31), 1-24.
31. Priotto, G.; Fogg, C.; Balasegaram, M.; Erphas, O.; Louga, A.; Checchi, F.; Salah, G.; Patrice, P., Three drug combinations for late-stage *Trypanosoma brucei gambiense* sleeping sickness: a randomized clinical trial in Uganda. *PLoS Clin Trials* **2006,** *1*, e39.
32. Maya, J. D.; Cassels, B. K.; Iturriaga-Vásquez, P.; Ferreira, J.; Faúndez, M.; Galanti, N.; Ferreira, A.; Morello, A., Mode of action of natural and synthetic drugs against *Trypanosoma cruzi* and their interaction with the mammalian host. *Comparative Biochemistry and Physiology* **2007,** *Part A* (146), 601-620.
33. Mäser, P.; Lüscher, A.; Kaminsky, R., Drug transport and drug resistance in African trypanosomes. *Drug Resistance Updates* **2003,** *6*, 281-290.
34. Shahi, S. K.; Krauth-Siegel, R. L.; Clayton, C. E., Overexpression of the putative thiol conjugate transporter TbMRPA causes melarsoprol resistance in *Trypanosoma brucei*. *Molecular Microbiology* **2002,** *43*, 1129-1138.

35. Iten, M.; Mett, H.; Evans, A.; Enyaru, J. C.; Brun, R.; Kaminsky, R., Alterations in ornithine decarboxylase characteristics account for tolerance of *Trypanosoma brucei rhodesiense* to D,L-alpha-difluoromethylornithine. *Antimicrobial Agents and Chemotherapy* **1997,** *41*, 1922-1925.

36. Ouellette, M., Biochemical and molecular mechanisms of drug resistance in parasites. *Tropical Medicine and International Health* **2001,** *6* (11), 874-882.

37. Anene, B. M.; Onah, D. N.; Nawa, Y., Drug resistance in pathogenic African trypanosomes: what hopes for the future? *Vet. Parasit.* **2001,** *96*, 83-100.

38. Sutherland, I. A.; Peregrine, A. S.; Lonsdale-Eccles, J. D.; Holmes, P. H., Reduced accumulation of isometamidium by drug-resistant *Trypanosoma congolense*. *Parasit. Res.* **1991,** *103*, 245-251.

39. Priotto, G.; Kasparian, S.; Mutombo, W., Nifurtimox-eflornithine combination therapy for second-stage African *Trypanosoma brucei gambiense* trypanosomiasis: a multicentre, randomised, phase III, non-inferiority trial. *The Lancet* **2009,** *374*, 56-64.

40. Keiser, J.; Stich, A.; Burri, C., New drugs for the treatment of Human African Trypanosomiasis: research and development. *TRENDS in Parasitology* **2001,** *17* (1), 42-49.

41. Berriman, M.; Ghedin, E.; Hertz-Fowler, C.; Blandin, G.; Renauld, H.; Bartholomeu, D. C.; Lennard, N. J.; Caler, E.; Hamlin, N. E.; Haas, B., et al., The genome of the African trypanosome *Trypanosoma brucei*. *Science* **2005,** *309* (5733), 416-422.

42. Cavalli, A.; Bolognesi, M. L., Neglected tropical diseases: Multi-target-directed ligands in the search for novel lead candidates against *Trypanosoma* and *Leishmania*. *J. Med. Chem.* **2009,** *52*, 7339-7359.

43. Morita, Y. S.; Paul, K. S.; Englund, P. T., Specialized fatty acid synthesis in African trypanosomes: Myristate for CPI anchors. *Science* **2000,** *288* (5463), 140-143.

44. Finkelstein, J. M., Parasitology-Peculiar lipid production. *Nature* **2006,** *442* (7106), 995-995.

45. Jones, S. M.; Urch, J. E.; Brun, R.; Harwood, J. L.; Berry, C.; Gilbert, I. H., Analogues of thiolactomycin as potential anti-malarial and anti-trypanosomal agents. *Bioorg. Med. Chem.* **2004,** *12* (4), 683-692.

46. Jones, S. M.; Urch, J. E.; Kaiser, M.; Brun, R.; Harwood, J. L.; Berry, C.; Gilbert, I. H., Analogues of thiolactomycin as potential antimalarial agents. *J. Med. Chem.* **2005,** *48* (19), 5932-5941.

47. Gibellini, F.; Hunter, W. N.; Smith, T. K., The ethanolamine branch of the Kennedy pathway is essential in the bloodstream form of *Trypanosoma brucei*. *Molecular Microbiology* **2009,** *73* (5), 826-843.

48. Mina, J. G.; Pan, S. Y.; Wansadhipathi, N. K.; Bruce, C. R.; Shams-Eldin, H.; Schwarz, R. T.; Steel, P. G.; Denny, P. W., The *Trypanosoma brucei* sphingolipid synthase, an essential enzyme and drug target. *Mol. Bioch. Parasit.* **2009,** *168* (1), 16-23.

49. Cavalcanti, D. P.; Fragoso, S. P.; Goldenberg, S.; de Souza, W.; Motta, M. C., The effect of topoisomerase II inhibitors on the kinetoplast ultrastructure. *Parasit. Res.* **2004,** *94*, 439-448.

50. Deterding, A.; Dungey, F. A.; Thompson, K.-A.; Steverding, D., Anti-trypanosomal activities of DNA topoisomerase inhibitors. *Acta Tropica* **2005,** *93*, 311-316.

51. Huang, T. L.; Eynde, J. J. V.; Mayence, A.; Collins, M. S.; Cushion, M. T.; Rattendi, D.; Londono, I.; Mazumder, L.; Bacchi, C. J.; Yarlett, N., Synthesis and SAR of alkanediamide-linked bisbenzamidines with anti-trypanosomal and anti-pneumocystis activity. *Bioorg. Med. Chem. Let.* **2009,** *19*, 5884-5886.

52. Barrett, M. P.; Mottram, J. C.; Coombs, G. H., Recent advances in identifying and validating drug targets in trypanosomes and leishmanias. *Trends in Microbiology* **1999,** *7* (2).

53. Kuettel, S.; Mosimann, M.; Maser, P.; Kaiser, M.; Brun, R.; Scapozza, L.; Perozzo, R., Adenosine kinase of *T. b. rhodesiense* Identified as the putative target of 4-[5-(4-phenoxyphenyl)-2H-pyrazol-3-yl]morpholine using chemical proteomics. *PloS Neglected Tropical Diseases* **2009,** *3* (8), 1-9.

54. Hellemond, J. J. v.; Bakker, B. M.; Tielens, A. G. M., Energy Metabolism and Its compartmentation in *Trypanosoma brucei*. *Advances in Microbial Physiology* **2005,** *50*, 202-226.

55. Bakker, B. M.; Michels, P. A. M.; Opperdoes, F. R.; Westerhoff, H. V., What controls glycolysis in bloodstream form *Trypanosoma brucei*? *J. Biol. Chem.* **1999,** *274* (21), 14551-14559.

56. Verlinde, C. L. M.; Hannaert, V.; Blonski, C.; Willson, M.; Périé, J. J.; Fothergill-Gilmore, L. A.; Opperdoes, F. R.; Gelb, M. H.; Hol, W. G. J.; Michels, P. A. M., Glycolysis as a target for the design of new anti-trypanosome drugs. *Drug Resistance Updates* **2001,** *4*, 50-65.

57. Chambers, J. W.; Kearns, M. T.; Morris, M. T.; Morris, J. C., Assembly of heterohexameric trypanosome hexokinases reveals that hexokinase 2 is a regulable enzyme. *J. Biol. Chem.* **2008,** *283* (22), 14963-14970.

58. Caceres, A. J.; Michels, P. A. M.; Hannaert, V., Genetic validation of aldolase and glyceraldehyde-3-phosphate dehydrogenase as drug targets in *Trypanosoma brucei*. *Mol. Bioch. Parasit.* **2010,** *169* (1), 50-54.

59. Olivares-Illana, V.; Perez-Montfort, R.; Lopez-Calahorra, F.; Costas, M.; Rodriguez-Romero, A.; de Gomez-Puyou, M. T.; Puyou, A. G., Structural differences in triosephosphate isomerase from different species and discovery of a multitrypanosomatid inhibitor. *Biochemistry* **2006,** *45* (8), 2556-2560.

60. Chevalier, N.; Bertrand, L.; Rider, M. H.; Opperdoes, F. R.; Rigden, D. J.; Michels, P. A. M., 6-Phosphofructo-2-kinase and fructose-2,6-bisphosphatase in trypanosomatidae - Molecular characterization, database searches, modelling studies and evolutionary analysis. *FEBS Journal* **2005,** *272* (14), 3542-3560.

61. Martinez-Oyanedel, J.; McNae, I. W.; Nowicki, M. W.; Keillor, J. W.; Michels, P. A. M.; Fothergill-Gilmore, L. A.; Walkinshaw, M. D., The first crystal structure of phosphofructokinase from an eukaryote: *Trypanosoma brucei*. *J. Mol. Biol.* **2007,** *366* (4), 1185-1198.

62. Chambers, J. W.; Fowler, M. L.; Morris, M. T.; Morris, J. C., The anti-trypanosomal agent lonidamine inhibits *Trypanosoma brucei* hexokinase 1. *Mol. Bioch. Parasit.* **2008,** *158* (2), 202-207.

63. Kotsikorou, E.; Sahota, G.; Oldfield, E., Bisphosphonate inhibition of phosphoglycerate kinase: Quantitative structure-activity relationship and pharmacophore modeling investigation. *J. Med. Chem.* **2006,** *49* (23), 6692-6703.

64. Nowicki, M. W.; Tulloch, L. B.; Worralll, L.; McNae, I. W.; Hannaert, V.; Michels, P. A. M.; Fothergill-Gilmore, L. A.; Walkinshaw, M. D.; Turner, N. J., Design, synthesis and trypanocidal activity of lead compounds based on inhibitors of parasite glycolysis. *Bioorg. Med. Chem.* **2008,** *16* (9), 5050-5061.

65. Bressi, J. C.; Choe, J.; Hough, M. T.; Buckner, F. S.; Van Voorhis, W. C.; Verlinde, C.; Hol, W. G. J.; Gelb, M. H., Adenosine analogues as inhibitors of *Trypanosoma brucei* phosphoglycerate kinase: Elucidation of a novel binding mode for a 2-amino-N-6-substituted adenosine. *J. Med. Chem.* **2000,** *43* (22), 4135-4150.

66. Mpamhanga, C. P.; Spinks, D.; Tulloch, L. B.; Shanks, E. J.; Robinson, D. A.; Collie, I. T.; Fairlamb, A. H.; Wyatt, P. G.; Frearson, J. A.; Hunter, W. N., et al., One scaffold, three binding modes: Novel and selective pteridine reductase-1 inhibitors derived from fragment hits discovered by virtual screening. *J. Med. Chem.* **2009,** *52*, 4454-4465.

67. Tulloch, L. B.; Martini, V. P.; Iulek, J.; Huggan, J. K.; Lee, J. H.; Gibson, C. L.; Smith, T. K.; Suckling, C. J.; Hunter, W. N., Structure-based design of pteridine reductase inhibitors targeting African sleeping sickness and the Leishmaniases. *J. Med. Chem.* **2010,** *53*, 221-229.

68. Torrie, L. S.; Wyllie, S.; Spinks, D.; Oza, S. L.; Thompson, S.; Harrison, J. R.; Gilbert, I. H.; Wyatt, P. G.; Fairlamb, A. H.; Frearson, J. A., Chemical validation of trypanothione synthetase: A potential drug target for Human Trypanosomiasis. *J. Biol. Chem.* **2009,** *284* (52), 36137-36145.

69. Naula, C.; Parsons, M.; Mottram, J. C., Protein kinases as drug targets in trypanosomes and Leishmania. *Biochimica Et Biophysica Acta-Proteins and Proteomics* **2005,** *1754* (1-2), 151-159.

70. Bahia, D.; Oliveira, L. M.; Lima, F. M.; Oliveira, P.; da Silveira, J. F.; Mortara, R. A.; Ruiz, J. C., The TryPIKinome of five human pathogenic

trypanosomatids: *Trypanosoma brucei*, *Trypanosoma cruzi*, *Leishmania major*, *Leishmania braziliensis* and *Leishmania infantum* - New tools for designing specific inhibitors. *Biochemical and Biophysical Research Communications* **2009,** *390* (3).

71. Mottram, J. C.; Smith, G., A family of trypanosome CDC2-related protein-kinases. *Gene* **1995,** *162* (1), 147-152.
72. Hammarton, T. C.; Kramer, S.; Tetley, L.; Boshart, M.; Mottram, J. C., *Trypanosoma brucei* Polo-like kinase is essential for basal body duplication, kDNA segregation and cytokinesis. *Molecular Microbiology* **2007,** *65* (5), 1229-1248.
73. Li, Z. Y.; Umeyama, T.; Wang, C. C., The aurora kinase in *Trypanosoma brucei* plays distinctive roles in metaphase-anaphase transition and cytokinetic initiation. *PLoS Pathogens* **2009,** *5* (9).
74. Urbaniak, M. D., Casein kinase 1 isoform 2 is essential for bloodstream form *Trypanosoma brucei*. *Mol. Bioch. Parasit.* **2009,** *166* (2), 183-185.
75. Heby, O.; Persson, L.; Rentala, M., Targeting the polyamine biosynthetic enzymes: a promising approach to therapy of African sleeping sickness, Chagas' disease, and leishmaniasis. *Amino Acids* **2007,** *33* (2), 359-366.
76. Coombs, G. H.; Mottram, J. C., Parasite proteinases and amino acid metabolism: possibilities for chemotherapeutic exploitation. *Parasitology* **1997,** *114*, S61-S80.
77. Spitznagel, D.; Ebikeme, C.; Biran, M.; Bhaird, N. N. A.; Bringaud, F.; Henehan, G. T. M.; Nolan, D. P., Alanine aminotransferase of *Trypanosoma brucei*: a key role in proline metabolism in procyclic life forms. *FEBS Journal* **2009,** *276* (23), 7187-7199.
78. Mott, B. T.; Ferreira, R. S.; Simeonov, A.; Jadhav, A.; Ang, K. K. H.; Leister, W.; Shen, M.; Silveira, J. T.; Doyle, P. S.; Arkin, M. R., et al., Identification and optimization of inhibitors of trypanosomal cysteine proteases: Cruzain, rhodesain, and TbCatB. *J. Med. Chem.* **2010,** *53* (1), 52-60.
79. Steverding, D.; Spackman, R. W.; Royle, H. J.; Glenn, R. J., Trypanocidal activities of trileucine methyl vinyl sulfone proteasome inhibitors. *Parasit. Res.* **2005,** *95* (1), 73-76.

80. Gigante, F.; Kaiser, M.; Brun, R.; Gilbert, I. H., SAR studies on azasterols as potential anti-trypanosomal and anti-leishmanial agents. *Bioorg. Med. Chem.* **2009,** *17* (16), 5950-5961.

81. Lyne, P. D., Structure-based virtual screening: an overview. *Drug Discovery Today* **2002,** *7* (20), 1047-1055.

82. Walters, W. P.; Stahl, T. M.; Murcko, A. M., Virtual screening: An overview. *Drug Discovery Today* **1998,** *3* (4), 160-178.

83. Joseph-McCarthy, D., Computational approaches to structure-based ligand design. *Pharmacology & Therapeutics* **1999,** *84* (2), 179-191.

84. Lipinski, C. A.; Lombardo, F.; Dominy, B. W.; Feeney, P. J., Experimental and computational approaches to estimate solubility and permeability in drug discovery and development settings. *Advanced Drug Delivery Reviews* **1997,** *23* (1-3), 3-25.

85. Yang, S. Y., Pharmacophore modeling and applications in drug discovery: Challenges and recent advances. *Drug Discovery Today* **2010,** *15* (11-12), 444-450.

86. Al-Balas, Q. A. *The Design and Synthesis of a New Lead against Tuberculosis*. University of Strathclyde, Glasgow, 2008.

87. Heath, R. J.; Rock, C. O., Fatty acid biosynthesis as a target for novel antibacterials. *Current Opinions and Investigations of Drugs* **2004,** *5* (2), 146-153.

88. Räz, B.; Iten, M.; Grether-Bühler, Y.; Kaminsky, R.; Brun, R., The Alamar Blue® assay to determine drug sensitivity of African trypanosomes (*T.b. rhodesiense* and *T.b. gambiense*) in vitro. *Acta Tropica* **1997,** *68* (2), 139-147.

89. Al-Balas, Q.; Anthony, N. G.; Al-Jaidi, B.; Alnimr, A.; Abbott, G.; Brown, A. K.; Taylor, R. C.; Besra, G. S.; McHugh, T. D.; Gillespie, S. H., et al., Identification of 2-Aminothiazole-4-Carboxylate Derivatives Active against Mycobacterium tuberculosis H37Rv and the beta-Ketoacyl-ACP Synthase mtFabH. *Plos One* **2009,** *4* (5).

90. Bligh, E. G.; Dyer, W. J., A rapid method of total lipid extraction and purification. *Canadian Journal of Biochemistry and Physiology* **1959,** *37* (8), 911-917.

91. Toba, S.; Srinivasan, J.; Maynard, A. J.; Sutter, J., Using pharmacophore models to gain insight into structural binding and virtual screening: An application study with CDK2 and human DHFR. *Journal of Chemical Information and Modeling* **2006,** *46*, 728-735.

92. Anderson, N. L.; Parish, N. M.; Richardson, J. P.; Pearson, T. W., Comparison of African Trypanosomes of different antigenic phenotypes, subspecies and life-cycle stages by two-dimensional gel-electrophoresis. *Mol. Bioch. Parasit.* **1985,** *16* (3), 299-314.

93. Coleman, P. G.; Welburn, S. C., Are fitness costs associated with resistance to human serum in *Trypanosoma brucei rhodesiense*? *Trends in Parasitology* **2004,** *20* (7), 311-315.

94. Owusu-Dapaah, G. Synthesis and evaluation of new antitrypanosomal agents. University of Strathclyde, Glasgow, 2008.

95. Henderson, G. B.; Ulrich, P.; Fairlamb, A. H.; Cerami, A., Synthesis of the trypanosomatid metabolites trypanothione, and n-1-mono-glutathionylspermidine and n-8-mono-glutathionylspermidine. ***J. Chem. Soc.****-Chemical Communications* **1986,** (8), 593-594.

96. Wilkinson, S. R.; Taylor, M. C.; Horn, D.; Kelly, J. M.; Cheeseman, I., A mechanism for cross-resistance to nifurtimox and benznidazole in trypanosomes. *PNAS* **2008,** *105* (13), 5022-5027.

97. Enanga, B.; Ariyanayagam, M. R.; Stewart, M. L.; Barrett, M. P., Activity of megazol, a trypanocidal nitroimidazole, is associated with DNA damage. *Antimicrobial Agents and Chemotherapy* **2003,** *47*, 3368-3370.

98. Barbosa, C. F.; Okuda, E. S.; Chung, M. C.; Ferreira, E. I.; Cicarelli, R. M. B., Rapid test for the evaluation of the activity of the prodrug hydroxymethylnitrofurazone in the processing of *Trypanosoma cruzi* messenger RNAs. *Brazilian Journal of Medical and Biological Research* **2007,** *40*, 33-39.

99. Hall, B. S.; Wu, X.; Hu, L.; Wilkinson, S. R., Exploiting the drug-activating properties of a novel trypanosomal nitroreductase. *Antimicrobial Agents and Chemotherapy* **2010,** *54* (3), 1193-1199.

100. Powers, J. P.; Li, S. Y.; Jaen, J. C.; Liu, J. Q.; Walker, N. P. C.; Wang, Z. L.; Wesche, H., Discovery and initial SAR of inhibitors of interleukin-1 receptor-associated kinase-4. *Bioorg. Med. Chem. Let.* **2006,** *16* (11), 2842-2845.

101. Sagi, K.; Fujita, K.; Sugiki, M.; Takahashi, M.; Takehana, S.; Tashiro, K.; Kayahara, T.; Yamanashi, M.; Fukuda, Y.; Oono, S., et al., Optimization of a coagulation factor VIIa inhibitor found in factor Xa inhibitor library. *Bioorg. Med. Chem.* **2005,** *13* (5), 1487-1496.

102. Drumm, J. E.; Deininger, D. D.; LeTiran, A.; Wang, T. S.; Grillot, A. L.; Liao, Y. S.; Ronkin, S. M.; Stamos, D. P.; Tang, Q.; Tian, S. K., et al., Facile preparation of fused ring azolylureas. *Tetrahedron Let.* **2007,** *48*, 5535-5538.

103. Hajduk, P. J.; Boyd, S.; Nettesheim, D.; Nienaber, V.; Severin, J.; Smith, R.; Davidson, D.; Rockway, T.; Fesik, S. W., Identification of novel inhibitors of urokinase via NMR-based screening. *J. Med. Chem.* **2000,** *43* (21), 3862-3866.

104. Gambert, R.; Kuratli, C.; Martin, R. E., Preparation of 5-amino-6-oxo-1,6-dihydro[1,2,4]triazine-3-carboxylic acid derivatives and synthesis of compound libraries thereof. *Tetrahedron Let.* **2004,** *45* (13), 2791-2795.

105. Lum, R. T.; Cheng, M.; Cristobal, C. P.; Goldfine, I. D.; Evans, J. L.; Keck, J. G.; Macsata, R. W.; Manchem, V. P.; Matsumoto, Y.; Park, S. J., et al., Design, synthesis, and structure-activity relationships of novel insulin receptor tyrosine kinase activators. *J. Med. Chem.* **2008,** *51* (19), 6173-6187.

106. Montalbetti, C.; Falque, V., Amide bond formation and peptide coupling. *Tetrahedron* **2005,** *61* (46), 10827-10852.

107. Kikugawa, Y.; Mitsui, K.; Sakamoto, T., N-Methoxydiacetamide - A new selective acetylating agent. *Tetrahedron Let.* **1990,** *31* (2), 243-246.

108. Stuart, D. R.; Bertrand-Laperle, M.; Burgess, K. M. N.; Fagnou, K., Indole synthesis via rhodium catalyzed oxidative coupling of acetanilides and internal alkynes. *J. Am. Chem. Soc.* **2008,** *130* (49), 16474-16475.

109. Fuwa, H.; Hiromoto, K.; Takahashi, Y.; Yokoshima, S.; Kan, T.; Fukuyama, T.; Iwatsubo, T.; Tomita, T.; Natsugari, H., Synthesis of biotinylated photoaffinity probes based on arylsulfonamide gamma-secretase inhibitors. *Bioorg. Med. Chem. Let.* **2006,** *16* (16), 4184-4189.

110. Wydysh, E. A.; Medghalchi, S. M.; Vadlamudi, A.; Townsend, C. A., Design and synthesis of small molecule glycerol 3-phosphate acyltransferase inhibitors. *J. Med. Chem.* **2009,** *52* (10), 3317-3327.

111. Zheng, X. X.; Oda, H.; Takamatsu, K.; Sugimoto, Y.; Tai, A.; Akaho, E.; Ali, H. I.; Oshiki, T.; Kakuta, H.; Sasaki, K., Analgesic agents without gastric damage: Design and synthesis of structurally simple benzenesulfonanilide-type cyclooxygenase-1 selective inhibitors. *Bioorg. Med. Chem.* **2007,** *15* (2), 1014-1021.

112. Hall, A.; Brown, S. H.; Chessell, I. P.; Chowdhury, A.; Clayton, N. M.; Coleman, T.; Giblin, G. M. P.; Hammond, B.; Healy, M. P.; Johnson, M. R., et al., 1,5-Biaryl pyrrole derivatives as EP_1 receptor antagonists: Structure–activity relationships of 4- and 5-substituted benzoic acid derivatives. *Bioorg. Med. Chem. Let.* **2007,** *17* 732-735.

113. Thorarensen, A.; Wakefield, B. D.; Romero, D. L.; Marotti, K. R.; Sweeney, M. T.; Zurenko, G. E.; Rohrer, D. C.; Han, F. S.; Bryant, G. L., Preparation of novel anthranilic acids as antibacterial agents. Extensive evaluation of alternative amide bioisosteres connecting the A- and the B-rings. *Bioorg. Med. Chem. Let.* **2007,** *17* (10), 2823-2827.

114. Ren, J.; Wang, S. M.; Wu, L. F.; Xu, Z. X.; Dong, B. H., Synthesis and properties of novel Y-shaped NLO molecules containing thiazole and imidazole chromophores. *Dyes and Pigments* **2008,** *76*, 310-314.

115. Aberle, N.; Catimel, J.; Nice, E. C.; Watson, K. G., Synthesis and biological evaluation of analogues of the anti-tumor alkaloid naamidine A. *Bioorg. Med. Chem. Let.* **2007,** *17*, 3741-3744.

116. Berry, D. A.; Gilbertsen, R. B.; Cook, P. D., Synthesis of 8-amino-3-deazaguanine via imidazole precursors. Antitumor activity and inhibition of purine nucleoside phosphorylase. *J. Med. Chem.* **1986,** *29*, 2034-2037.

117. Bouchet, M. J.; Rendon, A.; Wermuth, C. G.; Goeldner, M.; Hirth, C., Aryl diazo compounds and diazonium salts as potential irreversible probes of the γαμμα-aminobutyric-acid receptor. *J. Med. Chem.* **1987,** *30* (12), 2222-2227.

118. Lafrance, R. J.; Manning, H. W.; Vaughan, K., Open-chain nitrogen compounds: Synthesis and high resolution nuclear magnetic resonance spectroscopy of 3-(arylazo)-1,3-oxazolidines and 3-(arylazo)tetrahydro-1,3-oxazines. *J. Org. Chem.* **1985,** *50* (13), 2229-2232.

119. Trujillo, J. I.; Huang, H. C.; Neumann, W. L.; Mahoney, M. W.; Long, S.; Huang, W.; Garland, D. J.; Kusturin, C.; Abbas, Z.; South, M. S., et al., Design, synthesis, and biological evaluation of pyrazinones containing novel P1 needles as inhibitors of TF/VIIa. *Bioorg. Med. Chem. Let.* **2007,** *17* (16), 4568-4574.

120. Wagner-Wysiecka, E.; Jamrogiewic, M.; Fonari, M. S.; Biernat, J. F., Azomacrocyclic derivatives of imidazole: Synthesis, structure, and metal ion complexation properties. *Tetrahedron* **2007,** *63*, 4414-4421.

121. Barton, A.; Breukelman, S. P.; Kaye, P. T.; Meakins, G. D.; Morgan, D. J., The preparation of thiazole-4-carboxylates and thiazole-5-carboxylates, and an infrared study of their rotational isomers. *J. Chem. Soc.-Perkin Transactions 1* **1982,** (1), 159-164.

122. Ghosh, A. K.; Kim, J.-H., Stereoselective chloroacetate aldol reactions: Synthesis of acetate aldol equivalents and Darzens glycidic esters. *Org. Let.* **2004,** *6* (16), 2725-2728.

123. Krowicki, K.; Lown, J. W., Synthesis of novel imidazole-containing dna minor groove binding oligopeptides related to the antiviral antibiotic netropsin. *J. Org. Chem.* **1987,** *52* (16), 3493-3501.

124. South, M. S., Synthesis and reactions of halogenated thiazole isocyanate. *Journal of Heterocyclic Chemistry* **1991,** *28* (4), 1003-1011.

125. Hogberg, T.; Strom, P.; Ebner, M.; Ramsby, S., Cyanide as an efficient and mild catalyst in the aminolysis of esters. *J. Org. Chem.* **1987,** *52* (10), 2033-2036.

126. Hiebl, J.; Alberts, D. P.; Banyard, A. F.; Baresch, K.; Baumgartner, H.; Bernwieser, I.; Bhatnagar, P. K.; Blanka, M.; Bodenteich, M.; Chen, T., et al.,

Large-scale synthesis of hematoregulatory nonapeptide SK & F 107647 by fragment coupling. *Journal of Peptide Research* **1999,** *54* (1), 54-65.

127. Anthony, N. G.; Breen, D.; Clarke, J.; Donoghue, G.; Drummond, A. J.; Ellis, E. M.; Gemmell, C. G.; Helesbeux, J.-J.; Hunter, I. S.; Khalaf, A. I., et al., Antimicrobial lexitropsins containing amide, amidine, and alkene linking groups. *J. Med. Chem.* **2007,** *50*, 6116-6125.
128. Khalaf, A. I.; Waigh, R. D.; Drummond, A. J.; Pringle, B.; McGroarty, I.; Skellern, G. G.; Suckling, C. J., Distamycin analogues with enhanced lipophilicity: synthesis and antimicrobial activity. *J. Med. Chem.* **2004,** *47*, 2133-2156.
129. Ohemeng, K. A.; Roth, B., Receptor-based design of novel dihydrofolate reductase inhibitors: Benzimidazole and indole derivatives. *J. Med. Chem.* **1991,** *34*, 1383-1394.
130. Milbank, J. B. J.; Stevenson, R. J.; Ware, D. C.; Chang, J. Y. C.; Tercel, M.; Ahn, G. O.; Wilson, W. R.; Denny, W. A., Synthesis and evaluation of stable bidentate transition metal complexes of 1-(chloromethyl)-5-hydroxy-3-(5,6,7-trimethoxyindol-2-yl-carbonyl)-2,3-dihydro-1H-pyrrolo[3,2-*f*]quinoline (*seco*-6-azaCBI-TMI) as hypoxia selective cytotoxins. *J. Med. Chem.* **2009,** *52* (21), 6822-6834.
131. Pilipenko, A. S.; Gaidarzhi, A. N.; Butin, A. V., Recyclization of tosylamino derivatives of 2-aryl-5-benzylfuran to give indoles through two alternative pathways. *Chemistry of Heterocyclic Compounds* **2009,** *45* (3), 302-307.
132. Ragaini, F.; Song, J. S.; Ramage, D. L.; Geoffroy, G. L.; Yap, G. A. P.; Rheingold, A. L., Radical processes in the reduction of nitrobenzene promoted by iron carbonyl clusters. X-ray crystal-structures of $[Fe_3(CO)_9(\mu_3\text{-}NPh)]^{2-}$, $[HFe_3(CO)_9(\mu_3\text{-}NPh)]^-$, and the radical anion $[Fe_3(CO)_{11}]^{\cdot-}$. *Organometallics* **1995,** *14* (1), 387-400.
133. Cox, E. D.; Cook, J. M., The Pictet-Spengler condensation - A new direction for an old reaction. *Chemical Reviews* **1995,** *95* (6), 1797-1842.
134. Whaley, W. M.; Govindachari, T. R., The Pictet-Spengler synthesis of tetrahydroisoquinolines and related compounds. *Organic Reactions* **1951,** ***6***, 74.

135. Webb, K. S.; Seneviratne, V., A mild oxidation of aromatic amines *Tetrahedron Let.* **1995,** *36* (14), 2377-2378.

136. Bloom, J. D.; DiGrandi, M. J.; Dushin, R. G.; Curran, K. J.; Ross, A. A.; Norton, E. B.; Terefenko, E.; Jones, T. R.; Feld, B.; Lang, S. A., Thiourea inhibitors of herpes viruses. Part 1: Bis-(aryl)thiourea inhibitors of CMV. *Bioorg. Med. Chem. Let.* **2003,** *13* (17), 2929-2932.

137. Ueda, S.; Nagasawa, H., Copper-catalyzed synthesis of benzoxazoles via a regioselective C-H functionalization/C-O bond formation under an air atmosphere. *J. Org. Chem.* **2009,** *74* (11), 4272-4277.

138. Qian, X. H.; Li, Z. G.; Yang, Q., Highly efficient antitumor agents of heterocycles containing sulfur atom: Linear and angular thiazonaphthalimides against human lung cancer cell in vitro. *Bioorg. Med. Chem.* **2007,** *15*, 6846-6851.

139. Nagai, W.; Kirk, K. L.; Cohen, L. A., Synthesis of 2-amino-l-histidine and 2-aminohistamine. *J. Org. Chem.* **1973,** *38* (11), 1971-1974.